Promotion of neuroplasticity by modifying perineuronal nets using polysialic acid

Louise Adams

Supervisors: Dr Xuenong Bo, Professor Adina Michael-Titus and Professor John Priestley

A thesis submitted for the degree of Doctor of Philosophy

Centre for Neuroscience and Trauma, Blizard Institute, Barts and the London School of Medicine and Dentistry, Queen Mary University of London

Statement of Originality

I, Louise Adams, confirm that the research included within this thesis is my own work or that where it has been carried out in collaboration with, or supported by others, that this is duly acknowledged below and my contribution indicated. Previously published material is also acknowledged below.

I attest that I have exercised reasonable care to ensure that the work is original, and does not to the best of my knowledge break any UK law, infringe any third party's copyright or other Intellectual Property Right, or contain any confidential material.

I accept that the College has the right to use plagiarism detection software to check the electronic version of this thesis.

I confirm that this thesis has not been previously submitted for the award of a degree by this or any other university.

The copyright of this thesis rests with the author and no quotation from it or information derived from it may be published without the prior written consent of the author.

Signature: ***Louise Adams***

Date: 5th April 2015

Abstract

Polysialic acid (PSA) is a linear homopolymer formed of chains of 2,8-linked sialic acid. Found predominantly attached to the neural cell adhesion molecule, PSA acts to reduce cell-cell adhesion during development. It is also found in some areas of the adult central nervous system (CNS) associated with persistent neuroplasticity. Preliminary data from our laboratory indicated an inverse relationship between PSA expression and the formation of perineuronal nets (PNNs), specialised extracellular matrix structures with a role in limiting plasticity in the adult CNS. The primary aims of this thesis were to investigate this relationship in more detail, using *in vitro* models of PNN formation and *in vivo.* Also, to evaluate whether lentiviral vector-mediated PSA expression can enhance locomotor recovery and neuroplasticity in a rodent model of spinal cord injury. PNNs were heterogeneously distributed throughout the grey matter of the rat cervical spinal cord, and increased in numbers down the dorsoventral axis. Induced expression of PSA in the spinal cord of either naïve or injured rats did not alter the number or density of PNNs. Similarly, enzymatic removal of PSA from the surface of cultured embryonic neurons did not affect the formation of the PNNs. In a rodent model of cervical spinal cord injury, induced PSA expression resulted in an improvement in hindlimb, but not forelimb, locomotor function compared to animals injected with control virus. Interestingly, this was not associated with an increased density of serotonin or synaptophysin-labelled boutons in the areas of induced PSA expression. Taken together, the data presented in this thesis suggests that while induced PSA expression may contribute to improved locomotor function in a model of cervical spinal cord injury, this is not due to a reduction in the density or number of PNNs in the spinal cord.

Table of contents

List of Figures

List of Tables

List of Abbreviations

5-HT	5-hydroxytryptamine (serotonin)
AP	Anterioposterior
BBB	Basso, Beattie, Bresnahan scale
BDA	Biotin dextran amine
BDNF	Brain-derived neurotrophic factor
BRAL2	Brain link protein-2
BSCB	Blood-spinal cord barrier
ChABC	Chondroitinase ABC
ChAT	Choline acetyltransferase
CHL1	Close homologue L1
CMV	Cytomegalovirus
CNS	Central nervous system
CSPG	Chondroitin sulphate proteoglycan
CTB	Cholera toxin subunit B
DMEM	Dulbecco's modified Eagle medium
DRG	Dorsal root ganglion
ECM	Extracellular matrix
endo-N	Endoneuraminidase-N
FBS	Fetal bovine serum
FLS	Forelimb locomotor scale
FN-III	Fibronectin type 3 domain
GAG	Glycosaminoglycan
GAP-43	Growth-associated protein 43
GDNF	Glial-derived neurotrophic factor
GFAP	Glial fibrillary acidic protein
GFP	Green fluorescent protein
HAS	Hyaluronan synthase
HBSS	Hank's balanced salt solution
HEK293T	Human embryonic kidney 293T cell line
HSPG	Heparin sulphate proteoglycan
Ig	Immunoglobulin-like domain
LAR	Leucocyte antigen-related protein
LN1	Cartilage link protein-1

LV	Lentiviral
MAG	Myelin-associated glycoprotein
MAP2	Microtubule-associated protein 2
ML	Mediolateral
MMP	Matrix metalloproteinase
NCAM	Neural cell adhesion molecule
NCS-1	Neuronal calcium sensor-1
NeuN	Neuronal nuclei antigen N
NrCAM	Neuronal cell adhesion molecule
NT-3	Neurotrophin-3
OEC	Olfactory ensheathing cell
OMgp	Oligodendrocyte myelin glycoprotein
PNN	Perineuronal net
PSA	Polysialic acid
PST	Polysialyltransferase
PTEN	Phosphatase and tensin homologue
PTP	Protein tyrosine phosphatase sigma
ROS	Reactive oxygen species
SCI	Spinal cord injury
SEM	Standard error of the mean
STX	Sialyltransferase X
SVZ	Subventricular zone
WFA	*Wisteria floribunda* agglutinin

Acknowledgements

First and foremost, I would like to thank my supervisors Xuenong Bo, John Priestley and Adina Michael-Titus for giving me the opportunity to undertake my doctoral research, and for their continued help and support. Also, thanks to Spinal Research for supporting this project. Thanks also go to other members of Xuenong's laboratory, especially Yi Zhang and Sena Lee for help in the lab when I was just starting out. I would like to extend my gratitude to members to the past and present members of Adina's group, especially Ping Yip, I couldn't have done this without him and I'm so grateful for all of his help with the *in vivo* work.

I'd also like to thank all the amazing friends I have made during my time at the Blizard, especially Ruth Angus (the queen of all knowledge), Zoe Drymoussi, Susie Grey, Emal Waqif, Fiona Kenny, Sreekanth Reddy, Matthew Brooke and Laura Collopy. Special mention also goes to Gordon and Sam.

Special thanks, of course, goes to my lovely family, including the Gilvos, Jean and my new southern family, particularly Rob's parents, for their continued support. Thanks especially goes to my incredible Mum, she's the strongest person I know and has always given me unwavering support.

Finally, I'd like to thank Rob. I really couldn't have made it through the past few years without you and I'm looking forward to our future adventures!

_____

I'd like to dedicate this thesis to my Dad, for all his encouragement and support.

Chapter 1

Introduction

Chapter 1: Introduction

1.1 The neuronal extracellular matrix

The neuronal extracellular matrix (ECM) is a complex structure consisting of a large array of molecules that act to regulate cell growth and migration, in addition to synapse formation and plasticity. During development, dynamic changes occur within the matrix to regulate axonal sprouting and the formation of new synapses. When the majority of developmental neuroplasticity has occurred the composition of the ECM changes; molecules inhibitory to axonal growth are upregulated and the ECM plays a large part in the limitation of neuroplasticity in the adult central nervous system (CNS).

The neuronal ECM can be subdivided into three distinct regions, namely, (i) the basement membrane, (ii) the interstitial matrix and (iii) the perineuronal net (PNN). These subtypes are classified based on the ECM structure, in addition to location around neurons. The basement membrane is a specialised form of extracellular matrix, located between endothelial cells that line the vasculature of the CNS and the parenchyma. It is formed of type IV collagen, nidogen, agrin, heparin sulphate proteoglycan-2 (HSPG-2) and the glycoproteins laminin and fibronectin (reviewed by (Morris et al., 2014). The interstitial matrix is found throughout the spinal cord parenchyma, providing structural support to cells within the CNS. Containing structural molecules such as type IV collagen, laminin and fibronectin, the interstitial matrix differs from the basement membrane by containing a high proportion of chondroitin sulphate proteoglycans (CSPGs), supporting molecules hyaluronan and tenascin-R, but lacking HSPG-2 (Lau et al., 2013). Conversely, the PNN is only found surrounding certain neuronal populations in the adult CNS and predominantly consists of CSPGs, in addition to supporting molecules (Deepa et al., 2006; Galtrey et al., 2008). As the main scope of this thesis is to examine the relationship between the PNN and polysialic acid (PSA) in considerable detail, the distribution and composition of PNNs will be discussed further in section 1.1.1 below. The composition of the basement membrane, interstitial matrix and PNNs in the adult nervous system are summarised in Table 1.1 below

Molecule	Basement membrane	Interstitial matrix	Perineuronal net
Fibronectin	✓	✓	×
Laminin	✓	✓	×
Type IV collagen	✓	✓	×
Agrin	✓	×	×
Nidogen	✓	×	×
HSPGs	✓	×	×
CSPGs	×	✓	✓
Hyaluronan	×	✓	✓
Tenascin-R	×	✓	✓
Cartilage link protein-1	×	×	✓
Semaphorin 3A	×	×	✓

Table 1.1. Composition of the neuronal extracellular matrix.

1.1.1 Perineuronal net structure

First identified by Camillo Golgi in the late 19th century, the PNN was described as a reticular structure that envelopes the neuronal cell body. Improvements in techniques allowed detailed visualisation of this structure and it was subsequently determined that PNNs are largely formed of CSPGs, a large family of molecules that have an essential role in the restriction of neuroplasticity in the adult CNS, in addition to a number of supporting molecules, which are summarised in Table 1.1, above.

1.1.1.1 Chondroitin sulphate proteoglycans

Structurally, CSPGs consist of a core protein, which is covalently attached to a number of sulphated glycosaminoglycan (GAG) side chains. These GAG chains are post-translationally added to the core protein, the numbers of which are heterogeneous between CSPGs (Kjellen and Lindahl, 1991). Up to 100 GAG chains can be added to the core protein (Dyck and Karimi-Abdolrezaee, 2015) and the length of individual GAG chains can vary (Kjellen and

Lindahl, 1991; Bartus et al., 2012). Sulphation of CSPGs chains occurs via the action of chondroitin sulphotransferase enzymes, which add sulphate groups to specific residues of the GAG chains (Bartus et al., 2012). Five sulphation locations have been determined, named CS-A to CS-E. The pattern of sulphation varies on different CSPGs, at different stages of development and following trauma to the CNS (Bartus et al., 2012). This, in combination with the number and length of GAG chains attached to the core protein, has been shown to modulate the inhibitory functions of CSPGs (Nandini and Sugahara, 2006). For example, one study showed that CS-A is capable of inducing a more potent suppression of neurite outgrowth of cultured cerebellar granule neurons, compared with CS-C (Wang et al., 2008). However, other studies have disputed this finding and there are conflicting results as to which sulphation pattern can exert the strongest inhibition of axonal outgrowth.

Broadly speaking, CSPGs can be sub-classified into 3 families: (i) the lecticans, (ii) the matrix-associated proteoglycans and (iii) the cell-surface proteoglycans. The lecticans are the largest family of CSPGs and the most abundant class of molecule found in the neuronal extracellular matrix (Howell and Gottschall, 2012). Including neurocan, versican, aggrecan and brevican, they have distinct expression patterns in the developing CNS, which is believed in part to be due to their different structures (reviewed by (Howell and Gottschall, 2012)). The matrix-associated family contains the CSPG phosphacan, which is abundantly expressed throughout the developing and the adult CNS. While members of the lectican and matrix-associated CSPG families are secreted by astrocytes and neurons, the cell-surface proteoglycan NG2 is expressed by oligodendrocyte progenitor cells and microglia/macrophages, and shares little homology with other CSPGs (Siebert et al., 2014). Moreover, only members of the lectican and matrix-associated subgroups of CSPGs have been found condensed in PNNs (Deepa et al., 2006; Galtrey et al., 2008).

Results from structural studies have suggested that CSPGs are bound to long chains of hyaluronan, via a link protein, cartilage link protein-1 (LN1) in PNNs (Tsien, 2013). Furthermore, CSPGs can aggregate together, via an intermediate protein, tenascin-R, and may also bind the chemorepulsive guidance molecule semaphorin 3A (Vo et al., 2013).

1.1.1.2 Tenascin-R

Two members of the tenascin family, tenascin-R and tenascin-C, are abundantly expressed in the CNS. Tenascin-C is expressed during the development of the rodent CNS and is typically down-regulated in the adult nervous system, with the exception of a few limited brain regions associated with on-going neuroplasticity and following spinal cord injury (reviewed by Anlar 2012). On the other hand, expression of tenascin-R persists into adulthood, where it is heavily distributed throughout the extracellular matrix. Only tenascin-R has been localised to PNN structures in the rodent CNS, where it acts to stabilise connections between CSPGs (Aspberg et al., 1997). The importance of tenascin-R in maintaining the structure of the PNN was shown in studies using mice deficient in this protein. PNNs in the hippocampi and somatosensory cortex of tenascin-R deficient mice have an abnormal structure and contain reduced immunostaining for other PNN components, including hyaluronan, phosphacan, brevican and neurocan (Weber et al., 1999; Bruckner et al., 2000).

1.1.1.3 Link proteins

Out of the four identified link proteins only two have been observed in PNNs: LN1 and brain link protein 2 (BRAL2); they act to stabilise the connections between CSPGs and hyaluronan (Mörgelin et al., 1994; Carulli et al., 2010). Mounting evidence is suggesting a crucial role for LN1 in maintaining the integrity of the PNN structure. LN1 expression coincides with the formation of PNNs *in vivo*, therefore it has been proposed that LN1 acts as a 'trigger' for PNN formation in the CNS (Carulli et al., 2010). While the brains of LN1 deficient mice contain similar amounts of aggrecan, phosphacan, brevican and versican compared to wild-types animals, the condensation of these CSPGs into PNNs is reduced in LN1 knockout mice. PNNs in these mice appear thinner, and have a reduced amount of *Wisteria Floribunda* agglutinin (WFA; a lectin which binds to the *N*-acetylgalactosamine units found within the side chains of CSPGs) labelling (Carulli et al., 2010). In a separate study, LN1 deficiency led to the abnormal structure of PNN-like formations surrounding HEK293 cells *in vitro* (Kwok et al., 2010). Similarly to the brain of LN1 deficient mice, those lacking BRAL2 do not have a general reduction in CSPG expression in their brains, but condensation of these molecules into PNNs is disrupted (Bekku et al., 2012).

1.1.1.4 Hyaluronan

Hyaluronan is a glycosaminoglycan and is ubiquitously distributed throughout the neuronal extracellular matrix during development. While expression is generally reduced in the adult CNS it persists in PNNs, where it is believed to bind to CSPGs (Deepa et al., 2006; McRae and Porter, 2012). Hyaluronan is synthesised by the enzymes hyaluronan synthases (HAS), transmembrane proteins that are found on the surface of all PNN-expressing neurons (Kwok et al., 2010). Three HAS enzymes have been identified, HAS1-3, which are all differentially expressed during postnatal development in the CNS (Galtrey et al., 2008). As all PNNs have been shown to contain hyaluronan, it is likely that the PNN is anchored to the neuronal extracellular membrane via HAS enzymes and hyaluronan. To date only one study investigating the structure of the PNN in mice lacking one or more of the HAS enzymes has been conducted. Mice lacking the HAS3 isoform do not show any abnormalities in the structure or the number of WFA-labelled PNNs in their cortex or hippocampus (Arranz et al., 2014). However, the appearance of 'normal' PNNs in HAS3 knockout mice may be due to the continued expression of hyaluronan by other HAS isoforms. In an interesting *in vitro* study, HAS3, in addition to LN1 and aggrecan expression by a cell line that does not normally produce a pericellular matrix, led to the formation of a PNN-like structure surrounding HEK293 cells. Cells expressing LN1 and aggrecan only, in the absence of hyaluronan produced by HAS3, did not form this PNN-like structure (Kwok et al., 2010).

1.1.1.5 Semaphorin 3A

Recent work has identified the chemorepulsive axon guidance protein semaphorin 3A as a component of PNNs in the adult CNS. The semaphorins are the largest family of axon guidance molecules and are abundantly distributed throughout the CNS during development (Fiore and Püschel, 2003). Thus far, only semaphorin 3A has been identified in PNNs, where it interacts with the GAG side chains of CSPGs, as enzymatic removal of these GAG chains using chondroitinase ABC (ChABC) abolished semaphorin 3A immunolabelling within the PNN (Vo et al., 2013). As the finding of the presence of semaphorin 3A in PNNs was only recently discovered, there are no published studies on the structure of PNNs in mice lacking this protein. As current research suggests semaphorin 3A binds exclusively to the GAG chains of the CSPG molecules, it may be that knocking out this protein has minimal effect on the structure of the PNN.

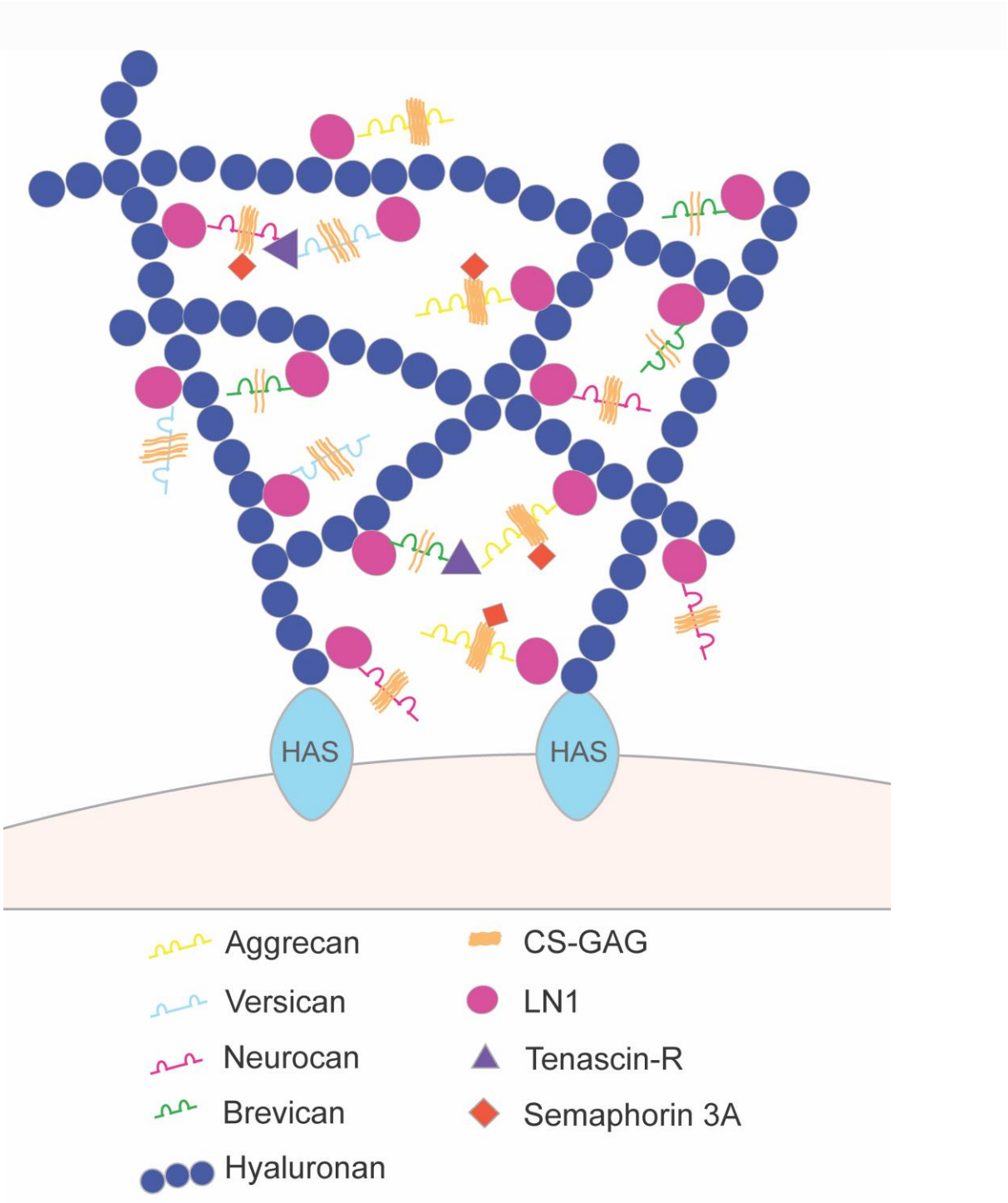

Figure 1.1. Structure of the perineuronal net.
PNNs predominantly consist of CSPGs, such as aggrecan, versican, neurocan and brevican, which are anchored to the extracellular membrane by HAS enzymes, which secrete hyaluronan molecules. CSPGs bind to hyaluronan via LN1, and are cross-linked via interactions with tenascin-R. Semaphorin 3A, a recently discovered component of PNNs, is speculated to bind to the GAG side chains of CSPGs. Adapted from Tsien 2013.

1.1.2 Distribution of perineuronal nets in the CNS

To date there have only been a handful of studies that have investigated the detailed distribution of PNNs in specific regions of the rodent CNS, including the cerebellum and spinal cord. For the most part, PNNs are detected using a combination of WFA labelling and antibodies raised against various members of the CSPG family. Generally, PNN immunolabelling detected by WFA lectin can be observed from the end of the first and second postnatal weeks in most brain regions. Cortical regions including the parietal, occipital and temporal cortices typically form PNNs at the end of the second postnatal week, with the appearance of adult-like PNNs observed at the end of the fifth week (Koppe et al., 1997). While the emergence of PNN structures in subcortical regions also occurs during the second week of postnatal development, some structures, such as the inferior colliculus and the red nucleus, form PNNs earlier. Adult-like PNNs are consistently observed by the end of the third week throughout all examined subcortical regions (Koppe et al., 1997). PNN formation in the deep cerebellar nuclei and spinal cord is observed from the first postnatal week (Carulli et al., 2007), and in the spinal cord, reaches adult levels by the third week (Galtrey et al., 2008).

To date, two studies have provided a thorough review of PNN formation in the cerebellum and spinal cord, by looking at the immunolabelling of individual PNN components, such as the CSPGs aggrecan and phosphacan, in addition to supporting molecules such as LN1 and hyaluronan (Carulli et al., 2007; Galtrey et al., 2008). As previously mentioned, WFA-PNN immunolabelling can be detected in the cerebellum from the end of the first postnatal week. Interestingly, while the lectican CSPG versican also condenses to form PNN structures at this time, it is not until the end of the second postnatal week that other lectican CSPGs, such as aggrecan and neurocan, in addition to supporting molecules LN1 and hyaluronan, are condensed into PNN structures (Carulli et al., 2007). Furthermore, although the general timescale of PNN development is similar in the deep cerebellar nuclei and the spinal cord, the temporal deposition of individual PNN components onto the neuronal surface is variable. For example, versican PNN immunolabelling can be detected in the cerebellum at the end of the first postnatal week; however, it is only observed in PNNs in the spinal cord from the third week. Aggrecan PNN immunolabelling however, is detected in the spinal cord from the end of the first postnatal week, but is not observed in the cerebellar PNNs

until the end of the second week. A tabular review of the two studies is shown below in Table 1.2.

PNN component	Cerebellum	Spinal cord
CSPGs		
Aggrecan	P14	P7
Neurocan	P14	P21
Phosphacan	P21	P14
Versican	P7	P21
Support molecules		
Hyaluronan	P14	P14
Link protein (LN1)	P14	P21
Tenascin-R	n/a	P14

Table 1.2. Expression of PNN components in cerebellum and spinal cord at different developmental periods.

Until recently, little data was available on the composition of PNNs and the phenotype of PNN-expressing neurons in the human CNS. One recent study has partly addressed this issue, and has provided a thorough histological examination of PNNs in the human spinal cord. Similarly to rodents, PNNs in the human spinal cord are heterogeneously distributed throughout the grey matter and contain a high proportion of CSPGs, in addition to hyaluronan, LN1 and tenascin-R (Jager et al., 2013).

1.1.3 Function of PNNs

Formation of PNNs has been shown to correspond to the postnatal time points at which developmental neuroplasticity is reduced throughout the nervous system. Consequently, this led to the hypothesis that the PNN may be involved in the restriction of neuroplasticity in the adult CNS. The first direct evidence to support this hypothesis came following the enzymatic degradation of the PNN using the bacterial enzyme ChABC, which cleaves the GAG side chains from the CSPG core protein. During postnatal development, but not in the adult CNS, monocular deprivation (that is, depriving one eye of visual input) results in a shift in the response of cortical neurons (situated in the visual cortex), such that the response to

inputs from the deprived eye are reduced and responses to inputs from the undeprived eye are increased - known as an ocular dominance shift. Administering ChABC to the visual cortex of adult rats led to an ocular-dominance shift following monocular deprivation, similar to the effect normally only observed in postnatal rats (Pizzorusso et al., 2002). Moreover, *in vitro* studies using ChABC to degrade PNNs resulted in an increase in the density of synaptic boutons contacting embryonic hippocampal neurons (Pyka et al., 2011).

Further evidence supporting the role of the PNN in the limitation of the neuroplasticity came from a combination of research using mice lacking one or more of the PNN components. Typically, these mice possess abnormalities in axonal rewiring or synaptic plasticity. For example, mice lacking LN1 have persistent ocular-dominance plasticity and elevated axonal sprouting following injury to the spinal cord (Carulli et al., 2010). Interestingly, although LN1-deficient mice have abnormal PNNs, the levels of inhibitory CSPGs in the brains of these mice is similar to wild-type mice, suggesting, it is the PNN, not the overall amount of inhibitory molecules in the brain that is critical for neuroplasticity (Carulli et al., 2010; Oohashi et al., 2015). BRAL2-deficient mice also possess PNNs with an abnormal structure, and have a reduction in the density of synapses in the deep cerebellar nuclei (Bekku et al., 2012). Interestingly, mice lacking the glycoprotein tenascin-R have normal synaptic structures of net-bearing neurons in the brain (Bruckner et al., 2000). However, additional studies have revealed a reduction in synaptic plasticity in the hippocampus (Bukalo et al., 2001).

Increasingly, a number of research groups are studying the effects of PNN degradation on neuroplasticity in the CNS. Using ChABC, mounting evidence suggests ChABC-mediated PNN breakdown can promote plasticity and behavioural recovery in rodent models of spinal cord injury (Bradbury et al., 2002; Barritt et al., 2006; Alilain et al., 2011). Moreover, ChABC-mediated PNN degradation in the spinal cord following stroke led to enhanced plasticity and locomotor recovery (Soleman et al., 2012). In the brain, PNNs have been associated with memory, as ChABC treatment enhanced memory and plasticity in mice (Romberg et al., 2013), in addition to increased plasticity and improvements in object recognition memory in two mouse models of tauopathy (Yang et al., 2015b). PNNs have also been shown to be involved in the maintenance of fear memories in the adult brain (Gogolla et al., 2009).

In addition to a critical role in the restriction of neuroplasticity in the adult CNS, recent findings have also indicated the PNNs may be involved in some sort of neuroprotection in pathological states. CSPGs have been shown to induce neuroprotection against the glutamate-mediated excitotoxicity of cultured neurons and in a separate study, PNN-expressing neurons were associated with reduced degeneration following oxidative stress, compared to neurons lacking PNNs (Cabungcal et al., 2013). The mechanism responsible for this is currently unknown and requires further research. Moreover, PNNs have been shown to prevent the lateral diffusion of AMPA receptors *in vitro* (Frischknecht et al., 2009).

1.1.4 Formation of PNNs

While it is now generally well-accepted that the formation of PNNs coincides with the timepoint at which most of the developmental neuroplasticity is concluding, there is little data available regarding the molecular events that underlie the formation of these structures *in vivo.* One thing that is known, however, is that neuronal activity correlates with the formation of PNNs, as chronic depolarisation has been shown to enhance PNN formation in a number of *in vitro* studies (Brückner and Grosche, 2001; Giamanco and Matthews, 2012). Moreover, a reduction in the formation of PNNs in animals raised with visual deprivation also suggests that neuronal activity *in vivo* can regulate the formation of PNNs (Brückner and Grosche, 2001; McRae et al., 2007). Linking in with this, the morphology of PNNs (meaning, the intensity of WFA labelling) in the deep cerebellar nuclei is dependent on presynaptic inputs to these neurons from Purkinje cells (Foscarin et al., 2011), such that reduced inputs from Purkinje cells results in less neurons with a PNN and a reduction in the thickness of PNNs (Carulli et al., 2013). Furthermore, it has been postulated that LN1 upregulation is important for the development of PNNs, as LN1 upregulation correlates with the timepoint of PNN formation, and animals lacking this molecule have deficits in PNN formation *in vivo* (Carulli et al., 2010). Other factors that can modulate the PNN include environmental stimuli, such as housing animals in an enriched environment. Interestingly, housing animals in an enriched environment results in a decrease in the proportion of neurons with a PNN in the deep cerebellar nuclei and reduces the intensity of WFA labelling of these PNNs, compared with controls (Foscarin et al., 2011).

As previously mentioned, upregulation of PNNs is associated with the closure of the critical period for neuroplasticity in the developing visual cortex (Pizzorusso et al., 2002). Interestingly, this phenomenon also coincides with the downregualtion of polysialic acid (PSA), a post-translational modification found preferentially attached to the neural cell adhesion molecule (NCAM) in the developing CNS (Di Cristo et al., 2007a). Moreover, closure of the critical period can be delayed by the continued expression of PSA in the visual cortex (Di Cristo et al., 2007a). This suggests that PSA expression is also a key regulator of neuroplasticity, and may exert this effect by modulating the formation of PNNs *in vivo.*

Preliminary research from our laboratory suggests a spatiotemporal relationship between PSA and PNNs in the postnatal rat spinal cord. During the first two weeks of postnatal development, PSA is abundantly distributed throughout the spinal cord and is found in both the grey and white matter. During this time, PNNs are not observed in the spinal cord. Towards the end of the second week of postnatal development, PSA expression is reduced and WFA-labelled PNNs can be detected in the spinal cord, the numbers of which continue to increase during the third and fourth postnatal weeks. By the end of the third week, PSA expression is solely confined to the anterior corticospinal tract, lamina X and the superficial dorsal horn (Figure 1.2).

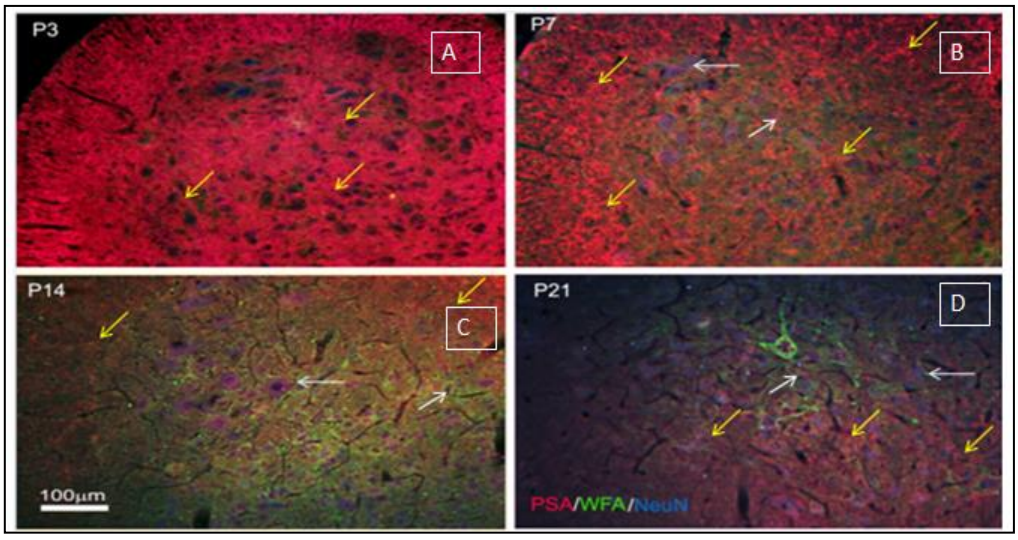

Figure 1.2. Inverse relationship between PSA and the expression of WFA-labelled PNNs in the postnatal rat spinal cord.
(A-B) During the first week of postnatal development, PSA expression is high throughout all regions of the spinal cord (yellow arrows). **(C)** Towards the end of the second postnatal week, PSA expression is reduced throughout the grey matter and weakly WFA-labelled PNNs

can be observed surrounding occasional neurons in the grey matter (white arrows). **(D)** By the end of the third postnatal week, PSA is only maintained in regions that continue to express PSA in the adult spinal cord, and the number of WFA-labelled PNNs is increased. Images courtesy of Dr Xuenong Bo.

As mounting evidence supports the critical role of PNNs in the limitation of plasticity in the adult nervous system, and that degrading this structure can induce significant recovery of function in preclinical models of SCI and stroke, in addition to mice with memory deficits, it is clear that PNNs require much further research. With little known about the molecular events that underlie PNN formation *in vivo,* this also requires further study. The inverse relationship between PSA expression and formation of PNNs in the spinal cord, in addition to the antagonistic effects of these molecules with respect to the closure of the critical period, suggests that PSA expression may be able to regulate the formation of PNNs *in vivo.* This will be examined in more detail in this thesis.

1.2 Polysialic acid

1.2.1. Neural cell adhesion molecule and polysialic acid - structure and biochemistry

As briefly mentioned, PSA is predominantly found attached to NCAM during the development of the nervous system. NCAMs are membrane-associated proteins and members of the immunoglobulin superfamily of adhesion molecules. Ubiquitously expressed throughout both the developing and adult CNS, NCAMs are found as three main isoforms: 180, 140 and 120 kDa (Bonfanti, 2006). The two larger isoforms are large, transmembrane proteins that consist of a cytoplasmic C-terminal domain and an extracellular N-terminal domain, that consists of five immunoglobulin-like domains and two fibronectin III domains (Figure 1.3A, Bonfanti, 2006). The smaller, 120 kDa isoform of NCAM does not possess a cytoplasmic domain but instead is attached to the extracellular membrane via a glycosylphosphatidylinositol anchor (Bonfanti, 2006).

A homophilic interaction between the 1st and 2nd Ig-like domains of the extracellular domains of NCAMs on opposing cell membranes leads to the formation of homodimers, which facilitates cell adhesion and neuronal differentiation. Conversely, this reduces cell

proliferation (Bonfanti, 2006). The formation of NCAM heterodimers is also common and has thus far been observed with the fibroblast growth factor receptor (FGFR) and the neurotrophin receptor TrkB. In addition, NCAM forms heterodimers with extracellular matrix molecules such as heparin sulphate proteoglycans (HSPGs) and CSPGs, such as neurocan and phosphacan (Kallapur and Akeson, 1992; Grumet et al., 1993; Friedlander et al., 1994; Kiselyov et al., 2003). Interactions between CSPGs and NCAM are thought to occur between the sulphated glycosaminoglycan side chains, as enzymatic digestion of these glycans using ChABC reduces the formation of NCAM-neurocan heterodimers (Friedlander et al., 1994).

One of the most frequent post-translational modifications of NCAM involves the addition of long chains of PSA to the 5th immunoglobulin (Ig)-like domain, in a process known as polysialylation. PSA is a linear homopolymer of 2, 8-linked sialic acid and is added to NCAM in the Golgi apparatus by the action of two polysialyltransferase enzymes; polysialyltransferase (PST) and sialyltransferase X (STX), which can also be referred to as ST8SiaIV and ST8SiaII, respectively (Eckhardt et al., 1995; Nakayama and Fukuda, 1996). These enzymes bind to NCAM at the 1st fibronectin type III (FN-III) domain, and catalyse the addition of PSA to the 5th Ig-like domain (Figure 1.3A, Mendiratta et al., 2005; Maness and Schachner, 2007). The extent of NCAM polysialylation is directly regulated by expression of the polysialyltransferase enzymes (Oka et al., 1995), which have distinct expression patterns throughout the CNS. The expression of STX is high during development, but expression is down-regulated in the adult CNS; but the opposite is true of PST (Hildebrandt et al., 1998; Ong et al., 1998).

Brains harvested from NCAM knockout mice have almost a complete loss of PSA expression, suggesting that the majority of PSA found in the CNS is bound to NCAM. Nonetheless, subsequent studies have revealed a number of other molecules that can be polysialylated, such as neuropilin-2, α subunit of the rat brain voltage-sensitive sodium channel, synaptic adhesion molecule and the polysialyltransferase enzymes themselves (Zuber et al., 1992; Mühlenhoff et al., 1996; Close and Colley, 1998; Curreli et al., 2007; Galuska et al., 2010). While much less is known about the effect of polysialylation on the function of these proteins, it is generally agreed that polysialylation of the sialyltransferase enzymes can regulate their ability to catalyse the addition of PSA onto NCAM (Close et al., 2000).

PSA has unusual biochemical properties; it occupies a large spatial area and has a large hydrated volume (Rutishauser, 1998; Johnson et al., 2005). When bound to NCAM it can increase its relative molecular mass by up to 30% and leads to a reduction in the homophilic interactions between NCAMs on opposing cellular membranes (Figure 1.3B-C). Consequently, this leads to a reduction in the adhesive force between cells and can increase the spacing between adjacent cells up to 15 nm (Yang et al., 1992). In addition to its effect on NCAM homophilic interactions, PSA has been shown to alter heterophilic interactions between NCAM and its binding partners (Storms and Rutishauser, 1998; Hane et al., 2015). One example of this is the association between NCAM and HSPGs (Storms and Rutishauser, 1998). Additionally, PSA binding to NCAM has been shown to enhance BDNF signalling via its TrkB receptors, and has been shown to impair the processing of proBDNF by plasmin when high concentrations of proBDNF are present (Hane et al., 2015).

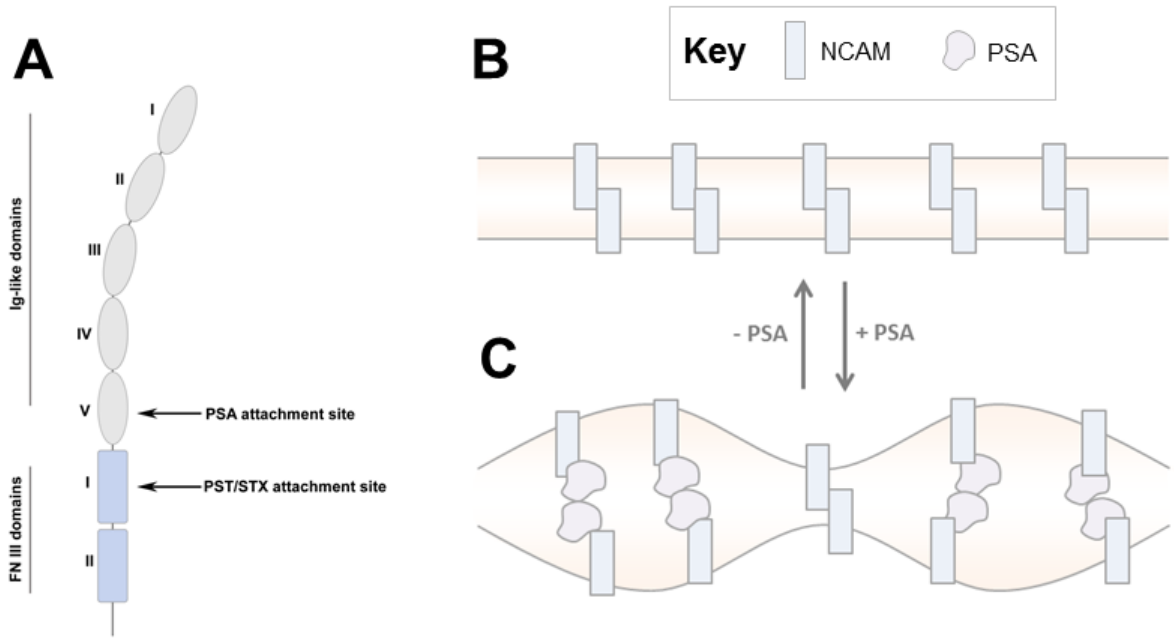

Figure 1.3. Structure and mechanism of PSA-NCAM.
(A) A member of the immunoglobulin superfamily of adhesion molecules, NCAM is formed of 5 immunoglobulin (Ig)-like domains and 2 fibronectin type-III (FN-III) domains. The polysialyltransferase enzymes bind to NCAM at the 1st FN-III domain, which catalyses the addition of PSA onto NCAM at the 5th Ig-like domain. **(B)** NCAMs on opposing cellular membranes can form homophilic interactions, leading to strong cell-cell adhesion. **(C)** In the presence of PSA the adhesive force of NCAMs on opposing membranes is reduced, leading to an increase in the size of the extracellular space. Adapted from Rutishauser (2008).

1.2.2. Expression of polysialic acid in the nervous system

1.2.2.1. Development

Generally absent during early developmental stages, PSA expression increases during mid-late embryonic development and is maintained during early post-natal development (Chuong and Edelman, 1984; Aaron and Chesselet, 1989; Nait Oumesmar et al., 1995b; Di Cristo et al., 2007a). Studies using mice deficient for one or more of the isoforms of NCAM have revealed the importance of PSA expression during development of the CNS. Mice deficient in NCAM have virtually no PSA in their brains and present with a minor reduction in body weight. Examining brain morphology revealed abnormalities in a number of brain

structures, such as a reduced size of the olfactory bulb and hippocampus (Tomasiewicz et al., 1993; Cremer et al., 1994b), in addition to behavioural deficits such as depression (Cremer et al., 1994a) and a reduction in spatial learning in NCAM-deficient mice (Cremer et al., 1994b). The relative reduction in size of the olfactory bulb in NCAM-deficient mice was revealed to be due to a deficit in migration of precursors from the subventricular zone to the olfactory bulbs (Hu et al., 1996).

Mice deficient in both polysialyltransferase enzymes lack expression of PSA in the brain, but expression of unpolysialylated NCAM is unchanged (Weinhold et al., 2005). PSA deficient mice present with a reduced body mass, precocious death and severe motor deficits, compared with wild-type mice. Examining brain morphology revealed abnormalities in a number of brain structures in PSA deficient mice, including a reduced olfactory bulb size, the accumulation of cells in the proximal rostral migratory stream, a smaller cross-sectional area of the corticospinal tract (at the level of the pyramids) and abnormal development of the mossy fibre tract of the hippocampus. Additionally, more than 80% of the PST/STX knockouts suffered from progressive hydrocephalus, due to enlargement of the lateral and third ventricles (Weinhold et al., 2005). The similarities in the phenotypes of NCAM or PSA knockout mice indicates that the deficits in brain structure and behaviour are most likely due to the lack of PSA, resulting in poor regulation of the adhesive properties of NCAM (Giza and Biederer, 2010).

Further evidence revealing the roles of PSA during development came from studies using the enzyme endoneuraminidase N (endo-N), to selectively remove PSA from the surface of NCAMs. In the developing corticospinal tract, PSA immunoreactivity is generally confined to regions associated with the formation of collateral axons, for example the entry of corticospinal axons into the spinal grey matter (Daston, Bastmeyer et al. 1996). Removing PSA from the developing corticospinal tract did not result in aberrant projections away from the typical path of the corticospinal tract but did, however, result in a reduced number of collateral branches into the spinal grey matter (Daston et al., 1996). In the visual cortex PSA is strongly expressed up to the end of the second postnatal week, following which expression steadily declines until it is virtually absent by postnatal day 28. Selectively removing PSA during the third postnatal week using endo-N resulted in early maturation of

inhibitory synapses in the visual cortex, in addition to the early onset of ocular dominance plasticity (Di Cristo et al., 2007a).

Taken together, these studies using NCAM, or PSA-deficient mice, or using endo-N to remove PSA *in vivo,* revealed the important role of PSA in neurodevelopment.

1.2.2.2. Adult

Although expression of PSA in the CNS is generally reduced during late stages of postnatal development, expression is maintained in areas typically associated with ongoing neuroplasticity and neurogenesis. In the adult brain there are two primary regions with sustained neurogenesis: the subgranular zone of the hippocampus and subventricular zone (SVZ) of the lateral ventricles.

Early research noted a population of PSA-expressing cells located in the granule cell layers of the dentate gyrus. Subsequent studies revealed these cells to be newly generated neurons, produced in the subgranular layer (Seki and Arai, 1991, 1993). Removing PSA from this region using endo-N resulted in the differentiation of these neural progenitor cells into neurons in the subgranular zone (Burgess et al., 2008). The SVZ is the most heavily studied area of neurogenesis in the adult brain. Newly generated neuronal precursors in the SVZ migrate to the olfactory bulbs of rodents, where they differentiate into inhibitory interneurons that form the granule cell layers of the olfactory bulb (Bonfanti et al., 1997). PSA expression is found on the neuronal precursors in the SVZ and persists as the cells migrate to the olfactory bulb. Upon reaching the olfactory bulb, PSA expression is reduced and these cells differentiate into inhibitory interneurons that form the granular cell layers (Bonfanti et al., 1997; Rockle et al., 2008). Removing PSA from this pathway using endo-N revealed the crucial role of PSA in the organisation and migration of cells from the SVZ to the olfactory bulb. These mice had smaller olfactory bulbs than controls and a disorganised rostral migratory stream (Battista and Rutishauser, 2010). Additionally, newly generated inhibitory interneurons were found in aberrant locations, such as the cortex and striatum, indicating a reduction in migration of progenitor cells out of the rostral migratory stream (Battista and Rutishauser, 2010).

While largely confined to the two main areas of ongoing neurogenesis, PSA expression can also be observed in a number of regions in the temporal lobe, such as the entorhinal and piriform cortices and other regions of the hippocampus such as CA1 and CA3 (Nacher et al., 2002). However, the function of continued PSA expression in these structures is poorly understood. Structures in the hypothalamus can also continue to express PSA, such as the suprachiasmatic nucleus (Glass et al., 1994), where PSA is believed to have a role in the regulation of circadian rhythms; and in the axons of neurosecretory cells and pituicytes that make up the hypothalamo-neurohypophysial system (Theodosis et al., 1994). In the spinal cord, PSA immunoreactivity is observed in the superficial layers of the dorsal horns and also surrounding the central canal. Interestingly, cells surrounding the central canal can share some characteristics with those in the SVZ (Hamilton et al., 2009), but there is no neurogenesis under normal physiological conditions. Nonetheless, *in vitro*, these cells are capable of producing neurospheres which can differentiate into neurons and glial cells (Dromard et al., 2008), suggesting that these cells may harbour a latent neurogenic ability. These findings further established the role of PSA in neurogenesis in the adult CNS.

1.2.2.3. Involvement in injury and disease

An increasing number of studies have noted an increase in levels of polysialylation following traumatic injury to the brain or spinal cord. PSA is transiently upregulated on both the ipsi- and contralateral sides of the spinal cord 4 days following dorsal rhizotomy lesion, in neurons, and levels are also elevated in astrocytes on the ipsilateral side of the spinal cord, 12 days post-injury (Bonfanti et al., 1996). Lesioning the entorhinal cortex resulted in a continuous elevation in PSA-NCAM levels in the denervated region of the dentate gyrus, starting 2 days post-lesion and the expression is maintained for over 60 days (Miller et al., 1994). The spatiotemporal relationship between PSA expression and axonal sprouting in the denervated dentate gyrus led to the hypothesis that re-expression of PSA following CNS injury may act as a pro-regenerative response, which may facilitate axonal sprouting and synaptogenesis. Subsequent studies have also noticed a relationship between PSA expression following CNS injury and attempts at axonal sprouting. PSA is upregulated in a number of cells in the perilesional area 7 days following controlled cortical impact injury (Harris et al., 2010; Budinich et al., 2012). These cells have a glial-like morphology and are

associated with sprouting axons positive for growth associated protein-43 (GAP-34) (Harris et al., 2010).

While much of this research has focused on PSA expression following traumatic injury to the CNS, one study has also noted alterations in PSA in a model of chemically-induced spinal cord injury. Lysolecithin-induced demyelination of the mouse spinal cord results in transient expression of PSA in Schwann cells, astrocytes and oligodendrocyte precursors, in and around the lesion site (Nait Oumesmar et al., 1995a). The novel finding of PSA upregulation in areas of demyelination has also been verified in human tissue samples using post-mortem brain samples from patients with multiple sclerosis (Charles et al., 2002).

With significant evidence supporting the role of PSA in plasticity in both the developing and adult CNS, and the evidence supporting a spatiotemporal correlation between PSA expression and axonal sprouting after injury, this led to a number of studies investigating whether induced PSA expression could lead to enhanced sprouting or regeneration, in addition to functional improvement in rodent models of CNS injury. Predominantly, these studies have relied on rodent models of spinal cord injury (SCI). The ability of induced PSA expression to mediate locomotor recovery in a rodent model of SCI will also be examined in this thesis, therefore, the pathophysiology of SCI, in addition to current research strategies to target neuroplasticity and axonal regeneration, including PSA, will be discussed in detail below.

1.3 Spinal cord injury – facts, figures and clinical manifestation

SCI is a devastating condition that affects an estimated 40,000 people in the United Kingdom, with a new occurrence every 8 hours (BackUp, 2016). Males are twice as likely to develop SCI and injuries are more prevalent in younger people, specifically, between the ages of 15 and 38 (SpinalResearch, 2016). Injuries are commonly caused by falls or road traffic accident (SpinalResearch, 2016), the impact of which can break one or more of the vertebrae thereby contusing or compressing the spinal cord. Additional causes of SCI, albeit those far less common, include stab injuries which directly penetrate the spinal cord, sports injuries and tumours (SpinalResearch, 2016). The annual cost of SCI in the UK is estimated at £1 billion, making this a large public health concern (SpinalResearch, 2016).

SCI patients may display a wide neurological deficit including loss of sensory, motor and autonomic functions. The extent of these deficits is dependent on both the location and size of the spinal cord lesion. For example, injuries occurring at the thoracic level will result in paralysis of the lower limbs (paraplegia) and loss of autonomic functions (bowel, bladder and sexual). In contrast, injuries occurring at the cervical level will result in paralysis of both upper and lower limbs (quadriplegia) and loss of autonomic functions. Injuries in the cervical region may also be associated with loss of respiratory function. Additional complications of SCI include autonomic dysreflexia, neuropathic pain, spasticity, frequent urinary tract infections (due to loss of bladder voiding reflexes) and depression. While these consequences of injury result in a drastic change to a patient's quality of life, a fraction of patients may have some preserved function due to the presence of spared spinal cord tissue that was not damaged by the injury.

1.4 Spinal cord injury pathophysiology

SCI pathophysiology is broadly subdivided into two stages, primary and secondary injury. The primary injury refers to the initial damage to the spinal cord and is frequently caused by the dislodgement of one or more of the vertebrae, which then contuses or compresses the spinal cord. This injury results in a focal area of cell death and haemorrhage, and initiates a cascade of secondary injury mechanisms, which results in the propagation of the injury and ultimately, a worsening of neurological outcome. There are a number of processes involved in the secondary injury phase, including inflammation, vascular disturbances and oxidative stress, which will be discussed in more detail in subsequent sections.

1.4.1 Vascular disturbances and the inflammatory response

The inflammatory response to SCI commences minutes after injury, persists for months, and involves a number of immune cells, both intrinsic to the spinal cord and originating in the periphery (Bowes and Yip, 2014). Of those found in the spinal cord, the first cellular responders are microglia, the resident immune cells of the CNS (David and Kroner, 2011). Typically, microglia exist in a quiescent state in the uninjured spinal cord, but are rapidly activated minutes after the initial spinal cord trauma (Davalos et al., 2005). Migrating to the injury epicentre, activated microglia act to seal off the injury site and clear away cellular

debris in an attempt to prevent the spread of damage to other parts of the spinal cord (Hines et al., 2009; Greenhalgh and David, 2014; Stirling et al., 2014). Activated microglial cells are still observed in the spinal cord weeks after the initial injury and are believed to be involved in the regulation of infiltration of peripheral immune cells into the spinal cord, in addition to the secretion of proinflammatory cytokines (Kigerl et al., 2009).

Secondary cellular responders to SCI include astrocytes, which rapidly proliferate, hypertrophy and increase production of intermediate filament proteins such as vimentin and glial fibrillary acidic protein (GFAP), in a process known as gliosis (Silver and Miller, 2004; Sofroniew and Vinters, 2010). Astrocytes also migrate to the lesion site, where they secrete CSPGs, molecules which aggregate with reactive astrocytes, to form a glial scar (Silver and Miller, 2004; Yuan and He, 2013). Early research suggested that the glial scar acts as a barrier to axonal growth and may be responsible for the poor recovery observed following SCI (Fawcett and Asher, 1999; Cregg et al., 2014). However, subsequent studies have suggested the glial scar may also have a beneficial role post-SCI by sealing off the lesion site, to prevent the spread of injury and enhance tissue preservation (Rolls et al., 2009). This was investigated in more detail in a novel study that investigated the development of gliosis and the extent of neurological improvement in a rodent model of SCI, using mice with ablated gliosis (due to the selective deletion of reactive astrocytes). Interestingly, these mice had a significantly worse neurological outcome post-injury, compared to control mice (Faulkner et al., 2004). Furthermore, histological examination revealed a significant reduction in the number of neurons and an increase in degenerating white matter, leucocyte infiltration and lesion size in these mice, compared with controls (Faulkner et al., 2004). Further details regarding the development of the glial scar and its contribution to poor neurological recovery following SCI will be discussed in section 1.4.4.

Under normal circumstances, the blood-spinal cord barrier (BSCB) consists of tightly compacted endothelial cells, ensheathed by perivascular cells (known as pericytes) and a basal lamina, which is contacted by the processes of astrocytes (Bartanusz et al., 2011). Collectively, these cellular populations compose the BSCB, which regulates the influx of molecules and cells from the blood into the spinal cord parenchyma (Echeverry et al., 2011). Within the first 24 hours post-SCI, there is a drastic upregulation of a number of matrix

metalloproteinases (MMPs), a family of zinc-dependent endopeptidases, which have a crucial role in extracellular matrix remodelling (reviewed by (Zhang et al., 2011). Following injury, the upregulation of MMPs such as MMP-3, -9 and -12 has been shown to promote the breakdown of the BSCB, via degradation of the endothelial tight junctions and basal lamina (Noble et al., 2002; Wells et al., 2003; Lee et al., 2014). This leads to an increase in the permeability of the BSCB, resulting in the influx of circulating inflammatory cells, such as macrophages/monocytes, neutrophils and leucocytes into the spinal cord (Trivedi et al., 2006).

Neutrophils, generally absent in the spinal cord, can cross the disrupted BSCB and enter the spinal cord parenchyma within a few hours after injury. Correlating with the extent of SCI damage, the number of neutrophils in the injured spinal cord peaks after 24 hours, but neutrophils are still observed in the cord three months post-injury (Beck et al., 2010). While initially acting to clear the injury site of cellular debris, neutrophils also secrete pro-inflammatory cytokines, which results in the recruitment of additional inflammatory cells, such as circulating monocytes, to the injury site. For a long while, this was believed to strongly contribute to secondary tissue damage and worsening neurological outcomes following SCI (Neirinckx et al., 2014). Interestingly, however, subsequent data has disputed this, and has suggested that the infiltration of neutrophils into the injured spinal cord may actually promote neurological recovery. For example, depleting the number of circulating neutrophils (and consequently reducing the number entering the injured spinal cord) was found to increase the amount of oxidised proteins observed in the injured spinal cord (de Castro et al., 2004). Moreover, in a separate study, this was shown to worsen locomotor function following SCI (Stirling et al., 2009). However, even considering these findings, neutrophils are generally still viewed to be a hindrance to spinal cord repair as the evidence supporting their role in the exacerbation of secondary tissue damage outweighs that supporting a beneficial role for neutrophils in the conservation of neurological function.

As previously mentioned, degradation of the BSCB also allows circulating monocytes/macrophages to enter the injured spinal cord (Glomsda et al., 2003). Migrating to the lesion epicentre, macrophages act in a similar capacity to microglial cells, where they act to phagocytose cellular debris in an attempt to prime the spinal cord for attempts at regeneration (David and Kroner, 2011; Greenhalgh and David, 2014). Additionally, however,

macrophages can contribute to axonal dieback, post-injury (Horn et al., 2008; Zhou et al., 2014b). The diverse functions of these cells led to the suggestion that there may be multiple phenotypes of macrophages that underlie each of these different roles. This has subsequently been demonstrated in a number of studies, which have noted two distinct subtypes of macrophages post-SCI; the classically activated M1 or the alternatively activated M2 phenotypes (Kigerl et al., 2009). M1 macrophages are considered pro-inflammatory and neurotoxic, while the M2 subset acts to promote tissue remodelling and axonal growth (David and Kroner, 2011). Activated microglia may therefore exacerbate secondary injury or promote repair of the spinal cord, based on which phenotype is predominantly expressed. A number of studies have revealed the predominance of M1 macrophages in the injured spinal cord for months after injury, which is believed to, in part, underlie the poor recovery of function following SCI (Kigerl et al., 2009; Chen et al., 2015). Attempts at driving macrophage polarisation towards the M2 phenotype in rodent models of SCI has resulted in improved tissue sparing and a significant neurological improvement (Gensel and Zhang, 2015; Zhang et al., 2015).

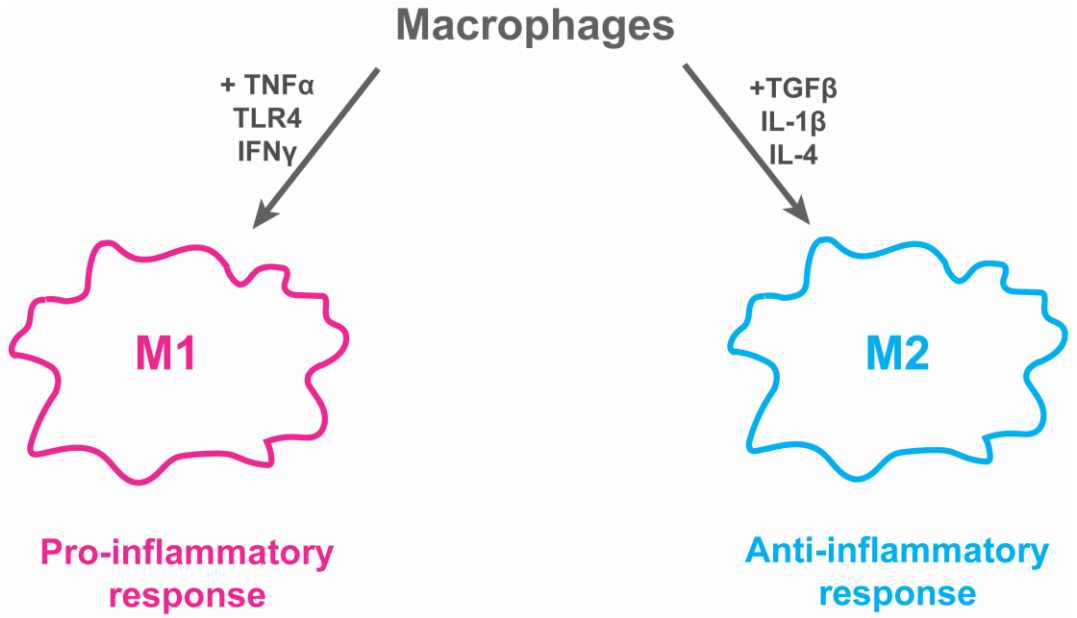

Figure 1.4. Macrophage polarisation.
Macrophages have diverse functions after injury to the spinal cord. Characterising macrophage polarisation has led to the identification of two distinct subtypes known as M1 and M2. These subtypes have a role in the pro-inflammatory and anti-inflammatory responses to SCI, respectively. Adapted from David and Kroner, 2011.

Responses of the adaptive immune system to SCI include infiltration of both B- and T-cells to the spinal cord, following breakdown of the BSCB (Jones et al., 2005; Bowes and Yip, 2014). Both B- and T-cell infiltration peaks approximately one week post-injury, however, B-cells display a biphasic response after SCI as a secondary peak is observed after four weeks (Bowes and Yip, 2014). After injury, both T- and B-cells are involved in a process known as SCI-induced autoimmunity, which involves these cells becoming 'autoreactive' and contributing to further secondary damage (Popovich et al., 1996; Ankeny et al., 2006). Improvement in locomotor function has been observed in mice devoid of mature T- and B-cells and is associated with enhanced axonal sprouting, remyelination and a reduced number of microglia/macrophages in the spinal cord (Wu et al., 2012). Despite some evidence suggesting a negative role of T-cells following injury to the nervous system, other studies have suggested that CD4+ T-cells can induce neuroprotection of facial motor neurons after transection of the facial nerve in mice (Serpe et al., 2003; Deboy et al., 2006).

1.4.2 Excitotoxicity and oxidative stress

Damage to the spinal cord vasculature can result in ischaemia in the injured cord. This, coupled with membrane depolarization can result in glutamate release, which can reach toxic levels within minutes of SCI (McAdoo et al., 1999). Activation of glutamate receptors on the cell surface, namely N-methyl-D-aspartate (NMDA) receptors can result in elevated cytoplasmic calcium concentrations, due to an influx of calcium from the extracellular space into the cell, in addition to calcium release from intracellular stores (Hausmann, 2003). This elevation in cytoplasmic calcium can activate a number of pathways that ultimately result in the apoptotic death of the cell (Hausmann, 2003).

In addition to glutamate-mediated excitotoxicity, post-SCI ischaemia can also lead to a rapid increase in the production of reactive oxygen species (ROS). ROS production peaks approximately 12 hours following SCI but is elevated for weeks post-injury (Xu et al., 2005). Polyunsaturated fatty acids make up a high proportion of cellular membranes and are highly sensitive to lipid peroxidation by ROS, which leads to cell death (Hall and Braughler, 1986).

1.4.3 Cell death

The primary injury to the spinal cord results in an immediate zone of necrotic cell death, including both neurons and glial cells such as oligodendrocytes (Liu et al., 1997). Secondary injury cascades amplify this cell death, which can worsen neurological outcomes following injury. For example, secondary injury mechanisms have been speculated to be responsible for the apoptotic death of neurons, observed between 4 and 6 hours after injury in the rat spinal cord (Crowe et al., 1997). Moreover, neuronal death has been shown to continue for up to 1 month post-SCI, both at the initial injury site and further along the spinal cord (Huang et al., 2007). This amplified neuronal death leads to the expansion of the lesion site, and worsening neurological outcomes.

Death of oligodendrocytes has been observed within 15 minutes of SCI in the rat and can persist for up to 3 weeks (Crowe et al., 1997). Similarly to neurons, the initial impact of the mechanical insult to the spinal cord results in a focal area of oligodendrocyte death (Liu et al., 1997). Following this, oligodendrocyte cell death continues in the days post-injury and is thought to be mediated by the high sensitivity of these cells to a number of secondary injury mechanisms, including glutamate and ATP-mediated excitotoxicity, oxidative stress and the release of pro-inflammatory cytokines from activated microglia and neutrophils (Crowe et al., 1997; Almad et al., 2011). Apoptotic oligodendrocytes have been observed up to 3 weeks following SCI in the rodent spinal cord, located both rostral and caudal to the lesion epicentre and associated with axons undergoing Wallerian degeneration (Crowe et al., 1997; Warden et al., 2001). This acute and delayed death of oligodendrocytes results in large areas of demyelinated axons. However, the extent of these and their contribution to the poor neurological recovery observed after SCI is debated due to conflicting data on the extent of remyelination of these fibres (Totoiu and Keirstead, 2005; Lasiene et al., 2008; Hesp et al., 2015).

1.4.4 Inhibitory molecules and the glial scar

Even following severe SCI, patients can regain some functional neurological improvement (Fawcett et al., 2007). One contributing mechanism to this functional improvement is that some axons can retain the capacity to regrow, or ‘sprout’. However, the ability of these sprouting fibres to reform substantial functional connections is severely limited and this is

believed to be at least partly due to the dynamic changes that occur in the neuronal extracellular matrix following SCI. The primary injury to the spinal cord results in immediate death of oligodendrocytes at the lesion site, and as previously mentioned, secondary injury mechanisms such as oxidative stress, and glutamate excitotoxicity, contribute to a second, delayed death of oligodendrocytes, which typically occurs 1 week post-injury (Crowe et al., 1997; Warden et al., 2001). Degenerating oligodendrocytes release a number of molecules, collectively known as the myelin-derived inhibitors, which are capable of restricting the neurite outgrowth of cultured neurons (Schwab and Caroni, 2008). These molecules are myelin-associated glycoprotein (MAG), oligodendrocyte-myelin glycoprotein (OMgp), neurite outgrowth inhibitor (Nogo), ephrin B3 and semaphorin 4D (GrandPré et al., 2000; Hunt et al., 2002; Huebner and Strittmatter, 2009). Following release from degenerating oligodendrocytes, MAG, OMgp and Nogo can bind to a range of receptors on the neuronal surface, such as members of the tumour necrosis factor family and LINGO-1, while ephrinB3 and semaphorin 4D signal via the EphA4 and plexin B1 receptors, respectively (Fournier et al., 2001; Wang et al., 2002; Mi et al., 2004; Benson et al., 2005). One of the first receptors to be identified was the Nogo-66 receptor, which can bind to MAG, OMgp and Nogo (Fournier et al., 2001; Liu et al., 2002). Downstream effects of Nogo-66 receptor activation are suppression of the Akt signalling pathway and activation of the Rho/ROCK signalling pathway, which ultimately initiates growth cone collapse via dysregulation of the actin cytoskeleton (Yiu and He, 2006).

In addition to the release of the myelin-derived inhibitory molecules from degenerating oligodendrocytes, as previously mentioned, a secondary class of molecules, known as CSPGs are secreted by reactive astrocytes (Silver and Miller, 2004). In the uninjured CNS, CSPGs are ubiquitously distributed throughout the adult spinal cord, both in the neuropil and within specialised ECM structures known as PNNs (see chapter 1.1 for more details on the neuronal extracellular matrix). After SCI, reactive astrocytes coupled with secreted CSPGs and infiltrating macrophages and fibroblasts, condense around the lesion site to form a glial scar (Figure 1.5).

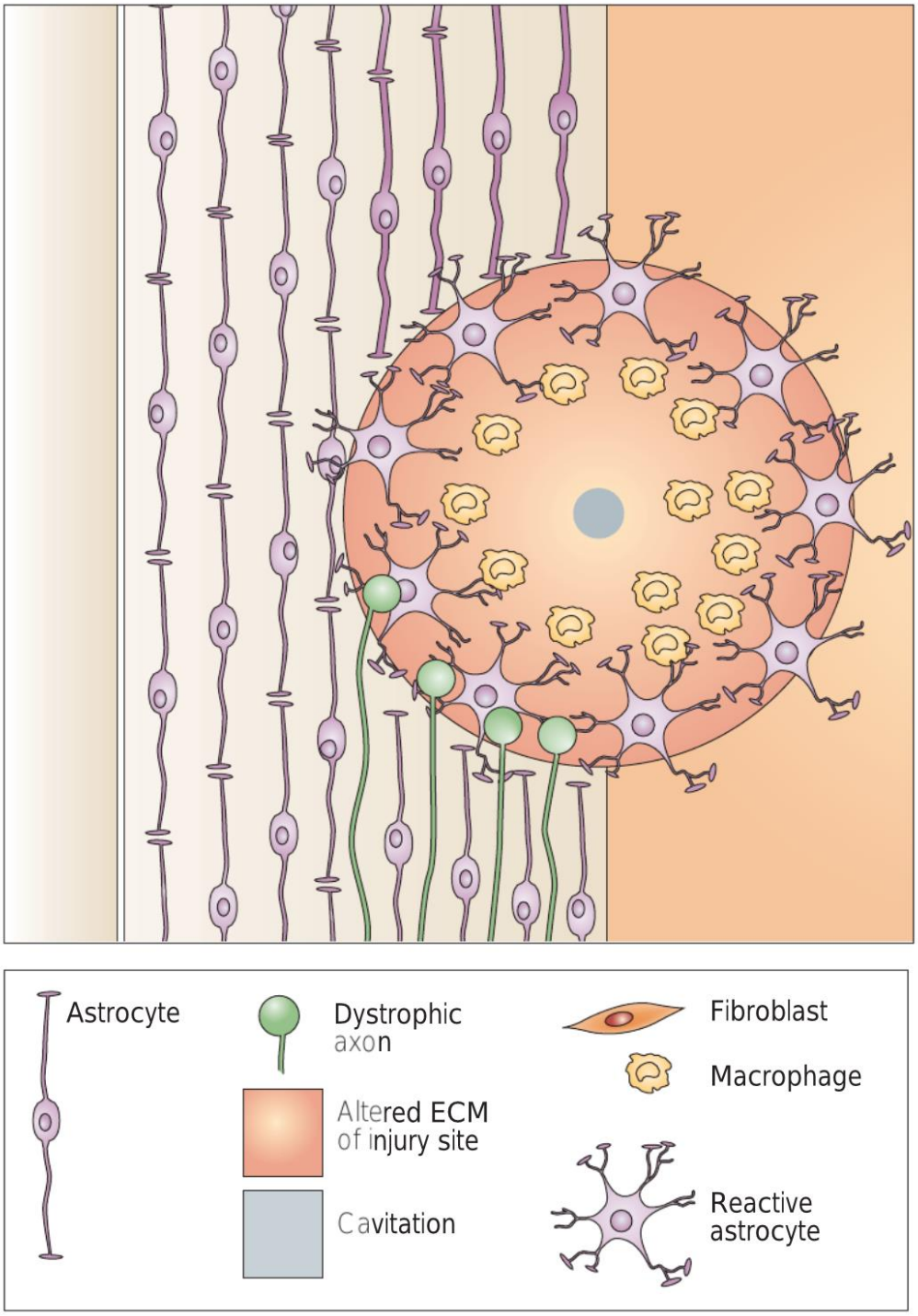

Figure 1.5. Classical glial scar structure.
Infiltrating macrophages, which act to clear the immediate lesion site from cellular debris are surrounded by reactive astrocytes, which secrete CSPGs. These cellular components and CSPGs form the glial scar, which acts as a barrier to axonal growth. Upon entering the environment of the scar, sprouting axons will lose their capacity for growth due to the formation of dystrophic growth cones (Silver and Miller, 2004).

Initially, the glial scar acts to limit the spread of secondary damage but its continued presence in the spinal cord has been shown to be a significant inhibitor of axonal sprouting

and/or regeneration. Upon reaching the glial scar, sprouting axons lose their capacity for growth as their growth cones become 'dystrophic', i.e. they take on a swollen appearance and contain a disorganised cytoskeleton (Li and Raisman, 1995; Tom et al., 2004). The high CSPG content of the glial scar has been proposed to be directly responsible for the formation of dystrophic growth cones and abortive axonal sprouting. In support of this hypothesis, a study revealed the poor neurite outgrowth of cultured dorsal root ganglion (DRG) neurons when plated on alternating strips of CSPGs and a growth-promoting substrate, such as laminin (Snow et al., 1990). Interestingly, neurites that extended onto the CSPG substrate were either repelled, or ceased to grow further and their growth cones became dystrophic (Snow et al., 1990). Building on these early experiments, subsequent studies modified this *in vitro* system to more accurately represent the concentration gradient of CSPGs within the glial scar, since typically, the concentration of CSPGs is at its highest at the inner-most regions (Tom et al., 2004). In this study, growth cones from cultured DRG neurons also formed swollen end bulbs following entry into the CSPG region, characteristic of the dystrophic growth cones which are observed *in vivo* (Tom et al., 2004).

For a long time, the mechanism underpinning the CSPG-induced formation of dystrophic growth cones was unknown. However, recent work has highlighted a number of different receptors that can bind to these molecules. One such receptor is protein tyrosine phosphatase sigma (PTPσ), which has been shown to interact with the CSPG GAG side chains (Shen et al., 2009). Additional receptors include members of the Nogo receptor family, NgR1, NgR3 and LAR (Dickendesher et al., 2012). Currently, the downstream effects of CSPG-receptor activation are poorly understood; however, activation of LAR is believed to activate the Rho/ROCK signalling pathway, which interestingly, is also activated by the binding of myelin-derived inhibitory molecules to their receptors (Fisher et al., 2011).

1.5 Strategies to promote spinal repair

For many years, the primary aim of therapies targeting repair of the injured spinal cord was to promote regeneration of damaged axons across the lesion site, with the hope of these axons forming functional connections beyond the lesion (Silver and Miller, 2004; Cregg et al., 2014). Whilst some regenerating axons are able to grow a few millimetres in the rodent

spinal cord following targeted pharmacological interventions, the translational ability of these drugs is under question, due to the difference in size between human and rodent spinal cords. In the human, regenerating fibres must grow centimetres to bridge the lesion site, then find appropriate target neurons and form functional synapses, compared to the 1 or 2 mm axonal growth required to bridge a spinal cord lesion in the rat.

Over the past decade it has become more apparent that the injured spinal cord is capable of spontaneous axonal sprouting and these sprouting fibres can connect with neurons spared by the initial injury to bypass the lesion site and form novel spinal circuits (Bareyre et al., 2004). Harnessing and amplifying this neuroplasticity to specific neuronal phenotypes could therefore lead to successful repair of the spinal cord in the absence of long-distance axonal regeneration. Because of this, a number of research laboratories are aiming to enhance this axonal sprouting by removing the inhibitory extracellular matrix molecules from the spinal cord and using rehabilitation to maintain these new synaptic connections. The next sections will discuss ways to promote regeneration and plasticity within the injured spinal cord.

1.5.1 Overcoming inhibition

1.5.1.1. Myelin-derived inhibitory molecules

As previously mentioned, a number of *in vitro* studies have highlighted the growth-restricting effects of the myelin-derived inhibitors and have suggested that removing or neutralising the inhibitory effect of these molecules may promote axonal growth, and thus, neurological recovery from SCI. However, attempts at confirming this data *in vivo* using knockout mice devoid of one or more of these molecules, and experimental models of SCI, has been met with mixed success. For example, inconsistent results have been observed in experiments using mice deficient in Nogo, with some studies noting poor regeneration following spinal lesions (Zheng et al., 2003; Lee et al., 2009) and others revealing a significant enhancement of regeneration in Nogo deficient mice (Kim et al., 2003). What is now clear is the differences between these studies may be due to differences in the underlying genetics of the mouse strains used to produce these knockouts (Dimou et al., 2006; Akbik et al., 2012). While studies using knockout mice yielded inconclusive data, interestingly, studies inhibiting downstream signalling of these molecules, or using function-

blocking antibodies to restrict their function, has resulted in promising results, showing an improvement in axonal regeneration and associated neurological function.

The discovery that Nogo, MAG and OMgp all bind to a common receptor, Nogo-66 receptor, led to the commencement of a series of studies utilising receptor antagonists in an attempt to block the action of these three molecules. Initial data noted enhanced regeneration of the corticospinal tract, sprouting of serotonergic fibres and associated locomotor recovery (GrandPré et al., 2002; Li and Strittmatter, 2003). However, an attempt at replicating this early study as part of the NIH "Facilities of Research-Spinal Cord Injury" project, yielded conflicting results (Steward et al., 2008). In a similar line of research, some groups have also investigated the effect of blocking LINGO-1, a co-receptor in the Nogo-receptor complex. These studies have noted enhanced regeneration of corticospinal and rubrospinal fibres, in addition to locomotor improvements, following intrathecal delivery of LINGO-1 antagonist in rodent models of SCI (Ji et al., 2006).

The convergence of the myelin-derived inhibitors on the Rho/ROCK signalling pathway led to the assumption that blocking this pathway would prevent the downstream effects of these molecules (i.e. prevent growth cone collapse). The enzyme C3 transferase, a potent inhibitor of the Rho signalling pathway, was initially shown to promote a significant recovery of locomotor function in a rodent model of injury, associated with enhanced regeneration of the corticospinal tract (Dergham et al., 2002). Subsequent studies have shown the efficacy of this enzyme in a number of different injury models and in both rats and mice, in addition to using an enzyme activity-deficient version of the protein (Boato et al., 2010).

Additional studies have targeted individual myelin-derived inhibitors by the use of, for example, function-blocking antibodies, and have shown promise in rodent models of SCI. Antibodies targeting Nogo-A were found to enhance axonal regeneration in the injured spinal cord, which was associated with an improvement in locomotor recovery (Liebscher et al., 2005). Subsequent studies have confirmed this data and have also shown a reduction in injury-related muscle spasms in rats following Nogo-A antibody treatment (Gonzenbach et al., 2010; Gonzenbach et al., 2012). The success of these rodent studies led to the development of experiments in non-human primate models of SCI, results of which mirrored those observed in rodents; enhanced regeneration of corticospinal neurons and

improvements in locomotor function were observed in the Nogo-A blocking antibody treated groups (Freund et al., 2006, 2009).

Although a partial recovery of function has been observed following neutralisation or blocking of the myelin-derived inhibitors, the lack of functional sprouting in mice lacking one or all three of these proteins after SCI indicates that these molecules may not be one of the main inhibitors of axonal regeneration after injury. Nonetheless, recently, the anti-Nogo antibody (ATI355) was tested for safety in patients with SCI. This was completed in 2011, but results of trials exploring the efficacy of this drug have not yet been published.

1.5.1.2. Glial-derived inhibitory molecules

Following results from early studies that noted the inhibitory effect of the glial scar on axonal growth and regeneration, a number of groups aimed to elucidate the main causes of this inhibition by examining the cellular molecular components of the glial scar in more detail. Initial observations suggested the CSPG molecules that form a large proportion of the glial scar are responsible for this limitation of axonal regeneration, and much research was performed to try to degrade CSPGs in the hope of promoting regeneration and spinal cord repair.

The finding that ChABC could remove the inhibitory GAG side chains from CSPGs *in vivo* and in culture, allowed the development of a pioneering study in 2002. In these experiments, ChABC was injected intrathecally following mid-cervical SCI, and was found to promote regeneration of lesioned corticospinal and sensory axons into the lesion site. This was also associated with a significant improvement in forelimb motor function (Bradbury et al., 2002). Subsequent studies have built on these initial experiments to investigate the use of ChABC in other models of SCI and using different delivery methods to the spinal cord. To date, ChABC-mediated axonal sprouting of both injured and uninjured spinal pathways has been observed, including the corticospinal (Barritt et al., 2006; Wang et al., 2011; Starkey et al., 2012), raphe-spinal (Barritt et al., 2006) and reticulospinal (Garcia-Alias et al., 2015) tracts. Further work has also investigated the efficacy of ChABC treatment on respiratory function following high-cervical SCI (Alilain et al., 2011) and on bladder function (Caggiano et al., 2005), and results have been promising. While earlier studies used a purified version

of the bacterial enzyme, this has been associated with some issues, including the lack of long-term stability of this enzyme *in vivo* (Lin et al., 2008; Bartus et al., 2014). In response to this, recent studies have commenced testing of viral vectors to drive expression of the ChABC gene *in vivo,* with results from these studies showing enhanced axonal regeneration, neuroplasticity and locomotor recovery following ChABC treatment (Zhao et al., 2011; James et al., 2015).

Interestingly, while previously thought to act to primarily promote regeneration and/or neuroplasticity, recent evidence also suggests ChABC treatment can modulate the phenotype of macrophages following SCI. Lentiviral vector-mediated ChABC treatment resulted in a significant increase in the density of M1-type macrophages 3 days post-injury, whereas, 2 weeks following injury, the density of M1 macrophages was reduced, but M2 macrophages were increased, compared to control groups (Bartus et al., 2014). More recent data also suggests that ChABC may increase the expression of anti-inflammatory cytokines, such as IL-10 (Didangelos et al., 2014).

With the success of ChABC in promoting regeneration and/or plasticity, in addition to a partial restoration of locomotor function in injured rodents, a number of studies have investigated the efficacy of ChABC combinatorial therapies, using, for example, another targeted therapeutic intervention. A popular combination is that of ChABC and administration of neurotrophins, or other growth factors. However, these studies have been met with mixed success. Combining ChABC and neurotrophin-3 (NT-3) administration following SCI resulted in improved locomotor function, enhanced serotonergic and corticospinal fibre sprouting, in addition to strengthening newly formed connections between corticospinal tract fibres and motor neurons (Hunanyan et al., 2013). Conversely, no long-term locomotor improvement was observed with ChABC administration in combination with a cocktail of growth factors and neurorehabilitation, although, there was noted to be enhanced sprouting of serotonergic and corticospinal fibres in this study (Alluin et al., 2014). Interestingly, a study utilising peripheral nerve grafts, to guide regenerating axons across the lesion site into distal regions of the spinal cord, in combination with brain-derived neurotrophic factor (BDNF) delivery and ChABC treatment showed no improvement in axonal regeneration or locomotor recovery (Tom et al., 2013). Other combinatorial therapies have included ChABC, Nogo-A function-blocking antibodies and

neurorehabilitation, which resulted in a synergistic improvement in locomotor function, with enhanced axonal regeneration and sprouting (Zhao et al., 2013), and ChABC and the adhesion molecule L1, which also showed improvements in locomotor function and anatomical plasticity (Lee et al., 2012). Following the success of ChABC treatment in promoting locomotor recovery in a number of rodent models of SCI, recently, a study involving ChABC in a canine model of severe chronic SCI has been approved (SpinalResearch, 2016).

The identification of a variety of CSPG receptors led a number of groups to try and promote axonal sprouting by blocking these receptors, or their downstream signalling mediators. Promising results were obtained from PTPσ knockout mice, which are capable of long-distance regeneration of the injured corticospinal tract (Fry et al., 2010). To date, two studies have aimed to modulate the PTPσ receptor, by either lentiviral-mediated delivery of RNA interference or creation of a PTPσ blocking peptide. Using a lentiviral vector to knockdown PTPσ *in vivo* resulted in improved hindlimb motor function post-SCI, compared with control-treated rats (Zhou et al., 2014a). Systemic administration of PTPσ blocking peptide led to improved motor function and bladder voiding and was associated with elevated sprouting of serotonergic fibres caudal to the lesion site, compared to control animals (Lang et al., 2015). Similarly, following the discovery of another CSPG receptor, LAR, studies aiming to block receptor activity using function-blocking peptides led to enhanced locomotor function following SCI, in addition to elevated regeneration of serotonergic fibres (Fisher et al., 2011). Comparable results were found in mice lacking LAR, in addition to enhanced regeneration of the corticospinal tract (Xu et al., 2015).

While most research targeting CSPGs and SCI uses the application of either function-blocking peptides or bacterial enzyme, to either block the activity of, or degrade CSPGs, respectively, some studies are investigating the endogenous molecules that are involved in the normal turnover of CSPGs *in vivo.* The ADAMTS family of proteases has been implicated in the degradation of CSPGs in the CNS, and expression of a number of these proteases has been found to increase following SCI in rodents (Tauchi et al., 2012a; Demircan et al., 2013). While research investigating these proteases is not as prolific as studies using ChABC, some groups have suggested ADAMTS-4 is capable of digesting CSPGs in the injured spinal cord, and administration of recombinant ADAMTS-4 has been shown to improve neurological

outcomes following injury, in addition to enhanced sprouting of serotonergic fibres (Tauchi et al., 2012b; Lemarchant et al., 2014).

Further strategies targeting CSPGs include attempts to neutralise the signalling of these molecules. As previously mentioned, activation of RhoA/ROCK signalling pathways occurs following receptor binding of the myelin-derived inhibitory molecules, and it was discovered that CSPGs also activate this pathway (Monnier et al., 2003). As strategies targeting this pathway were discussed in section 1.5.1.1, it will not be discussed in more detail here.

1.5.1.3 Intracellular inhibition

It is now generally well-established that most neuronal subtypes lose the capacity to fully regenerate in the injured adult CNS. While a large part of this is caused by extracellular factors, such as inhibitory extracellular matrix molecules and the down-regulation of several important growth-promoting molecules, mounting evidence suggests that a number of intracellular molecules may be at least partly responsible for the poor axonal regeneration of neurons observed in the adult CNS.

One of the best characterised intrinsic modulators of the regenerative function of neurons is the level of cyclic AMP (cAMP). Early studies noted that the growth-promoting effect on myelin of neurons isolated from early postnatal rat pups was due to high intracellular cAMP levels (Cai et al., 2001). Conversely, neurons from later postnatal time points showed a reduction in cAMP levels, and showed a drastic reduction in axonal outgrowth following contact with myelin. Increasing cAMP levels overcame this myelin-based inhibition of axonal outgrowth (Cai et al., 2001). Building from this initial study, it was noted that pre-conditioning peripheral nerve injury, previously shown to enhance regeneration of injured sensory axons *in vivo*, resulted in increased cAMP levels in DRG neurons, and direct administration of cAMP to DRG neurons prior to SCI mimicked the effect of a preconditioning lesion (Neumann et al., 2002; Qiu et al., 2002). Although an interesting observation, this is obviously clinically non-viable, so new studies were aimed at elucidating a pharmacological intervention that could be used post-SCI to raise intracellular cAMP levels. One of the first studies to do this used the phosphodiesterase 4 inhibitor, rolipram (Nikulina et al., 2004). Administered 2 weeks following SCI and embryonic spinal tissue

transplant, rolipram was found to improve axonal regeneration into the transplant, which was accompanied by an improvement in locomotor function and reduced levels of gliosis (Nikulina et al., 2004). Subsequent research has built on this initial experiment, to include other models of SCI (Kajana and Goshgarian, 2009; Costa et al., 2013) and different combinations of rolipram administration, including combinatorial therapies with cell transplantation (Dai et al., 2009; Bretzner et al., 2010), neurorehabilitation (Dai et al., 2009), and neurotrophin delivery (Lu et al., 2004).

A number of studies have characterised a relatively recently discovered intracellular inhibitor of axonal regeneration, namely PTEN. A negative regulator of mTOR, PTEN is highly expressed in adult corticospinal neurons, which undergo limited axonal regeneration following injury to the spinal cord (Liu et al., 2010). Conditional deletion of PTEN in corticospinal neurons was found to promote sprouting of the uninjured corticospinal tract, in addition to enhancing regeneration of injured corticospinal fibres through the lesion site in two distinct models of SCI (Liu et al., 2010). Since this was published, there have been a number of studies confirming the link between ablation or knockdown of PTEN and enhanced regeneration of corticospinal fibres in a number of different injury models, and also showing improved locomotor recovery in these animals (Zukor et al., 2013; Danilov and Steward, 2015; Du et al., 2015). Interestingly, strong regeneration of injured corticospinal neurons was observed following conditional ablation of PTEN one year following SCI (Du et al., 2015).

Following the promising results observed by deletion of PTEN alone, some groups have started investigating combinatorial therapies, to try to target multiple factors that have been shown to restrict recovery from SCI. As previously mentioned, Nogo is a myelin-derived inhibitory molecule found to exert a significant restriction on neuronal regeneration *in vivo.* Interestingly, double-mutant mice lacking all isoforms of Nogo and with conditional PTEN deletion, do not show an increase in compensatory sprouting following pyramidotomy, compared to animals lacking PTEN alone (Geoffroy et al., 2015). Conversely, regeneration of injured corticospinal fibres past the caudal border of the lesion following thoracic-level SCI was enhanced in double-mutant mice, compared to those lacking PTEN deletion alone, however, this was not associated with significant locomotor recovery (Geoffroy et al., 2015). Additionally, one notable study co-deleted PTEN and SOCS3,

another intrinsic regulator of regeneration, which promoted elevated sprouting of uninjured corticospinal neurons and partial restoration of locomotor recovery, compared to single deletion of SOCS3 (Jin et al., 2015).

Other strategies showing success in improving the intrinsic growth capacity of neurons, thereby allowing axonal growth in non-permissive environments, include targeting microtubule stabilisation using the cancer drug Taxol and overexpression of neuronal calcium sensor-1 (NCS-1) in the sensorimotor cortex (Yip et al., 2010; Hellal et al., 2011). In addition, targeting the repulsive guidance molecule – an inhibitor of axonal growth that is expressed in neurons, leucocytes and the glial scar after SCI (Schwab et al., 2005) – or its receptor, neogenin, has been shown to promote regeneration and locomotor recovery in rodent models of SCI (Hata et al., 2006; Tassew et al., 2014).

1.5.2 Cell transplantation

As previously mentioned, one of the immediate consequences of SCI is the necrotic death of neurons at the injury epicentre. Secondary pathological mechanisms lead to further death of neurons distal from the injury site, which also contributes to the death of other cells such as oligodendrocytes. Although numerous studies have documented the ability of neuroplasticity to promote significant recovery of function lost by a SCI in rodent models, a number of groups believe full recovery will not be possible unless there is a replacement of the cells lost by the injury.

1.5.2.1. Schwann cells

As previously mentioned, there is typically a perimeter of spared tissue following SCI. Axons in this spared region can undergo demyelination due to the on-going apoptosis of oligodendrocytes that persists for up to 3 weeks post-injury (Crowe et al., 1997; Warden et al., 2001). While remyelination of these axons is common, their myelin sheath remains thin which leads to reduced neuronal function (Crowe et al., 1997).

Schwann cells, the myelinating cell type in the peripheral nervous system, have been shown to be able to remyelinate rodent CNS axons *in vivo* (Zhang et al., 2013). Therefore, the primary aim of these studies is to remyelinate the demyelinated axons following SCI, to promote the recovery of locomotor function. In addition to this myelinating ability of

transplanted Schwann cells, following *ex vivo* engineering to express, for example, growth factors, Schwann cells have also been shown to increase axonal regeneration and sprouting. The *ex vivo* engineering of Schwann cells to selectively over-express the neurotrophin glial-derived neurotrophic factor (GDNF) resulted in the regeneration of descending propriospinal neurons beyond the spinal cord lesion, which was accompanied by a partial improvement in locomotor function (Deng et al., 2013). In a separate study, a synergistic effect was observed following the transplantation of Schwann cells engineered to express both neurotrophins and ChABC into the injured spinal cord (Kanno et al., 2014). Animals receiving these transplants had significant locomotor recovery, which was associated with regeneration of corticospinal, serotonergic and propriospinal fibres, compared to animals that received control transplants (Kanno et al., 2014).

The ability of Schwann cells to both remyelinate demyelinated fibres, enhance axonal regeneration and promote partial locomotor recovery suggests they may be very useful as part of a combinatorial therapy to treat SCI in the future. Based on the thorough preclinical data showing the efficacy of transplanted Schwann cells in promoting locomotor recovery following SCI, recently, a phase I clinical trial was approved to investigate the safety of autologous Schwann cells isolated from the sural nerve in acute and chronic SCI.

1.5.2.2. Olfactory ensheathing cells

A specialised population of glial cells in the olfactory mucosa, known as olfactory ensheathing cells (OECs), have been trialled in rodent models of SCI. These cells can be purified from either the olfactory bulb or the olfactory mucosa and are believed to provide channels through which regenerating neurons can grow and eventually form functional connections with target cells (Raisman and Li, 2007). Early studies noted the enhanced regeneration of the injured corticospinal tract and a partial recovery of locomotor function in rats that received OEC transplantation, either at the time of injury or up to 2 months post-lesion (Lu et al., 2002; Keyvan-Fouladi et al., 2003). In addition, OEC transplants promoted the restoration of supraspinal control of breathing in rats with a high cervical injury (Li et al., 2003). Since the publication of these studies there has been a large volume of research

conducted using these cell transplants, with variable results (Takami et al., 2002; Steward et al., 2006; Stamegna et al., 2011).

Based on the success of many of the rodent studies described above, a small study investigating the therapeutic benefit of OEC transplantation in companion dogs with chronic SCI was performed. Results from this study showed a modest improvement in interlimb coordination in dogs that received OEC transplants, compared to those that received control treatments. However there was no improvement in long-tract functionality. Importantly, there were no long-term adverse effects of this treatment (Granger et al., 2012). Following on from this translational study, another research group recently performed a small clinical trial investigating the use of OEC transplantation, the results of which received widespread media attention. A single patient with an ASIA-classified complete SCI received an autologous OEC transplant into the lesion site, in addition to surgical removal of scar tissue, autologous peripheral nerve graft and extensive neurorehabilitation (Tabakow et al., 2014). Nineteen months post-surgery, the patient showed improved trunk stability, voluntary movement of the lower limbs and partial recovery of sensation (Tabakow et al., 2014). It was speculated that this functional recovery is due to long-distance axonal regeneration facilitated by the OEC transplantation (Tabakow et al., 2014). However, the results from this study should be treated with caution, as this was only performed on one patient, who received multiple treatments, including an autologous nerve graft and intense rehabilitation.

1.5.3. Rehabilitation

While selective drugs targeting the promotion of regeneration or plasticity after SCI have resulted in modest improvement in functional recovery in animal models, combining these therapeutic interventions with motor rehabilitation has, in some cases, produced extensive recovery of function. Rehabilitation protocols include enriched cages, treadmill training, or pellet retrieval tasks and can, as previously mentioned, be used in combination with targeted pharmacological interventions or can be used as a monotherapy (Houle and Côté, 2013; Sandrow-Feinberg and Houlé, 2015). Exercise and rehabilitation procedures have been shown to modify the spinal cord, to make it more permissible for plasticity and regeneration in many ways, including down-regulation of PTEN, increased levels of

neurotrophins and a reduction in inflammation (Hutchinson et al., 2004; Ying et al., 2005; Liu et al., 2012). Interestingly, exercise has been shown to increase expression of PNNs in the spinal cord of injured rats (Wang et al., 2011; Smith et al., 2015).

One notable example of the beneficial effect of exercise is a study investigating the combination of ChABC and neurorehabilitation. While ChABC treatment alone has been shown to promote locomotor recovery and enhanced axonal sprouting in a number of different injury models, combining treatment with rehabilitative therapy resulted in a significant improvement in forelimb function after C4 level dorsal column lesion in rats (García-Alías et al., 2009). Conflicting results have been obtained with a Nogo-A function blocking antibody and rehabilitation; one study noted a reduction in muscle spasms, however, the other noted no benefit of dual treatment on locomotor recovery (Maier et al., 2009; Gonzenbach et al., 2010).

Interestingly, there are also some beneficial effects of rehabilitative therapy, in the absence of targeted drug therapies (Houle and Côté, 2013). However, rehabilitation must be approached carefully. Mounting evidence suggests that targeted rehabilitation to improve a specific feature of motor function can lead to impairments in other functions. One key example of this was highlighted in another study combining ChABC and either task-specific or general rehabilitation. This study noted that general locomotor rehabilitation resulted in a worsening of performance on a pellet-reaching task, compared to animals treated with ChABC only (García-Alías et al., 2009).

Thus, for studies investigating neurorehabilitation, the type of rehabilitation used (general locomotor versus task-specific), must be carefully decided upon before the study commences. Other research has revealed that the time and duration of rehabilitation can have a significant effect on locomotor outcomes, therefore must also be carefully investigated.

1.5.4 Adhesion molecules

Many classes of adhesion molecules have been examined in preclinical models of SCI to determine their efficacy at supporting axonal regeneration and/or neuroplasticity. This includes integrins and members of the immunoglobulin superfamily.

1.5.4.1 Integrins

The integrins are a large family of transmembrane proteins that primarily function to mediate cell-ECM interactions. Composed of an alpha and beta subunit, of which there are 18 and 8, respectively, 24 integrins can be generated in total, each with specific roles (Eva and Fawcett, 2014). In the CNS, integrins are ubiquitously expressed and found on both neurons and glial cells (Eva and Fawcett, 2014). Recent evidence suggests that the growth-restrictive effects of the myelin-derived inhibitory molecules, in addition to CSPGs, may be partially mediated by integrin signalling (Goh et al., 2008; Hu and Strittmatter, 2008; Tan et al., 2011).

The ubiquity of integrins throughout both the injured and naïve nervous system means that directly modulating integrin function can have multiple effects post-lesion. Many studies targeting integrins, such as $\alpha D\beta 2$ (also called CD11d/CD18) and $\alpha v\beta 3$ integrin, have been shown to reduce the systemic immune response to spinal cord injury, with some vasculature effects (Gris et al., 2004; Han et al., 2010; Bao et al., 2011). There is less data, however, to support the pro-regenerative consequences of integrin manipulation within the damaged spinal cord. While it is generally well-established that integrin signalling is necessary for axonal growth within the CNS, data showing enhanced axonal regeneration as a consequence of integrin expression post-SCI is limited (Lemons and Condic, 2008; Eva and Fawcett, 2014). One notable study, however, noted increased regeneration of damaged sensory axons into the lesion site of a dorsal column crush injury, following transgenic expression of $\alpha 9$ integrin (Andrews et al., 2009). However, it should be noted that regeneration beyond the lesion site was not observed in this study. More recent work has shown that co-expressing $\alpha 9$ integrin and kindlin-1 (which binds to the integrin β subunit to regulate integrin activation) in DRG neurons can promote long-distance regeneration of sensory axons into the spinal cord after dorsal root crush (Cheah et al., 2016).

1.5.4.2 Immunoglobulin superfamily

Members of the immunoglobulin superfamily of adhesion molecules have been shown to promote axonal regeneration and/or neuroplasticity and associated locomotor

improvement in a number of rodent models of SCI. The L1 cell adhesion molecule is widely expressed in the CNS during development and is believed to be associated with axon guidance and cell migration (Maness and Schachner, 2007). Early research noted administering L1-Fc (a soluble dimer composed of L1 and immunoglobulin Fc) could improve locomotor recovery following contusion injury to the thoracic spinal cord (Roonprapunt et al., 2003). Subsequent studies have utilised an adeno-associated viral vector to induce expression of L1, and a function-triggering monoclonal antibody to stimulate L1 activation *in vivo,* which have both promoted locomotor recovery following thoracic level compression injury in mice (Chen et al., 2007; Loers et al., 2014). Histological data from these studies indicated that L1-mediated locomotor recovery may be associated with enhanced regeneration, or axonal sprouting of serotonergic fibres, a reduction in astrogliosis and secretion of the inhibitory proteoglycan NG2, when administered focally using a viral vector (Chen et al., 2007). Interestingly, L1-mediated locomotor recovery was associated with neuroprotection of motor neurons and parvalbumin-positive interneurons, in addition to a reduction in the size of the glial scar, and enhanced growth of dopaminergic fibres caudal to the lesion following treatment with L1 monoclonal antibody (Loers et al., 2014).

The close homologue of L1 (CHL1), another member of the immunoglobulin superfamily of adhesion molecules, is upregulated within 24 hours post-SCI, at and around the lesion site (Jakovcevski et al., 2007; Wu et al., 2011). Found in NG2-positive cells, and at later time points in reactive astrocytes, elevated CHL1 expression persists for up to 8 weeks post-lesion (Wu et al., 2011). While studies in CHL1 knockout mice have shown an improvement in locomotor function following mid-thoracic level SCI, there have been no studies to date that have tried to knock down CHL1 post-lesion to evaluate this in more detail (Jakovcevski et al., 2007). To date, up- or down-regulation of other members of the L1 family, such as neurofascin and the neuronal cell adhesion molecule (NrCAM), have not been investigated in rodent models of SCI.

The distribution and function of neural cell adhesion molecules (NCAMs) have been extensively studied in the CNS, and can be modulated to promote significant locomotor recovery in rodent models of SCI. As previously mentioned, the main scope of this thesis is to investigate polysialylation of NCAM so studies investigating PSA and SCI will be discussed in extensive detail in section 1.5.4.4 below.

1.5.4.3 Other molecules

Other classes of adhesion molecules include cadherins, calpains and neuroligins. However, currently, there is little data available regarding their involvement in the pathophysiology of SCI, or how modulation of their function is correlated with functional improvement.

1.5.4.4 Polysialic acid

Utilising the unique biochemical properties of PSA to promote recovery in experimental models of SCI has progressed in two main directions. Firstly, transplantation of genetically modified Schwann cells that were engineered *ex vivo* to express polysialyltransferase, or secondly, direct expression of polysialyltransferase in the injured spinal cord. Each of these approaches will be discussed in detail below.

The ability of transplanted Schwann cells to myelinate CNS axons following trauma to the spinal cord has been well documented and has been shown to promote some behavioural improvement in experimental models of SCI (Yang et al., 2015a). However, these studies have a number of important caveats, such as the death of Schwann cells following transplantation and the poor integration of surviving cells into the host spinal cord (Pearse et al., 2007). The ability of PSA to facilitate cell migration during development of the CNS led to the hypothesis that engineering PSA expression on cultured Schwann cells may enable transplanted cells to migrate further into the host spinal cord.

Preliminary work utilised a retroviral vector to express the STX transgene in cultured Schwann cells isolated from the rat sciatic nerve. Cells transduced by the viral vector were strongly immunopositive for PSA and survived well *in vitro*. Importantly, PSA-Schwann cells migrated approximately 50% further than wild-type cells in a scratch assay and retained their myelinating ability (Lavdas et al., 2006). Subsequent studies aimed to transplant PSA-expressing Schwann cells into the injured mouse spinal cord to assess locomotor recovery. Animals that received transplants of PSA-Schwann cells rostral to SCI had improved motor function, compared to mice that received either control Schwann cells or no transplant at all. Interestingly, these animals had a significant increase in the density of serotonergic axons caudal to the injury, but not in the lesion site, and an increase in remyelination by

resident Schwann cells (Papastefanaki et al., 2007). Further research has built on this initial study and has investigated the therapeutic potential of PSA-Schwann cells in different models of SCI. In one study, PSA-Schwann cells showed improved survival up to 30 days following transplantation caudal to T8 dorsal column crush injury. PSA-Schwann cells migrated a further distance than control counterparts, and reduced the reactive response of astrocytes that is normally observed following Schwann cell transplantation into the injured spinal cord (Luo et al., 2010). A more recent study revealed similar findings following transplantation of PSA-Schwann cells into the injury epicentre, one week following moderate contusion at T8/9 spinal level. PSA-Schwann cells migrated significantly further than control cells. However, no difference was observed in the reactivity of astrocytes at the injury epicentre between cell types. Interestingly, there was also a significant increase in the density of serotonergic axons in the centre of the graft and an increase in corticospinal axons both in the centre of the graft and caudal to the leading edge of the transplant. Rats that received PSA-Schwann cells had a modest improvement in hindlimb function, compared to those that received control cells (Ghosh et al., 2012).

The ability of PSA expression to promote axonal regeneration following SCI has been documented in a number of rodent models. The first study to do this used a lentiviral vector carrying the polysialyltransferase gene to selectively express PSA in astrocytes following thoracic corticospinal tract lesion. Mice that received injections of PST lentivirus had elevated sprouting of corticospinal axons crossing the caudal border of the lesion, than those treated with control virus (El Maarouf et al., 2006). Detailed histological assessment also revealed a large number of non-dystrophic growth cones associated with regions of PSA expression (El Maarouf et al., 2006). Following on from this work, other groups have used lentiviral vectors to express PSA at the lesion site in a number of rodent models of injury. Injecting lentivirus carrying the PST gene (LV/PST) into the lesion site after dorsal column transection resulted in increased regeneration of sensory axons, compared with animals that received LV/GFP (Zhang et al., 2007b). In a separate group of LV/PST treated animals, the sciatic nerve was crushed immediately following SCI to initiate a pro-regenerative response in these neurons. Animals that received sciatic nerve crush, in addition to LV/PST treatment had significantly more CTB-labelled sensory axons in and rostral to the lesion site,

compared to those that received crush and treatment with control virus (Zhang et al., 2007b).

One of the limitations of using viral vectors to selectively express PSA in the spinal cord after injury is the relatively small area transduced by the virus. To obtain a large area of expression, multiple injections need to be performed to the spinal cord, which may be counter-productive. Recent research has identified two 9 amino acid peptides that can mimic the role of PSA in culture and in the developing chick retina. Soaking a collagen gel in this peptide, followed by subsequent transplantation into the lesion site after thoracic-level dorsal column hemisection promoted a significant improvement in hindlimb motor function, compared to mice that received control peptide. Additionally, these mice regained controlled bladder voiding faster and showed an increase in the density of serotonergic fibres both in the lesion site and in the caudal side of the lesion (Marino et al., 2009). These findings were verified in another study, in which mice received continuous infusion of PSA mimetic for 2 weeks post-T8 compression injury. Mice treated with one of the two different PSA mimetics had a significant improvement in hindlimb motor function, compared with animals that received control peptide (Mehanna et al., 2010; Pan et al., 2014). Interestingly, a PSA mimetic has also been shown to preserve neurons in the ventral horn, both rostral and caudal to the lesion and induce sprouting of serotonergic and catecholinergic neurons above and below the injury epicentre (Mehanna et al., 2010; Pan et al., 2014). Recent work has revealed another two mimetic peptides, vinorelbine and epirubicin, however, their efficacy at promoting repair and locomotor improvements in SCI has not yet been examined (Loers et al., 2016).

1.6. Hypotheses and aims

Based on the previously mentioned preliminary data, we hypothesise that PSA expression can restrict the formation of the PNN. Moreover, we speculate that the large, hydrated volume of PSA can prevent WFA-binding to its site within the PNN.

There are three main aims for this thesis. Firstly, to map the distribution of two PNN components, neurocan and LN1, and the PNN-binding lectin WFA, in the adult rat cervical spinal cord. We hypothesise that these components will be heterogeneously distributed throughout different laminae of the spinal cord and we also expect to see high levels of co-

localisation between these markers within PNN structures. Secondly, to investigate the proposed relationship between PSA and the PNN, using both *in vitro* and *in vivo* models. It is speculated that removal of PSA from primary neuronal cultures will increase development of the PNN, which will be associated with a reduction in the density of synapses contacting PNN-expressing neurons *in vitro*. Furthermore, we hypothesise that *in vivo*, induced PSA expression using a lentiviral vector carrying the transgene for the polysialyltransferase enzyme (LV/PST) will reduce binding of the WFA to its specific site within the PNN. Finally, we will investigate the behavioural effects of induced PSA expression rostral and caudal to a mid-cervical lateral hemisection lesion, using LV/PST, in adult rats. Synaptic inputs to transduced neurons will be examined 6 weeks following injection of LV/PST. We hypothesise that LV/PST treated rats will show a significantly elevated locomotor recovery, compared with animals that received injections of control virus, carrying the transgene for green fluorescent protein (LV/GFP) only. Additionally, we expect the density of synaptic inputs to transduced neurons to be increased in animals that received LV/PST injections, compared to controls.

Chapter 2

Methods

Chapter 2: Materials and methods

2.1. Cell culture

2.1.1. Primary cortical and hippocampal cell culture

Timed-pregnant Wistar rats (Charles River UK), gestation day 18, were sacrificed by CO_2 asphyxiation followed by decapitation. Embryos were rapidly removed and placed in ice-cold Hank's buffered salt solution (HBSS) (Sigma-Aldrich, UK). Embryos were decapitated and the heads placed in fresh HBSS. Skin and skull were removed from each head and the brain transferred into a fresh dish filled with HBSS. After each brain was split into 2 cerebral hemispheres with the dura removed, the hippocampi and cortices were collected in separate tubes containing fresh HBSS. Brain tissue was chemically dissociated using 0.125% trypsin-EDTA solution (Sigma-Aldrich, UK) for 8 minutes at 37°C. Modified medium which contained Neurobasal medium, 100 units/ml penicillin / 100 μg/ml streptomycin, 1% B27 supplement without vitamin A, 0.5 mM GlutaMAX and 10% foetal bovine serum (FBS) (all Life Technologies, UK) was added to each tube to inactivate the trypsin. The tissue was mechanically dissociated using a 1 ml pipette tip and the resulting cell suspension was filtered through a sterile 70 μm cell strainer (VWR, UK). Cells were collected by centrifugation at 1000 rpm for 5 minutes, then resuspended in modified Neurobasal medium without any FBS. Cells were plated at a density of 50,000 or 100,000 cells/cm^2 on 13 mm poly-D-lysine with or without laminin coated glass coverslips.

2.1.2. Preparation of coverslips for culture

For poly-D-lysine coating, 13 mm glass coverslips were sterilised in 70% ethanol and then autoclaved in an enclosed container. Coverslips were coated with 100 μg/ml poly-D-lysine solution, overnight at 37°C and 5% CO_2 and then were washed in sterile distilled water four times and once in sterile PBS, before cell plating.

For coating with poly-D-lysine and laminin, coverslips were initially incubated in poly-D-lysine, as above. After several washes in sterile distilled water, the poly-D-lysine- treated coverslips were incubated in laminin (2 μg/ml, Life Technologies) for three hours at 37°C

and 5% CO_2. Coverslips were rinsed four times in sterile distilled water and then once in sterile PBS, prior to cell plating.

2.1.3. Treatment of primary cells with endoneuraminidase-N

To investigate the effect of PSA on the development of PNNs and synaptogenesis *in vitro*, PSA was removed from the surface of cultured hippocampal cells using endoneuraminidase-N (endo-N, ABC Scientific). Endo-N was diluted in modified Neurobasal medium to concentrations of 40, 80, 160 or 200 ng/ml. 4 days after plating, cells received a 50% medium change with endo-N containing medium, resulting in final endo-N concentrations of 20, 40, 80 or 100 ng/ml, respectively. All subsequent medium changes contained endo-N. Control cells received medium changes containing vehicle only (phosphate-buffered saline).

2.1.4. HEK293T cell culture

Human embryonic kidney 293 (HEK293T) cells were plated at a density of 40,000 cells/cm^2. Cells were maintained in modified Dulbecco's Modified Eagle Medium (DMEM, Life Technologies) supplemented with 100 units/ml penicillin / 100 µg/ml streptomycin and 10% FBS, at 37°C and 5% CO_2. Cells were split at a ratio of 1:3 when they reached a confluency of approximately 80%.

2.2. Lentiviral vector production

2.2.1. Preparation of transfer vector

Green fluorescent protein (GFP) cDNA was fused to the C-terminal of mouse polysialyltransferase (PST) cDNA, to generate PST-GFP. PST-GFP and mCherry cDNAs were subcloned into the transfer vector pRRL, with each cDNA under the control of an independent human synapsin I promoter. GFP cDNA was subcloned into two separate pRRL transfer vectors, one under the control of a human synapsin I promoter and the other under the control of a cytomegalovirus (CMV) promoter (Figure 2.1).

Plasmid vectors were transformed into DH5α competent cells (Life Technologies, UK) using the heat shock method according to the manufacturer's instructions. The bacteria were then streaked on Lysogeny broth agar plates containing 50 µg/ml ampicillin and incubated

overnight at 37°C. Single colonies were selected and grown in terrific broth overnight at 37°C. Plasmid DNA was isolated using QIAprep Miniprep kits and QIAprep Midiprep kits (Qiagen). To verify insertion of cDNA into plasmids, isolated DNA was digested using appropriate restriction enzymes and fragments were separated on a 0.8% agarose gel. Concentration of plasmid DNA was determined using a NanoDrop UV spectrophotometer. Plasmid DNA was diluted to a final concentration of 1 µg/µl and stored at -20°C until needed for production of lentiviral vectors.

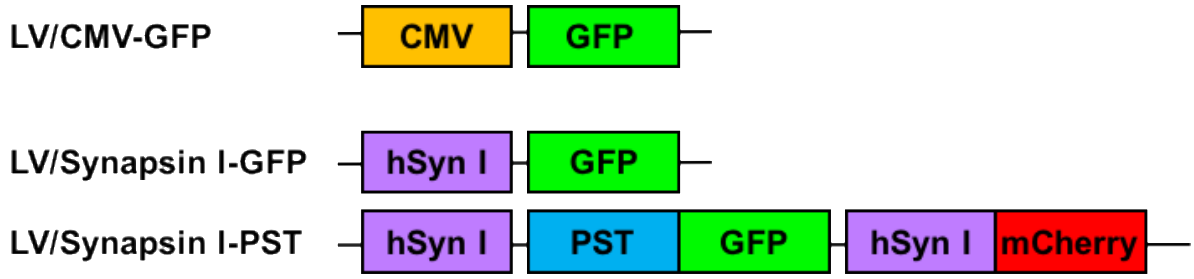

Figure 2.1. Schematic of transfer vectors for lentiviral vectors.
CMV: cytomegalovirus promoter sequence, GFP: green fluorescent protein, hSyn-1: human synapsin I promoter sequence, PST: polysialyltransferase.

2.2.2. Production of lentiviral vectors

HEK293T cells were expanded as described previously (see section 2.1.4). To package the lentivirus, cells that were passaged at least 3 times after thawing from liquid nitrogen storage were re-plated at a density of 3 x 10^6 cells per 10 cm dish, which had been pre-coated with 10 µg/ml poly-D-lysine. When cells reached 80-85% confluency, transfection was carried out using the calcium precipitation method. Two hours before transfection, cells received a full medium change. Sterile water, 0.1 X Tris-EDTA (TE) and envelope, pack and transfer plasmids (Table 2.1) were mixed together by gentle vortexing. Calcium chloride (2.5 M, $CaCl_2$) was added and the solution was mixed. An equal volume of 2 X HEPES-buffered saline (HBS) was added to the mixture at a rate of two drops per second, while the solution was vortexed at high speed. 1 ml was immediately added to each 10 cm dish, which was gently rocked to ensure even dispersion of solution.

Reagent	Amount of solution (µl)
H_20	1080
0.1 X TE	1500
ENV plasmid (1 µg/µl)	21
PACK plasmid (1 µg/µl)	39
Transfer vector (1 µg/µl)	60
2.5M $CaCl_2$	300

Table 2.1. Composition and volumes of transfection mixture for production of lentiviral vectors for six 10 cm dishes.

Cells were incubated for 14 hours before the medium was replaced with 9 ml DMEM-GlutaMAX supplemented with 2% FBS and 100 units/ml penicillin / 100µg/ml streptomycin. Medium containing the viral vectors was harvested 48 hours after transfection. Cell debris was removed by centrifugation at 1000 x *g* for 10 minutes and then filtered through a sterile 0.45 µm syringe filter.

To concentrate the lentiviral vectors for use *in vivo*, supernatant from three dishes was decanted into sterile Ultracone centrifugation tubes (28 ml size) and centrifuged using the Sorvall SureSpin 630/36 swing bucket rotor for 2.5 hours at 25,000 x *g* at 4°C. After centrifugation, the supernatant was carefully aspirated and the pellet re-suspended in 60 µl sterile 0.01 M phosphate buffered saline (PBS). The virus was stored in 10 µl aliquots at -80°C until required.

2.2.3. Titration of lentiviral vectors

To titrate lentiviral vectors, HEK293T cells were seeded at a density of 5 x 10^5 cells into each well of a 6-well plate, which was pre-coated with poly-D-lysine. Viral stocks were serially diluted to 0.1, 0.01 and 0.001 µl/ml in modified DMEM (see section 2.1.4), and 1 ml diluted virus and 1 ml medium was added to cells. 24 hours later, the medium was replaced with modified DMEM. Cells were fixed after a further 24 hours and the number of transduced cells was counted using an inverted fluorescence microscope using a 10x objective lens. The number of viral transducing units (TU) was calculated according to the formula below.

TU/ml = Number transduced cells (at 10x objective lens) x dilution x 700 fields of view

Lentiviral vectors driven by the synapsin I promoter (LV/Synapsin I-GFP and LV/Synapsin I-PST) were not titered as this titration method did not work, seemingly due to the lack of synapsin I expression in HEK293T cells. The titre of LV/CMV-GFP was 1.7 x 10^{10} TU/ml.

2.3. Animals and surgeries

All surgical procedures were performed in accordance with the Animals (Scientific Procedures) Act 1986. Adult Wistar rats (weight 125-200 g, Charles River UK) were used to optimise surgical procedures and test lentivirus transduction. Adult female Wistar rats (weight 200-225g, Charles River UK) were used for the spinal cord injury experiments. All animals were housed in groups under a 12 hour light/dark cycle with *ad libitum* access to food and water.

To prepare for surgery, all animals (unless otherwise stated) were anaesthetised using a combination of ketamine (60 mg/kg, Ketaset®, Fort Dodge) and medetomidine (0.25 mg/kg, Dormitor®, Pfizer). The surgical area was shaved and cleansed with iodine solution.

2.3.1. Optimising surgical procedures

2.3.1.1. Lentiviral vector delivery to cortex

To optimise the procedure for injecting lentiviral vectors into the CNS, animals (*n*=2) were deeply anaesthetised with 4% isoflurane (IsoFlo®) and positioned in a stereotaxic frame. A 2 cm midline incision was made to reveal the skull. Each animal received 3 injections into the left sensorimotor cortex at coordinates defined as anteroposterior (AP) and mediolateral (ML): (i) AP: 1.0 mm ML: -1.5 mm (ii) AP: 1.5 mm, ML: -2.5 mm (iii) AP: 2.0 mm, ML: -3.5 mm, relative to bregma. The lentiviral vector used carried a GFP cDNA under the control of a cytomegalovirus (CMV) promoter (LV/CMV-GFP). Another 3 injections of lentiviral GFP vector under the control of a synapsin I promoter (LV/Synapsin I-GFP) were carried out at coordinates: (i) AP: 1.0 mm, ML: 1.5 mm (ii) AP: 1.5 mm, ML: 2.5 mm (iii) AP: 2.0 mm, ML: 3.5 mm, relative to bregma. All injections were carried out at the depth of 2 mm from the surface of the skull. To assess the optimal procedure for injecting viral vectors into the CNS, lentiviral vectors were delivered using a Hamilton syringe via a directly attached 33-gauge steel needle or a glass microneedle. All injections were performed at a flow rate of 0.2 µl/min and 1 µl vector was delivered per site.

In a second study, animals received unilateral injections of lentiviral vector carrying PST-GFP and mCherry cDNAs (LV/Synapsin I-PST) into the forelimb sensorimotor cortex, at coordinates: AP: 1.5 mm, ML: -2.5 mm, relative to bregma. Injections were performed using a glass microneedle at a depth of 2 mm from the surface of the skull and a flow rate of 0.2 µl/min.

In a third study, animals (*n*=6) received two LV/Synapsin I-GFP injections at coordinates: (i) AP: 1.5 mm, ML: -2.5 mm (ii) AP: -1.5 mm, ML: -2.5 mm, relative to bregma, and two LV/Synapsin I-PST injections at coordinates: (i) AP: 1.5 mm, ML: 2.5 mm (ii) AP: -1.5 mm, ML: 2.5 mm, relative to bregma. All injections were performed at a depth of 2 mm below the skull surface. Injections were performed at a flow rate of 0.2 µl/min (2 µl/site) using a glass microneedle. The wound was sutured and animals were allowed to recover in a heated chamber.

Animals from the first two studies were deeply anaesthetised with pentobarbital (50 mg/kg, Euthatal®, intraperitoneal, Merial Animal Health Ltd) then underwent perfusion-fixation

(see section 2.3.3) at 2 weeks post-surgery, before brains were harvested for immunofluorescent staining. Animals from the third study were deeply anaesthetised with pentobarbital (50 mg/kg, Euthatal®, intraperitoneal, Merial Animal Health Ltd) then underwent perfusion-fixation (see section 2.3.4) at either 4 weeks (*n*=3) or 6 weeks (*n*=3) post-surgery, before brains were harvested for immunofluorescent staining.

2.3.1.2. Lentiviral vector delivery to the cervical spinal cord

To identify cell types transduced by lentiviral vectors in the spinal cord, animals (*n*=2) received unilateral injections of LV/CMV-GFP into the cervical spinal cord. A dorsal midline incision was made between the 4th and 7th cervical laminae and the vertebral column was exposed. A hemi-laminectomy on the left hand side was performed at C6 and C7, following which the dura was cut to expose the dorsal surface of the spinal cord. Injections were delivered using a glass micropipette attached to a Hamilton syringe via a water-filled polyethene tube, into the intermediate grey matter. All injections were performed at a flow rate of 0.2 µl/min (2 µl/site). After injection, the muscle and skin were sutured and animals received buprenorphine (0.01 mg/kg) and saline subcutaneously, twice daily for 2 days.

In another experiment, animals (*n*=2) received injections of viral vectors immediately following cervical lateral hemisection injury. A hemi-laminectomy was performed on the left side between the 4th and 7th cervical spinal cord segments, following which an incision was made in the dura to expose the dorsal surface of the spinal cord. A sharp microblade was used to make an incision at the spinal cord midline between the 5th and 6th cervical segments, which was then extended laterally using microscissors. Immediately following injury, rats received 1 injection of LV/Synapsin I-PST rostrally and 1 injection of LV/Synapsin-I-GFP caudally to the injury.

Animals from these studies underwent perfusion fixation at 2 weeks post-surgery and the spinal cords were collected for histological analysis.

2.3.2. Spinal cord injury and intraspinal lentiviral vector injections study

2.3.2.1. Experimental timeline

Animals received training at behavioural tasks for up to two weeks prior to surgery (see chapter 2.4 for details) and baseline values for all behavioural assessments were obtained up to three days prior to surgery. Animals were assigned into one of five groups; (i) hemisection + LV/Synapsin I-PST, (ii) hemisection + LV/Synapsin I-GFP, (iii) LV/Synapsin I-PST injection only, (iv) LV/Synapsin I-GFP injection only, (v) sham (laminectomy only). Testing of locomotor function was carried out on the next day following surgery and weekly for the duration of the experiment. All animals received unilateral injections of the anterograde neuronal tracer, biotin dextran amine (BDA) into the primary sensorimotor cortex two weeks before collection of tissue for histology (Figure 2.2).

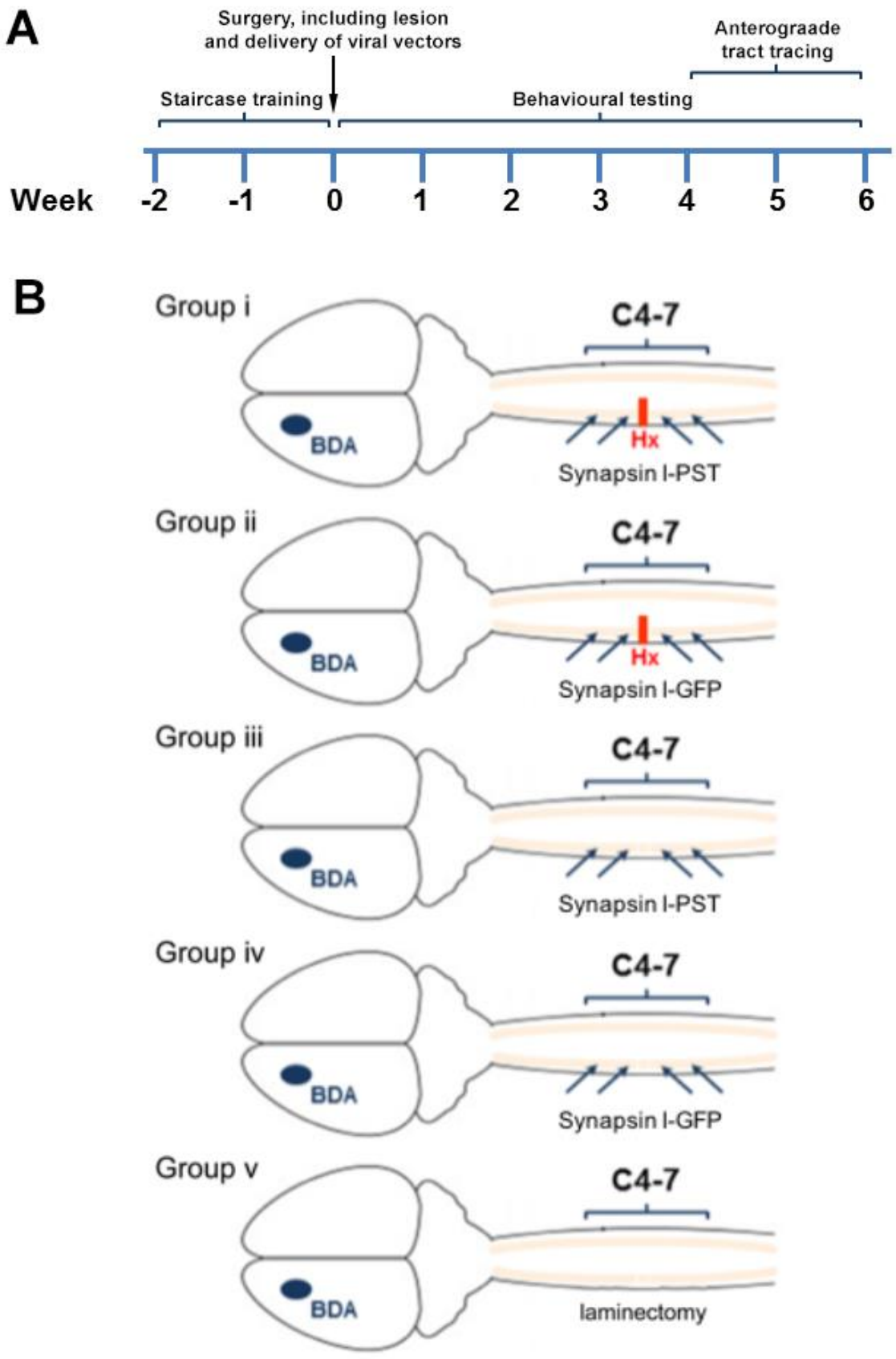
A
Surgery, including lesion
and delivery of viral vectors
Anterograade
tract tracing
Staircase training
Behavioural testing
Week
-2
-1
0
1
2
3
4
5
6
B
Group i
C4-7
BDA
Hx
Synapsin I-PST
Group ii
C4-7
BDA
Hx
Synapsin I-GFP
Group iii
C4-7
BDA
Synapsin I-PST
Group iv
C4-7
BDA
Synapsin I-GFP
Group v
C4-7
BDA
laminectomy

➤ **Figure 2.2. Timeline and schematic for SCI experiments**
(A) Animals were trained on the Montoya staircase test daily for 2 weeks prior to surgery. Furthermore, during this time, animals were also habituated to a number of other behavioural tasks (see chapter 2.4 for details). Surgery (including laminectomy, lesion and delivery of lentiviral vectors) was performed on day 0, and then locomotor function was examined for 6 weeks. Two weeks prior to sacrifice, animals received injections of the anterograde neuronal tracer biotin dextran amine (BDA) to the cortex that was ipsilateral to the injury. **(B)** Animals received lateral hemisection injury at C5/6, followed with 4 intraspinal injections of either LV/Synapsin I-PST or LV/Synapsin I-GFP alone without the injury. The control surgery group received a laminectomy only. All animals received unilateral injections of BDA into the ipsilateral sensorimotor cortex.

2.3.2.2. Cervical lateral hemisection

A dorsal midline incision was made between the second and seventh cervical laminae and the vertebral column was exposed. A hemi-laminectomy was performed on the left side between the C4 and C7, following which an incision was made in the dura to expose the dorsal surface of the spinal cord. A sharp microblade was used to make an initial incision at C5/C6, which was extended laterally to ensure complete lateral hemisection of the spinal cord (Figure 2.3A).

2.3.2.3. Intraspinal injections of lentiviral vectors

Immediately following the hemisection lesion animals were prepared for intraspinal injections. Each animal received four injections of either LV/Synapsin I-GFP (*n*=8) or LV/Synapsin I-PST (*n*=12), at two sites rostral and two sites caudal to the lateral hemisection site (approximately 0.5 and 1.5 mm rostral and caudal to the lesion). Injections were delivered using a glass micropipette attached to a Hamilton syringe via a water-filled polyethene tube at a flow rate of 0.2 µl/min (1 µl/site). After injection, muscle and skin were sutured and animals were left to recover in a warm chamber.

A separate group of animals received LV/Synapsin I-GFP (*n*=6) or LV/Synapsin I-PST (*n*=5) injections in the absence of hemisection injury (Figure 2.3B), or sham surgery (laminectomy only, n=4).

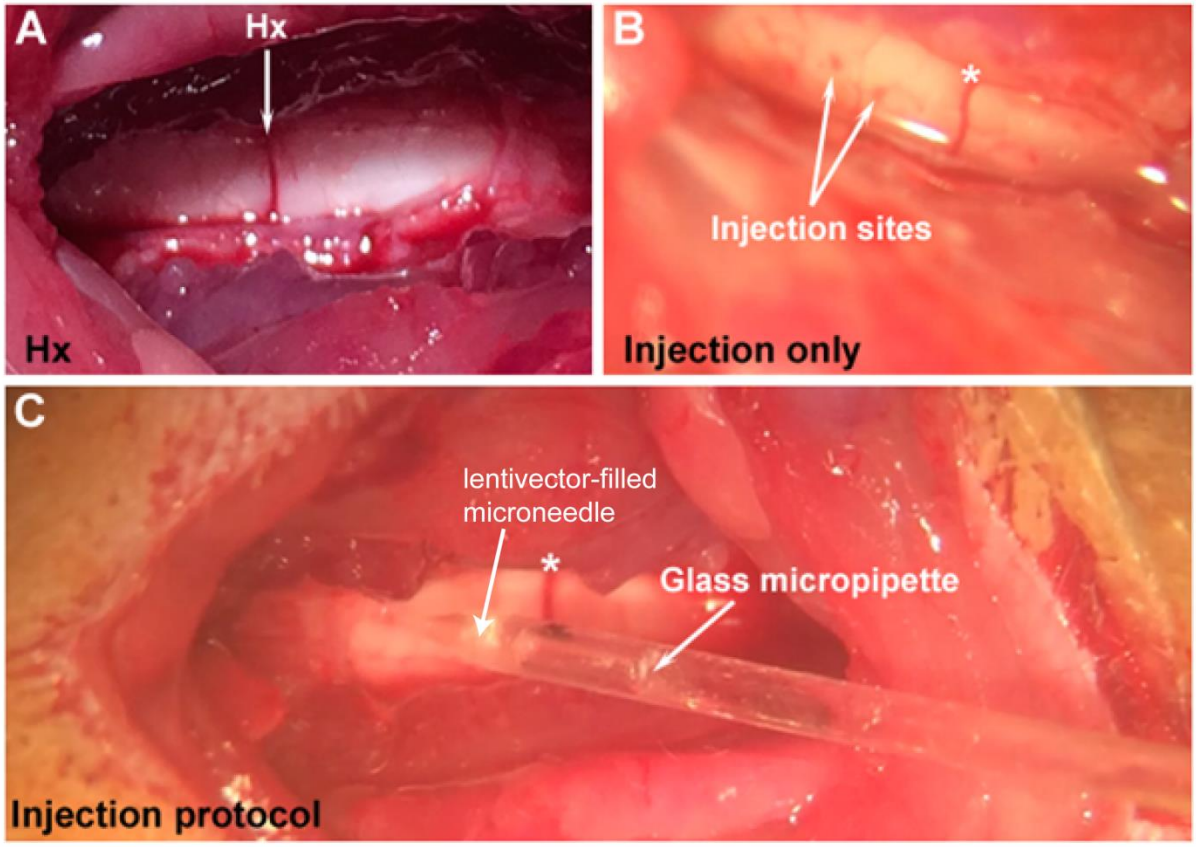

Figure 2.3. Representative surgical images of the lateral hemisection and microinjection of lentiviral vector into the spinal cord.
(A) Laminectomy was performed between C4-C7 and lateral hemisection (Hx) injury was performed at C5/6. **(B)** A representative image showing lentiviral vector injection sites into the uninjured spinal cord. **(C)** A representative image showing lentiviral vector at the end of the glass microneedle being delivered into the uninjured cervical spinal cord. * denotes blood vessel.

2.3.2.4. Post-operative care

All animals received buprenorphine (0.01 mg/kg, subcutaneous) and sterile saline (3ml, Vetivex), immediately following surgery and twice daily for 4 days. In agreement with Home Office instructions, animals that lost 20% body mass were immediately culled. Paws were inspected daily for signs of autotomy. If observed, rats received topical treatment of anti-chew spray and Fuciderm® (Dechra) gel, 3 times per day until the skin healed. If autotomy persisted and penetrated beyond the superficial skin layers of the digits, animals were culled.

2.3.2.5. Anterograde tract tracing

To investigate whether lentiviral vector-mediated PSA expression can promote sprouting of the uninjured corticospinal tract, rats received unilateral injections of BDA (10%; 10 000 MW, Life Technologies, UK). Rats were anaesthetised with 4% isoflurane and placed in a stereotaxic frame. Seven burr holes (0.7 mm diameter) were drilled through the skull, ipsilateral to the site of lateral hemisection, at coordinates defined as anteroposterior (AP) and mediolateral (ML): (i) AP: -1.5 mm, ML: 2.5 mm; (ii) AP: -0.5 mm, ML: 3.5 mm (iii) AP: -0.5 mm, ML: 2.5 mm; (iv) AP: + 0.5 mm, ML: 3.5 mm; (v) AP: + 1.0 mm, ML: 1.5 mm; and (vi) AP: 1.5 mm, ML: 2.5 mm; and (vii) AP: 2.0 mm, ML: 3.5 mm, relative to bregma. BDA (0.8 µl/site) was injected at a flow rate of 0.2 µl/min using a 26 G needle attached to a Hamilton syringe via a water-filled polyethene tube. Injections were carried out at a depth of 2 mm below the skull. Animals were left to recover in a warm chamber before being transferred to clean cages. Animals received buprenorphine (0.01 mg/kg, subcutaneous) and saline (3 ml, subcutaneous) twice daily, for two days.

2.3.2.6. Exclusion criteria

A total of 6 animals in the hemisection + LV/Synapsin I-PST group were excluded from the study. Three animals developed severe autotomy of the contralateral hindlimb, between 2 and 3 weeks post-surgery and were culled as per Home Office instructions. Another two animals were excluded due to incomplete lesions and a further did not recover from BDA injections.

One animal from the hemisection + LV/Synapsin I-GFP group did not recover from surgery.

Thus, final group sizes for this study were as follows: hemisection + LV/Synapsin 1-PST (*n*=6), hemisection + LV/Synapsin I-GFP (*n*=7), LV/Synapsin I-PST alone (*n*=5), LV/Synapsin I-GFP (*n*=6), and laminectomy alone (*n*=3).

2.3.3. Perfusion-fixation

At the end of the study, the animals were deeply anaesthetised using pentobarbital (50 mg/kg, Euthatal®, intraperitoneal, Merial Animal Health Ltd). The thoracic cavity was opened and a needle was inserted into the ascending aorta, via the left ventricle. The right

atrium was cut and perfused with 0.9% saline followed by 4% paraformaldehyde in 0.1 M phosphate buffer, for 8 minutes. The brain and spinal cord were collected and post-fixed in 4% paraformaldehyde overnight at 4°C. Tissue was cryoprotected in 20% sucrose in 0.1 M phosphate buffer for at least two days at 4°C.

2.3.4. Tissue processing (spinal cord)

Following cryoprotection in 20% sucrose, spinal cords were cut into 15 mm tissue blocks, containing the lesion and injection sites. Tissue was embedded in optimum cutting temperature (OCT) mounting medium (VWR, UK), rapidly frozen on dry ice and stored at -20°C until further processed.

Spinal cords were sectioned serially (15 µm thick) in the horizontal plane and thaw-mounted onto Superfrost Plus microscope slides. Sections were air dried and stored at -20°C until further processed.

2.3.5. Tissue processing (brain)

Large brain sections (3-5 mm thick) containing the injection regions were embedded in OCT mounting medium, rapidly frozen on dry ice and stored at -20°C until needed. Coronal sections (20 µm thick) were collected and thaw-mounted on to Superfrost Plus slides. Tissue sections were air dried and stored at -20°C until further processed.

2.4 Behavioural testing

All behavioural testing and analysis was done by a blinded assessor.

2.4.1 Open field locomotor assessment

Rats were habituated to the open field (approximately 1 metre diameter) daily, starting 1 week prior to surgery. For the behavioural testing, animals were placed in the open field and allowed to freely explore for 4 minutes. Fore- and hindlimb locomotor function was assessed in real-time using the forelimb locomotor scale (FLS) and Basso, Beattie, Bresnahan scale (BBB), respectively. Open field locomotor assessment was performed daily for 7 days post-surgery, then every other day for the remainder of the study.

2.4.2 Montoya staircase

Skilled forelimb reaching was assessed using the Montoya staircase test. Animals were trained to retrieve food pellets from the staircase daily for 2 weeks before surgery. Baseline testing values were obtained 2 days before surgery then animals were tested twice weekly, beginning 3 days post-surgery. Animals were placed in the staircase for 20 minutes, with one food pellet per step. The number of pellets consumed and displaced was recorded.

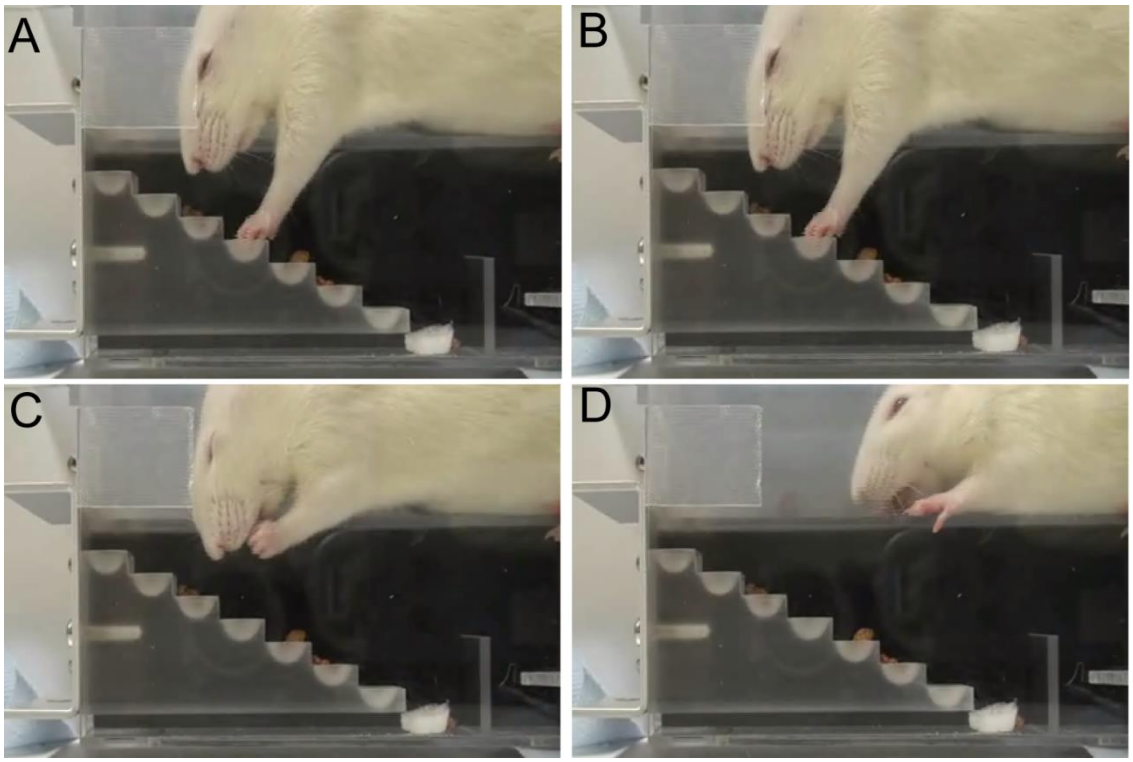

Figure 2.4. Montoya staircase test.
(A-D). Animals were placed inside the Montoya staircase and allowed to grab a food pellet from the steps. The number of food pellets displaced and eaten was recorded. Images provided courtesy of Dr Zhuo-Hao Liu.

2.4.3 Grid exploratory test

Animals were habituated to the grid exploratory apparatus daily, for 1 week prior to surgery. Baseline data was obtained 2 days before surgery and then animals were tested once per week starting 7 days post-surgery. Rats were placed on a metal grid (1 metre x 1 metre with gaps measuring 50 x 50 mm) and allowed to freely explore for 35 steps. This was recorded using a video camera and the number of hindlimb missteps (when the entire surface of the foot misses the wire and protrudes through the bottom of the grid, Figure 2.5) was counted retrospectively.

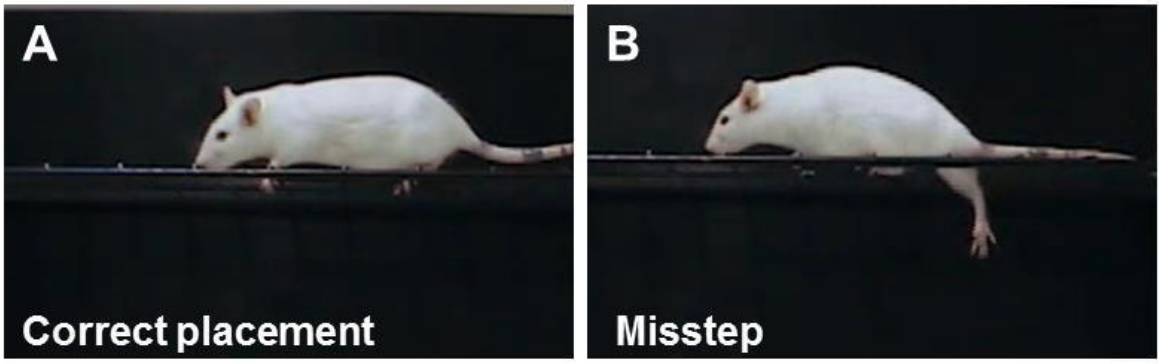

Figure 2.5. Grid exploratory test.
Animals were left to roam on a metal grid and the number of missteps was manually counted by a blinded assessor. **(A)** Generally, animals can place paws on the metal grid while exploring. **(B)** Missteps were defined as when the entire paw missed the grid and protruded through the grid.

2.4.4 Automated gait analysis

Automated gait analysis was performed using the Catwalk-XT system (Noldus). This consists of an enclosed linear glass walkway, which emits LED light that is completely internally reflected. When an animal moves down the walkway, the LED light is refracted at the areas where the paw contacts the glass surface. This refracted light is detected by a video camera attached underneath the walkway, which inputs to a computer for data analysis.

Animals were habituated to the Catwalk-XT apparatus daily, for 3 days before surgery. Individual animals were placed at one end of the walkway, and allowed to walk freely until they entered their home cage, which was placed at the other end of the walkway. Baseline data was obtained 2 days before surgery and then animals were tested once per week, starting 3 weeks post-lesion. Three complete runs were analysed per animal at each time point. A complete run was defined as between 1.5 and 10 seconds in duration, during which the animal did not pause when it was moving along the walkway. Data was analysed using the Catwalk-XT software provided by the manufacturer.

2.4.5 Plantar heat test (Hargreave's method)

Hindlimb responses to thermal stimuli were assessed using the plantar heat test (Hargreave's method). Rats were habituated in plastic boxes over a glass plate for 20 minutes. An infrared heat source (Ugo Basile) was placed beneath the glass plate, which

was situated over the centre of the plantar surface of the hind paw. The heat source was switched on and the latency to paw withdrawal was recorded. Each hind paw was tested 3 times, with at least 5 minutes resting time in between each test.

2.4.6 Von Frey

Hindlimb responses to tactile stimuli were assessed by Von Frey filaments (Ugo Basile 37450/277, Linton Instruments) using a simplified up-down method (Bonin et al., 2014). Animals were habituated in plastic boxes placed over a wire mesh, for 20 minutes. Each hindpaw was tested 5 times using Von Frey filaments of various diameters and responses to each filament were recorded.

2.5 Immunofluorescence

2.5.1 Immunohistochemistry (tissue sections)

Slides containing the tissue sections were rinsed three times in 0.01 M PBS then incubated in blocking solution (10% normal goat, or normal donkey, serum in 0.01 M PBS + 0.2% Triton-X-100 (PBS-T)) for 2 hours. The blocking solution was removed and slides were incubated in the appropriate primary antibodies (Table 2.2), overnight at room temperature. Next day, slides were washed in PBS and incubated in the appropriate fluorescent (Alexa Fluor®, Life Technologies)-conjugated secondary antibody, diluted in PBS-T, for 2 hours. Unbound secondary antibody was removed from slides by washing in PBS and slides were cover slipped using DAPI Fluoromount-G (Southern Biotech, UK).

2.5.2 *Wisteria floribunda* agglutinin labelling

Lectin from *Wisteria floribunda* agglutinin (WFA) was used to detect perineuronal nets (PNNs) in tissue sections. Sections were washed in Tris buffered saline (TBS) then incubated in biotinylated WFA lectin (Sigma Aldrich) diluted in TBS + 0.2% Triton-X-100 (TBS-T) to a final concentration of 50 μg/ml, overnight at room temperature. Unbound lectin was removed by washing with TBS then labelling was detected by incubation with fluorescence-conjugated streptavidin (Life Technologies), for two hours. Slides were washed in TBS and cover slipped with DAPI Fluoromount-G.

2.5.3 Immunocytochemistry (cell cultures)

Coverslips were rinsed once in TBS and incubated in 10% normal donkey serum in TBS-T, for 1 hour at room temperature. Coverslips were incubated in either WFA-lectin or primary antibody (for dilutions see Table 2.2), overnight at room temperature. The following day coverslips were washed in TBS and incubated in secondary antibody for 35 minutes, at room temperature. Unbound secondary antibody was removed by washing in TBS then coverslips were mounted using DAPI Fluoromount-G.

Antibody (species)	Source	Cell immunostaining	Tissue immunostaining
Primary antibodies			
NeuN (mouse)	Chemicon (Millipore)	-	1:100
GFAP (rabbit)	Dako	1:1000	1:1000
Iba1 (rabbit)	Wako	-	1:500
Cartilage link protein-1 (goat)	R & D Systems	1:100	1:100
Neurocan (sheep)	R & D Systems	1:500	1:500
Parvalbumin	Swant	-	1:1000
5-HT (rabbit)	Immunostar	-	1:2000
GAD67 (mouse)	Chemicon (Millipore)	-	1:250
ChAT (Goat)	Chemicon (Millipore)	-	1:100
Calbindin	Cell Signalling Technologies	-	1:250
Synaptophysin (rabbit)	Cell Signalling Technologies	1:100	1:100
MAP2 (mouse)	Chemicon (Millipore)	1:100	-
MAP2 (rabbit)	Chemicon (Millipore)	1:1000	-
PSA (mouse IgM)	Hybridoma Bank	1:500	1:500
Lectin for PNN labelling			
WFA	Sigma, L1766	10 μg/ml	50 μg/ml

Table 2.2. Concentrations of primary antibodies used for immunofluorescence.

2.6 Data analysis and statistics

All data and statistical analysis was performed by a blinded assessor. All images were captured using a Leica Epifluorescence microscope (unless otherwise stated) and all analysis was performed using ImageJ (National Institute for Health).

2.6.1 Percentage of neurons with a PNN

2.6.1.1 Dissociated hippocampal cultures

To quantify the percentage of neurons with a PNN in dissociated hippocampal cultures, the number of WFA, LN1 or neurocan-positive PNNs was expressed as a percentage of the number of MAP2-labelled neurons. Forty images taken with a 20x objective were analysed per experiment and three independent experiments were analysed. Statistical significance was determined using a two-way ANOVA.

2.6.1.2 Following lentiviral vector injection to spinal cord

The number of GFP or mCherry-positive neurons was manually counted using the Cell Counter Plugin on ImageJ. The number of WFA, LN1 or neurocan-labelled PNNs surrounding transduced neurons was also counted and expressed as a percentage of the total number of transduced neurons. For each animal, three spinal cord sections were quantified, encompassing the intermediate grey matter and the ventral horn. Statistical significance was determined using a two-way ANOVA.

2.6.2 Density of synaptic inputs to neurons

2.6.2.1. Dissociated hippocampal cultures

The density of synaptophysin-labelled boutons contacting individual PNN-expressing hippocampal neurons was quantified using a custom script on ImageJ created by Prof. John Priestley. Thirty images of PNN-expressing neurons taken at 40x objective lens were captured per experiment and three independent experiments were quantified in total. The synaptophysin labelling is overlapped with the MAP2 labelling, to assess the area occupied by synaptophysin immunolabelling that was in contact with a MAP2-positive neuronal cell body. The area occupied by synaptophysin labelling was presented as a percentage of the

area of the neuronal cell body. Statistical significance was determined using a two-way ANOVA.

2.6.2.2. Following lentiviral vector injection into the spinal cord

The density of synaptophysin and serotonin-positive boutons on individual transduced neurons was quantified using the same script described above. For each animal, three spinal cord sections were quantified, encompassing the intermediate grey matter and the ventral horn. Statistical significance was determined using a two-way ANOVA.

2.6.3 Density of individual PNNs

2.6.3.1. Dissociated hippocampal cultures

The density of individual PNNs was analysed using a custom script on Image J created by Prof. John Priestley. Thirty high magnification (40x objective) images were captured per experiment and the area occupied by PNN labelling was manually thresholded using Image J. The area occupied by individual PNNs was converted into μm^2 and three independent experiments were analysed in total. Statistical significance was determined using a two-way ANOVA.

2.6.3.2. Following lentiviral vector delivery into the spinal cord

The density of WFA, LN1 or neurocan-labelled PNNs surrounding transduced neurons was quantified using the same script that measured the density of synaptic inputs to transduced neurons. Data was obtained from three spinal cord sections per animal, encompassing the intermediate grey matter and the ventral horn. Statistical significance was determined using a two-way ANOVA.

2.6.4 PSA expression

2.6.4.1. Dissociated hippocampal cultures

Twenty images were captured per experiment using a 20x objective. The area occupied by PSA immunolabelling was quantified in a 500 μm x 500 μm box, using a custom script designed for Image J. The area occupied by PSA was reported as a percentage of the area of

the quantification box and three independent experiments were quantified. Statistical significance was determined using a one- or a two-way ANOVA.

2.6.4.2. Lentiviral vector delivery into the spinal cord

For each animal, images encompassing all injection sites were taken using a 20x objective lens on three spinal cord sections (intermediate grey matter and ventral horn). The area occupied by PSA labelling was manually thresholded on Image J and quantified using the 'measure' function. The values obtained were converted into μm^2. Statistical significance was determined using a two-way ANOVA.

2.6.5 Behavioural tests

A two-way repeated measures ANOVA was used to compare open field locomotor function, performance at the grid exploratory test and performance at the Montoya staircase test in animals that received either lateral hemisection injury or laminectomy only, and either injections of LV/PST or LV/GFP. A two-way ANOVA was used to compare the responses to thermal and mechanical stimuli in these animals.

2.6.6. Statistical analysis

All data in this thesis is presented as mean $\pm$ standard error of the mean (SEM) and statistical analysis was performed using GraphPad Prism software. Statistical significance was determined when $p<0.05$ for all experiments.

Chapter 3

Distribution of perineuronal net molecules in the cervical spinal cord

Chapter 3: Distribution of perineuronal net molecules in the cervical spinal cord

3.1 Introduction

3.1.1 The neuronal extracellular matrix

As previously mentioned in section 1.1.1, the neuronal extracellular matrix can be subdivided into three distinct regions, namely (i) basement membrane (ii) the interstitial matrix and (iii) the PNN, which are classified based on their localisation and structure (Barros et al., 2011). With different molecular components found in each type of extracellular matrix, they all have varying functions and can respond differently to injury or diseases of the nervous system (Barros et al., 2011). As the detailed structure and function of the extracellular matrix was previously described in detail, it will only be touched upon here.

The PNN is a specialised form of extracellular matrix, which has previously been observed to surround some populations of neurons during early postnatal development stages in the CNS, and throughout adulthood (Carulli et al., 2007; Galtrey et al., 2008). Compared to both the basement membrane and the interstitial matrix, the PNN does not contain the 'classical' extracellular matrix molecules such as collagen, laminin and fibronectin, but contains a high proportion of CSPGs and supporting molecules (Carulli et al., 2007; Galtrey et al., 2008). This underlies the main function of the PNN, which is the restriction of neuroplasticity and the stabilisation of synapses in the adult CNS (Pizzorusso et al., 2002).

The PNN can be detected in brain and spinal cord tissue sections using lectin from WFA, which binds to N-acetylgalactosamine units that compose the GAG side chains of CSPGs (Rhodes and Fawcett, 2004). Additionally, antibodies have been raised against a number of components of the PNN, such as LN1, tenascin-R, semaphorin 3A and individual CSPGs such as neurocan, aggrecan, brevican, phosphacan and versican (Carulli et al., 2007; Galtrey et al., 2008). The hyaluronan backbone of the PNN can be reliably detected using a biotinylated hyaluronan binding protein (Carulli et al., 2007; Galtrey et al., 2008).

To date, there have been a number of studies that have examined the distribution and development of PNNs in the CNS, using a combinatorial approach of immunohistochemistry and *in situ* hybridization. While the general structure and composition of these structures are consistent between the brain and the spinal cord, there are regional differences in the subtypes of CSPGs expressed in PNNs (Galtrey et al., 2008). Additionally, some studies have investigated the phenotype of PNN-expressing neurons (Vitellaro-Zuccarello et al., 2007). What is lacking in these studies is a quantitative assessment of the types and relative amounts of synaptic inputs to PNN-expressing neurons. As mounting evidence suggests enzymatic degradation of PNNs following SCI can enhance both axonal regeneration and sprouting, in addition to the density of synaptic boutons, understanding the type of synaptic connections to PNN-expressing neurons is crucial.

3.1.2 Aims

The primary aim of this study was to investigate the distribution of WFA-labelled PNNs in the rat cervical spinal cord, and to compare this with PNNs immunolabelled using antibodies raised against LN1 and neurocan. LN1 and neurocan were selected as PNN markers as mounting evidence supports the vital role of LN1 for PNN formation, and as neurocan has previously been shown to bind to NCAM (Friedlander et al., 1994; Carulli et al., 2010). Additionally, the relative density of synaptic inputs to PNN-expressing neurons was studied.

3.2 Results

3.2.1 General characteristics of perineuronal net labelling in the cervical spinal cord

Epifluorescence images of adult rat cervical spinal cord sections revealed the close association between the pericellular PNN and the neuronal cell body (Figure 3.1A-C), and under higher-power confocal microscopy it was possible to visualise the 'honeycomb' structure of the PNN on the surface of ventral horn neurons (Figure 3.1D-F). To determine whether PNNs are found heterogeneously distributed throughout the grey matter of the spinal cord, different regions of the cervical spinal cord were analysed for PNNs.

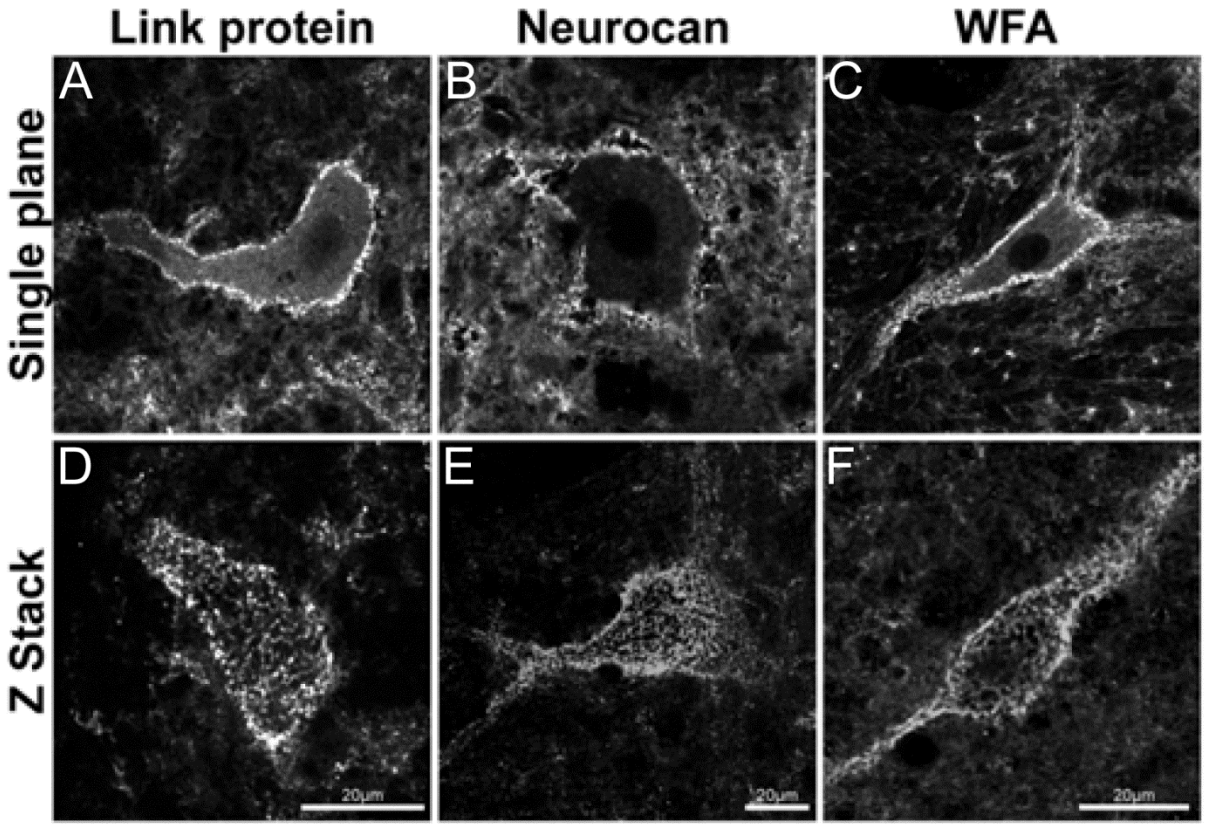

Figure 3.1. Structure of PNNs in the cervical spinal cord.
PNNs were detected in spinal cord tissue using antibodies against link protein (LN1) and neurocan, or lectin from WFA. **(A-C)** In the grey matter, PNNs are found surrounding the neuronal cell body (single plane). **(D-F)** High magnification confocal imaging of single neurons revealed the 'honeycomb' structure of the PNN on the neuronal surface.

3.2.2 PNN expression in the dorsal horn

To investigate the proportion of neurons with a PNN in the cervical spinal cord dorsal horn, sections were double-labelled using antibodies against neuronal nuclei antigen (NeuN), to label neuronal cells, and the PNN components; LN1 or neurocan, or WFA (Figure 3.2A-C). In the dorsal horn, WFA labelling was sparse and the percentage of neurons surrounded by a PNN was low (5.2 ± 0.6 %, Figure 3.2C, D). LN1 or neurocan-positive PNNs were found at a similar frequency to those labelled with WFA (LN1, 4.4 ± 1.1 %; neurocan, 7.0 ± 2.9 %, Figures 3.2A-D). A comparison of PNN density detected by each marker, calculated as a percentage of NeuN labelling, showed no significant difference between the density of LN1-positive or WFA-labelled PNNs in the dorsal horn (LN1, 38.5 ± 2.3%; WFA 37.9 ± 1.8% Figure 3.2E). Interestingly, the density of neurocan-positive PNNs was significantly less compared with those positive for LN1 or WFA (28.0 ± 2.4 %, Figure 3.2E). No significant difference was

observed in the mean size of neurons expressing LN1, neurocan or WFA-labelled PNNs (Supplementary Figure 1A).

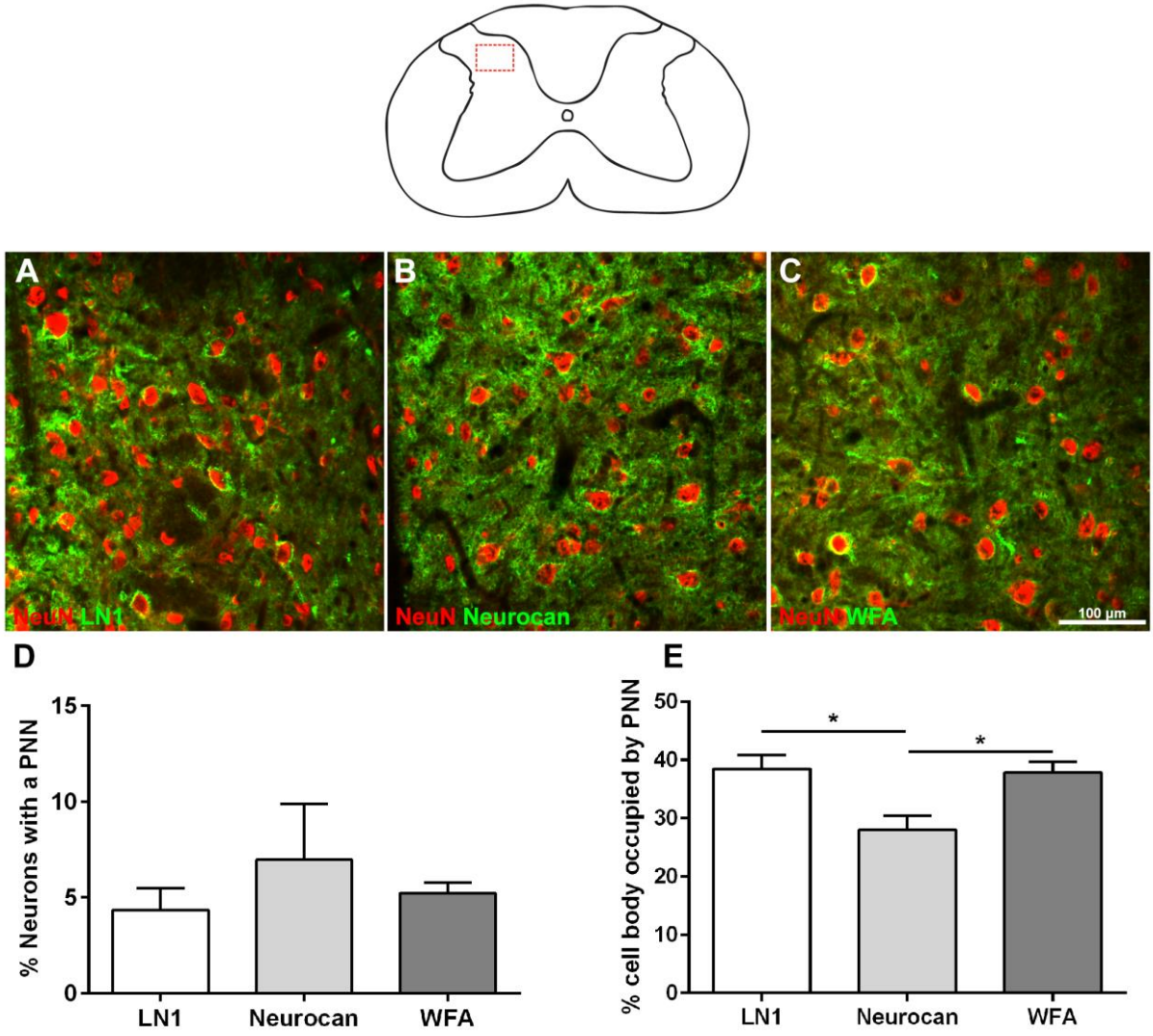

Figure 3.2 PNNs in the dorsal horn.
(A-C) Double fluorescent labelling was used to assess the proportion of neurons surrounded by PNNs in the dorsal horn. LN1, neurocan or WFA-labelled PNNs were associated with NeuN-positive neuronal cell bodies. **(D)** Quantification of the percentage of neurons with a PNN revealed no difference between the three PNN markers (n=3, p>0.05, one-way ANOVA). **(E)** Quantification of the area of the neuronal cell body occupied by PNN labelling revealed a significant difference between neurocan-containing PNNs, compared with LN1-positive or WFA-labelled PNNs. n=3, * $p < 0.05$, one-way ANOVA, Tukey's post hoc.

To assess the relationship between WFA-labelled and LN1 or neurocan-positive PNNs, double fluorescent labelling was performed using WFA and either LN1 or neurocan antibody. WFA labelling within PNNs ranged in intensity, as did LN1 or neurocan staining

intensity (Figure 3.3). LN1-immunoreactivity was strong in 71% of WFA-labelled PNNs (Figure 3.3A, arrows) and neurocan was strong in 67% of WFA-labelled PNNs (Figure 3.3B, arrows, Summary Figure 3.20).

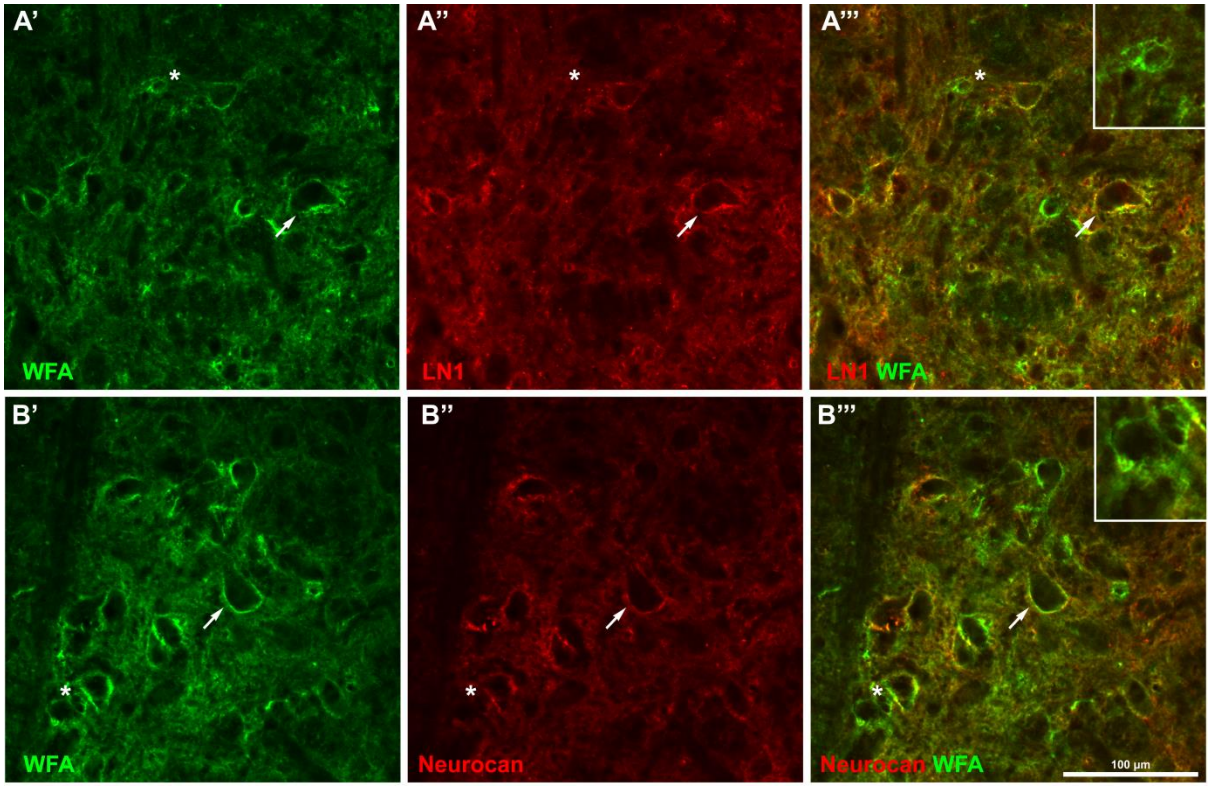

Figure 3.3. Co-localisation of WFA-labelled PNNs with LN1 or neurocan in the dorsal horn. Double-labelling was used to reveal the association between WFA-labelled PNNs and LN1 or neurocan in the dorsal horn region of the spinal cord. **(A'-A''')** WFA-labelled PNNs contained high levels of LN1 (arrows). Remaining PNNs are weak for LN1 (asterisks). **(B'-B''')** Some WFA-labelled PNNs are strong for neurocan while others are weakly labelled (asterisks). Scale bar 100 µm.

To assess the density of synaptic boutons in contact with PNN-expressing neurons, sections stained with WFA were double-labelled with ChAT (cholinergic fibres), 5-HT (serotonergic fibres) or GAD67 (GABAergic fibres). The area occupied by immunopositive synaptic boutons was calculated as a percentage of the size of the cell surface. The density of inhibitory terminals in contact with the surface of PNN-expressing dorsal horn neurons was relatively high (GAD67, 14.5 ± 1.4 % Figure 3.4A). The density of serotonergic and cholinergic immunopositive boutons contacting PNN-expressing neurons was low (5-HT, 4.7 ± 1.2 %; ChAT, 1.1 ± 0.3 %, Figure 3.4B-C, Summary Figure 3.20). To investigate whether a

relationship existed between the density of synaptic input and the size of the PNN, a linear regression analysis was performed for the PNN size with density of synaptic inputs to individual PNN-expressing neurons. There was no correlation between the extent of WFA labelling versus the density of synaptic input on PNN-expressing neurons for GABAergic, serotonergic or cholinergic synaptic boutons (R^2 = 0.14, 0.29, 0.17, respectively, Figures 3.4D-F).

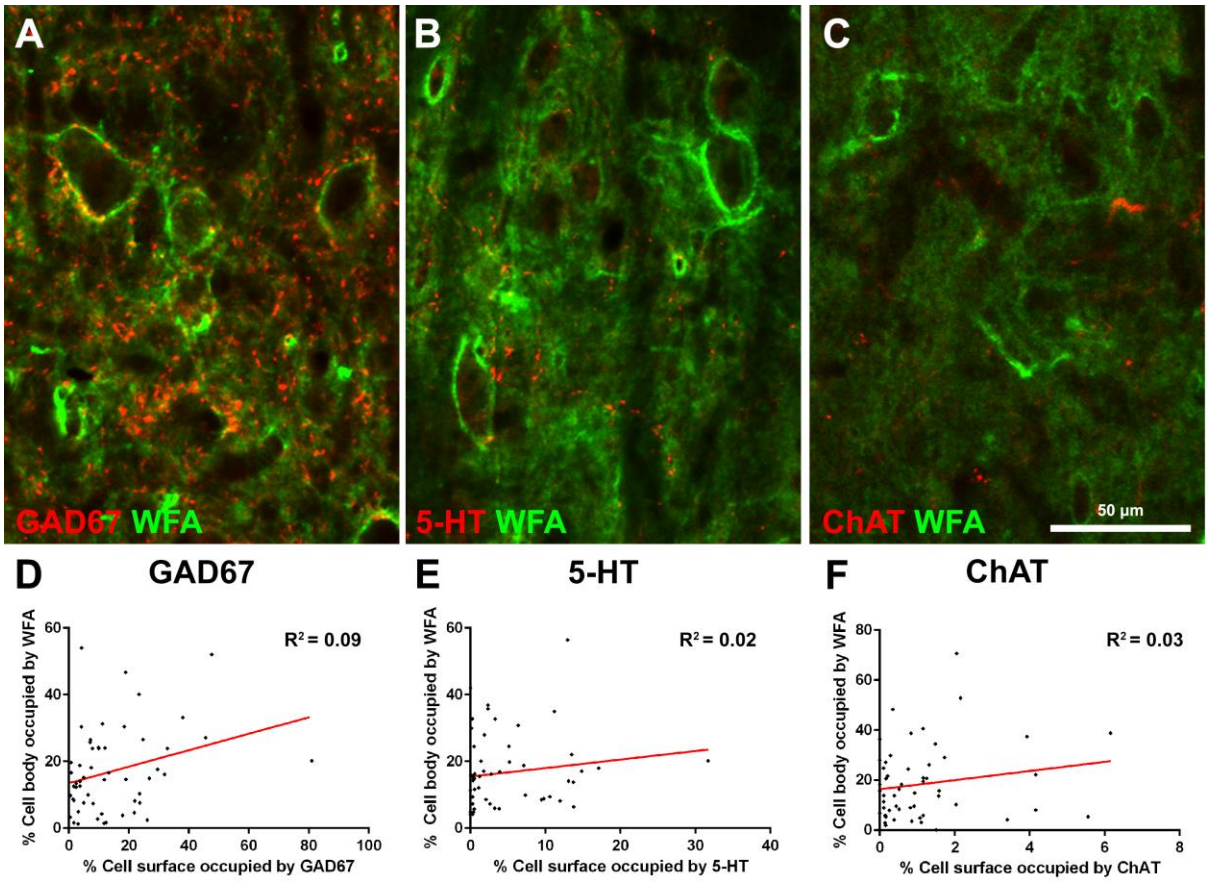

Figure 3.4. Synaptic inputs to PNN-expressing neurons in the dorsal horn.
Double-labelling using WFA lectin and antibodies against GAD67, 5-HT or ChAT was used to assess the relationship between the PNN and the density of synaptic input to PNN-expressing neurons. **(A)** neurons with a PNN received moderate levels of inhibitory input. **(B, C)** PNN-expressing neurons received sparse serotonergic and cholinergic input. **(D-F)** the density of inhibitory, serotonergic or cholinergic synaptic inputs to PNN-expressing neurons does not correlate with the density of WFA labelling (linear regression, R^2 = 0.09, 0.02 and 0.03, respectively).

3.2.3 Intermediate grey matter

For this study the intermediate grey matter (IMG) has been subdivided into three regions; (i) dorsal IMG encompasses lamina VI and the dorsal region of VII, (ii) lamina X, as defined by

Bror Rexed, (iii) ventral IMG, which includes the ventral region of lamina VII and dorsal regions of lamina VIII. Each region of the IMG will be discussed in separate sections in this subchapter.

3.2.3.1 PNN expression in the dorsal IMG

PNNs were found throughout the dorsal IMG and could be detected by LN1 and neurocan antibodies, or WFA (Figures 3.5A-C, respectively). No significant difference was observed between the percentage of neurons with a LN1-positive PNN or those labelled by WFA (LN1, 9.5 ± 1.0 %; WFA, 12.3 ± 0.6 %, Figure 3.5D). The proportion of neurons with a neurocan-positive PNN was significantly reduced, compared to WFA-labelled PNNs (7.4 ± 0.1 %, $p < 0.05$; one-way ANOVA, Tukey's post hoc, Figure 3.5D). Although there was a difference in the number of neurocan and WFA PNNs in the dorsal IMG, the density of individual PNNs was unchanged for all examined markers (Figure 3.5E). No significant difference was observed in the size of neurons with PNNs positive for LN1, neurocan or labelled by WFA (Supplementary Figure 1B)

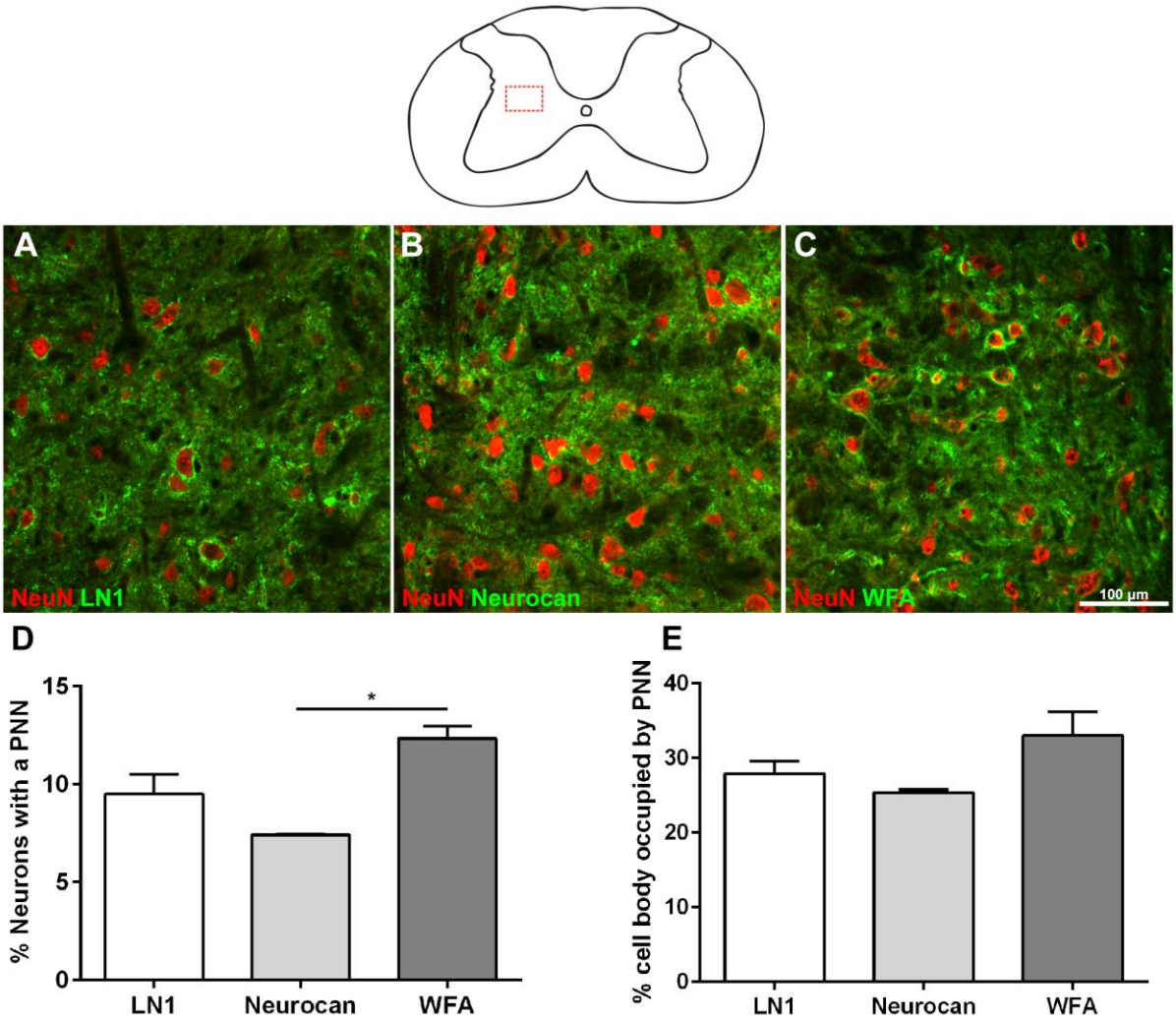

Figure 3.5. PNN expression in the dorsal IMG.
(A-C) LN1, neurocan or WFA-labelled PNNs were found surrounding neurons in the dorsal IMG region of the spinal cord. **(D)** Analysis of the proportion of neurons with a PNN revealed a significant reduction in the percentage of neurons with a neurocan-positive PNN, compared to those labelled by WFA (n =3, $p < 0.05$, one-way ANOVA, Tukey's post hoc). **(E)** No significant difference in the densities of PNNs with the three markers (n=3, p>0.05, one-way ANOVA). Scale bar = 100 µm.

The density of individual WFA-labelled PNNs was variable in the dorsal IMG (Figure 3.6). Strong LN1 immunolabelling was present in 65% of WFA-labelled PNNs (Figure 3.6A, arrows). Similar number of PNNs contained strong neurocan immunoreactivity (61%, Figure 3.6B, arrows, Summary Figure 3.20). A subpopulation of PNNs were strongly labelled by WFA but had weak LN1 or neurocan immunolabelling (Figure 3.6, asterisks).

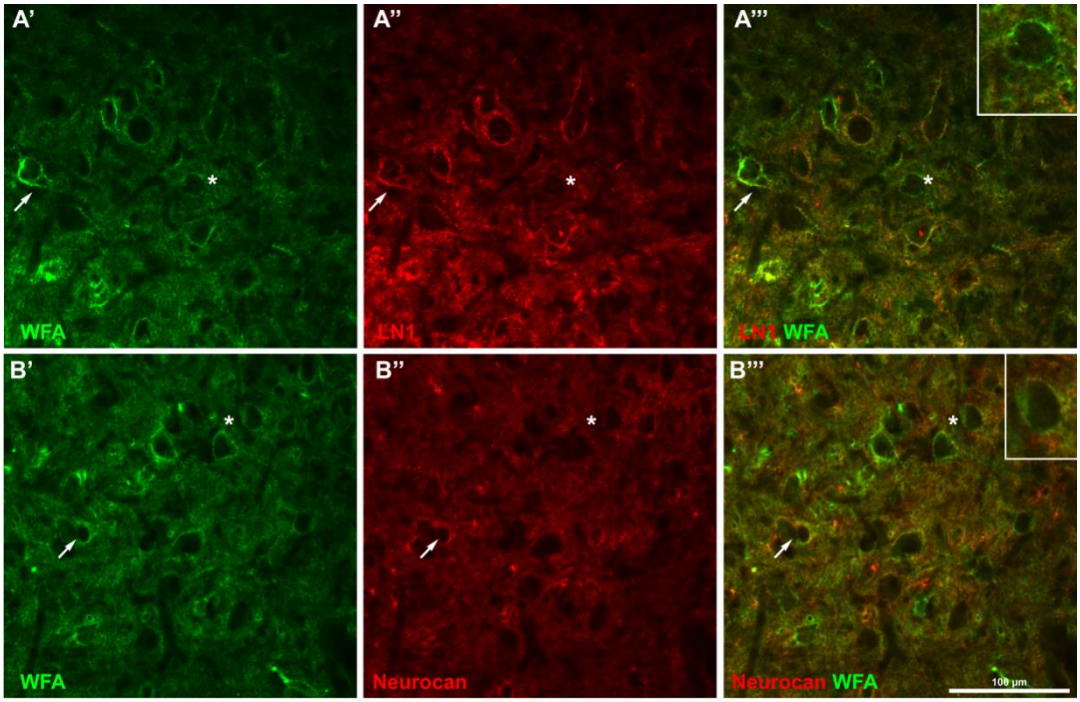

Figure 3.6. Colocalisation of different PNN components in neurones located in the dorsal IMG.
(A) Intensity of LN1 staining was variable between WFA-labelled PNNs. WFA-labelled PNNs can display weak (asterisks) or strong (arrows) LN1 immunoreactivity **(B)** Variable co-immunostaining was also present for neurocan between different neurons. Scale bar = 100 µm.

PNN-expressing neurons in the dorsal-IMG received a similar density of cholinergic and serotonergic inputs (cholinergic, 2.0 ± 0.7 %; serotonergic, 2.8 ± 0.9 %, Figure 3.7B-C). The density of GABAergic synaptic boutons contacting PNN-expressing neurons was much higher (27.9 ± 5.0 %, Figure 3.7A, Summary Figure 3.20). There was no correlation between the density of PNN labelling and the density of synaptic input to PNN-expressing neurons in the dorsal-IMG (GAD67 R^2=0.04; 5-HT R^2=0.08; ChAT R^2=0.01, linear regression, Figure 3.7D-E).

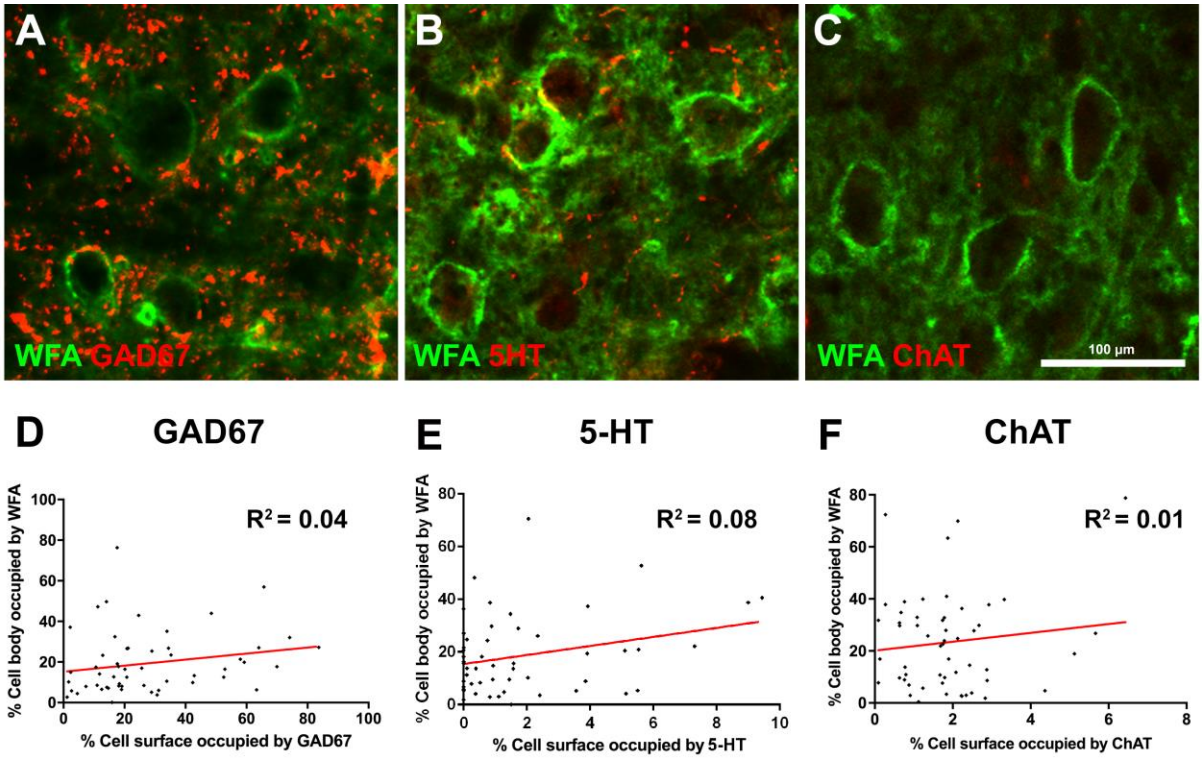

Figure 3.7. Synaptic inputs to PNN-expressing neurons in the dorsal-IMG
The relationship between synaptic inputs to PNN-expressing neurons and density of WFA labelling was assessed. **(A)** Neurons in the dorsal-IMG that express WFA-labelled PNNs receive moderate levels of inhibitory input (GAD67). **(B)** The density of serotonergic boutons in contact with these neurons is low. **(C)** PNN-expressing neurons receive sparse cholinergic input. **(D-F)** No correlation was observed between the density of inhibitory, serotonergic or cholinergic inputs to individual PNN-expressing neurons and the density of PNN labelling neurons (linear regression).

3.2.3.2 PNN expression in lamina X

Lamina X consists of a small region of grey matter surrounding the central canal. A population of small diameter neurons in lamina X were surrounded by a dense, WFA-labelled PNN. These neurons can be observed in horizontal sections of spinal cord, in small columns that are found parallel to the central canal (Figure 3.8A). LN1 or neurocan labelling in lamina X was generally much weaker compared with WFA (Figure 3.8C, E). Some LN1 or neurocan-containing PNNs could be detected in lamina X, however, labelling was generally weak. Few of the WFA-labelled PNNs contained LN1 (23%) or neurocan (21%).

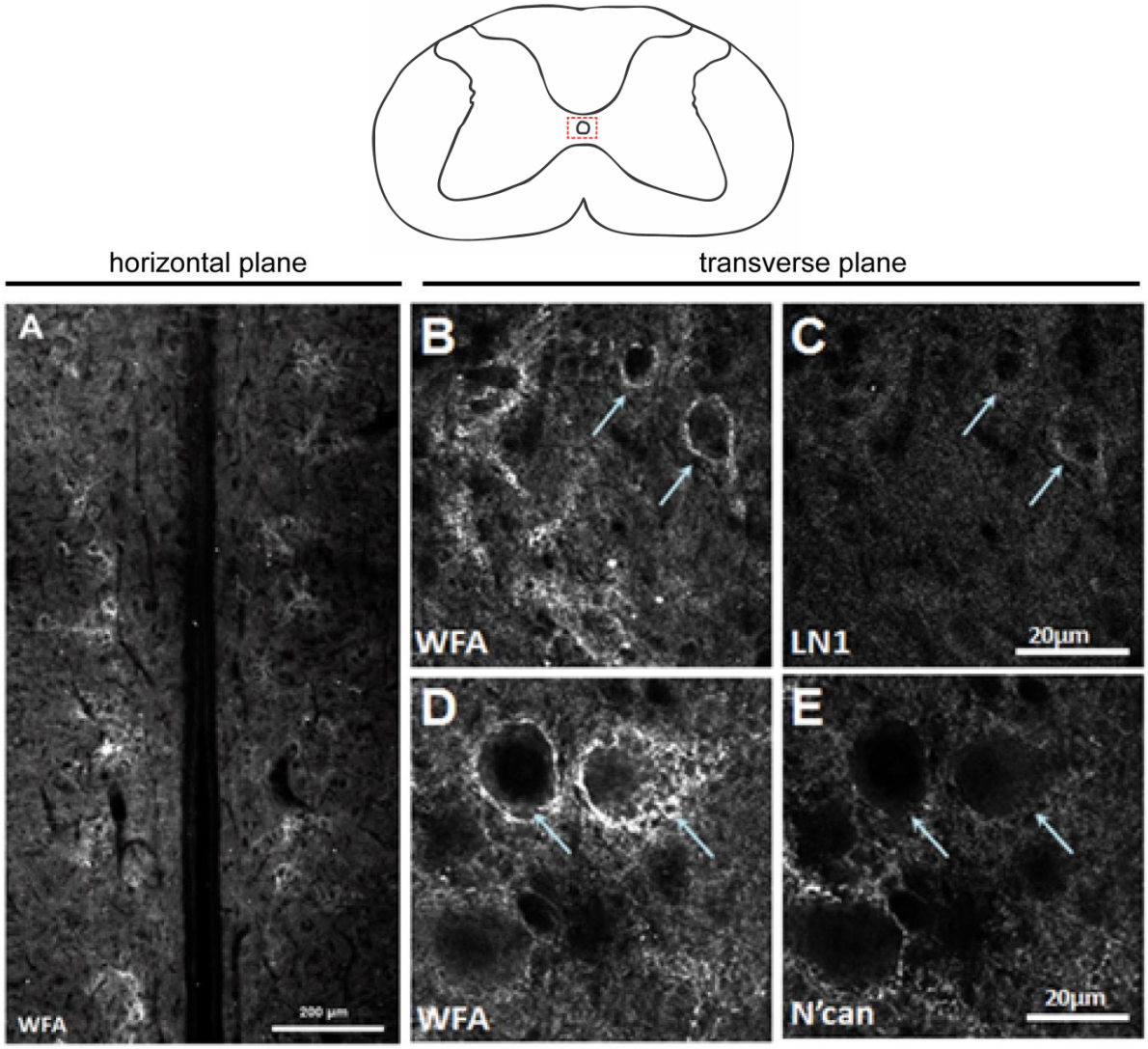

Figure 3.8. Neurons in lamina X expresses dense WFA-labelled PNN.
(A) A population of neurons in lamina X located parallel to the central canal were surrounded by WFA-labelled PNNs when spinal cord was cut in the horizontal plane. **(B-C)** WFA-labelled PNNs in lamina X were weakly immunopositive for LN1. **(D-E)** Neurocan labelling was weak in these PNNs. Scale bars; A = 200 µm, B-E = 20 µm.

Lamina X is the location of a cholinergic population of neurons known as central canal cluster neurons (Barber et al., 1984; Miles et al., 2007). To determine whether the PNN-expressing neurons were part of this neuronal population, sections were double-labelled with WFA and ChAT. PNN-expressing in lamina X neurons were non-cholinergic and the density of cholinergic immunoreactive terminals contacting these neurons was low (Figure 3.9A, B). The density of serotonin immunoreactive terminals contacting individual PNN-expressing neurons was also low (Figure 3.9C), but higher numbers of inhibitory boutons contacted these neurons (Figure 3.9E). Double fluorescent labelling was performed using

WFA lectin and antibodies against calbindin or parvalbumin to determine whether the lamina X PNN-expressing neurons were immunopositive for either of these proteins. Occasional calbindin immunoreactive neurons were observed in lamina X, however, none were surrounded by a WFA-labelled PNN (Figure 3.9D). Interestingly, a proportion of PNN-expressing neurons were found to contain parvalbumin (Figure 3.10, arrows).

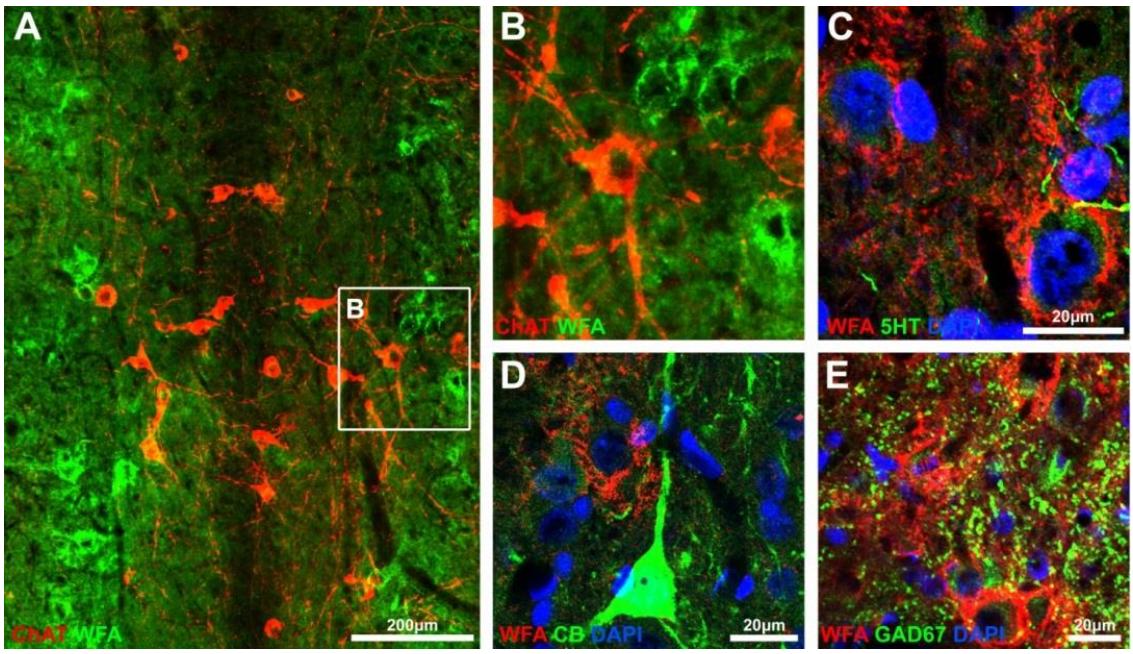

Figure 3.9. Density of synaptic terminals contacting lamina X PNN-expressing neurons. **(A-B)** Neurons with a dense, WFA-labelled PNN in lamina X were non-cholinergic, and a low proportion of the cell body had cholinergic bouton contacts. **(C)** The density of serotonergic terminals contacting PNN-expressing neurons was low. **(D)** The calcium-binding protein calbindin was not expressed by these neurons. **(E)** The density of inhibitory boutons contacting lamina X PNN-expressing neurons was relatively high.

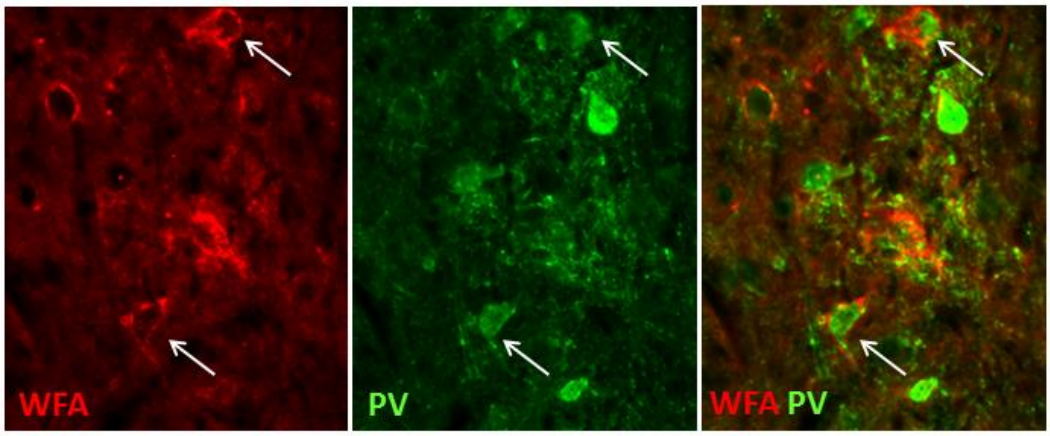

Figure 3.10. Colocalisation of parvalbumin and PNN immunolabelling in lamina X
To assess whether the lamina X PNN-expressing neurons contained the calcium binding protein parvalbumin (PV), sections were double-labelled for WFA and antibody against PV Some of the PNN-expressing neurons were positive for parvalbumin (arrows).

A second neuronal population expressing strong WFA-labelled PNNs was present in lamina X (Figure 3.11A, arrows). These neurons were large in diameter, with cell bodies near or at the midline, which projected to both sides of the spinal cord. However, there was a sparse number of these neurons with only one or two observable neurons per section of spinal cord (intermediate grey). These neurons had PNNs that were weakly immunopositive for LN1 (Figure 3.11B) or neurocan (Figure 3.11C). The density of inhibitory synaptic boutons contacting the neurons was low (Figure 3.11D), as was the density of serotonergic or cholinergic terminals (Figure 3.11E-F).

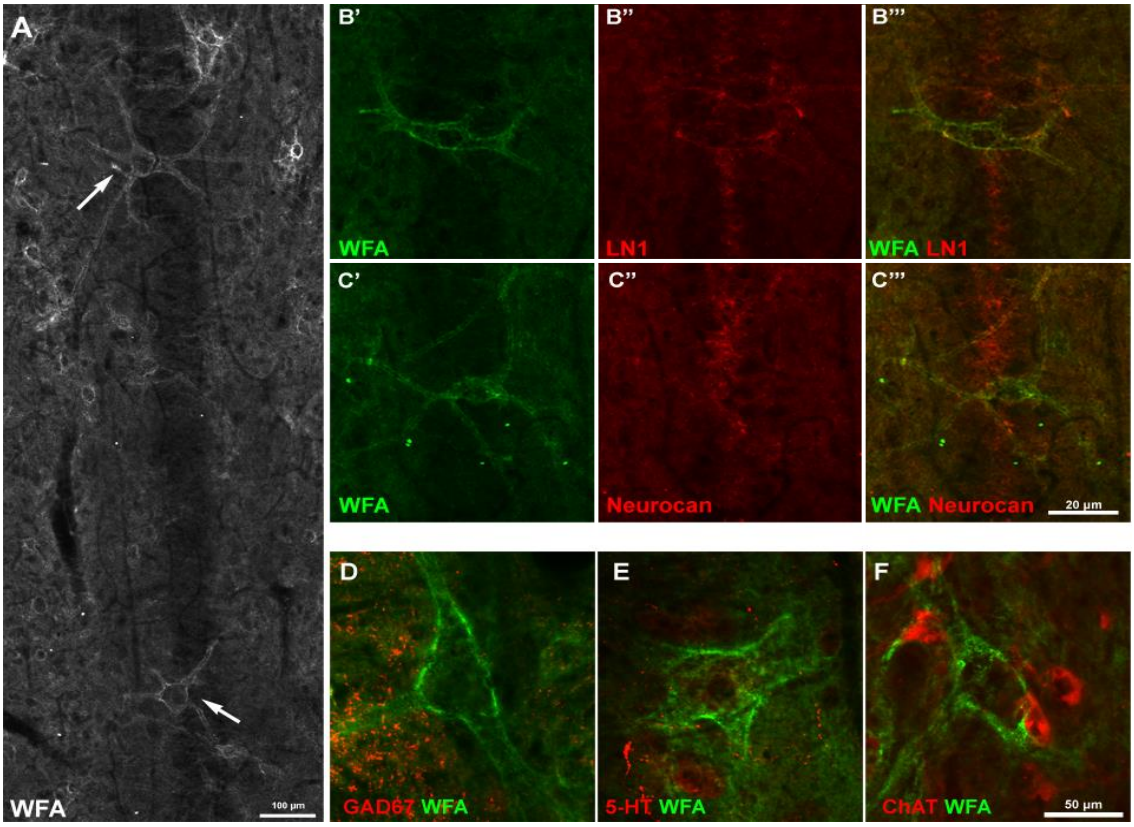

Figure 3.11. Large diameter neurons in lamina X expresses a dense WFA-labelled PNN
(A) A small population of large neurons in lamina X were surrounded by a WFA-labelled PNN (arrows). The cell body of these neurons was close to the spinal midline. **(B)** These PNN-expressing neurons in lamina X were weakly immunopositive for LN1. **(C)** These neurons were also weakly immunopositive for neurocan (C''). **(D-F)** The density of GABAergic, serotonergic or cholinergic boutons in contact with these lamina X PNN-expressing neurons was low.

3.2.3.3 PNN expression in the ventral IMG

Throughout the ventral IMG, PNN-labelled neurons were immunopositive for LN1 or neurocan which could be detected by WFA labelling (Figure 3.12A-C, respectively). No difference was observed in the percentage of neurons expressing a LN1 or a neurocan-positive PNN (LN1, 11.1 ± 1.9 %; neurocan, 12.7 ± 3.5%) or those labelled by WFA (14.5 ± 0.9 %, Figure 3.12D). No difference was observed in the densities of PNNs or the size of neurons expressing PNNs (Figure 12E, Supplementary Figure 1C, respectively).

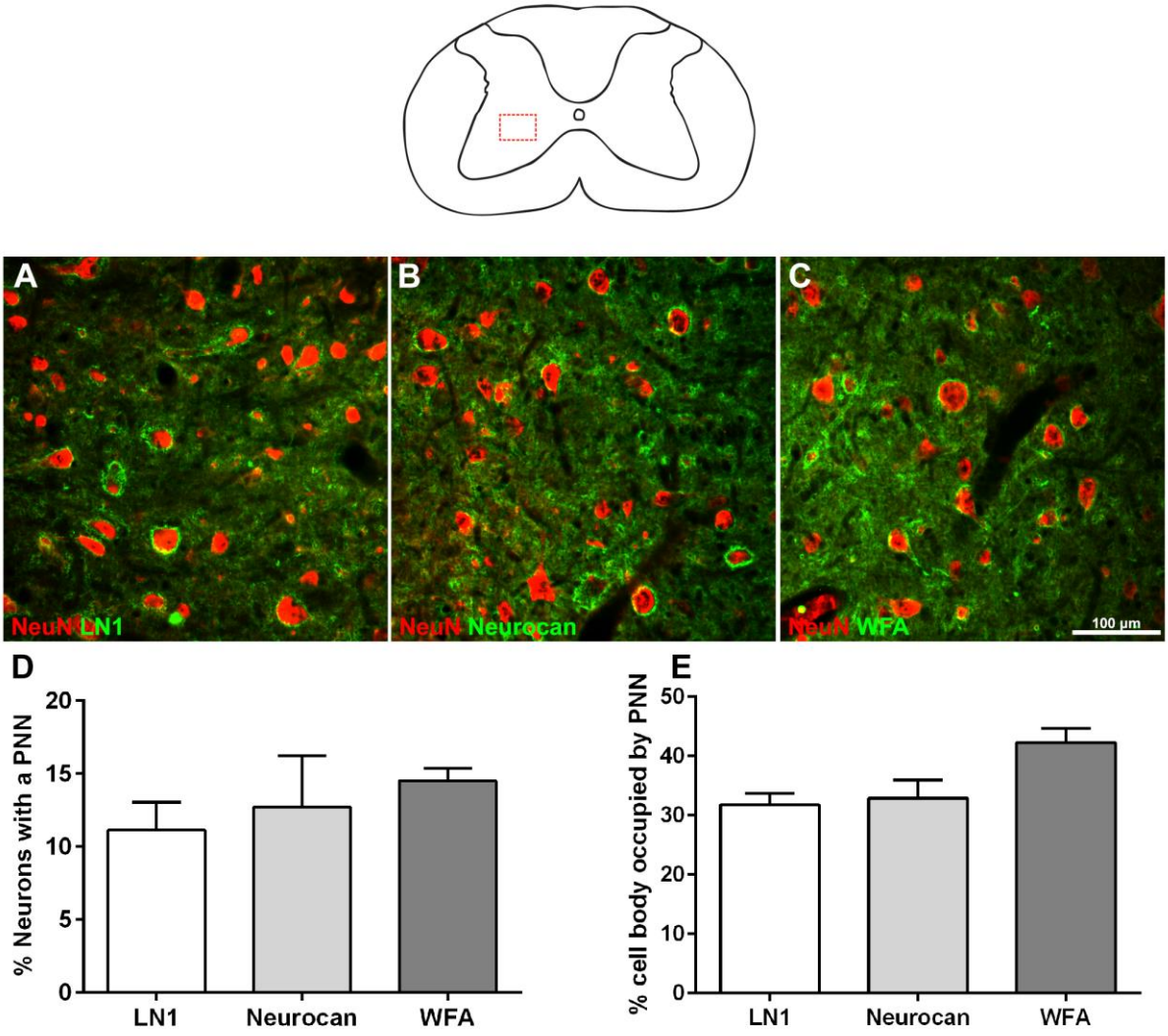

Figure 3.12. PNN-expressing neurons in the ventral IMG.
(A-C) PNNs labelled with LN1, neurocan or WFA were observed in the ventral IMG. **(D)** Quantification of the percentage of neurons with a PNN revealed no difference between the three PNN markers examined. **(E)** Quantification of the area of the neuronal cell body occupied by PNN labelling revealed no significant difference between LN1, neurocan or WFA-labelled PNNs (n=3, p>0.05, one-way ANOVA). Scale bar = 100 µm.

WFA labelling of individual PNNs varied in intensity (Figure 3.13). The proportion of WFA-labelled PNNs expressing high levels of LN1 immunoreactivity was 62.3% (Figure 3.13A, arrows). Similar numbers of PNNs (59.8%) had high neurocan immunoreactivity (Figure 3.13B, arrows, Summary Figure 3.20).

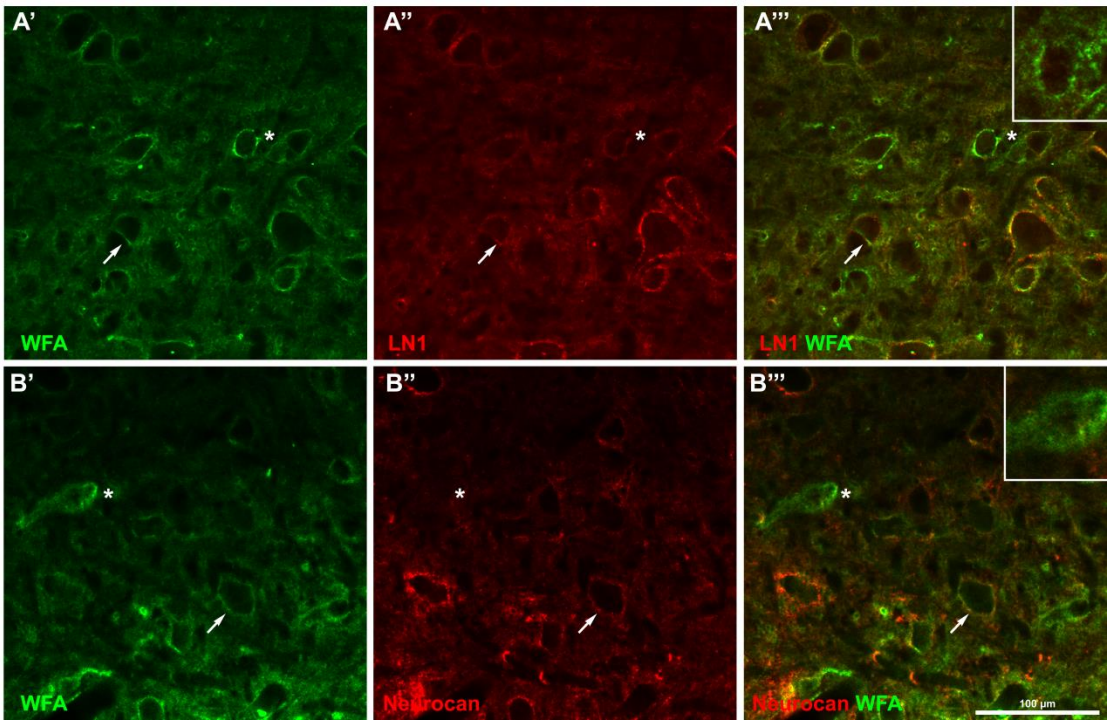

Figure 3.13. Co-localisation between various PNN components in the neurons located in the ventral IMG.
(A) WFA-labelled and LN1-positive PNNs show a partial overlap in the ventral IMG. WFA-labelled PNNs contained a mixture of strong (arrows) or weak LN1-immunolabelling (asterisks). **(B)** WFA-labelled PNNs can also co-localise with neurocan immunolabelling. Scale bar = 100 µm.

The density of inhibitory boutons in contact with ventral IMG PNN-expressing neurons was 24% ± 1.9% (Figure 3.14A). By comparison, the densities of serotonergic (5.1 ± 1.2%) and cholinergic (7.0 ± 1.3%) terminals were relatively low (Figure 3.14B-C, Summary Figure 3.20). There was no correlation between the density of the PNN and the density of synaptic terminals contacting PNN-expressing neurons (GAD67 R^2=-0.07, 5-HT R^2=0.09, ChAT R^2=0.002, linear regression, Figure 3.14D-F).

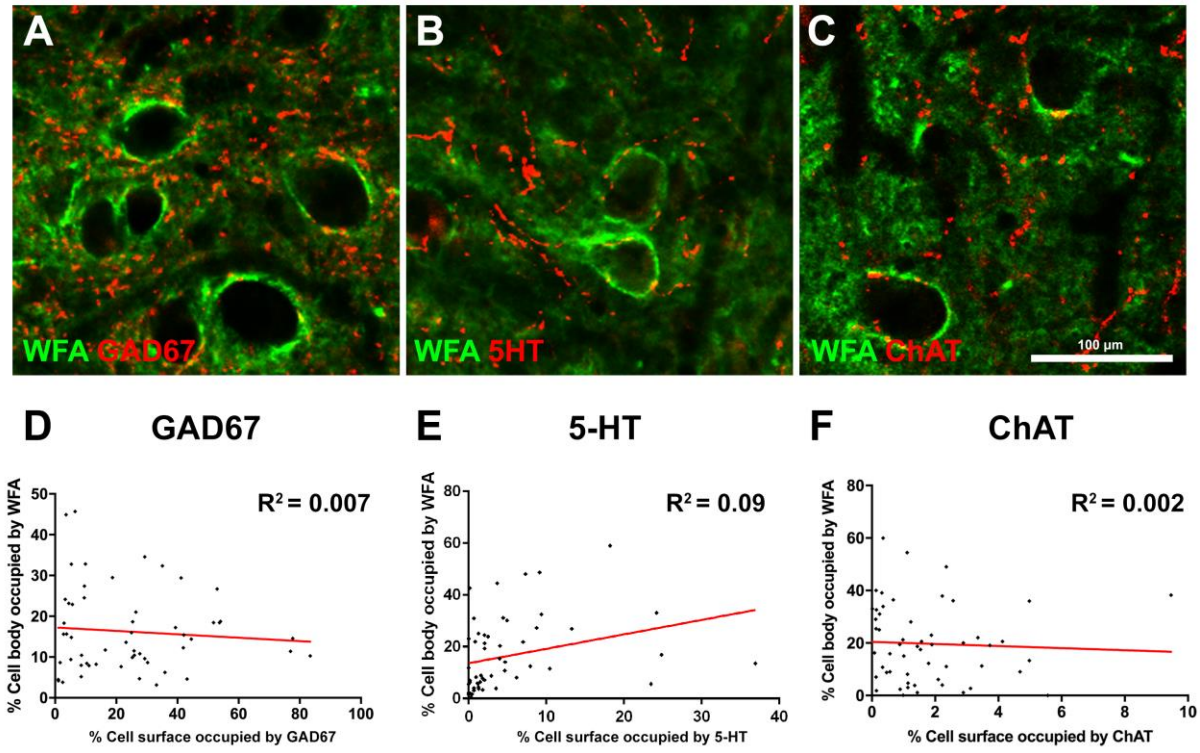

Figure 3.14. Synaptic inputs to PNN-expressing neurons in the ventral IMG
(A-C) Representative photomicrographs showing synaptic inputs to PNN-expressing neurons in the ventral-IMG. **(A)** The density of inhibitory boutons contacting PNN-expressing neurons in the ventral IMG was relatively high. **(B)** PNN-expressing neurons were contacted by low numbers of serotonergic terminals. **(C)** Similarly, the density of cholinergic boutons contacting PNN-expressing neurons was low. **(D-F)** There was no correlation between the density of inhibitory, serotonergic or cholinergic boutons on individual PNN-expressing neurons and the density of WFA immunolabelling. (linear regression). Scale bar = 100 µm.

3.2.4 PNN expression in the ventral horn

Ventral horn neurons had the highest proportion of PNNs, compared with other regions of the spinal cord (Figure 3.15). No significant difference was observed between the percentage of neurons with a LN1 (14.3 ± 1.5 %) or neurocan (16.3 ± 2.1 %) containing PNN or those labelled by WFA (17.8 ± 0.4 %, Figure 3.15D). Low magnification images revealed a difference in PNN expression throughout the ventral horns (Figure 3.15A-C). Bright LN1 and neurocan immunolabelling was found around motor neurons, identified based on their large cell body size and location in the lateral regions of the ventral horns (Figure 3.15A-B). Interneurons were identified based on their smaller cell body. Weak WFA-immunolabelling was present around motor neurons, but stronger WFA-immunolabelling surrounded

smaller-diameter interneurons located in the medial region of the ventral horns (Figure 3.15C).

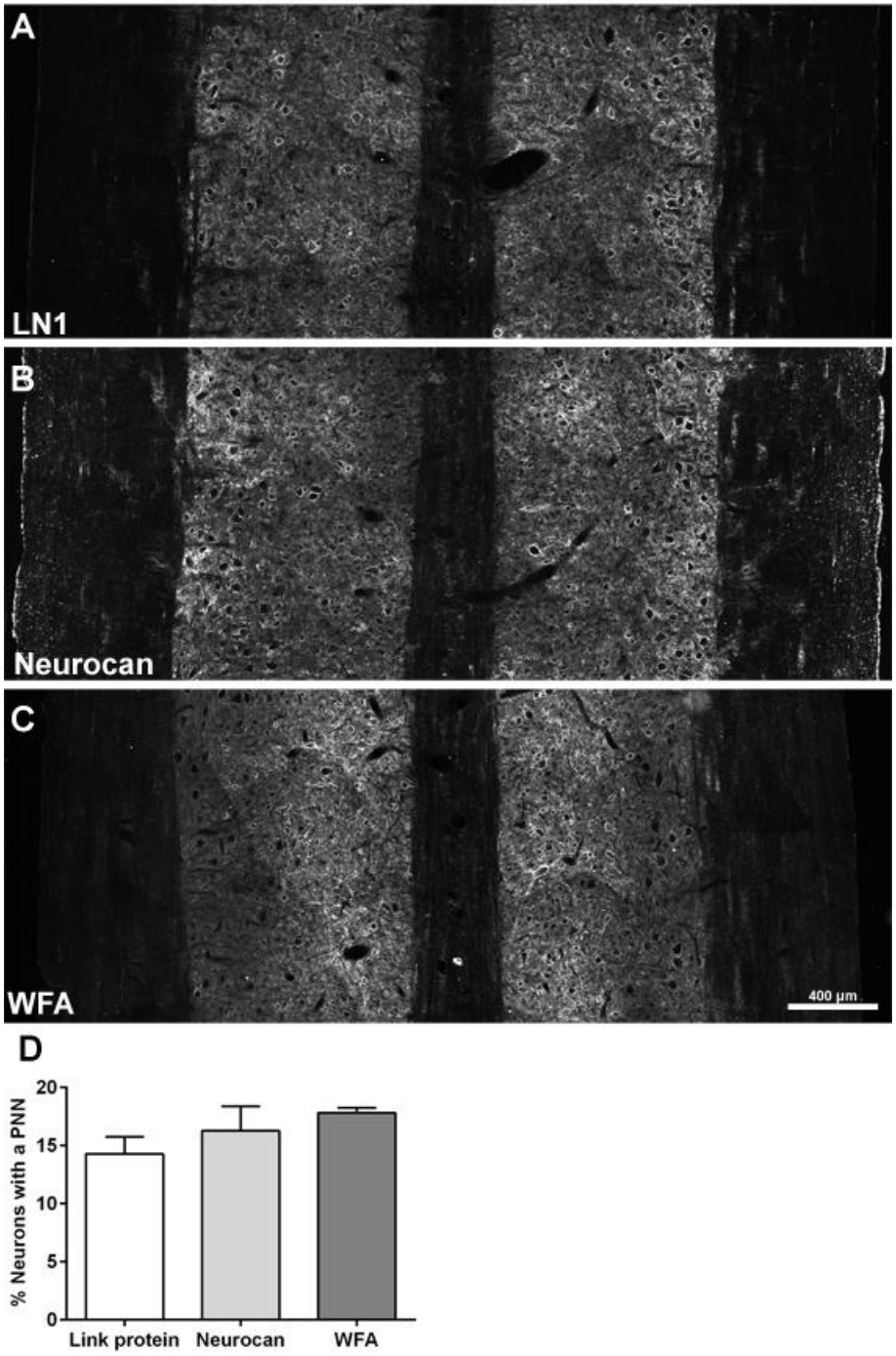

Figure 3.15. PNN-expressing neurons in the ventral horn.
Neurons in the ventral horn were surrounded by LN1 **(A)**, neurocan **(B)** or WFA-labelled PNN **(C)**. **(D)** The percentage of neurons with a PNN was not significantly different for all three PNN markers (n=3, p>0.05, one-way ANOVA).

Due to the apparent difference in PNN expression between motor neurons and interneurons in the ventral horns, the density of PNNs was analysed separately for both neuronal cell types. No significant difference was observed between the densities of LN1 (18.7 ± 2.5 %) or neurocan-positive (20.5 ± 1.4 %) PNNs surrounding motor neurons (Figure 3.16A, B, G). The density of WFA-labelled PNNs on motor neurons was significantly lower than those positive for LN1 or neurocan (6.8 ± 0.9 %, $p<0.01$, one-way ANOVA, Figure 3.16C,G). No significant difference was observed in the densities of PNNs surrounding interneurons (Figure 3.16D-F, H). There was no difference in the average size of either motor- or interneurons expressing LN1, neurocan or WFA-labelled PNNs in the ventral horn (Supplementary Figures 1D-E).

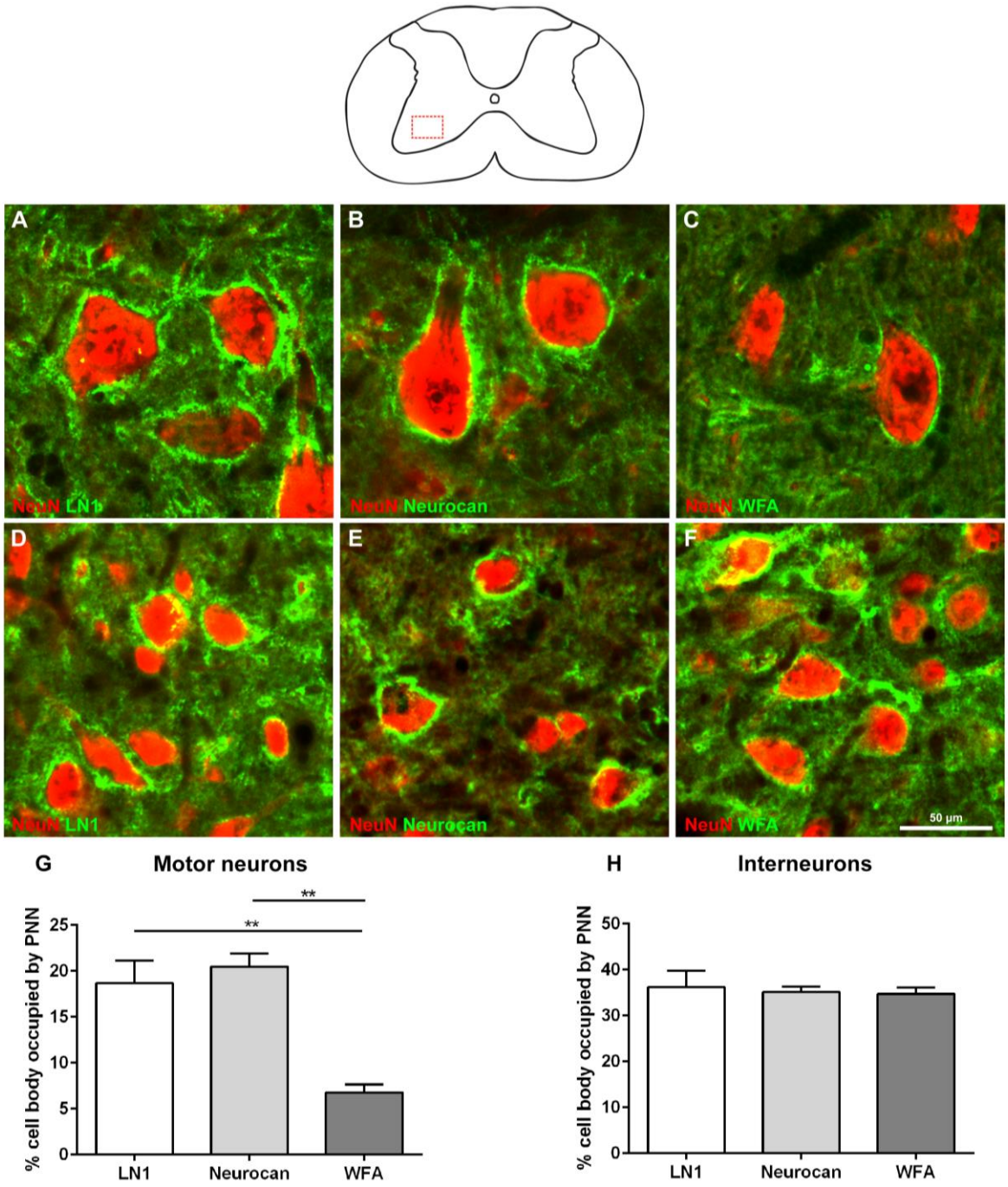

Figure 3.16. PNNs surrounding motor neurons and interneurons in the ventral horn. **(A-C)** Ventral horn motor neurons are surrounded by PNNs positive for LN1 or neurocan, or labelled by WFA. **(D-F)** Interneurons in the ventral horn have LN1 or neurocan-positive PNNs, and some are labelled by WFA. **(G)** Density of individual WFA-labelled PNNs was significantly lower than those positive for LN1 or neurocan (n=3, $^{**}p$<0.01, one-way ANOVA). **(H)** No difference was observed in the densities of individual PNNs found on interneurons (n=3, p>0.05, one-way ANOVA).

As previously mentioned, the density of WFA-labelled PNNs on motor neurons was significantly lower than the density of LN1 or neurocan immunopositive PNNs. To evaluate

whether motor neurons surrounded by weakly-labelled WFA PNNs contained LN1 or neurocan, double fluorescent labelling was performed. WFA-labelled PNNs were found on mostly large motor neurons and almost all of these (94%) were immunopositive for LN1 (Figure 3.17A) or neurocan (88%, Figure 3.17B, Summary Figure 3.20). A large proportion of WFA-labelled PNNs found on interneurons were immunopositive for LN1 (63%, Figure 3.17C) or neurocan (54%, Figure 3.17D, Summary Figure 3.20).

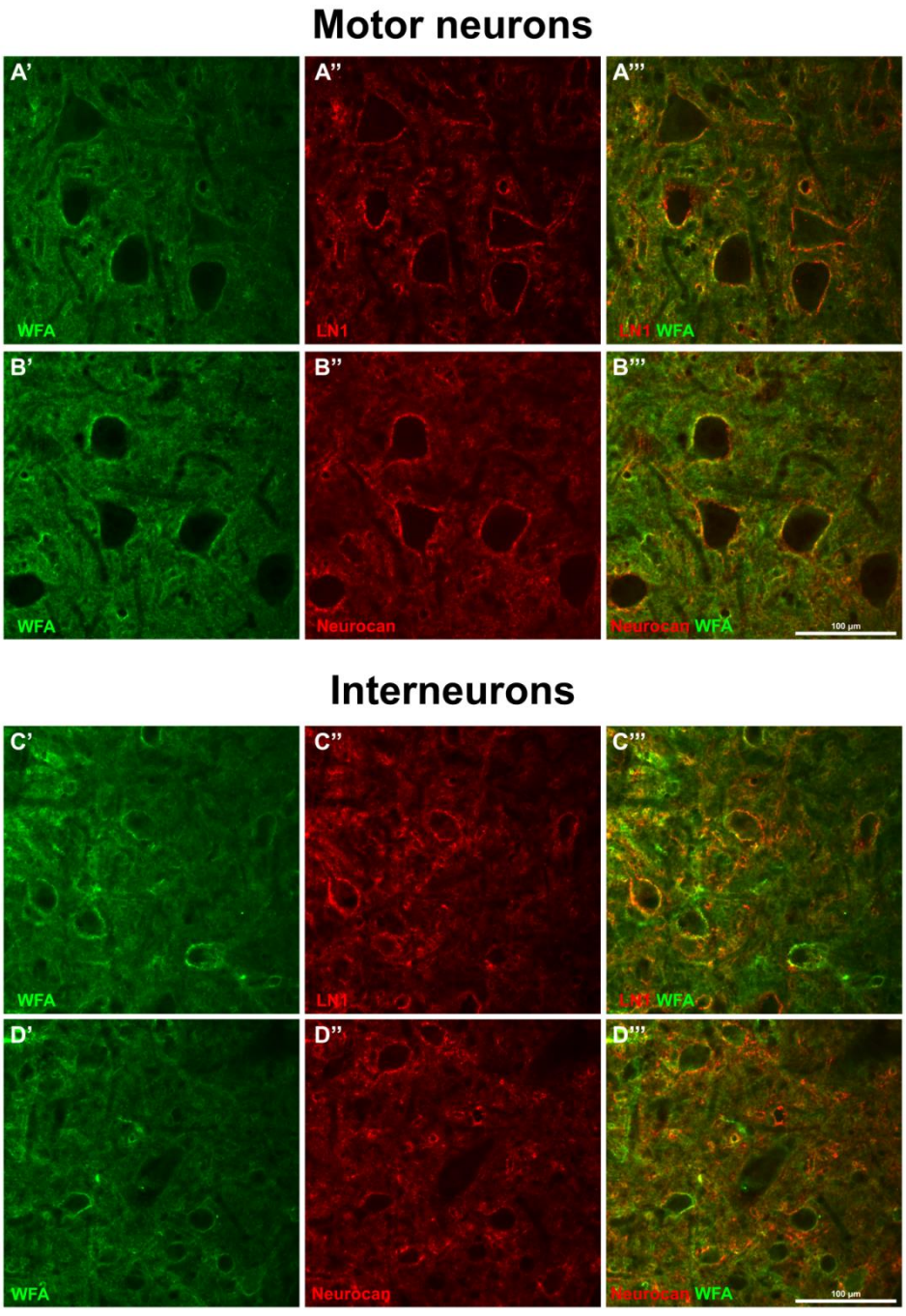

Figure 3.17. Co-localisation between WFA and LN1 or neurocan immunolabelling of PNN-expressing neurons in the ventral horn

(A) WFA-labelled PNNs were found around motor neurons in the ventral horn and almost all of these PNNs were immunopositive for LN1. **(B)** Many of the PNNs surrounding motor neurons were immunopositive for neurocan. **(C-D)** WFA-labelled PNNs on interneurons were immunopositive for LN1 and neurocan. Scale bar = 100 μm.

The density of GABAergic terminals in contact with PNN-expressing motor neurons was 20.0 ± 1.3%. (Figure 3.18A). The density of serotonergic and cholinergic boutons was much lower (5-HT, 8.1 ± 1.1 %; ChAT, 9.5 ± 1.7 %, Figure 3.18B-C, summary Figure 3.20). There was no correlation between the density of synaptic inputs to individual PNN-expressing motor neurons and the density of WFA labelling (GAD67 R^2= 0.05; 5-HT R^2= 0.11 and ChAT R^2 = 0.003, linear regression, Figure 3.18D-F).

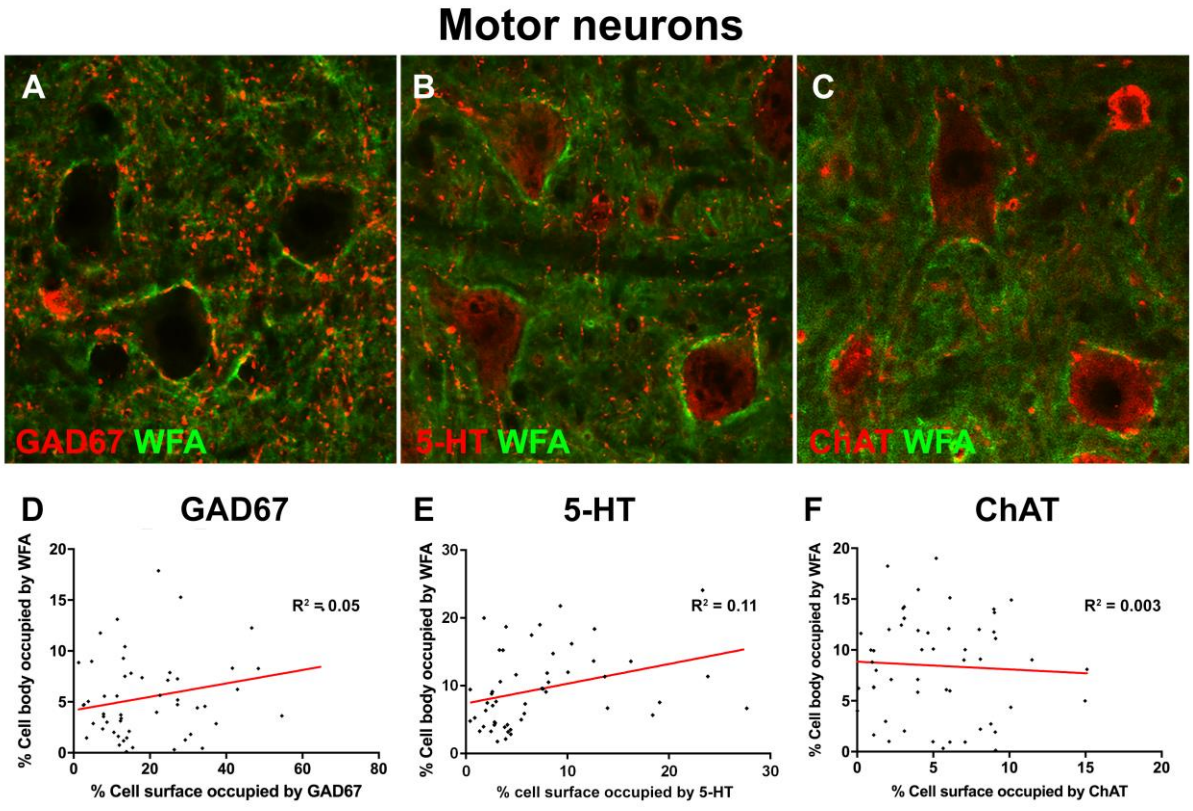

Figure 3.18. Density of synaptic boutons in contact with PNN-expressing motor neurons in the ventral horn.
Representative photomicrographs illustrating the density of synaptic inputs to PNN-expressing motor neurons in the ventral horn. **(A-C)** The density of inhibitory boutons in contact with PNN-expressing motor neurons was relatively high. Conversely, the density of serotonergic and cholinergic terminals in contact with these neurons was considerably lower. **(D-F)** There was no correlation between the density of inhibitory, serotonergic or

cholinergic inputs to PNN-expressing neurons and the density of WFA labelling on motor neurons (linear regression). Scale bar = 100 μm.

The density of GABAergic contacts to PNN-expressing interneurons was 26.2 ± 2.3% (Figure 3.19A), while serotonergic and cholinergic inputs were again much lower (5-HT 3.5 ± 0.3 %, ChAT 2.3 ± 0.2 %, Figure 3.19B,C, summary Figure 3.20). There was no correlation between the density of synaptic inputs to PNN-expressing interneurons in the ventral horn and the density of WFA immunolabelling (GAD67 R^2= 0.21; 5-HT R^2= 0.09 and ChAT R^2 = 0.03, linear regression, Figure 3.19D-F).

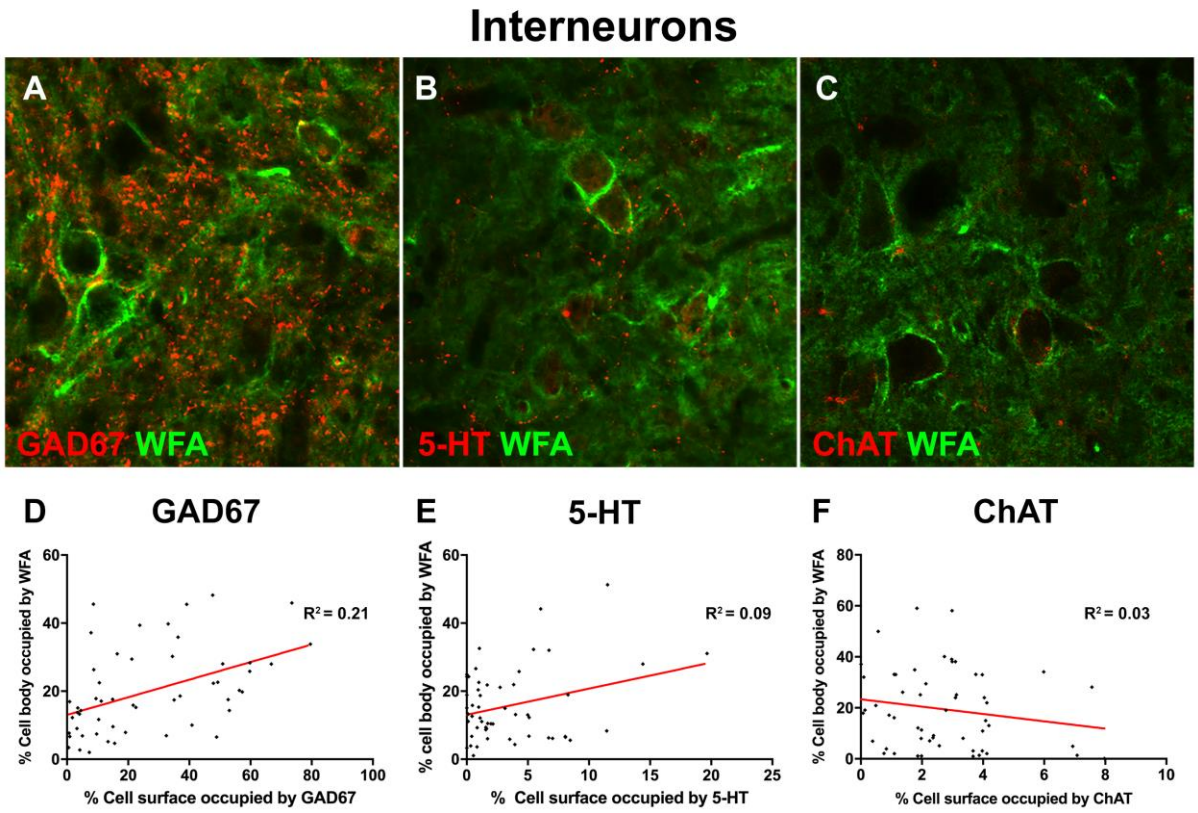

Figure 3.19. Density of synaptic boutons in contact with PNN-expressing interneurons in the ventral horn.
Representative photomicrographs illustrating the density of synaptic inputs to PNN-expressing interneurons in the ventral horn. **(A-C)** The density of inhibitory boutons contacting with PNN-expressing interneurons was relatively high. Conversely, the density of serotonergic and cholinergic terminals in contact with these neurons was considerably lower. **(D-F)** There was no correlation between the density of inhibitory, serotonergic or cholinergic inputs to PNN-expressing neurons and the density of WFA labelling on inter neurons (linear regression). Scale bar = 100 μm.

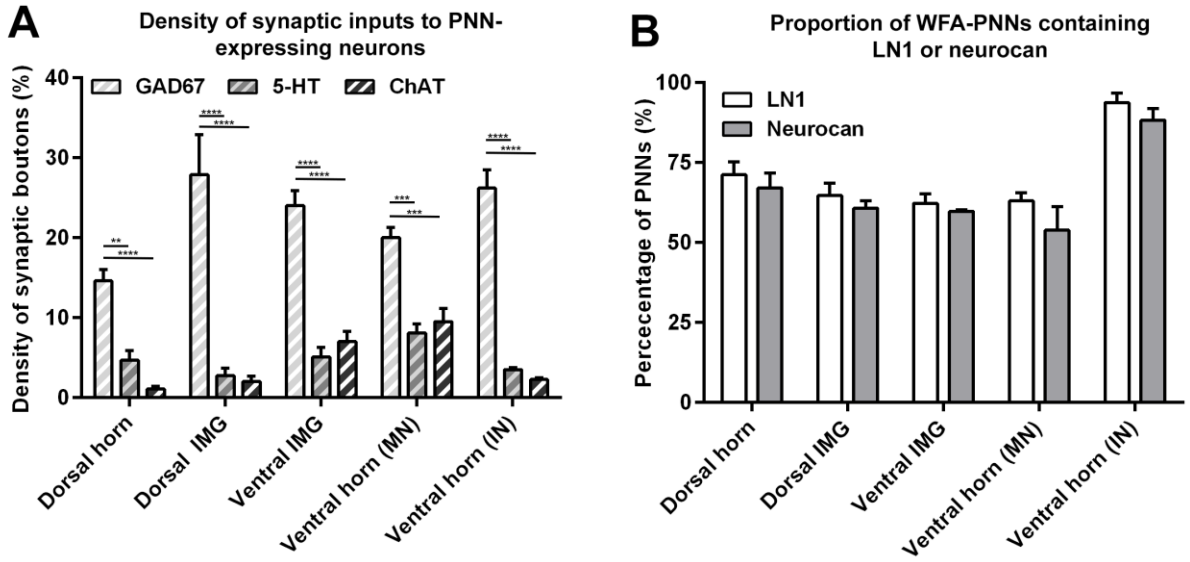

Figure 3.20. Summaries of the density of synaptic inputs to PNN-expressing neurons and the overlap of PNN components.

(A) Summary of the percentage of the cell body of PNN-expressing neurons contacted by specific types of synaptic inputs. At all spinal cord regions examined there was a significant difference in the density of GAD65-labelled boutons contacting neurons, compared with boutons labelled with 5-HT or ChAT. **(B)** Summary of the proportion of WFA-labelled PNNs double-labelled with LN1 or neurocan antibodies. There was no significant difference in the proportion of WFA-labelled PNNs labelled with LN1 compared with those labelled with neurocan. Significance was determined using a two-way ANOVA, ** denotes $p < 0.01$, *** denotes $p < 0.001$ and **** denotes $p < 0.0001$.

3.3 Discussion

3.3.1 PNNs are heterogeneously distributed throughout the cervical spinal cord

In the cervical spinal cord of adult Wistar rats there was a heterogeneous distribution of WFA-labelled PNNs throughout the grey matter. There was a dorso-ventral increase in the proportion of neurons ensheathed by PNNs detected by WFA, LN1 and the CSPG neurocan. However, there was in general no difference in the percentage of neurons expressing PNNs that were labelled with WFA, LN1 or neurocan in all spinal cord regions examined, with one notable exception in the more dorsal region of the intermediate grey matter. In contrast to previously published observations, the proportion of neurons with a PNN did not exceed 20% for any of the examined markers. Previous data suggests that between 20 and 40% of neurons express WFA-labelled or LN1-containing PNNs in the intermediate grey matter and the ventral horn (Galtrey et al., 2008). The disparity between the data in this study and others may be explained by the use of different rat strains; such that this study used Wistar

rats, while the published study by Galtrey and co-workers used Sprague Dawley rats. Although there is currently no data available concerning the difference in the extracellular matrix, or more specifically, the PNN, in different rat strains, Sprague Dawley and Wistar rats are known to exhibit differences in their behaviour and response to neuronal insult (Mills et al., 2001; Walberer et al., 2006). Therefore, it is reasonable to suggest there may also be strain-related differences in the extracellular matrix. Moreover, other factors that could have contributed to the differential results observed could be the age of the animals, the use of antibodies from different suppliers, in addition to the method of tissue preparation and the method of histological staining. It should also be noted that to date, the only other available study that investigated the distribution of extracellular matrix molecules in the spinal cord subdivided the cord into distinct anatomical regions, as classified by Rexed (Watson et al., 2008). The purpose of this study was to investigate the distribution of PNN molecules throughout broad distinct regions of the spinal cord, namely; dorsal horn, intermediate grey matter (either dorsal or ventral) and ventral horn, thus rendering it difficult to perform direct comparisons between the published study and this one.

In the dorsal horn, the density of neurocan-immunopositive PNNs was significantly lower than those detected by LN1 or WFA. This result concurs with other published studies, which have also noted weaker neurocan labelling in the dorsal horn, when compared with WFA or LN1 immunostaining (Galtrey et al., 2008). Although neurocan levels were generally low in the dorsal horn, we noted stronger neurocan immunostaining in PNNs found in other anatomical regions of the spinal cord. Interestingly, other studies have revealed consistent low levels of neurocan immunostaining in all PNNs found throughout all regions of the spinal cord, whereas immunolabelling for other CSPGs, such as aggrecan and phosphacan was strong (Galtrey et al., 2008). The differences between our results and those obtained in other studies may be explained by the use of a different supplier of neurocan primary antibody, or again, may be explained by the difference in rat species used.

Interestingly, there was a remarkable difference in the expression of PNNs in the ventral horns observed in this study. Neurons in the ventral horn can be broadly classified as motor- or interneurons. Alpha motor neurons were identified in this study by their large cell body size and their location in the motor neuron pools at the lateral grey matter of the

ventral horns. These motor neurons, located in lateral motor neurons pools, were densely immunolabelled using LN1 and neurocan antibodies, but poorly labelled by WFA. Conversely, PNNs surrounding smaller interneurons in the ventral horns were strongly labelled by WFA and weakly immunostained for LN1 or neurocan. Motor neuron pools are found both medially and laterally in the spinal cord, in lamina IX. Only one published study has characterised the intensity of PNN immunostaining in lamina IX of the rat cervical spinal cord. Similarly to the findings in this study, Galtrey and co-workers also noted 'weak' WFA staining intensity and 'strong' neurocan labelling intensity surrounding neurons in lamina IX. Interestingly, in contrast with our observations in this study, neurocan intensity was defined as 'weak' in lamina IX. Unfortunately, the terms 'weak' or 'strong' were not clearly defined in the published methodology, which makes it difficult to identify the cause for this variability. However, similar results were also obtained in another study (Vitellaro-Zuccarello et al., 2007).

3.3.2 No correlation between PNN density and the density of synaptic inputs to PNN-expressing neurons

As the detailed phenotypes of PNN-expressing neurons have been explored by other groups (Vitellaro-Zuccarello et al., 2007), this was not examined in this study. Instead, this study aimed to characterise the relative amounts of synaptic inputs to PNN-expressing neurons in the spinal cord and whether this correlated with the density of WFA-immunostaining. In all examined spinal cord regions, the density of individual WFA-binding PNNs was not correlated with the density of specific types of synaptic boutons (GABAergic, serotonergic or cholinergic) that made contact with these PNN-expressing neurons.

3.3.3 A subpopulation of neurons in lamina X express dense PNNs

A small proportion of neurons in lamina X, a region of the spinal cord grey matter located surrounding the central canal, were surrounded by a thick, WFA-labelled PNN. Previous studies have also observed PNN immunostaining in lamina X, however, the neurons expressing these structures has not been characterised. Using a variety of cellular and synaptic markers, this study determined these cells to be negative for ChAT and the calcium

binding protein, calbindin, however, a small proportion of these neurons were immunopositive for parvalbumin. Cholinergic and serotonergic inputs to these neurons were low, but they received a moderate level of inhibitory (GAD67) inputs.

Although information is lacking regarding the function of lamina X neurons as a whole, a number of different neuronal phenotypes and some of their associated functions have been identified in the spinal cord. Some of the best characterised neurons in lamina X are positive for ChAT and were termed the central canal cluster neurons (Barber et al., 1984; Miles et al., 2007). These neurons are found throughout the entire rostrocaudal extent of the spinal cord bilaterally, adjacent to the central canal. The lack of ChAT expression in PNN-expressing neurons indicates that these neurons do not belong to the cluster neuron population. Additional studies have revealed dense networks of propriospinal neurons in lamina X (Masson et al., 1991; Siebert et al., 2010a; Siebert et al., 2010b), in addition to a population of neurons in the thoracic and lumbar regions of the spinal cord, which are activated during stimulated fictive locomotion (Dai et al., 2005).

3.4 Conclusions

In summary, this is the first concise study regarding the expression of PNNs within the cervical spinal cord. We have shown that PNNs, namely WFA, LN1 and neurocan are present around neurons and that the levels of each PNN differs between different locations of the spinal cord, including dorsal horn, intermediate laminae and ventral horn. Further study with others PNN components may aid our understanding of the PNN distribution and their expression after spinal cord injury.

Chapter 4

Investigation of the relationship between PSA and the PNN *in vitro*

Chapter 4: Investigation of the relationship between PSA and the PNN *in vitro*

4.1 Introduction

In vivo studies have been widely used to study the temporal development of PNNs and how these structures can regulate plasticity in the nervous system. Cells can be simply modified *in vitro* using techniques such as gene silencing (using, for example, shRNA or siRNA) genome editing, enzyme treatments and injury modalities. Thus, *in vitro* models provide a good system to investigate factors that can alter the structure or development of PNNs, without the expense or ethical concerns of *in vivo* animal experimentation. To date, there have been a number of cell culture systems used to model PNNs, including primary neurons isolated from the embryonic rodent brain, organotypic slice cultures and cell lines. Each of these culture models will be discussed in turn, below.

4.1.1 Primary neuronal cultures

Two main types of primary dissociated cultures have been used to model the development of PNNs *in vitro:* cortical and hippocampal neurons. Cortical neurons can be isolated from the embryonic or early postnatal brain and survive well in culture when they adhere onto a two dimensional substrate. One of the most common methods of isolating cortical neurons is to use embryonic day 18 rat pups, which results in a heterogeneous population of cells, including neurons and astrocytes. Cultured cortical neurons can form PNNs during the second week *in vitro*, and can be labelled by WFA lectin, in addition to antibodies raised against CSPGs such as neurocan and phosphacan, and the supporting molecule hyaluronan (Miyata et al., 2005). Cortical neurons can also be isolated from mouse pups (embryonic day 16), which are at a similar stage of development to embryonic day 18 rat pups. Similarly, PNNs formed in these cultures contain CSPGs and the supporting molecule hyaluronan (Giamanco and Matthews, 2012). These studies have helped to reveal interesting details regarding the cellular contributions to the PNN. For example, the removal

of astrocytes from cortical cultures did not lead to alterations in WFA labelling of PNNs (Miyata et al., 2005).

Similarly to cortical neurons, neurons isolated from the hippocampus for *in* vitro modelling of the PNN are generally collected from the brain of either embryonic day 18 rat, or embryonic day 16 mouse pups (John et al., 2006; Geissler et al., 2013). While little is known about the precise cellular components of these cultures, some studies have noted a proportion of NG2-positive cells, in addition to low numbers of nestin-positive cells at 7 and 14 days *in vitro* (DIV). It is likely that at least a fraction of these cells correspond to oligodendrocyte progenitors, however, this has not yet been confirmed in studies looking at PNN development (Pyka et al., 2011; Geissler et al., 2013). PNNs form in dissociated hippocampal cultures during the second week *in vitro*, and are found associated with neurons, where they ensheathe the cell body, proximal dendrites and axon initial segment (John et al., 2006). Sharing a similar composition to those observed *in vivo,* hippocampal PNNs contain CSPGs, can be labelled by WFA lectin and also contain the supporting molecules hyaluronan and tenascin-R (Pyka et al., 2011; Geissler et al., 2013). Cultured hippocampal neurons have been used to investigate the effect of ChABC-mediated degradation of PNNs on synaptic plasticity and synaptogenesis (Pyka et al., 2011).

4.1.2 Cell lines

While commonly used cell lines such as the human embryonic kidney 293 (HEK293) line can express PNN components such as aggrecan, tenascin-R and LN1, they do not typically secrete a pericellular matrix. Transfecting cells with plasmids encoding a hyaluronan synthase enzyme (HAS3) and LN1 can result in the formation of a PNN-like structure that binds WFA lectin, similar to those observed *in vivo* and in primary neuronal cultures (Kwok et al., 2010). This culture system has been used to investigate the components of the PNN in more detail, such as which molecules are necessary for PNN formation and maintenance *in vitro* (discussed in chapter 1.1.1, (Kwok et al., 2010)).

4.1.4 Slice cultures

Organotypic slice cultures can be generated from CNS tissue, typically obtained either during embryonic or early postnatal development, from a number of regions of the nervous system (Lein et al., 2011; Humpel, 2015). Cultures survive well *in vitro*, can easily be manipulated using a variety of compounds or genome editing techniques and are widely used for electrophysiological recordings. Organotypic cultures provide a more sophisticated cell culture model than dissociated cultures which adhere onto a two-dimensional substrate, and more accurately represent the environment observed *in vivo,* due to their heterogeneous cellular composition and three-dimensional architecture (Lein et al., 2011). Slice cultures derived from regions of the nervous system that typically express PNNs *in vivo*, such as the hippocampus and the cortex, express PNNs, which contain CSPGs and can be detected by WFA labelling (Bruckner et al., 2004; Bruckner et al., 2006).

4.1.5 Aims

The primary aims of this chapter were to investigate the development of PNNs in primary neuronal cultures, and to assess whether premature removal of PSA led to an increase in the proportion of neurons with PNNs. Additionally, to examine whether PSA removal could affect synapse formation *in vitro.*

4.2 Results

4.2.1 Optimisation and characterisation of primary cortical cultures

Previous studies modelling PNNs *in vitro* commonly used high density cultures derived from the embryonic brain (Miyata et al., 2005; Giamanco et al., 2010). To identify the optimal plating density of cortical cultures required in this study, cultures were plated at 50,000 or 100,000 cells/cm^2, onto poly-D-lysine (PDL) coated coverslips. At 1 DIV, neuronal cells from both plating densities were strongly adherent to the coverslips and exhibited small neurites. After 7 DIV, neurons in lower density cultures were homogenously distributed across the coverslip and neurites had extended in length, which could be clearly observed with bright field microscopy (Figure 4.1A). Conversely, neurons in higher density cultures at 7 DIV had aggregated into large cellular clumps and presented long and thick neurites (Figure 4.1B). To assess whether the formation of clumps in higher density cultures was due to insufficient PDL coating of coverslips, 3 concentrations of PDL were tested; 10, 50 and 100 μg/ml. Neurons plated on coverslips coated with either 50 or 100 μg/ml PDL adhered to coverslips and extended short neurites after 1 DIV. After 7 DIV, neurons in the lower density cultures had extended long neurites and were homogeneously distributed across coverslips pre-treated with the various concentrations of PDL used (Figure 4.1A, C, E). Conversely, higher density cultures formed large cellular clumps, which extended long and thick bunches of neurites, irrespective of the PDL concentrations used (Figure 4.1B, D, F).

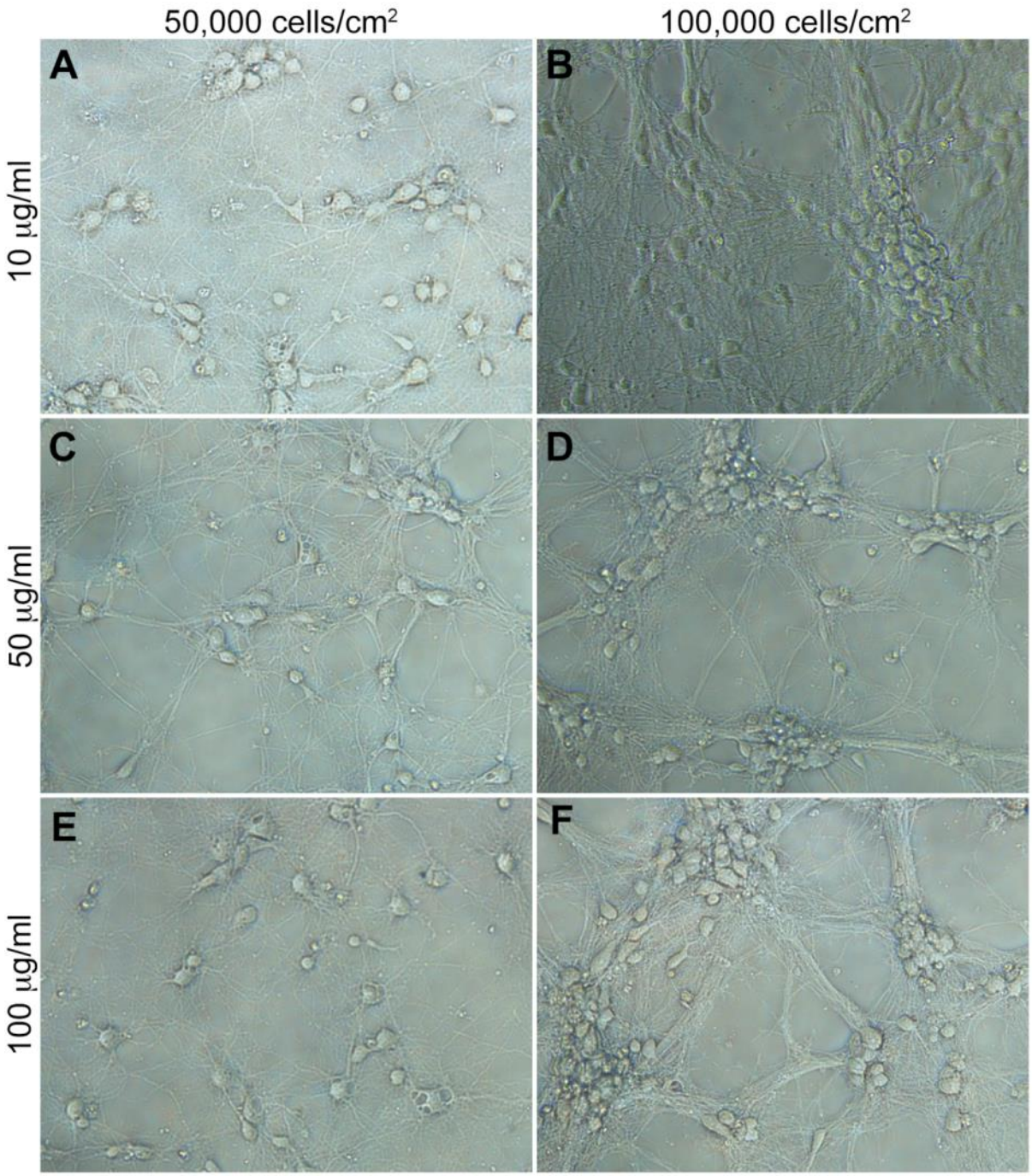

Figure 4.1. Cultured cortical neurons plated at high density formed large cellular clumps after 7 DIV.

To optimise plating density for cultured cortical neurons, two cell densities (50,000 and 100,000 cells/cm^2) were seeded onto PDL-plated coverslips and examined under light microscopy. **(A)** Neurons plated at low density were homogenously distributed across the coverslip, and extended long neurites by 7 DIV. **(B)** Neurons plated at higher density formed large cellular clumps by 7 DIV. **(C-F)** To determine whether inadequate coverslip coating was causing the formation of large cellular aggregates, an additional two concentrations of PDL (50 and 100 µg/ml) were tested. The PDL concentration had no effect on the formation of cellular clumps.

In a separate experiment, cultures were plated on coverslips coated with 100 μg/ml PDL followed by laminin (2 μg/ml), to assess whether this could prevent the formation of clumps within high density cultures (Figure 4.2). Plating with PDL and laminin did not lead to any gross improvement in cell distribution in lower density cultures examined under light microscopy (Figure 4.2A, C) nor did it prevent the formation of cellular clumps in higher density cultures (Figure 4.2B, D). Based on this data, all subsequent experiments were carried out on neurons cultured at the lower density (50,000 cells/cm^2), on coverslips coated with 100 μg/ml PDL only.

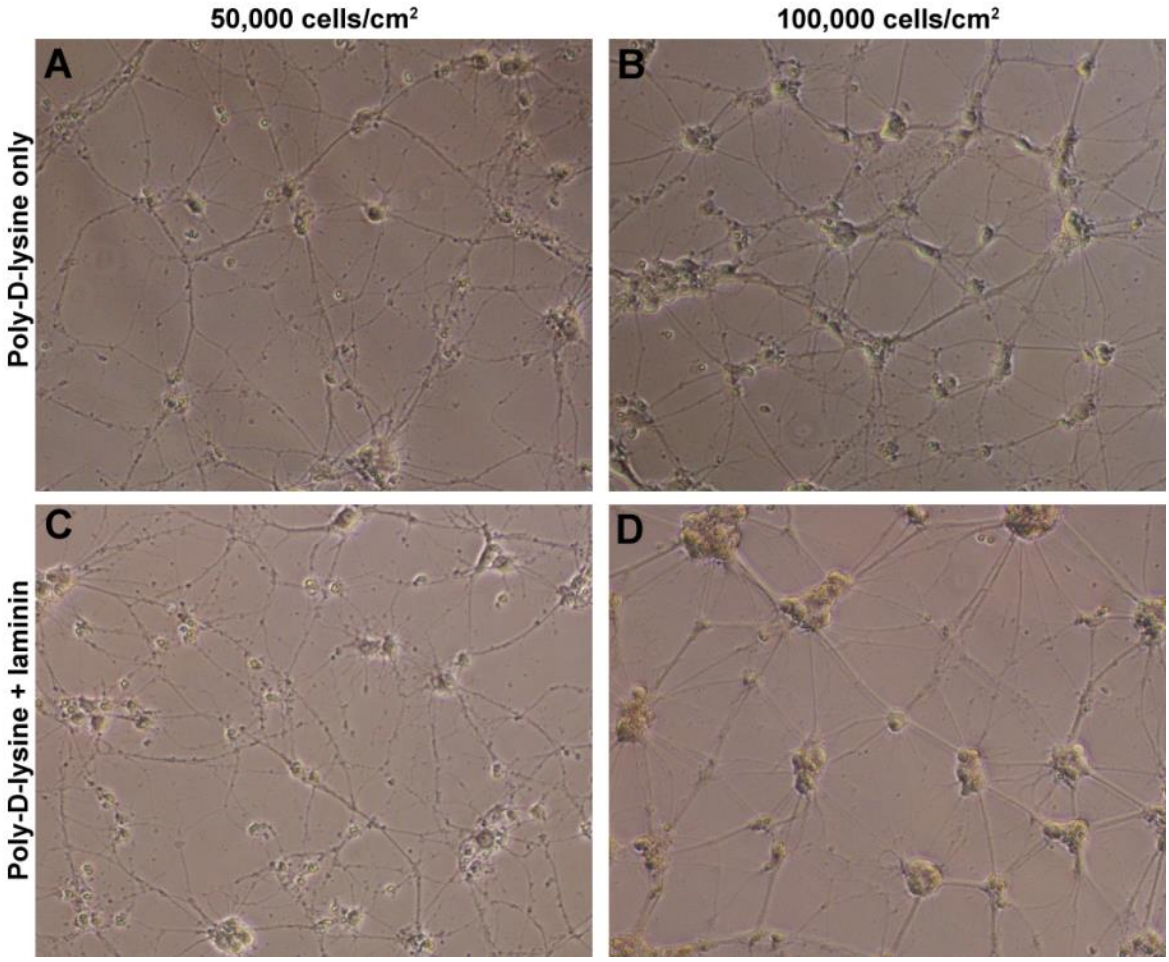

Figure 4.2. Treating coverslips with PDL and laminin did not affect the formation of cellular aggregates.
(A, C) Plating dissociated cortical cultures at lower density on PDL and laminin coated glass coverslips did not grossly alter cell survival or neurite outgrowth compared to PDL only. **(B, D)** Higher density cultures still formed large cellular clumps when plated on PDL and laminin coated coverslips compared to PDL only.

Previously published research has suggested that PNN components can be produced by neurons and astrocytes *in vitro.* To identify whether the cultures used in this study were of a heterogeneous cellular composition, including neurons and astrocytes, cells were fixed at various time points (7, 14 and 21 DIV), then immunolabelled for microtubule-associated protein 2 (MAP2) and glial fibrillary acidic protein (GFAP) to identify neurons and astrocytes, respectively (Figure 4.3). After 7 DIV, neurons can be identified in the cultures using MAP2 (Figure 4.3A), which labels both the neuronal cell body and dendrites. By 14 DIV, the number of MAP2-positive neurons had remained qualitatively consistent, but the dendrites protruding from the neuronal cell body had increased in length and were entangling dendrites from other neurons (Figure 4.3B). Neurons in 21 DIV cultures appeared similar to those in 14 DIV cultures (Figure 4.3C). Astrocytes have been shown to secrete a number of proteoglycans that compose PNNs in the adult CNS, therefore it was important to study whether astrocytes were present in these cultures (Miyata et al., 2005). A common astrocyte marker, GFAP, was used to identify astrocytes (Figure 4.3 D-F). After 7 DIV, qualitative assessment detected only a few GFAP-positive cells in culture, which exhibited a typical astrocytic fibrous and branched morphology (Figure 4.3A). By 14 DIV, the numbers of these astrocytic cells had increased (Figure 4.3B), and at 21 DIV it had increased further (Figure 4.3C).

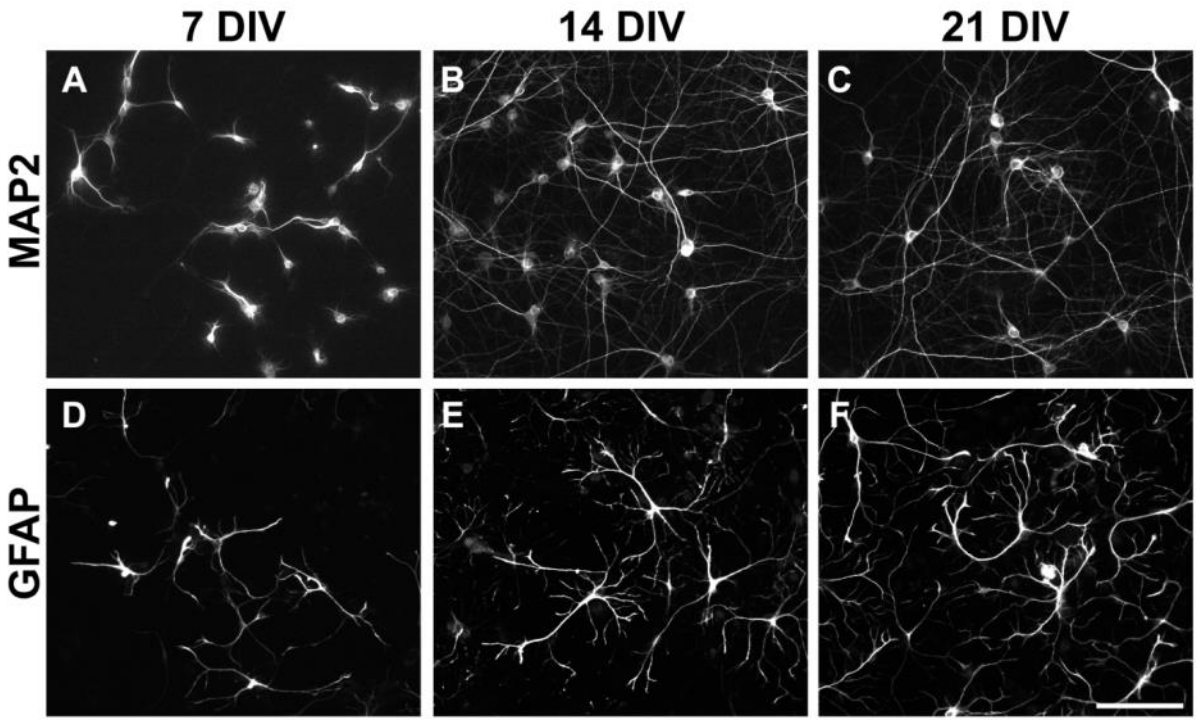

Figure 4.3. Neurons and astrocytes are present in dissociated primary cortical cultures.

(A-C) MAP2-labelled neurons could be observed in dissociated cortical cultures at 7, 14 and 21 DIV. **(A)** At 7 DIV, neurons with extended neurites were observed. **(B,C)** Neurite length had dramatically increased by 14 and 21 DIV**. (D-F)** GFAP immunostaining revealed the continued presence and a temporal increase in the number of astrocytes in dissociated primary cortical cultures. Scale bar = 100 μm.

4.2.2 Characterisation of PNNs in dissociated primary cortical cultures

As previously mentioned, PNNs can be detected both *in vivo* and *in vitro,* using antibodies raised against the supporting protein LN1 or CSPGs such as neurocan, and using a biotinylated lectin, WFA. Double-fluorescent labelling using PNN markers and MAP2 was performed, to verify PNN production in dissociated cortical cultures (Figure 4.4).

LN1 labelling was predominantly co-localised with MAP2 immunostaining of the neuronal cell body, and on some MAP2-labelled proximal dendrites (Figure 4.4A, arrows). Interestingly, LN1 labelling was also observed on a neurite-like structure, originating from the cell body that was not MAP2-positive (arrowhead). Neurocan labelling was similar in morphology to that of LN1, and co-localised with MAP2 immunolabelling of the neuronal cell body and proximal dendrites (Figure 4.4B, arrows). Similarly, neurocan labelling was commonly observed on a MAP2-negative structure (arrowheads). Conversely, WFA labelling was different in morphology to that observed with LN1 and neurocan antibodies and was granular in appearance (Figure 4.4C). WFA labelling co-localised with MAP2-positive neuronal cell bodies and some dendrites (arrows).

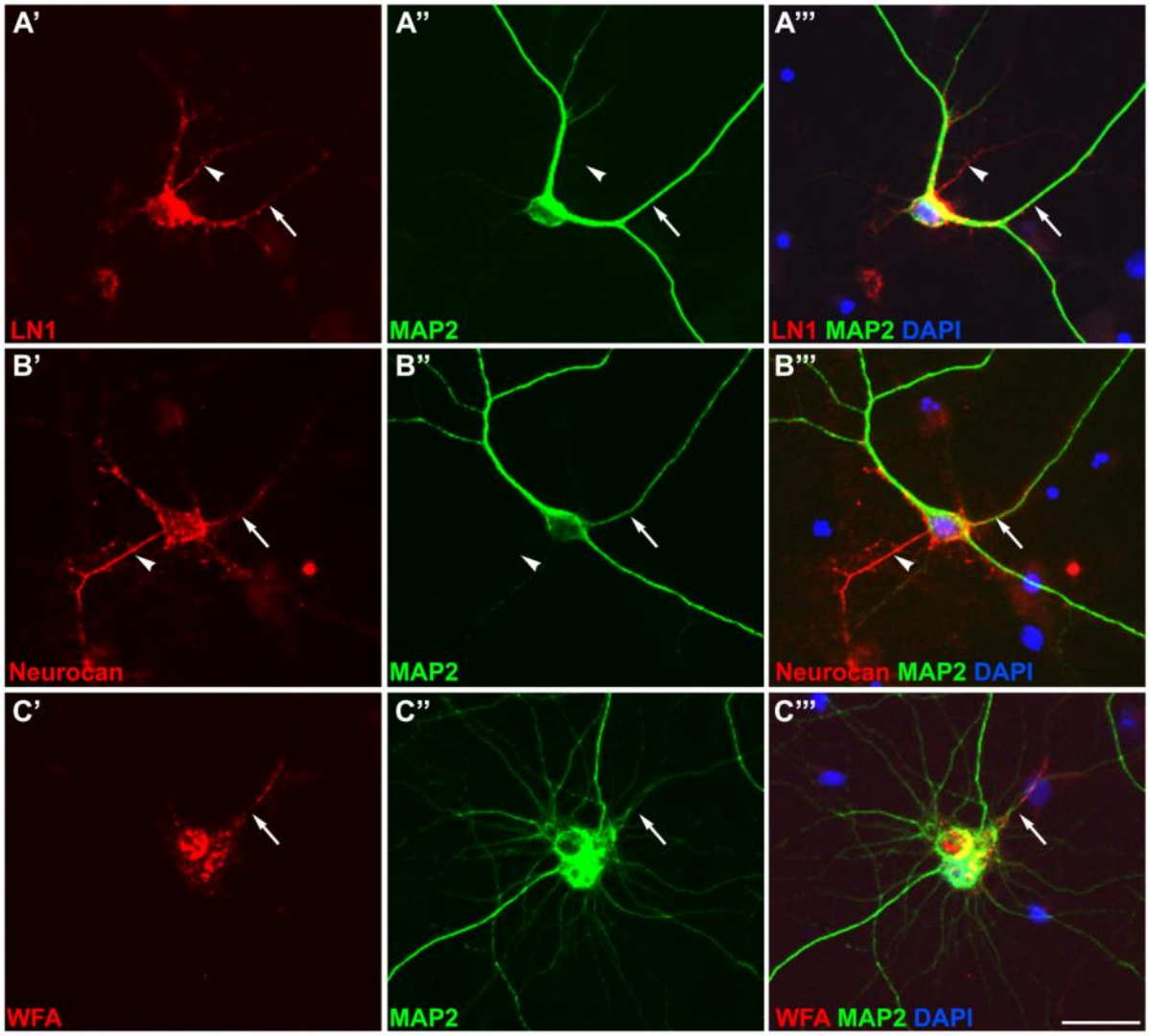

Figure 4.4. PNN labelling was observed on primary cultured cortical neurons.
(A) LN1-labelled PNNs were observed around some cortical neurons. LN1 labelling co-localises with MAP2 labelling of the neuronal cell body and proximal dendrites (arrows), and was also found on a neurite-like structure, that was not labelled by MAP2 (arrowheads). **(B)** Similarly to LN1 immunostaining, neurocan labelling was observed in PNNs surrounding cultured cortical neurons, and showed partial co-localisation with MAP2 immunostaining. **(C)** WFA labelling was granular in appearance and was also present on the neuronal cell body. Scale bar = 25 μm.

Previous studies have indicated two types of WFA-labelling are observed in cultures derived from the cortex, termed granular and pericellular labelling (Miyata et al., 2005). However, there is no other information available regarding the localisation of these labelling patterns on neurons.

Upon closer examination of the cultures from this study at 14 DIV, only pericellular labelling could be identified with the LN1 antibody (Figure 4.5A, arrows). Interestingly, however, neurocan-labelled PNNs could be classified as pericellular (Figure 4.5B, arrows) or granular (arrowheads). WFA labelling was observed as a granular morphology only (Figure 4,5C). Similarly, in 21 DIV cultures LN1 was observed as a pericellular morphology only (Figure 4.5D) and only neurocan labelling was observed as being both pericellular or granular (Figure 4.5E, arrows and arrowheads, respectively). WFA was observed in granular PNNs only (Figure 4.5F). It was not determined whether granular labelling was intracellular or extracellular.

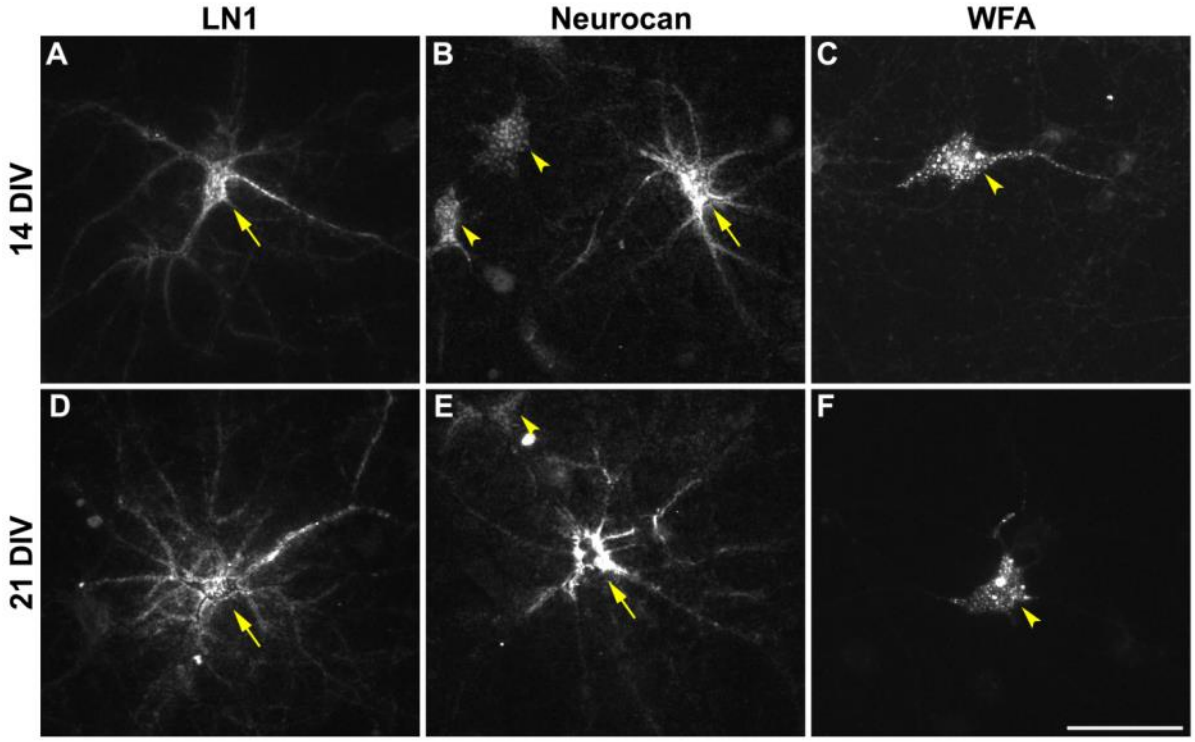

Figure 4.5. PNNs were observed in cortical cultures at 14 and 21 DIV.
PNN immunolabelling could be observed at both 14 and 21 DIV using LN1 or neurocan antibodies and WFA lectin. **(A, D)** LN1 labelling was classified as pericellular (arrows). **(B, E)** Neurocan labelling was observed to be either pericellular (arrows) or granular (arrowheads). **(C, F)** Interestingly, only WFA labelling was observed as granular at both 14 and 21 DIV (arrowheads). Scale bar = 50 μm.

To assess the co-localisation between LN1 or neurocan PNNs, and those labelled with WFA, cells were double-labelled with either LN1 or neurocan antibodies, and WFA. Neurocan and LN1 double labelling was not performed due to cross-species reactivity between the two

primary antibodies. As previously mentioned, neurocan and WFA labelling were both observed as a granular morphology in some of the cultured cortical neurons. Double-fluorescent labelling revealed a partial co-localisation of neurocan and WFA labelling within these granular PNNs (Figure 4.6A). Conversely, granular LN1 labelling was not observed *in vitro* and thus, was not observed as co-localising with WFA-labelled granular PNNs (Figure 4.6B). Since WFA labelling was absent in a pericellular form, there was no co-localisation between neurocan pericellular labelling and WFA (Figure 4.6C). Similarly, there was no co-localisation observed between LN1 pericellular staining and WFA labelling (Figure 4.6.D).

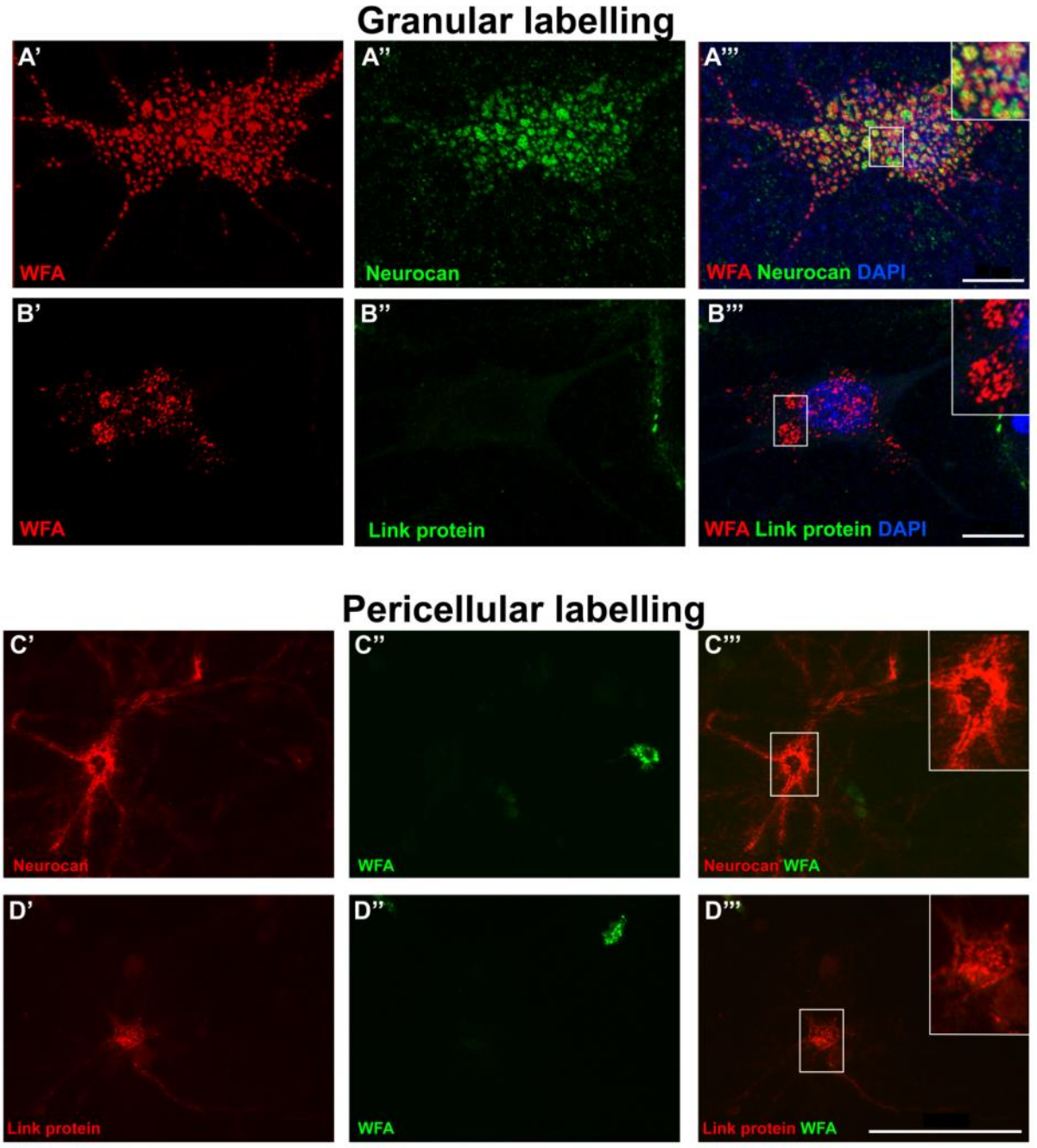

➤ **Figure 4.6. WFA labelling co-localised with neurocan in granular PNNs of primary cortical neurons.**
(A) WFA labelling was only observed in a granular morphology. Neurocan immunostaining partially co-localised with WFA labelling within these granular PNNs. **(B)** No co-localisation between WFA and LN1 in granular PNNs was observed. **(C)** WFA labelling was absent in pericellular PNNs that could be labelled by neurocan antibody. **(D)** Similarly, WFA was also absent in LN1-labelled pericellular PNNs. Highlighted areas are magnified in the top right corner of each image. Scale bar = 10 μm (A, B) or 100 μm (C, D).

4.2.3 Characterisation of PNNs in dissociated primary hippocampal cultures

As previously described in chapter 4.1.2 above, it has been reported that PNNs can also be observed in dissociated hippocampal cultures isolated from the embryonic rat brain (Pyka et al., 2011). Therefore, the purpose of this study was to determine whether the expression of PNNs was similar between neurons from different anatomical regions of the embryonic rat brain. Similarly to those observed in cortical cultures, PNNs can be labelled with LN1 or neurocan antibody or WFA and show a partial co-localisation with MAP2 immunostaining in hippocampal cultures (Figure 4.7). At 14 DIV, LN1-labelled PNNs predominantly exhibited a pericellular morphology, and were found on the neuronal cell body and proximal dendrites (Figure 4.7A, arrows). A MAP2-positive neurite was also labelled by LN1 (arrowhead). Likewise, neurocan-labelled PNNs were found on the neuronal cell body and proximal dendrites at 14 DIV (Figure 4.7B, arrows). There was also neurocan labelling on a neurite that was not labelled by MAP2 (arrowhead). WFA labelling in hippocampal cultures had a granular morphology, and co-localised with MAP2 immunostaining (Figure 4.7C, arrow). In 21 DIV cultures, all 3 PNN markers appeared similar in morphology, and showed a partial co-localisation with MAP2 immunostaining (Figure 4.7D-F).

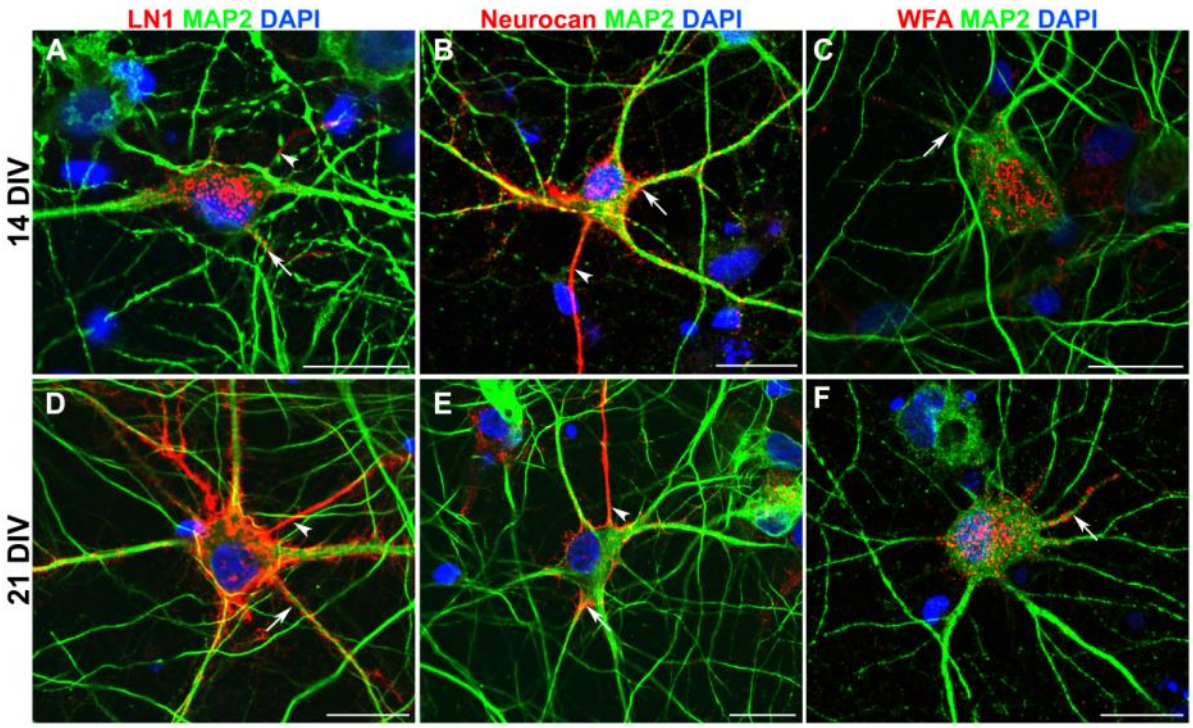

Figure 4.7. PNN immunolabelling in dissociated primary hippocampal cultures.
(A) After 14 DIV, hippocampal neurons identified by MAP2 labelling exhibited PNNs that were detected by the LN1 antibody. This showed co-localisation on the neuronal cell body and occasional dendrites (arrows), but additionally could be found on a MAP2-negative neurite (arrowhead). **(B)** Similarly, neurocan labelling was observed in PNNs surrounding the hippocampal neuronal cell body and dendrites (arrows) and on a neurite-like structure that was not labelled by MAP2 (arrowhead). **(C)** WFA immunostaining was granular in morphology and was found primarily on the neuronal cell body. **(D-F)** After 21 DIV there was no gross morphological difference in PNNs examined for LN1, neurocan or WFA. Scale bar = 20 μm.

Similarly to PNNs observed surrounding neurons isolated from the cortex, PNNs in hippocampal cultures could be classified as either granular or pericellular, based on their morphology (Figure 4.8). Granular labelling appeared as a punctate labelling pattern, which was predominantly observed on the neuronal cell body, with weaker dendritic staining (Figure 4.8A, C). On the other hand, pericellular labelling was observed as a diffuse labelling pattern, found closely associated with the cell body and with strong dendritic staining (Figure 4.8B, D). Interestingly, both LN1 and neurocan could be observed as granular and pericellular PNNs, which contradicted data observed in cortical cultures, in which LN1 was absent from granular PNNs (Figure 4.8). WFA labelling was absent in pericellular PNNs, and was only found as a granular labelling pattern (Figure 4.7C, F).

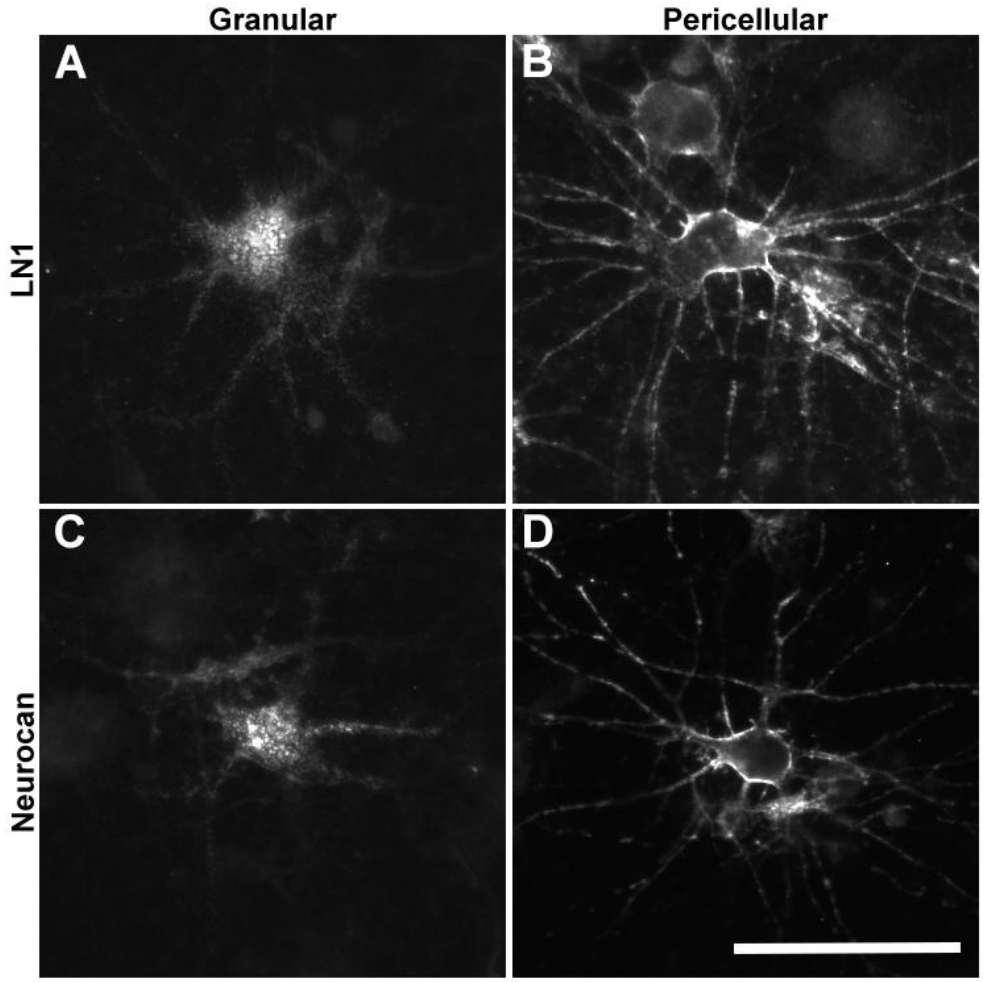

Figure 4.8. Granular and pericellular PNNs were present on primary cultured hippocampal neurons.
Diffuse and granular PNNs were observed in hippocampal cultures. **(A)** LN1 labelling was observed in granular PNNs. **(B)** LN1 labelling was also observed in pericellular PNNs, which exhibited prominent dendritic staining. **(C, D)** Similarly, neurocan was observed in granular and pericellular PNNs. Scale bar = 100 μm.

4.2.4 Addition of endoneuraminidase N can selectively remove PSA from the surface of cultured hippocampal neurons

Polysialic acid (PSA) can be observed surrounding cultured hippocampal neurons at 7, 14 and 21 DIV. Previous research has shown that an enzyme, endoneuraminidase N (endo-N), can be used *in vitro* to selectively remove PSA from the surface of cultured cells (Dityatev et al., 2004). To identify the optimal concentration of endo-N needed to remove PSA from the cultures, cells were treated with 40, 80 or 100 ng/ml endo-N after 4 DIV for an additional three days. Cultures were fixed at 7 DIV and immunolabelled for PSA. Untreated cultures showed robust PSA labelling (24.9 $\pm$ 2.0 %, Figure 4.9.A, E). As expected, Endo-N treatment

resulted in a drastic reduction in PSA labelling (Figure 4.9B-D). Quantification of the density of PSA labelling in endo-N treated cultures revealed a significant reduction in the area occupied by PSA labelling, at all endo-N concentrations examined (40 ng/ml; $0.01 \pm 0.003\%$, 80 ng/ml; $0.007 \pm 0.005\%$, 100 ng/ml; $0.004 \pm 0.002\%$, Figure 4.9E).

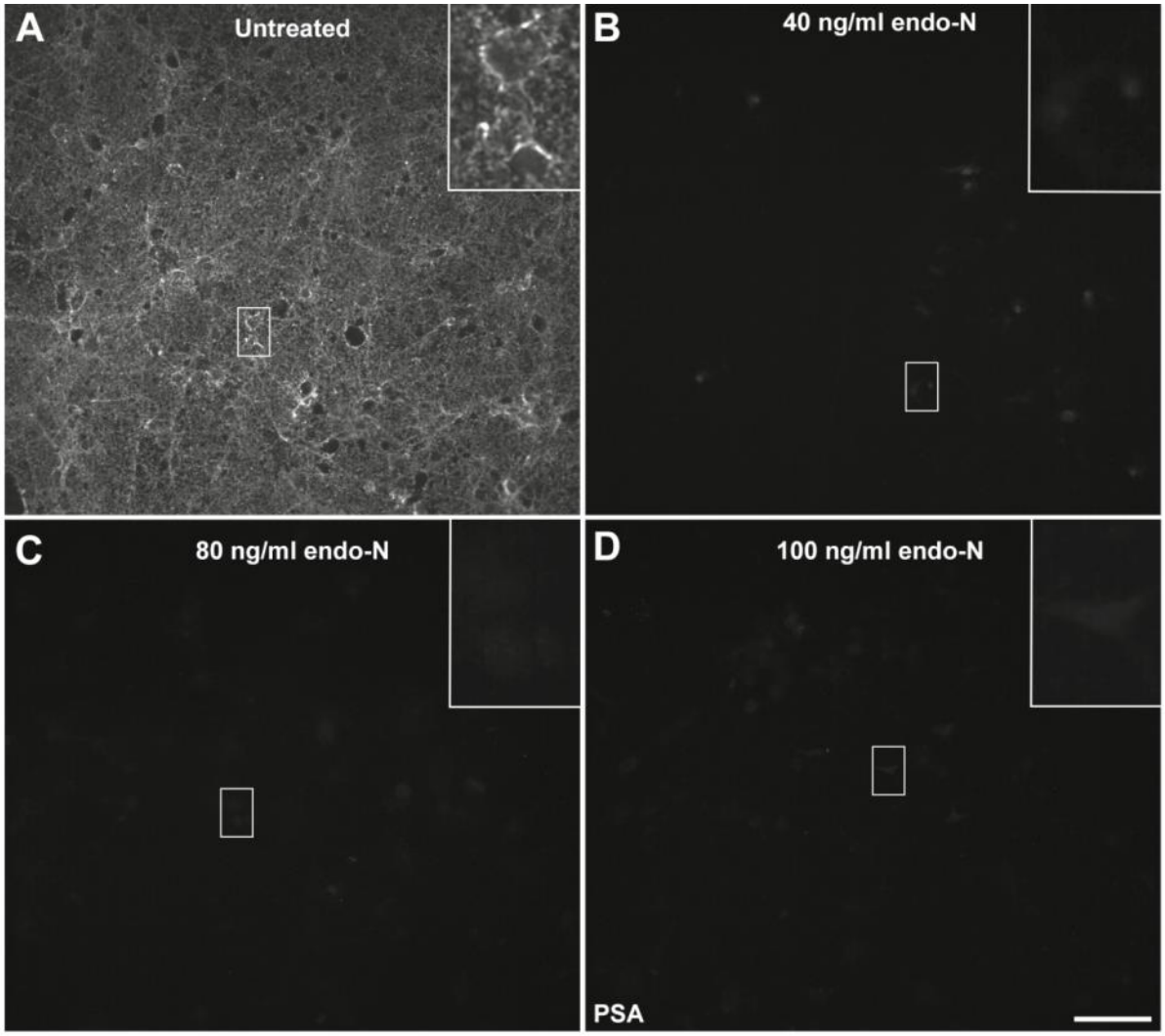
A
Untreated
B
40 ng/ml endo-N
C
80 ng/ml endo-N
D
100 ng/ml endo-N
PSA

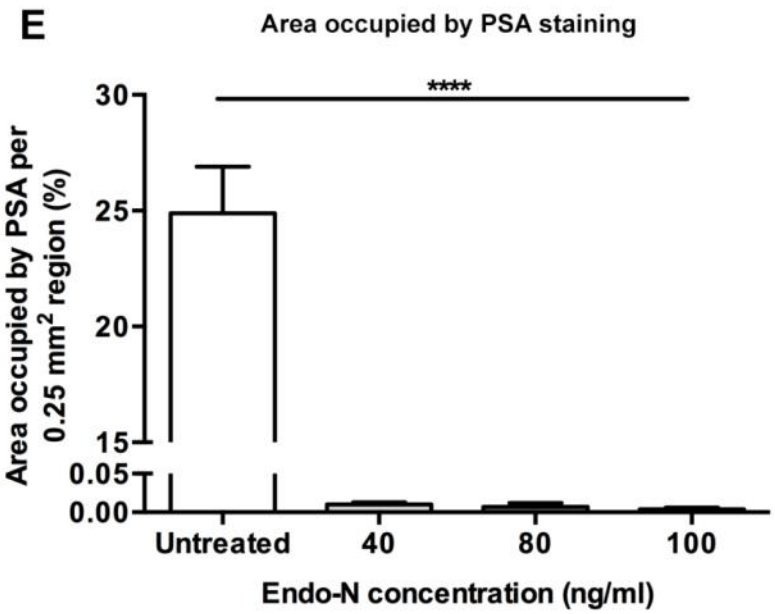
E
Area occupied by PSA staining
****
Area occupied by PSA per 0.25 mm² region (%)
30
25
20
15
0.05
0.00
Untreated
40
80
100
Endo-N concentration (ng/ml)

➤ **Figure 4.9. PSA expression in primary hippocampal cultures treated with endo-N.**
(A) PSA labelling was robust following 7 DIV. **(B-D)** Endo-N treatment resulted in a drastic reduction in PSA labelling, at all concentrations tested. **(E)** Quantification of the density of PSA labelling following endo-N treatment revealed a significant reduction in the area occupied by PSA immunostaining. *n*=3 independent experiments. ****denotes *p*<0.0001, one-way ANOVA, Bonferroni's post-hoc test). Scale bar = 100 μm.

To investigate whether treating cultured hippocampal neurons with endo-N could affect neuronal survival, cells were treated with endo-N as above, and immunolabelled using the MAP2 antibody. Untreated cultures contained a high density (45.1 ± 1.2 cells/field of view, Figure 4.10A, E) of MAP2-labelled neurons at 7 DIV, from which long MAP2 labelled dendrites had covered a large proportion of the coverslip. Treating cultures with endo-N, at all concentrations, resulted in a strong and dose-dependent reduction in the average number of MAP2-labelled neurons per field of view (40 ng/ml; 19.2 ± 1.1, 80 ng/ml 5.2 ± 1.3, 100 ng/ml; 2.8 ± 0.7 cells, Figure 4.10 E).

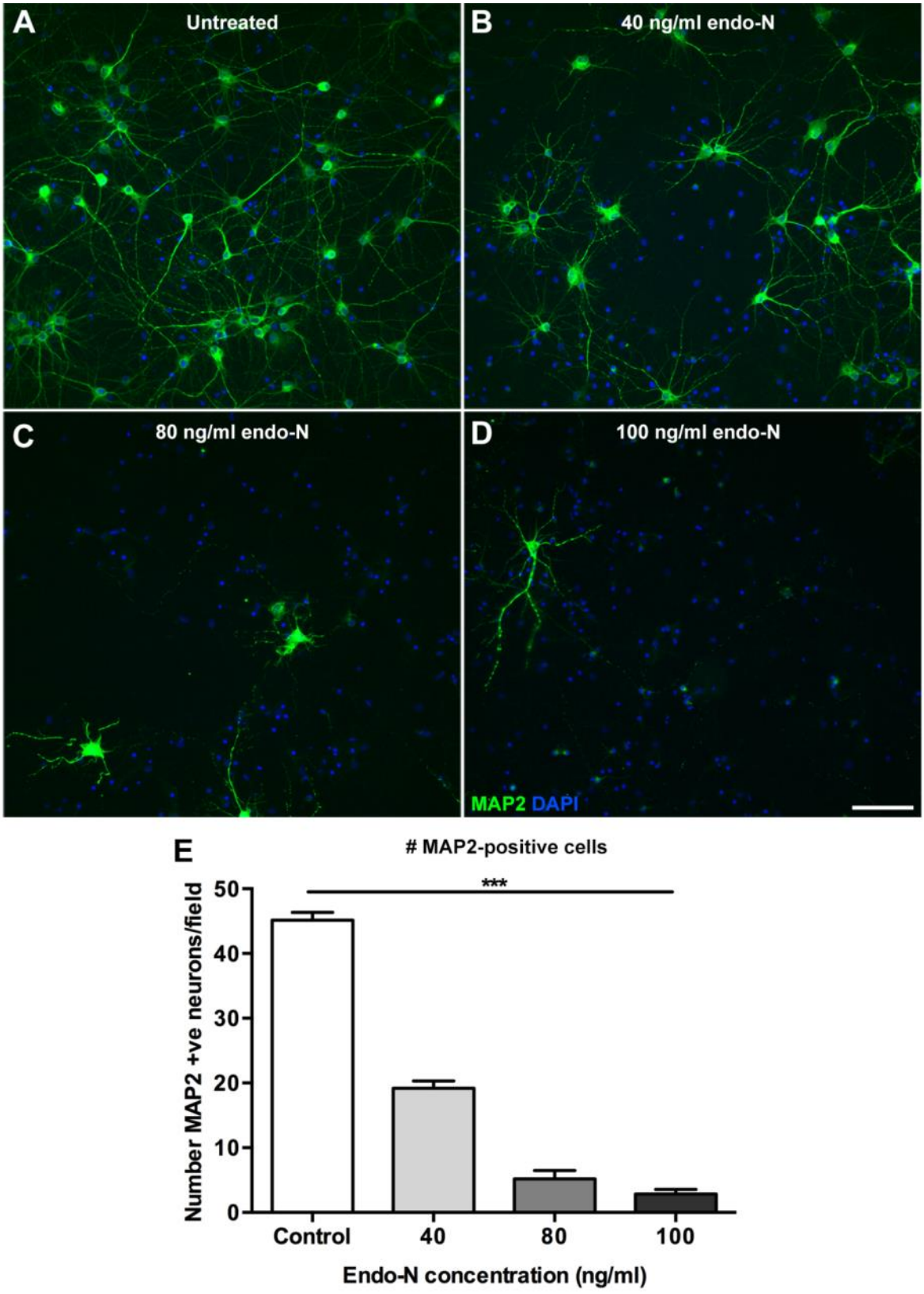

Figure 4.10. Reduction of MAP2-positive neurons following endo-N treatment.
(A) At 7 DIV, there was a high number of MAP2-positive neurons in culture. **(B-D)** After endo-N treatment, the numbers of MAP2-immunolabelled neurons were reduced in a dose-dependent manner. **(E)** Quantification of the number of MAP2-positive neurons per field of

view in the presence of endo-N. A significant decrease in the number of neurons in culture was observed with increasing endo-N concentrations. *n=3* independent experiments. ***p<0.001, one-way ANOVA, Bonferroni's post-hoc test. Scale bar = 100 μm.

As endo-N concentrations from 40 - 100 ng/ml resulted in a significant reduction in the number of MAP2-immunopositive neurons *in vitro*, a concentration of 20 ng/ml was tested in a subsequent study. Strong PSA labelling was observed in untreated hippocampal cultures after 14 DIV (39.6 ± 3.1 %, Figure 4.11A, E), and less in 21 DIV cultures (29 ± 3.6%, Figure 4.11 C, E). Treating cultures with 20 ng/ml endo-N significantly reduced the density of PSA labelling at both 14 and 21 DIV (14 DIV 0.3 ± 0.02%; 21 DIV 0.03 ± 0.09%, Figure 4.11E).

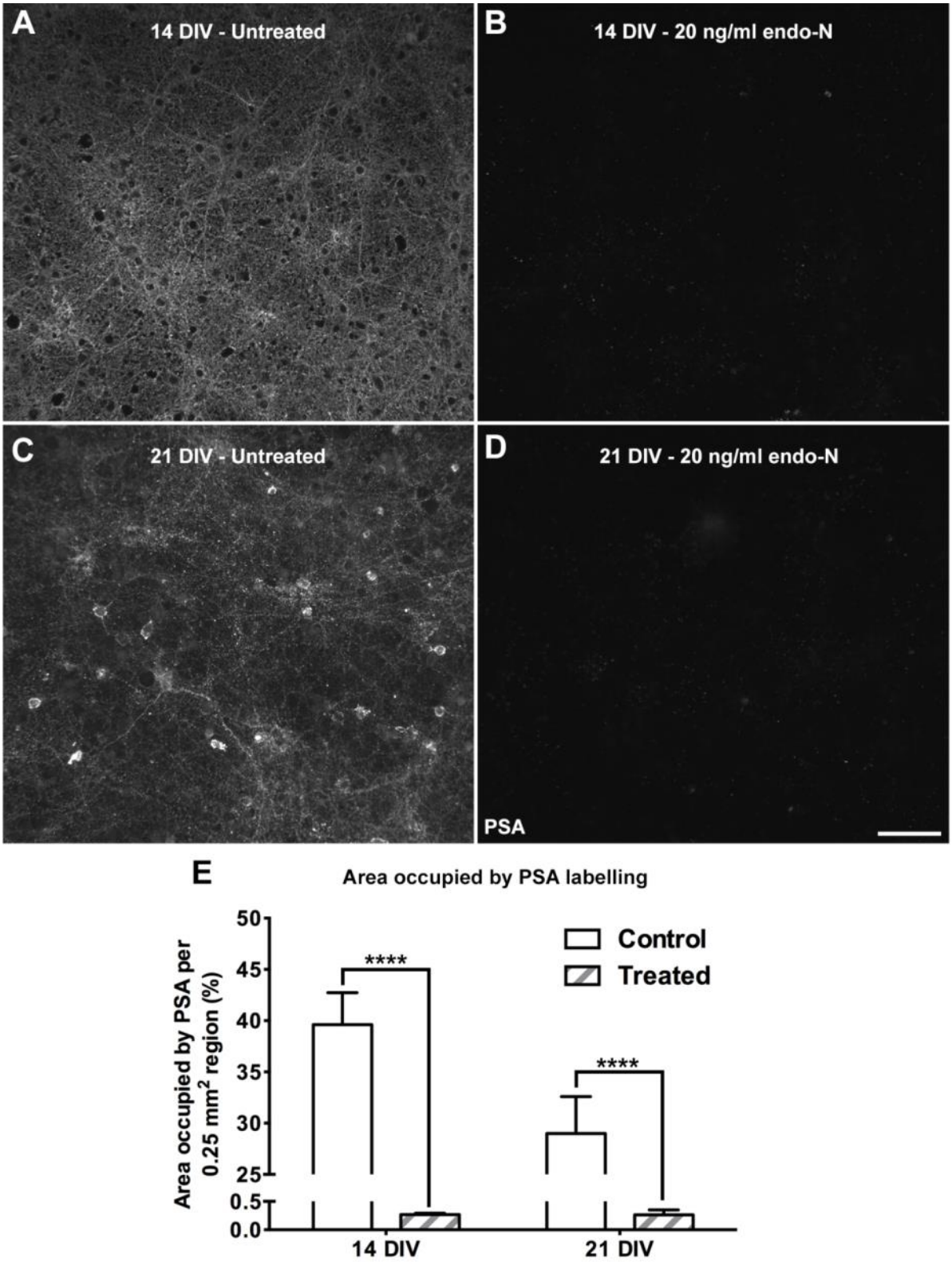

Figure 4.11. Treating hippocampal cultures with 20 ng/ml endo-N reduced PSA labelling at 14 and 21 DIV.

(A) Strong PSA labelling was observed in hippocampal cultures at 14 DIV. **(B)** Continuous endo-N treatment from 4 DIV almost completely ablated PSA immunolabelling in 14 DIV cultures. **(C)** PSA labelling in 21 DIV hippocampal cultures was strong; however, it was

reduced in comparison to 14 DIV cultures. **(D)** PSA labelling was drastically reduced in 21 DIV cultures following endo-N treatment. **(E)** Quantification of the percentage area occupied by PSA labelling following endo-N treatment. PSA labelling was significantly reduced at both 14 and 21 DIV following endo-N treatment. *n=3* independent experiments. ****p<0.0001, two-way ANOVA. Scale bar = 100 μm.

The previous examination of endo-N concentrations at 40 – 100 ng/ml showed that the treatment resulted in neuronal cell death. To check that the continuous treatment with 20 ng/ml endo-N did not affect neuronal survival, cells were fixed at 14 and 21 DIV and immunolabelled with MAP2 antibody (Figure 4.12). At 20 ng/ml endo-N, no significant difference was observed in the average number of MAP2-positive cells at 14 DIV in control (57.3 ± 2.1 cells/field of view) or treated cultures (57.9 ± 2.5, Figure 4.12 A-B, E). Similarly the number of MAP2-positive cells at 21 DIV was unchanged with endo-N treatment (control 61.4 ± 1.8; treated 62 ± 0.9, Figure 4.12C-E). This data suggests endo-N at a concentration of 20 ng/ml was sufficient to reduce PSA expression without having any detrimental effect on the neuronal cells in culture.

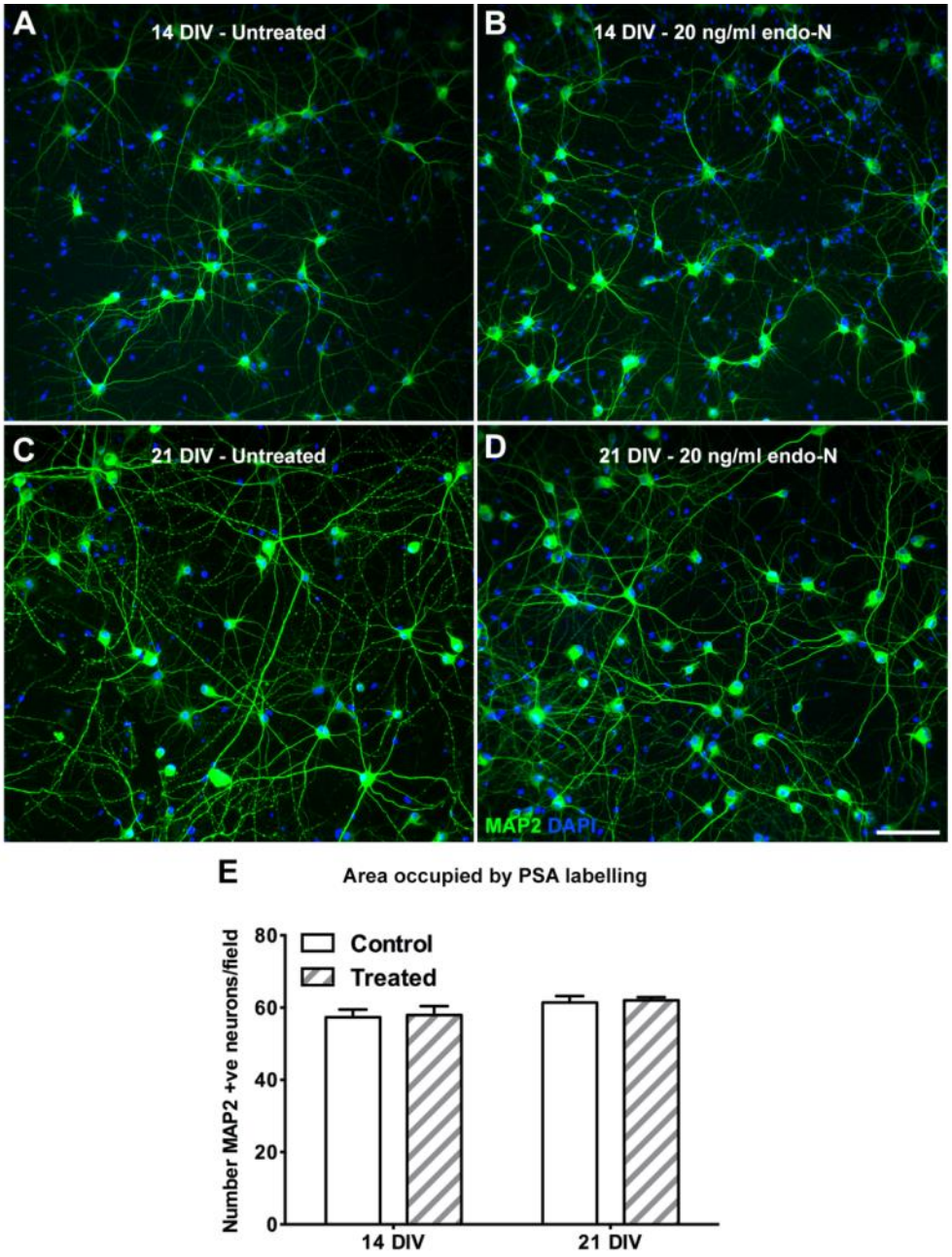

Figure 4.12. Treating hippocampal cultures with 20 ng/ml endo-N did not affect neuronal survival.
(A-D) Representative photomicrographs illustrating MAP2 immunostaining of 14 and 21 DIV hippocampal cultures, with or without endo-N treatment. **(E)** Quantification of the number of MAP2-positive cells per field. The number of MAP2-positive cells was not significantly different following endo-N treatment, at both 14 and 21 DIV. *n=3* independent experiments. $p>0.05$, two-way ANOVA. Scale bar = 100 μm.

4.2.4 Treating cultures with endo-N does not alter the development of the PNN

Previous unpublished data from our laboratory indicated that there may be an inverse relationship between PSA expression and the formation of the PNN in the postnatal rat CNS.

To assess whether removing PSA from the cultured cells could alter the proportion of neurons with a PNN *in vitro,* cultures were continuously treated with 20 ng/ml endo-N starting after 4 DIV, then fixed at 14 or 21 DIV. This endo-N concentration was selected from previous experiments that showed a significant reduction in PSA labelling in treated cultures, without a reduction in the number of neurons. To quantify the proportion of neurons with a PNN, cells were double-labelled with the MAP2 antibody and either LN1/neurocan antibody or WFA. After 14 DIV, the percentage of neurons with a PNN was different between the three PNN markers examined in this study. While a similar percentage of neurons had PNNs immunolabelled with LN1 (4.7 $\pm$ 1.2%, Figure 4.13A) or neurocan (3.3 $\pm$ 0.7%, Figure 4.13B), a slightly higher percentage had WFA labelling (8.1 $\pm$ 2.4%, Figure 4.13C). Following endo-N treatment, there was no change in the average percentage of neurons with a PNN, labelled with LN1 (3.3 $\pm$ 1.0%, Figure 4.13A), neurocan (2.7 $\pm$ 0.4, Figure 4.13B) or WFA (11.5 $\pm$ 4.1, Figure 4.13C). Interestingly, between 14 and 21 DIV, there was a slight, but non-significant increase in the proportion of neurons with a LN1 or neurocan-labelled PNN in untreated cultures (21 DIV untreated; LN1 7.0 $\pm$ 0.8%; neurocan 6.1 $\pm$ 0.4%, Figure 4.13A,B). There was no significant difference in the percentage of neurons with a WFA-labelled PNN between 14 and 21 DIV cultures (21 DIV untreated; 8.7 $\pm$ 1.4%, Figure 4.13C). Quantification of the percentage of neurons with a PNN in 21 DIV cultures revealed no significant change following endo-N treatment compared to control cultures (LN1 5.2 $\pm$ 1.1%; neurocan 5.6 $\pm$ 0.6%; WFA 11.4 $\pm$ 2.1%).

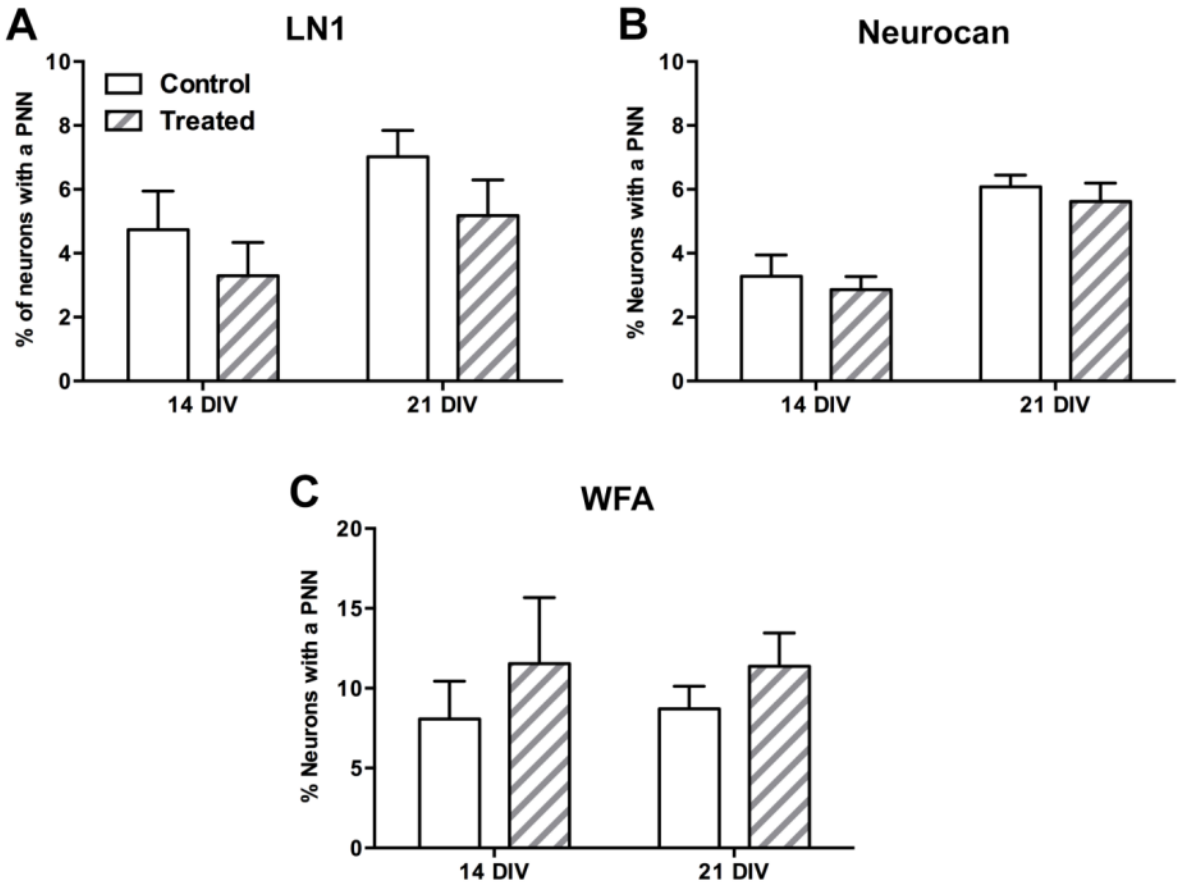

Figure 4.13. Endo-N treatment does not alter the proportion of neurons with PNNs *in vitro.*

Quantification of the percentage of neurons with either a LN1, neurocan or WFA labelled PNN, following continuous treatment with endo-N. **(A)** The proportion of neurons with a LN1-labelled PNN was marginally increased between 14 and 21 DIV. Treating cells with endo-N from 4 DIV did not alter the proportion of neurons with a LN1-labelled PNN, at either time point. **(B)** Similarly, the percentage of cultured hippocampal neurons with a neurocan-labelled PNN increased between 14 and 21 DIV. The percentage of neurons with a neurocan-labelled PNN was unchanged following endo-N treatment. **(C)** There was no change in the proportion of neurons with a WFA-labelled PNN, at either 14 or 21 DIV following endo-N treatment. *n=3* independent experiments. $p>0.05$, two-way ANOVA.

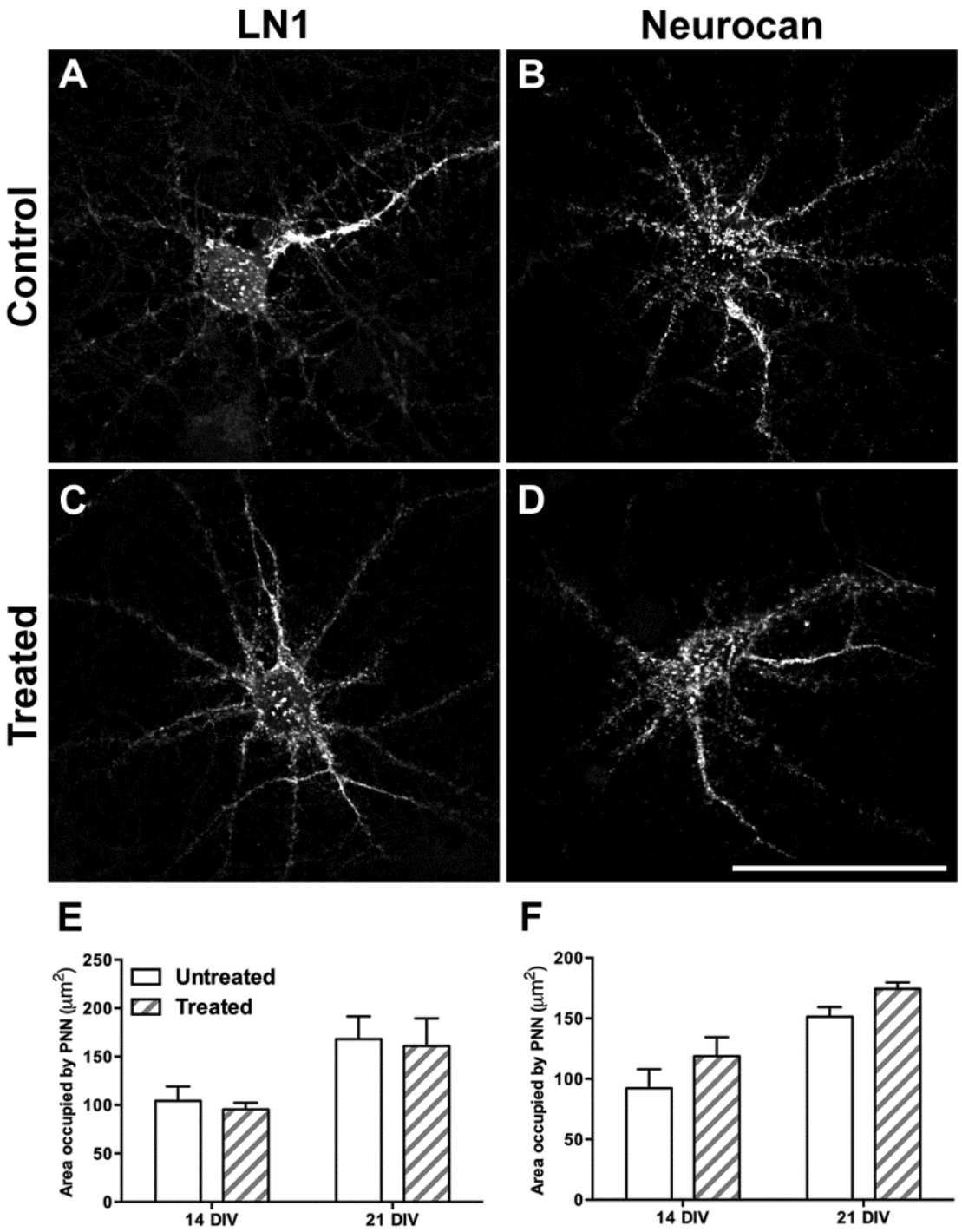

Figure 4.14. Endo-N treatment does not alter the density of PNN immunolabelling.
(A-D) Representative photomicrographs showing the density of individual PNNs following endo-N treatment. **(E)** Quantification of the density of individual LN1-labelled PNNs. There was no difference in the density of individual LN1 PNNs at either 14 or 21 DIV following endo-N treatment ($p>0.05$, two-way ANOVA). **(F)** Similarly, there was no difference in the density of neurocan labelled PNNs following endo-N treatment. *n=3* independent experiments. $p>0.05$, two-way ANOVA. Scale bar = 50 μm.

4.2.5 Endo-N treatment does not alter the density of synaptophysin immunolabelling *in vitro*

To assess whether the general density of synaptophysin labelling was altered following endo-N treatment, cells were immunolabelled with an antibody raised against synaptophysin. The immunolabelling was robust in both control and endo-N treated cultures, at both 14 and 21 DIV (Figure 4.15A-D). Quantification of synaptophysin immunostaining revealed no difference between the area occupied by labelling in endo-N treated cultures, at either 14 or 21 DIV. There was, however, a moderate increase in synaptophysin immunolabelling between 14 and 21 DIV (Figure 4.15E).

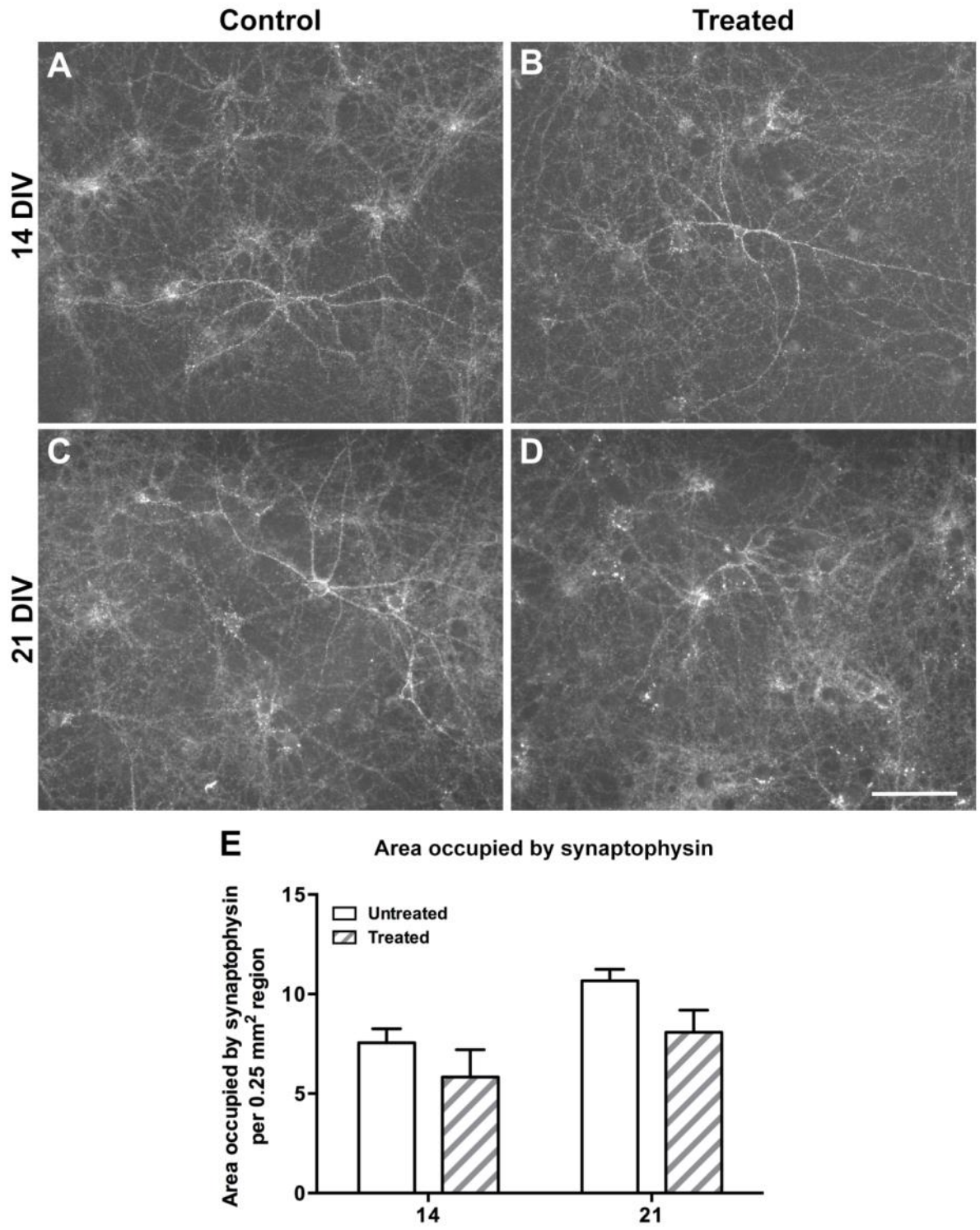

Figure 4.15. The density of synaptophysin immunostaining *in vitro* is unchanged by endo-N treatment.

(A-D) Representative photomicrographs showing the global density of synaptophysin labelling in control hippocampal cultures and following endo-N treatment. **(E)** Quantification of the density of synaptophysin labelling. There is a moderate increase in the area occupied by synaptophysin immunostaining between 14 and 21 DIV. Endo-N treatment did not affect the density of synaptophysin immunolabelling at either examined time point. *n=3* independent experiments. $p>0.05$, two-way ANOVA. Scale bar = 100 μm.

4.2.6 The density of synaptic inputs to PNN-expressing neurons is unchanged following endo-N treatment

Although the global density of synaptophysin labelling appeared to be unchanged following endo-N treatment when compared with control cultures, it was possible that the density of synaptic inputs to individual PNN-expressing neurons may be altered. To assess this, cells were triple immunostained using antibodies raised against MAP2, synaptophysin and either LN1 or neurocan. WFA, MAP2 and synaptophysin triple immunolabelling could not be reliably performed, due to the difference in buffers required for WFA and synaptophysin staining. At 14 DIV, neurons surrounded by LN1-positive PNNs received sparse contact from synaptophysin-immunopositive boutons (0.5 $\pm$ 0.1%, Figure 4.16A, E). This was increased by 21 DIV (1.0 $\pm$ 0.2%, Figure 4.16B, E). There was no difference in the density of synaptophysin labelling contacting PNN-expressing neurons following endo-N treatment (14DIV 0.2 $\pm$ 0.2%; 21DIV 0.8 $\pm$ 0.1%, p>0.05, two-way ANOVA, Figure 4.16C-E). Similarly, neurons surrounded by neurocan-labelled PNNs received sparse contact from synaptophysin-positive boutons at 14 DIV (0.3 $\pm$ 0.04%, Figure 4.17A), which was marginally increased by 21 DIV (0.6 $\pm$ 0.1%, Figure 4.17C). Following endo-N treatment, there was no difference in the density of synaptophysin labelling contacting neurons with a neurocan-labelled PNN at either 14 or 21 DIV (14DIV 0.3 $\pm$ 0.1%, 21DIV 0.5 $\pm$ 0.1%, p>0.05, two-way ANOVA, Figure 4.17C-E).

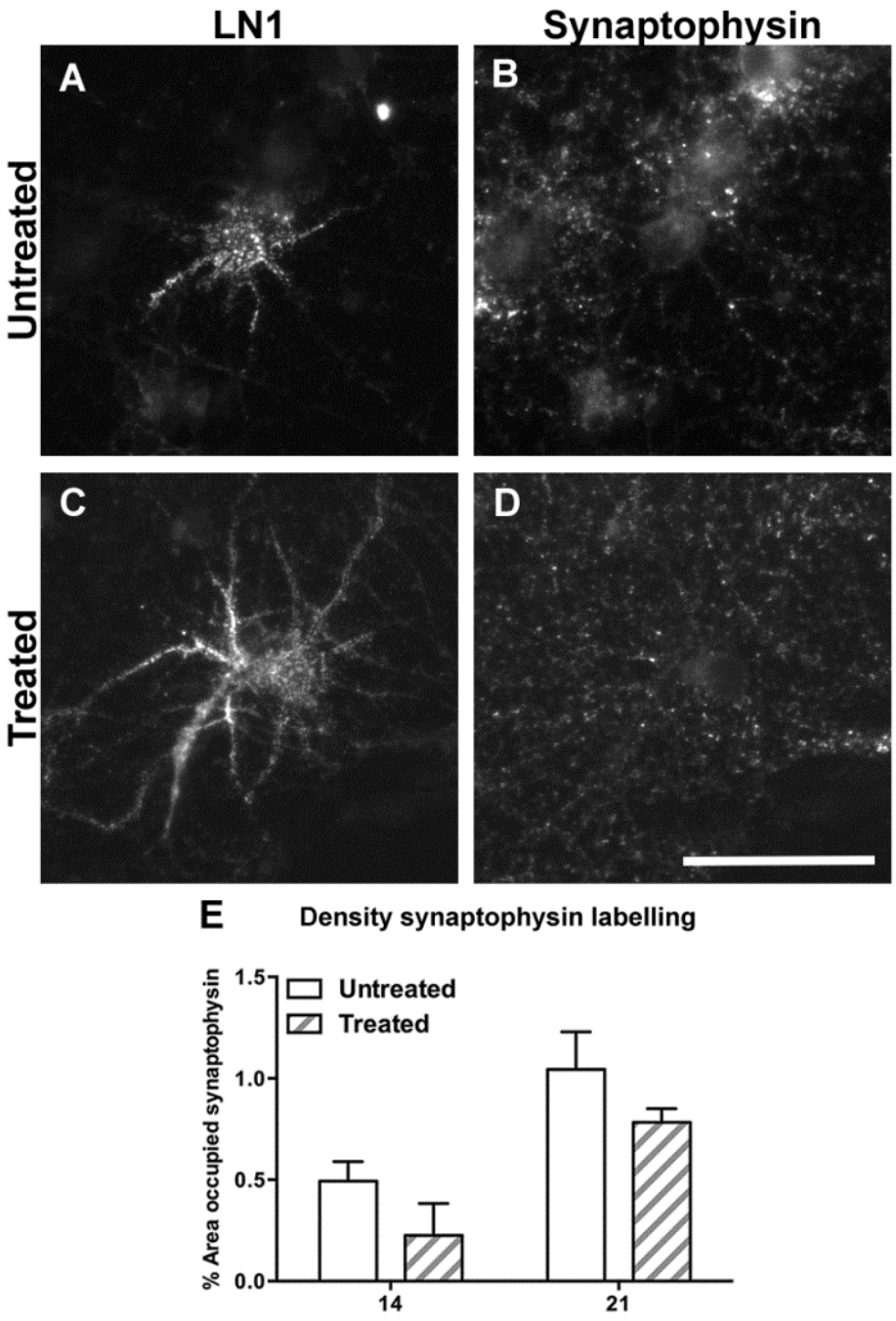

Figure 4.16. The density of synaptophysin-positive inputs to neurons with a LN1-positive PNN was unchanged following endo-N treatment.
(A-D) Representative images showing the density of synaptophysin-immunopostive boutons in contact with neurons expressing LN1-labelled PNNs after 14 DIV. **(E)** There was a moderate increase in the density of synaptophysin boutons contacting PNN-expressing neurons between 14 and 21 DIV. There was no difference between control and endo-N treated cultures. *n=3* independent experiments. $p>0.05$, two-way ANOVA. Scale bar = 50 μm.

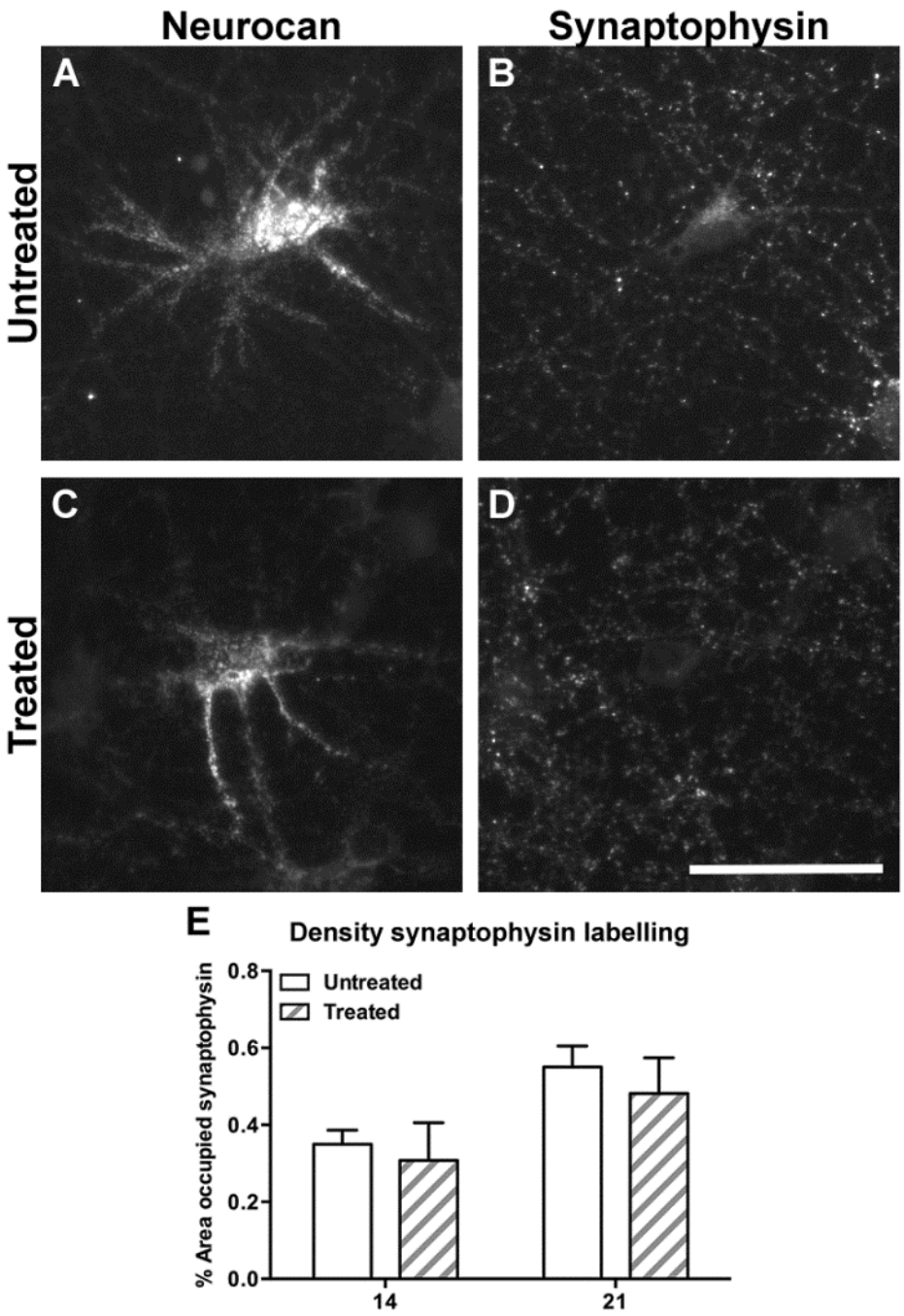

Figure 4.17. The density of synaptophysin-positive inputs to neurons with a neurocan-labelled PNN was unchanged following endo-N treatment.
(A-D) Representative images showing the density of synaptophysin-immunopositive boutons in contact with neurons expressing neurocan-labelled PNNs after 14 DIV. **(E)** There was a moderate increase in the density of synaptophysin boutons contacting PNN-expressing neurons between 14 and 21 DIV. There was no difference between control and endo-N treated cultures. *n=3* independent experiments. $p>0.05$, two-way ANOVA. Scale bar = 50 μm.

4.3 Discussion

To summarise the data presented in this chapter, PNNs were observed in dissociated primary cell cultures originating from the embryonic rat cortex and hippocampus. These PNNs were detected using WFA lectin, in addition to antibodies raised against PNN components LN1 and neurocan. Treating hippocampal cells with endo-N to remove PSA from the surface of cultured cells did not affect the percentage of neurons with a PNN, as hypothesised, or affect the density of individual PNNs. Finally, endo-N treatment did not reduce the density of synaptophysin immunolabelling in hippocampal cultures.

4.3.1 Characterisation of PNNs *in vitro*

The development of PNNs in primary cultures isolated from the developing cortex or hippocampus has been established previously (Miyata et al., 2005; Pyka et al., 2011). Similar to those observed in brain and spinal cord tissue sections, PNNs *in vitro* have previously been shown to bind WFA lectin, as in this study, in addition to supporting molecules, such as tenascin-R and LN1, and CSPGs such as brevican, phosphacan and neurocan (Miyata et al., 2005; John et al., 2006; Giamanco and Matthews, 2012). In both cortical and hippocampal cultures, PNNs were observed on the neuronal cell body and proximal dendrites, as demonstrated by co-localisation between PNN immunolabelling and MAP2 immunoreactivity. Additionally, PNN labelling was observed on another neurite-like structure, that was devoid of MAP2 staining. This probably corresponds to the axon initial segment, which has previously been shown to be ensheathed by a dense pericellular matrix, both *in vitro* and in tissue sections (Bruckner et al., 2006; John et al., 2006). Neuronal phenotypes expressing PNNs *in vitro* have been well established and thus were not examined in this study. Generally, PNNs are observed surrounding parvalbumin-positive interneurons in cultures originating from the embryonic cortex, which also corroborates findings from tissue sections (Pizzorusso et al., 2002; Miyata et al., 2005). It is likely that at least a proportion of the neurons in the hippocampal cultures used in this study are positive for parvalbumin, and that a fraction of these neurons express PNNs.

Previous research has suggested the formation of two types of WFA-labelled PNNs in cortical cultures, which have been termed granular and pericellular PNNs (Miyata et al., 2005). It could be speculated that granular PNNs represent less developed structures, while

pericellular PNNs are more mature. In the data presented in this chapter, WFA labelling was exclusively found as granular PNNs. Conversely, neurocan was found as both granular and pericellular PNNs, and partially co-localised with WFA in granular structures. Co-localisation between WFA and LN1 was not observed in either cortical or hippocampal cultures, despite LN1 being observed in both pericellular and granular structures. Double-labelling of PNNs by neurocan and WFA has been observed in other studies (Miyata et al., 2005), as has double-labelling by LN1 and WFA (Giamanco et al., 2010). The lack of co-localisation between LN1 and WFA in this study may explain the absence of pericellular WFA-labelled PNNs. LN1 is believed to stabilise connections between hyaluronan and CSPGs (Tsien, 2013) and mounting evidence supports a crucial role for this protein in the development of the PNN. For example, one study noted the production of a condensed, pericellular matrix following expression of LN1, in combination with hyaluronan synthase, which was not produced following expression of hyaluronan synthase alone (Kwok et al., 2010). Furthermore, transgenic mice lacking LN1 expression in the brain, have a drastic reduction in both the number and density of WFA-labelled PNNs in the cortex (Carulli et al., 2010; Suttkus et al., 2014). Taken together, these experiments suggest a key role for LN1 in the development of a pericellular matrix, such as PNNs. Double-labelling for LN1 and neurocan could not be performed in this study due to cross-reactivity between primary antibodies. Co-localisation between LN1 and other CSPGs, such as brevican, has been observed in pericellular PNNs *in vitro*, previously (Giamanco et al., 2010). Thus, it is likely that there would be some degree of LN1 and neurocan co-localisation in these cultures, probably in pericellular PNNs.

4.3.2 The relationship between PSA expression and development of the PNN *in vitro*

In vivo, PNNs develop after the critical period for neuroplasticity, and are believed to act to stabilise synaptic connections and also to restrict experience-dependent plasticity, for example ocular dominance plasticity (Pizzorusso et al., 2002; Wang and Fawcett, 2012). Conversely, it has been noted in a separate study that PSA expression, abundant during the late stages of embryonic development, and in the early postnatal development is down-regulated towards the end of the critical period. It has been proposed that PSA down-regulation may regulate the onset of ocular dominance plasticity in the visual cortex (Di Cristo et al., 2007b). Unpublished data from our laboratory has revealed a spatiotemporal

relationship between PSA down-regulation and expression of PNNs in the postnatal rat nervous system. In the spinal cord, for example, PSA expression was widespread throughout the first two weeks of postnatal development, following which, levels declined and occasional WFA-labelled PNNs were formed (unpublished observations, Dr Xuenong Bo and Dr Yi Zhang). Between the second and third postnatal weeks, PSA expression was down-regulated and the number of PNNs increased (unpublished observation). This led to the hypothesis that PSA down-regulation may act as a molecular switch for the development of the PNN *in vivo*. The initial data presented in this chapter may also support a role for PSA down-regulation in the development of PNNs. After 14 DIV, PSA expression was robust in hippocampal cultures. While occasional PNNs could be observed at this time point, the percentage of neurons with a PNN had increased by 21 DIV. Within the same timeframe, PSA expression had decreased and the density of synaptophysin immunolabelling had increased. A gradual increase in the density of synaptophysin labelling in hippocampal cultures has been identified previously, and is believed to reflect the maturation of cultures with time (Fletcher et al., 1991; Harrill et al., 2015). While there is no current data to suggest a correlation between the density of synaptic proteins and PNN markers *in vitro*, it is likely that the increase in synaptophysin immunostaining and the change in the proportion of neurons with a PNN, are linked. Previous studies have revealed the close association between PNNs and synaptic boutons *in vitro,* suggesting the PNNs have a crucial role in the development and stabilisation of synapses (Miyata et al., 2005; Geissler et al., 2013).

To assess the hypothesised relationship between PSA and PNNs in more detail, hippocampal cultures were treated with endo-N, starting after 4 DIV. Endo-N has been widely used *in vivo* to selectively remove PSA from the surface of the neural cell adhesion molecule, to investigate the role of PSA in axon guidance and synaptogenesis in specific brain regions (Daston et al., 1996; McRae et al., 2007). As expected, PSA labelling in endo-N treated cultures was almost completely absent. The concentration of endo-N used in this study was selected based on a series of experiments that noted a dose-dependent death of cultured hippocampal neurons at higher concentrations of endo-N. Interestingly, there was no difference in the percentage of neurons with a PNN, or the density of PNN labelling on individual neurons, following endo-N treatment. To date, this is the first study to directly

investigate whether PSA can regulate PNN formation *in vitro*. While it is now generally believed that neuronal activity can modulate PNN formation both in cultures and also *in vivo*, for example in the rodent visual cortex and the barrel cortex (Pizzorusso et al., 2002; McRae et al., 2007), the molecular mechanisms underlying PNN development are poorly understood. Recently, it has been proposed that LN1 upregulation underlies the formation of PNNs in the rat cerebellum and visual cortex (Carulli et al., 2007; Carulli et al., 2010). It has also been suggested that closure of the critical period, and thus, PNN formation, can be modulated by the ratio of chondroitin-4 to chondroitin-6 sulphation *in vivo* (Miyata et al., 2012).

From the data presented in this thesis, although PSA down-regulation apparently corresponds to an increase in the proportion of neurons with a PNN *in vitro*, it is likely that PSA down-regulation is not a critical factor for the development of PNNs, at least *in vitro*, as endo-N treated cultures showed no difference in PNN formation. Nonetheless, it would still be interesting to investigate PNN formation in mice lacking the polysialyltransferase enzymes PST and STX. Mice devoid of both polysialyltransferase enzymes have a complete loss of PSA *in vivo* and have gross abnormalities in brain structure (Weinhold et al., 2005). At present, there is no data available as to whether these mice show any abnormalities in the extracellular matrix. It would be interesting to investigate this at different time points during postnatal development.

4.3.3 The relationship between PSA expression and synaptogenesis *in vitro*

We speculated here that early removal of PSA from primary hippocampal cultures would lead to an increase in the proportion of PNNs. We also hypothesised that if there was an increase in PNNs, this may restrict the formation of synapses on PNN-expressing neurons and consequently, lead to a reduction in the density of synaptophysin immunolabelling *in vitro*. Although there was no alteration in either the number or density of PNNs with endo-N treatment, as PSA has a crucial role in axonal pathfinding and synaptogenesis, we hypothesised that endo-N-mediated PSA removal could still affect synapse formation *in vitro.* Currently, the only other study investigating the density of synaptic labelling in endo-N treated hippocampal cultures noted a reduction in the density of synaptophysin-labelled boutons contacting neuronal dendrites, compared to control cultures (Dityatev et al., 2004). In a heterogeneous culture system, containing hippocampal neurons isolated from NCAM$^{+/+}$

and NCAM$^{-/-}$ mice, a lower density of synapses was found on NCAM$^{+/+}$ neurons after treatment of the cultures with endo-N (Dityatev et al., 2004). In the data presented in this thesis, endo-N treatment did not affect the general density of synaptophysin labelling *in vitro*, or the density of synaptophysin-labelled boutons contacting individual PNN-expressing neurons. There are a number of crucial differences between the Dityatev *et al.* study and the data presented in this thesis, which may explain the conflicting results obtained, namely, differences in the species and age of animals used for culture (rat embryonic day 18 here, and mouse postnatal day 1-3 in the study by Dityatev and collaborators). Furthermore, Dityatev *et al.*, quantified inputs to neuronal dendrites, which could not be performed in this study due to limitations with the Image J script used for quantification; this script only allowed quantification of inputs to the neuronal cell body. Additionally, their study used a higher (10-fold difference) concentration of endo-N (Dityatev et al., 2004). Such a high endo-N concentration was not assessed in the study presented in this thesis. However, treating cells with endo-N, diluted to half of this concentration, resulted in a strong reduction in the number of MAP2-positive neurons observed in culture, indicating that high concentrations of endo-N led to significant neurotoxicity. This has also been observed in another study (Vutskits et al., 2001). It must also be taken into consideration that while the concentration of endo-N drastically reduced PSA labelling *in vitro*, there was some residual PSA expression observed, which may have promoted synapse formation.

In this study, synaptophysin immunolabelling was used to identify synapses, due to its robust use in other studies, in addition to strong localisation at presynaptic terminals. While synaptophysin is still considered a good marker for the labelling of synapses both *in vitro* and *in vivo,* it is becoming increasingly common is to use dual fluorescent labelling, with pre- and post-synaptic markers, such as bassoon and PSD-95, respectively (Pyka et al., 2011). Quantification of the number of double-labelled boutons is hypothesised to give a more accurate estimate of the number of active synapses, compared to the use of synaptophysin immunolabelling alone. However, this dual staining technique, like synaptophysin labelling, cannot distinguish between excitatory or inhibitory synaptic boutons. This requires specific antibodies, raised against vesicular transporters for either glutamate (VGLUT) or GABA (VGAT). This may be an interesting future experiment, to investigate whether PSA removal

from hippocampal neurons can affect the density of different types of synaptic inputs to PNN-expressing neurons *in vitro.*

The experiments to investigate the effect of PSA removal on the development of PNNs in this thesis were performed using primary hippocampal neurons, as opposed to cortical neurons or organotypic slice cultures, for two main reasons. Firstly, hippocampal cultures are widely used to model synaptogenesis *in vitro.* Secondly, previous research has suggested chemical digestion of parts of PNNs can increase the number of synapses in hippocampal cultures (Pyka et al., 2011). As the hypothesis of this chapter was to investigate whether PSA can modulate the structure of PNNs, and thereby alter the number of synapses, this seemed an appropriate model. However, it must also be noted that using a two-dimensional culture system has its flaws, and does not accurately represent the environment *in vivo*. For example, neurons *in vivo* are surrounded by a network of glial cells and ECM molecules, which is impossible to replicate using a two-dimensional culture system. Moreover, PSA expression *in vitro*, at least in the cellular model used in this study, does not follow the same developmental pattern observed *in vivo*. For example, *in vivo*, PSA expression in the hippocampus is down-regulated during early post-natal development, with the exception of the dentate gyrus (Seki and Arai, 1991; Di Cristo et al., 2007a). Conversely, cultured hippocampal neurons maintain strong PSA expression during the third week *in vitro*, beyond the time-point at which PSA would normally be down-regulated *in vivo.* For these reasons, it may be prudent to repeat this study using organotypic slice cultures, which more accurately represent the natural spatiotemporal expression of PSA *in vivo,* in addition to maintaining the complex cytoarchitecture of the brain *in vitro*.

One of the main caveats of this study is the lack of short time-points for quantification of the proportion of neurons with a PNN and the density of synaptophysin immunolabelling. The main reason that 14 DIV was selected as the earliest time-point is due to the poor PNN and synaptophysin immunostaining prior to this *in vitro.* Very few PNN-bearing neurons were observed at 7 DIV, which made accurate quantification extremely difficult. Moreover, synaptophysin labelling was weak at 7 DIV, and detection of synaptophysin-positive boutons by the quantification program used in this study was poor, rendering quantification inaccurate.

4.4 Conclusions

Taken together, the results from this study indicate that although the timing of PSA reduction in cultured hippocampal neurons that have not been treated with endo-N seemingly corresponds to an increase in the proportion of neurons with a PNN, it is unlikely that PSA down-regulation has a direct role in PNN formation, at least *in vitro*, as treating cultured neurons with endo-N did not alter either the proportion of neurons expressing PNNs or the density of individuals PNNs.

Chapter 5

Optimisation of lentiviral vectors for use in the central nervous system

Chapter 5: Optimisation of lentiviral vectors for use in the central nervous system

5.1 Introduction

The data generated in the previous chapter of this thesis showed no difference in either the proportion of neurons with a PNN, or the density of PNNs on individual neurons following removal of PSA from cultured hippocampal neurons. However, there were a number of limitations with this study, as discussed in chapter 4.3, which may have affected the results from these experiments. One of the most likely caveats, is the two-dimensional cell cultures used for these experiments, which do not represent the complex cytoarchitecture of the brain. Consequently, it was decided to further investigate the proposed relationship between PSA and the PNN *in vivo,* using a viral vector to selectively express the polysialyltransferase gene in neurons and subsequently use immunolabelling to examine the effect of induced PSA expression on both the number and density of PNNs. Before undertaking these experiments, there were a number of factors to be deliberated, such as the type and pseudotype of viral vector used, in addition to the delivery method of viral vectors, to ensure robust transgene expression in the desired cell type and region of the CNS. These factors will be discussed in more detail below.

5.1.1 The use of lentiviral vectors in the CNS

The use of viral vectors to selectively express a gene of interest in the CNS is increasing in popularity. While different vectors are principally used for other tissues, the most commonly used in the CNS are derived from the adeno-associated virus, or lentivirus.

Lentiviral (LV) vectors consist of a genome formed of single-stranded RNA, which is surrounded by the viral capsid and then ensheathed by an envelope (Baron, 1996). Following entry into the host cells, the RNA genome is reverse transcribed into double-stranded DNA, which subsequently integrates into the host genome, resulting in long-term transgene expression (Baron, 1996). Unfortunately, some vectors show a preference for integration into the sites of regularly active genes, which carries a high risk of insertional mutagenesis. Consequently, a group of non-integrating retroviral vectors have been

engineered, which retain the ability to successfully transduce neurons and glial cells *in vivo* (Rahim et al., 2009).

Including the human immunodeficiency virus (HIV), simian immunodeficiency virus (SIV) and feline immunodeficiency virus (FIV), LV vectors can transduce both dividing and non-dividing cells and produce long-lasting transgene expression (Azzouz et al., 2004). Interestingly, some vectors can be uptaken by either the neuronal cell body or the axon terminal, facilitating their use as neuroanatomical tracers (Beier et al., 2011; Hutson et al., 2012).

Commonly, LV vectors are pseudotyped using glycoprotein from the vesicular stomatitis virus (VSV-G), allowing transduction of a broad range of cell types (Liehl et al., 2007; Yaguchi et al., 2013). Cell-type specific targeting can be achieved by altering the cellular tropism, using different envelope proteins; for example, pseudotyping with glycoprotein from the rabies virus resulted in selective transduction of astrocytes (Liehl et al., 2007). What is far more common, however, is to drive gene expression in target cells using a cell-type specific promoter sequence. The use of a ubiquitous promoter sequence, such as that from cytomegalovirus (CMV), will drive transgene expression in a number of CNS cell types, including neurons and astrocytes (Li et al., 2010). Conversely, using cell-type specific promoters, such as synapsin I or GFAP, results in transgene expression in exclusively neurons or astrocytes, respectively (Hioki et al., 2007; Li et al., 2010; Yaguchi et al., 2013).

LV vectors have previously been used to either induce expression of a gene of interest, or as a delivery system for small hairpin RNA (shRNA) to suppress the expression of target genes in the CNS (reviewed by (Parr-Brownlie et al., 2015). Coupled with the ability to direct transgene expression to pre-determined cell types, in addition to improvements in the safety of viral vectors, this has led to a surge of research attempting to harness this technology to deliver drug treatments to the injured or diseased nervous system (Yip et al., 2006; Weishaupt et al., 2014).

5.1.2 Methods of lentiviral vector administration to the CNS

Many studies, particularly those that use viral vectors to deliver drug treatment to the injured CNS require the precise delivery of vectors to specific regions of the brain or spinal cord. The most common method of focal delivery is the direct injection of vectors into the CNS parenchyma. One of the main advantages of this method, is that it allows the precise

delivery of vectors to specific regions of the CNS, thereby allowing targeting to pre-determined neuronal populations (Cetin et al., 2006). Additionally, this technique is highly reproducible and causes very little damage to the CNS (Cetin et al., 2006). However, diffusion of vectors away from the initial injection site is often limited, and multiple injections may be required to deliver vectors to large regions of the CNS (Parr-Brownlie et al., 2015).

Other types of viral vector, namely adeno-associated vectors, can transduce a wide area of the CNS following delivery into either (i) the cerebrospinal fluid (CSF), typically via the lateral ventricles or cisterna magna, or (ii) the periphery (using intravenous injections) (Stone et al., 2008; Shen et al., 2013). This is not possible with LV vectors, which require direct delivery to the parenchyma to allow the robust transduction of CNS cell types.

5.1.3 Aims

The work presented in this chapter had the following aims; i) to generate LV vectors carrying the transgene for the polysialyltransferase (PST) enzyme or the control transgene GFP; ii) to optimise the methodology for LV vector delivery to the CNS suitable for use *in vivo*; iii) to optimise the promoter sequence needed to drive high levels of transgene expression in neurons; iv) to conduct a pilot study, investigating whether induced expression of PSA in the adult sensorimotor cortex can reduce WFA-binding within the PNN.

5.2 Results

5.2.1 Generation of lentiviral vectors

The methodology for the production and titration of LV vectors, is described in chapter 2.2. A total of 3 LV vectors were generated in this study: i) carrying the transgene for GFP, under the control of a CMV promoter (LV/CMV-GFP), to act as the control vector; ii) carrying the transgene for GFP under the control of a human synapsin I promoter (LV/Synapsin I-GFP), to provide a second control for the overexpression of PST via the synapsin I promoter; iii) carrying the transgenes for PST, fused to GFP, and mCherry, under the control of two separate human synapsin I promoters (LV/Synapsin I-PST), to provide expression of PST.

5.2.2 Optimisation of the viral vector delivery method

There are several methods through which LV vectors have been delivered directly into the CNS, in particular via a Hamilton syringe with a 33G steel needle or a glass micropipette (Cetin et al., 2006; Yip et al., 2006). To compare these delivery methods, rats received bilateral injections of LV/GFP into the sensorimotor cortex, delivered using either a steel needle or glass micropipette (one hemisphere received LV/CMV-GFP injection, the other received LV/Synapsin-1 injection). Injections delivered by either the steel needle or the glass micropipette resulted in successful transduction of cortical cells, which could be observed 2 weeks post-injection as large regions of GFP-positive cells (Figure 5.1). The injection performed using the steel needle resulted in a clearly identifiable needle tract, which was filled with autofluorescent cells (Figure 5.1A, arrowheads). By contrast, no clear needle tract could be observed following injection delivered using the glass micropipette, and no autofluorescent cells were identified (Figure 5.1B). This data suggests that delivering LV vectors using a glass micropipette resulted in very limited tissue damage compared to a steel needle; thus, subsequent injections were performed using this methodology.

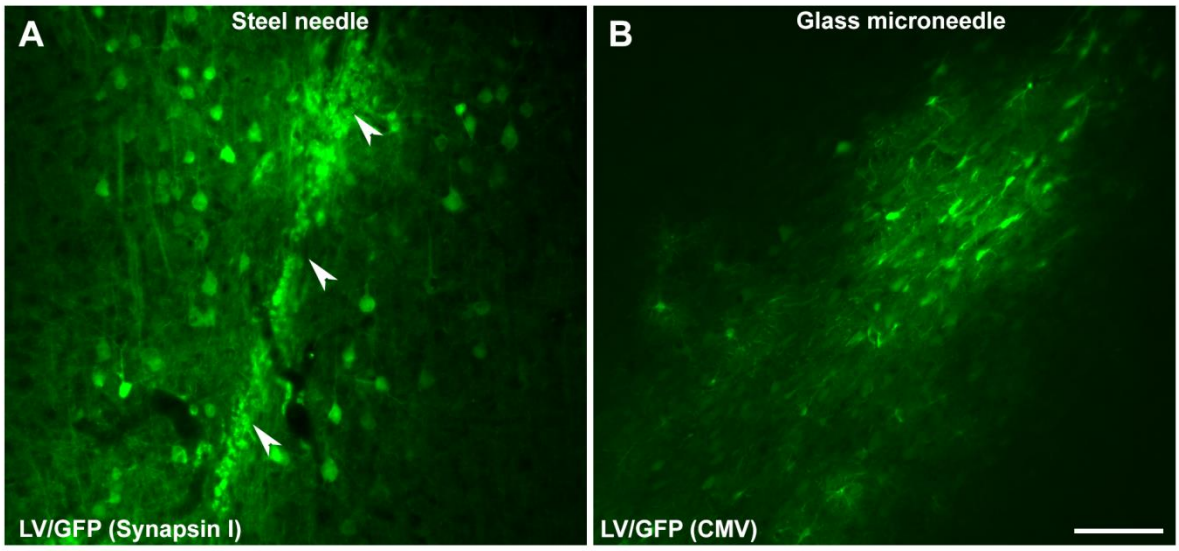

Figure 5.1. Intraparenchymal injections delivered using a steel needle resulted in greater damage to the cortex compared to a glass micropipette.
(A) Delivery of LV vector to the sensorimotor cortex using a steel needle resulted in strong transduction of cells near the injection site, which could be identified by GFP expression 2 weeks post-injection. A distinct needle tract damage to the cortical parenchyma was observed, indicated by autofluorescent cells along the needle tract (arrowheads). **(B)** Similarly, delivering LV vector to the cortex using a glass micropipette resulted in

transduction of cells at the injection site, identified by GFP expression, with minimal needle tract damage to the cortical parenchyma. Scale bar = 100 μm.

5.2.3 Cell types transduced by lentiviral vectors following injection to the cortex

As mentioned in chapter 5.1.1, targeted expression of LV vectors can be obtained using cell-type specific promoter sequences to drive transgene expression. For this study, it was important to obtain robust and specific transgene expression in neurons. Previous research has noted strong transgene expression in neurons, and also glial cells, when driven by a CMV promoter sequence, or exclusive transgene expression in neurons when expression was driven by synapsin I promoter sequence. To study the effect of different promoters and to determine the optimal promoter sequence for high transgene expression in neurons, rats received bilateral injections of LV/CMV-GFP and LV/Synapsin I-GFP to the sensorimotor cortex. Coronal brain sections of the injection sites were immunolabelled with antibodies raised against GFAP (astrocytes), NeuN (neurons) or Iba1 (microglia) to identify cell types transduced by each vector.

Two weeks following injection of the viral vectors, large areas of GFP-positive cells could be identified in the cortex, indicating successful transduction of, and strong transgene expression in cortical cells, by both LV/CMV-GFP and LV/Synapsin I-GFP (Figure 5.2). The LV/CMV-GFP injection resulted in transgene expression in a heterogeneous population of cells, including both neurons and astrocytes. A large number of GFP-positive cells was strongly co-labelled with GFAP, indicating that a large proportion of these cells were astrocytes (Figure 5.2A'-A''', arrowheads). However, co-localisation between GFP-positive cells and NeuN was weak, with only occasional double-labelled cells observed (Figure 5.2B'-B''', arrowheads). No co-localisation could be observed between Iba1 and GFP (Figure 5.2C'-C'''), suggesting that transgene expression in microglial cells did not occur.

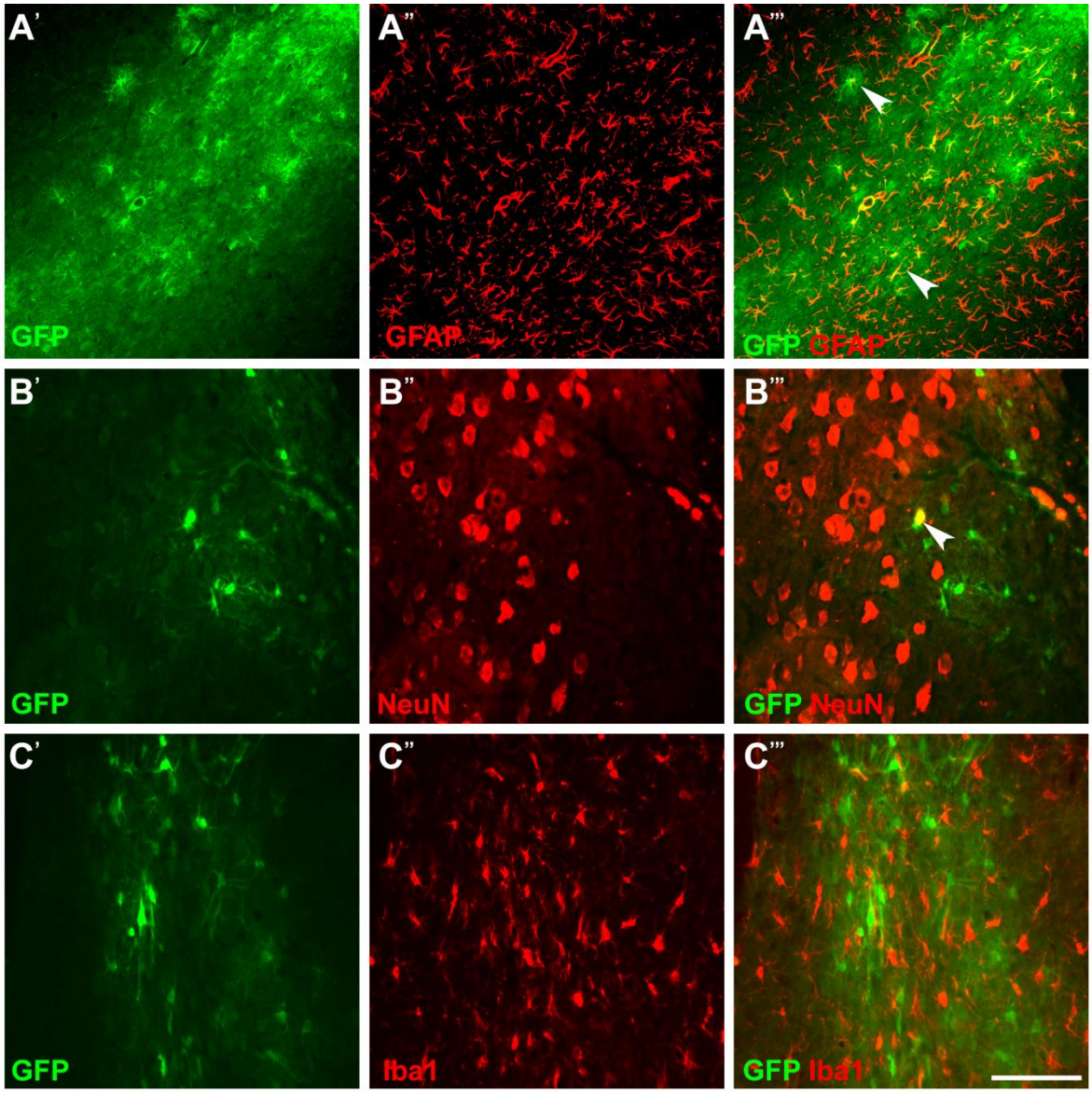

Figure 5.2. Expression of LV/CMV-GFP reporter gene was strong in astrocytes following injection into the sensorimotor cortex

Qualitative assessment was used to identify the type of cells with expression of LV/CMV-GFP reporter gene, 2 weeks following injection into the sensorimotor cortex. **(A'-C')** Strong expression of the viral reporter gene (GFP) was observed at 2 weeks post injection. **(A'-A''')** Frequent co-localisation was observed between GFP-positive cells and GFAP immunolabelling (arrowheads). **(B'-B''')** Weak co-localisation was observed between GFP and NeuN labelling, but some double-labelled cells could be identified (arrowhead). **(C'-C''')** No co-localisation between GFP and Iba1 labelling was observed. Scale bar = 100 μm.

Similarly to LV/CMV-GFP, LV/Synapsin I-GFP injection resulted in a large area of transduced cells in the cortex, which could be identified by strong GFP expression (Figure 5.3). Fluorescent immunostaining using cell-type specific antibodies revealed no co-localisation

between GFP and GFAP labelling (Figure 5.3A'-A'''). Conversely, strong co-localisation could be observed between GFP and NeuN labelling (Figure 5.3B), indicating that LV/Synapsin I-GFP could drive strong transgene expression in transduced cortical neurons. No co-localisation was also observed between Iba1 labelling and GFP, suggesting poor reporter gene expression in cortical microglial cells (Figure 5.3C'-C''').

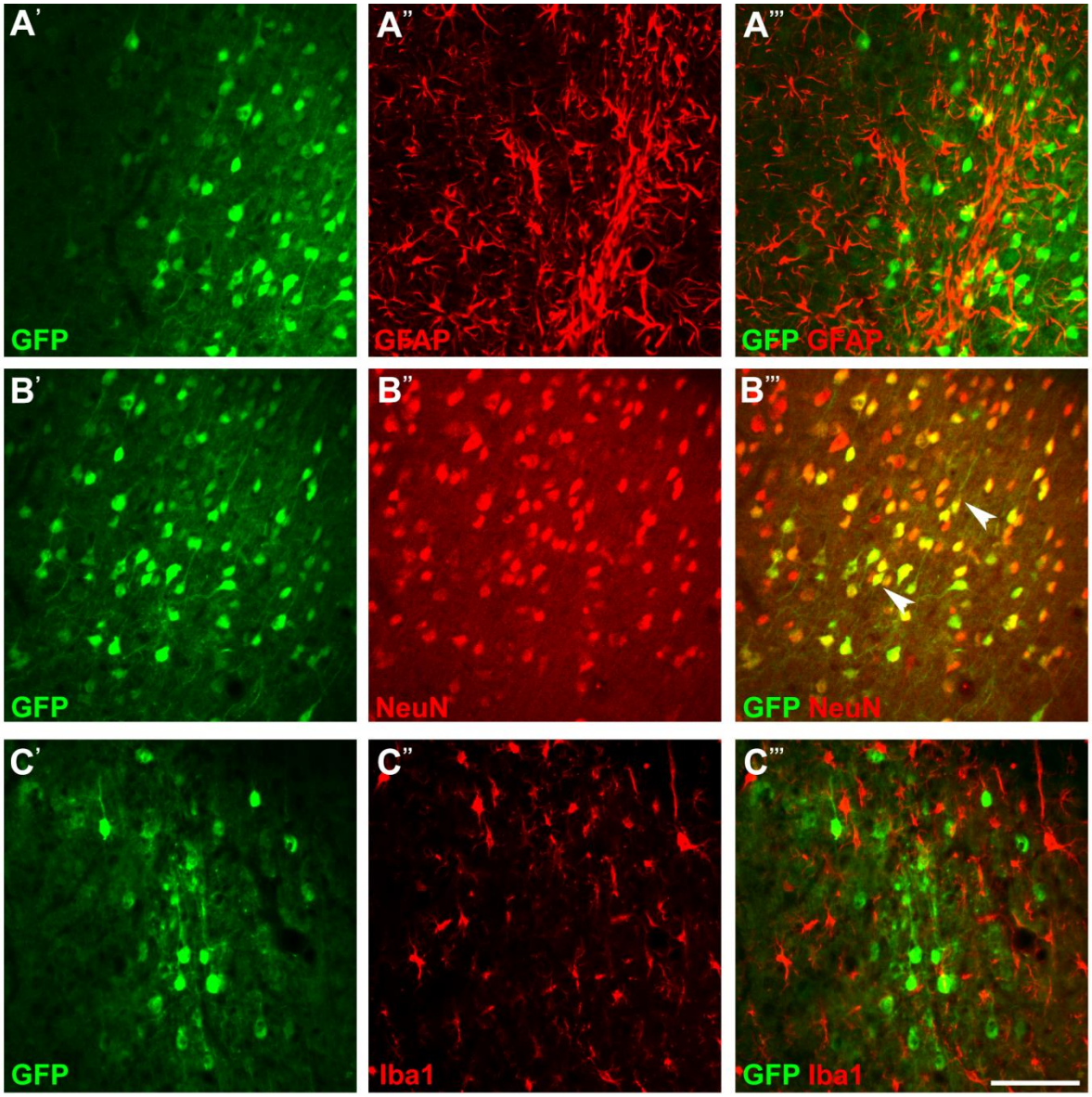

Figure 5.3. Expression of LV/Synapsin I-GFP reporter gene was exclusively neuronal. Qualitative assessment was used to identify the type of cells with expression of LV/Synapsin I-GFP reporter gene at 2 weeks following injection into the sensorimotor cortex. **(A'-C')** Expression of the viral reporter gene (GFP) was strong at 2 weeks post injection. **(A'-A''')** No co-localisation was observed between GFP and GFAP immunostaining. **(B'-B''')** GFP co-localised exclusively with NeuN-immunopositive neurons (arrowheads). **(C'-C''')** No co-localisation was observed between GFP and Iba1 labelling. Scale bar = 100 μm.

In a separate study, animals received unilateral injections of LV/Synapsin I-PST, which can independently express PST and the red mCherry fluorescent protein into the sensorimotor cortex. To identify the cell types transduced by LV/Synapsin I-PST, brains were harvested 2 weeks post-injection, and coronal sections were immunolabelled with primary antibodies raised against GFAP, NeuN or Iba1. LV/Synapsin I-PST injection resulted in successful reporter gene expression in cortical cells, which could be identified by strong mCherry expression (Figure 5.4A'-C'). No co-localisation was observed between mCherry-positive cells and GFAP immunolabelling, suggesting that Synapsin I promoter sequence did not drive transgene expression in cortical astrocytes (Figure 5.4A'-A'''). Conversely, strong co-localisation was observed between mCherry-positive cells and NeuN labelling (Figure 5.4B'-B'''), indicating strong transgene expression in cortical neurons. No co-localisation was observed between Iba1 labelling and mCherry (Figure 5.4C'-C''').

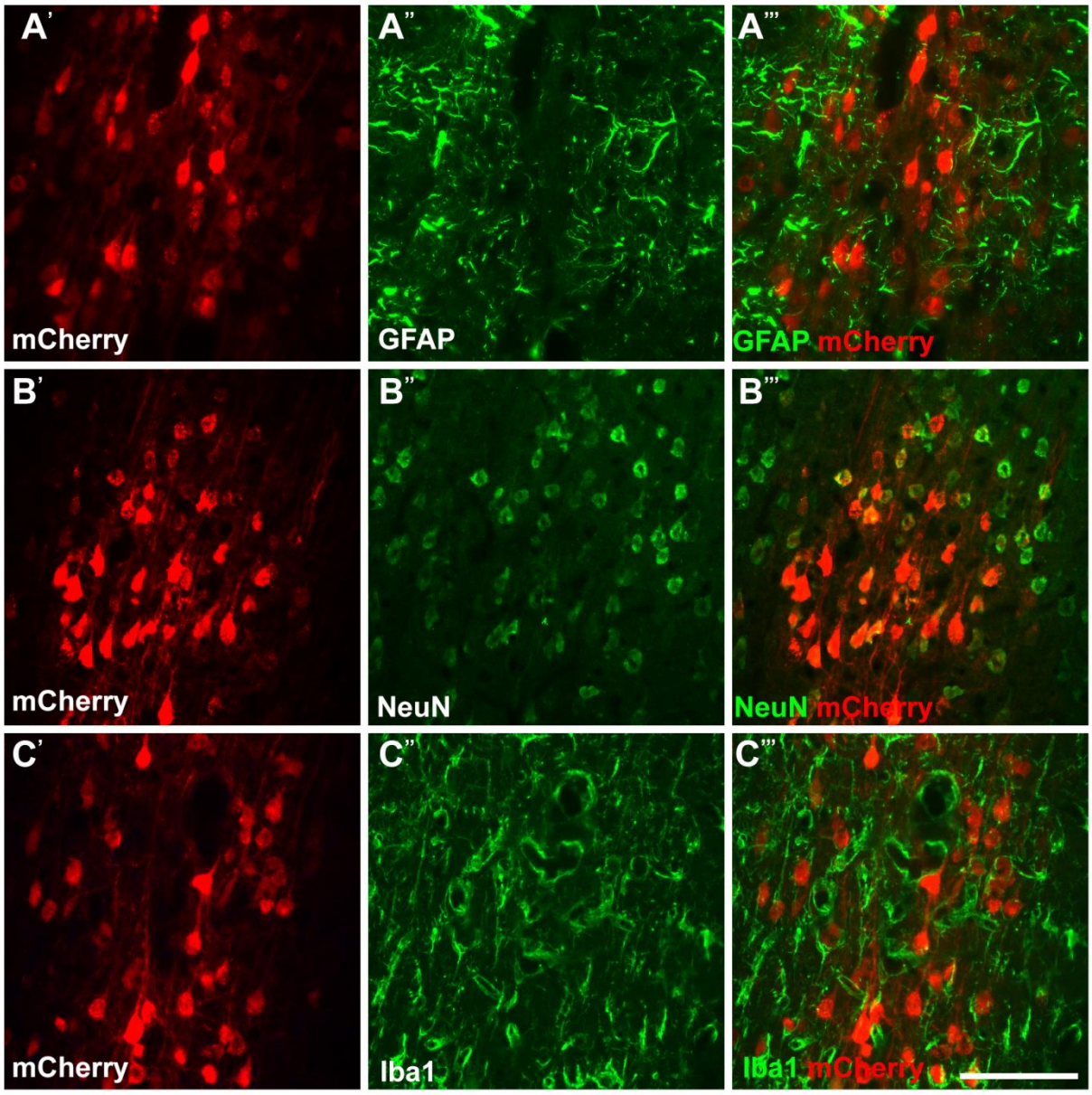

Figure 5.4. Expression of LV/Synapsin I-PST reporter gene was exclusively neuronal. Qualitative assessment was used to identify the type of cells containing expression of LV/Synapsin I-PST reporter gene at 2 weeks following injection into the sensorimotor cortex. **(A'-C')** Strong expression of the viral reporter gene (mCherry) was observed at 2 weeks post injection. **(A'-A''')** No co-localisation was observed between GFAP immunostaining and mCherry. **(B'-B''')** mCherry co-localised exclusively with NeuN-positive neurons. **(C'-C''')** No co-localisation was observed between Iba1 labelling and mCherry. Scale bar = 100 µm.

In summary, these experiments suggest that following injection into the adult rat cortex, LV vectors under the control of a CMV promoter restricted transgene expression to astrocytes, with weak transgene expression in neurons. Conversely, LV vectors under the control of the human synapsin I promoter restricted transgene expression to neurons, as expected,

illustrated by the strong co-localisation between GFP- or mCherry-positive cells and NeuN immunolabelling.

5.2.4 Cell types transduced by lentiviral vectors following injection to the cervical spinal cord

5.2.4.1 Uninjured spinal cord

Previous research suggests that different promoter sequences are required to drive transgene expression in neurons in different regions of the CNS. For example, using LV vectors with the transgene under the control of the CMV promoter results in low transgene expression in cortical neurons, compared to the use of LV vectors with the transgene under the control of the PGK promoter. Conversely, the opposite is true with cerebellar granular neurons (Li et al., 2010). To assess whether transgene expression driven by the CMV promoter was higher in the spinal cord, compared to previous data obtained in the sensorimotor cortex, rats received a unilateral injection of LV/CMV-GFP into the intermediate grey matter and ventral horn at C6/C7 spinal cord level. Horizontal spinal cord sections containing the injection site were collected at 2 weeks post injection and immunolabelled for neurons, astrocytes and microglia using the cell-type specific markers NeuN, GFAP and Iba1, respectively. Similarly to data obtained following cortical injection, LV/CMV-GFP intraspinal injection resulted in strong co-localisation of GFP-positive cells and GFAP (Figure 5.5A'-A''', arrowheads). Co-localisation between NeuN labelling and GFP-positive cells was weak, however, occasional double-labelled cells could be identified (Figure 5.5B'-B''', arrowheads). Furthermore, a few of these double-labelled neurons were motor neurons, based on their size and location within the ventral horn. Co-localisation between Iba1 and GFP-positive cells was absent, suggesting that CMV promoter cannot drive transgene expression in spinal cord microglial cells (Figure 5.5C'-C''').

As this data supports previous findings using LV/CMV-GFP in the sensorimotor cortex, it was decided to continue future experiments using LV vectors with the transgene under the control of the human synapsin I promoter, i.e. LV/Synapsin I-GFP (control) and LV/Synapsin I-PST.

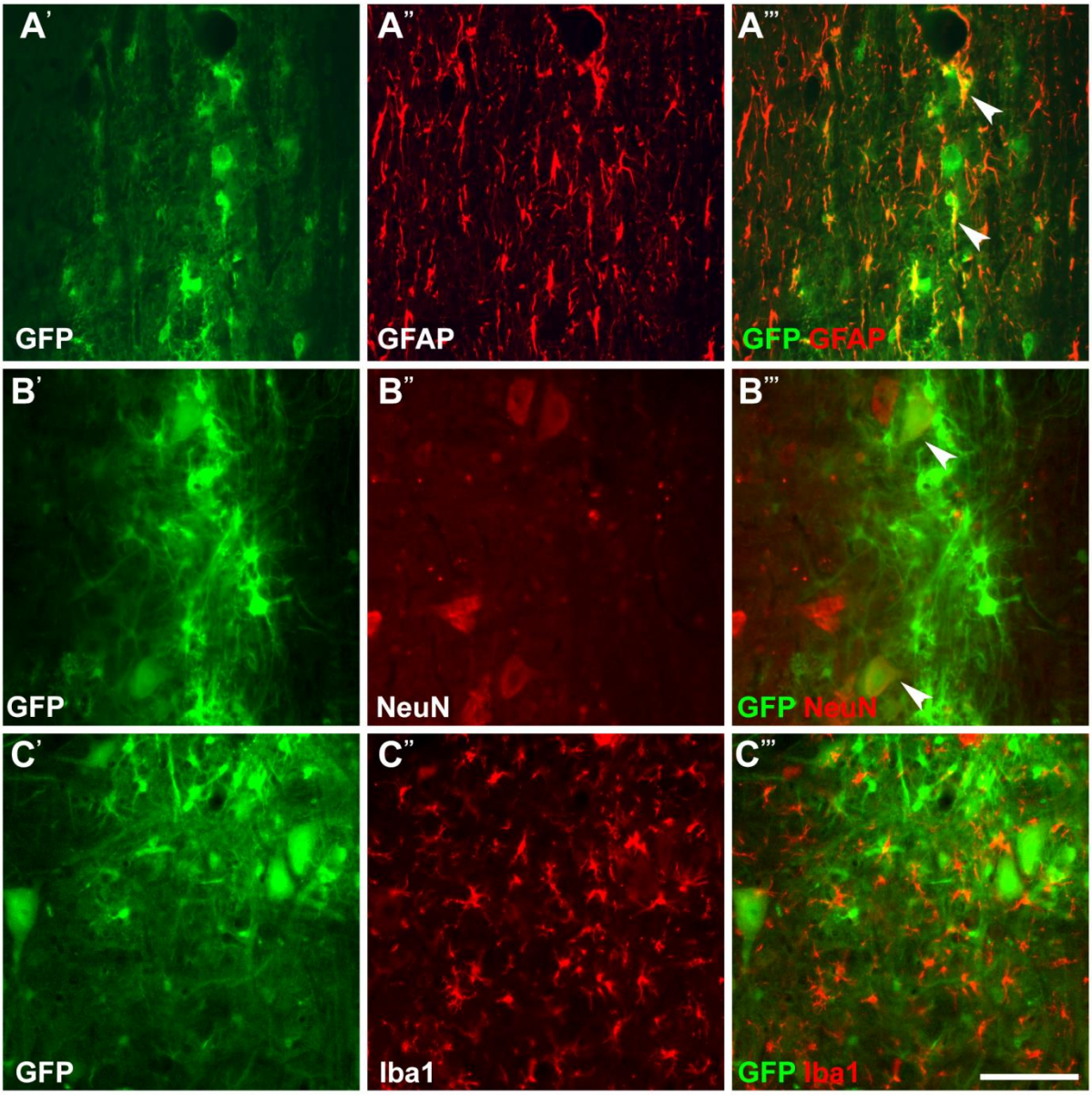

Figure 5.5. Expression of LV/CMV-GFP reporter gene was strong in neurons and astrocytes in the uninjured cervical spinal cord.
Qualitative assessment was used to identify the type of cells transduced by LV/CMV-GFP at 2 weeks following injection into the sensorimotor cortex. **(A'-C')** Strong expression of the viral reporter gene (GFP) was observed at 2 weeks post injection. **(A'-A''')** Frequent co-localisation between GFAP labelling and GFP was observed (arrowheads). **(B-B''')** GFP co-localised with NeuN immunolabelling, but was relatively scarce (arrowheads). **(C'-C''')** No-localisation was observed between GFP and Iba1-labelled cells. Scale bar = 100 μm.

5.2.4.2 Injured spinal cord

To assess transgene expression in cell types following injury to the spinal cord, and to ensure this was consistent with data obtained from the uninjured animals, rats received a

lateral hemisection lesion at C5/C6 spinal cord level and injections of LV/Synapsin I-GFP (control) and LV/Synapsin I-PST (containing a mCherry driven by an independent synapsin I promoter) were carried out rostrally and caudally to the injury site. The spinal cords were harvested 2 weeks after surgery and horizontal sections containing the injury and injection sites were immunolabelled for astrocytes, neurons and microglia using the cell-type antibodies, GFAP, NeuN and Iba1, respectively. A dense network of GFP-positive cells expressed by LV/Synapsin I-GFP was observed rostral to the lesion site, and a similar sized area of mCherry-positive cells expressed by LV/Synapsin I-PST was observed caudal to the lesion (Figures 5.6 and 5.7, respectively). These cells were found exclusively in the grey matter, ipsilateral to the lesion site, in the intermediate grey matter and in the ventral horn. None of the GFP or mCherry-positive cells exhibited co-localisation with GFAP or Iba1 immunolabelling, indicating these cells were not astrocytes or microglia, respectively (Figure 5.6A & C, 5.7 A & C). As expected, strong co-localisation was observed between GFP and mCherry with NeuN positive neurons (Figure 5.6B & 5.7B).

This data suggests that LV/Synapsin I-GFP or LV/Synapsin 1-PST can selectively express transgenes in neurons in the injured cervical spinal cord. Furthermore, the hemisection injury per se did not alter the tropism of LV vectors under the control of human synapsin I promoter.

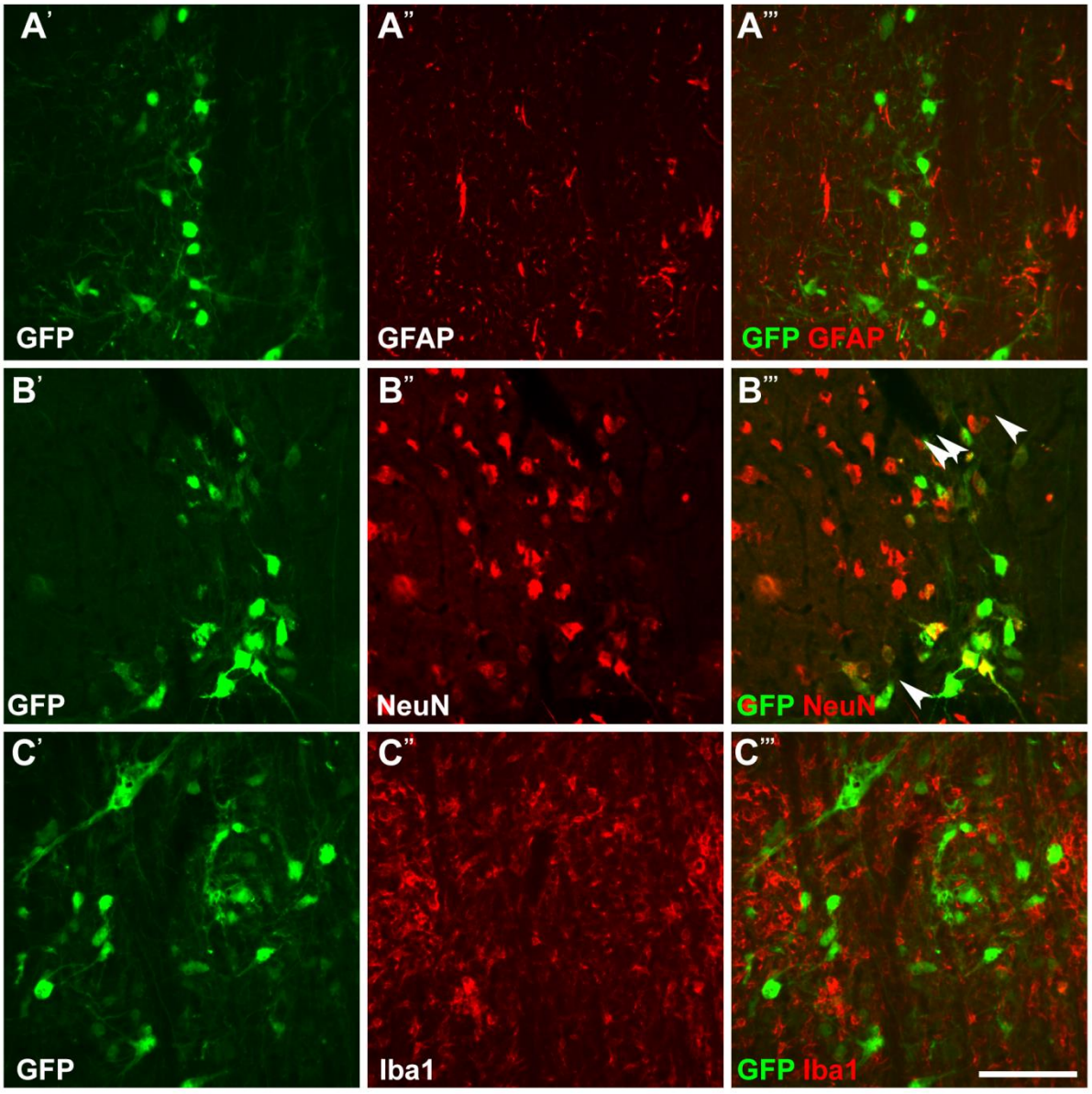

Figure 5.6. Expression of LV/Synapsin I-GFP reporter gene was strong in neurons in the injured cervical spinal cord.

Qualitative assessment was used to determine the cell types expressing LV/Synapsin I-GFP reporter gene at 2 weeks following injection to the injured cervical spinal cord. LV/Synapsin I-GFP and LV/Synapsin I-PST was injected rostrally and caudally, respectively, to a mid-cervical hemisection lesion and immunolabelling was used to assess the cell types transduced by each vector. **(A'-A"')** GFP-positive cells did not co-localise with GFAP labelling. **(B'-B"')** Strong co-localisation was observed between GFP and NeuN, suggesting that transduced cells were neurons. **(C'-C"')** No co-localisation between Iba1 and GFP was observed. Scale bar = 100 μm.

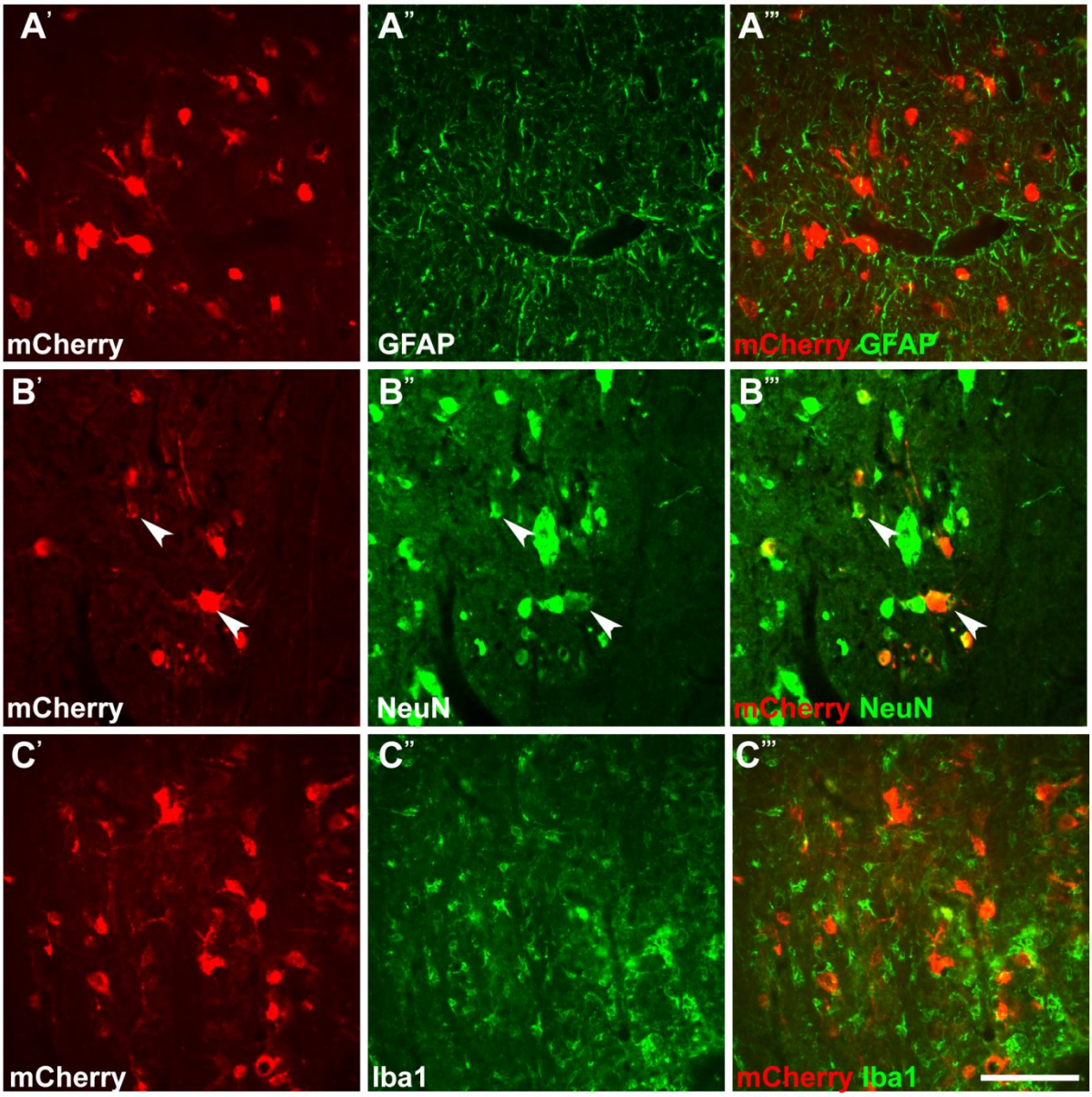

Figure 5.7. Expression of LV/Synapsin I-PST reporter gene was strong in neurons in the injured cervical spinal cord.

Qualitative assessment was used to determine the cell types expressing LV/Synapsin I-PST reporter gene at 2 weeks following injection to the injured cervical spinal cord. **(A'-A"'),** mCherry-positive cells expressed no co-localisation with GFAP labelling. **(B'-B"')** Strong co-localisation was observed between mCherry and NeuN, suggesting that transduced cells were neurons. **(C'-C"')** No co-localisation between Iba1 and mCherry was observed. Scale bar = 100 μm.

5.2.5 Polysialic acid production by the lentiviral vectors

To investigate whether the injection of LV vectors into the CNS resulted in polysialic acid (PSA) expression, tissue sections were immunostained and analysed at 2 weeks post-injection.

5.2.5.1 Cortex

PSA expression is weak in the sensorimotor cortex of the adult rat brain, following down-regulation during early stages of postnatal development (Di Cristo et al., 2007b). After 2 weeks post-injection of LV/Synapsin I-GFP (control), PSA labelling was indeed absent from the cortex and no immunolabelling was observed surrounding transduced neurons (Figure 5.8A'-A'''). Conversely, at 2 weeks post-injection of LV/Synapsin I-PST, PSA labelling was observed in the cortex surrounding neurons transduced by LV (Figure 5.8B'-B'''). A separate population of transduced neurons contained intracellular PSA labelling, which co-localised with mCherry (Figure 5.8C'-C'''). As the LV/Synapsin I-PST contained a transgene for GFP which is fused to the C-terminus of the PST gene, it was possible that this perceived intracellular PSA labelling could be GFP signal rather than true PSA immunostaining. To investigate this, tissue sections were incubated with PSA secondary antibody only, with the primary antibody omitted from the immunostaining. The data showed mCherry-positive neurons did not contain any intracellular labelling (Figure 5.8D), suggesting that the previously observed green signal was in fact true PSA immunostaining.

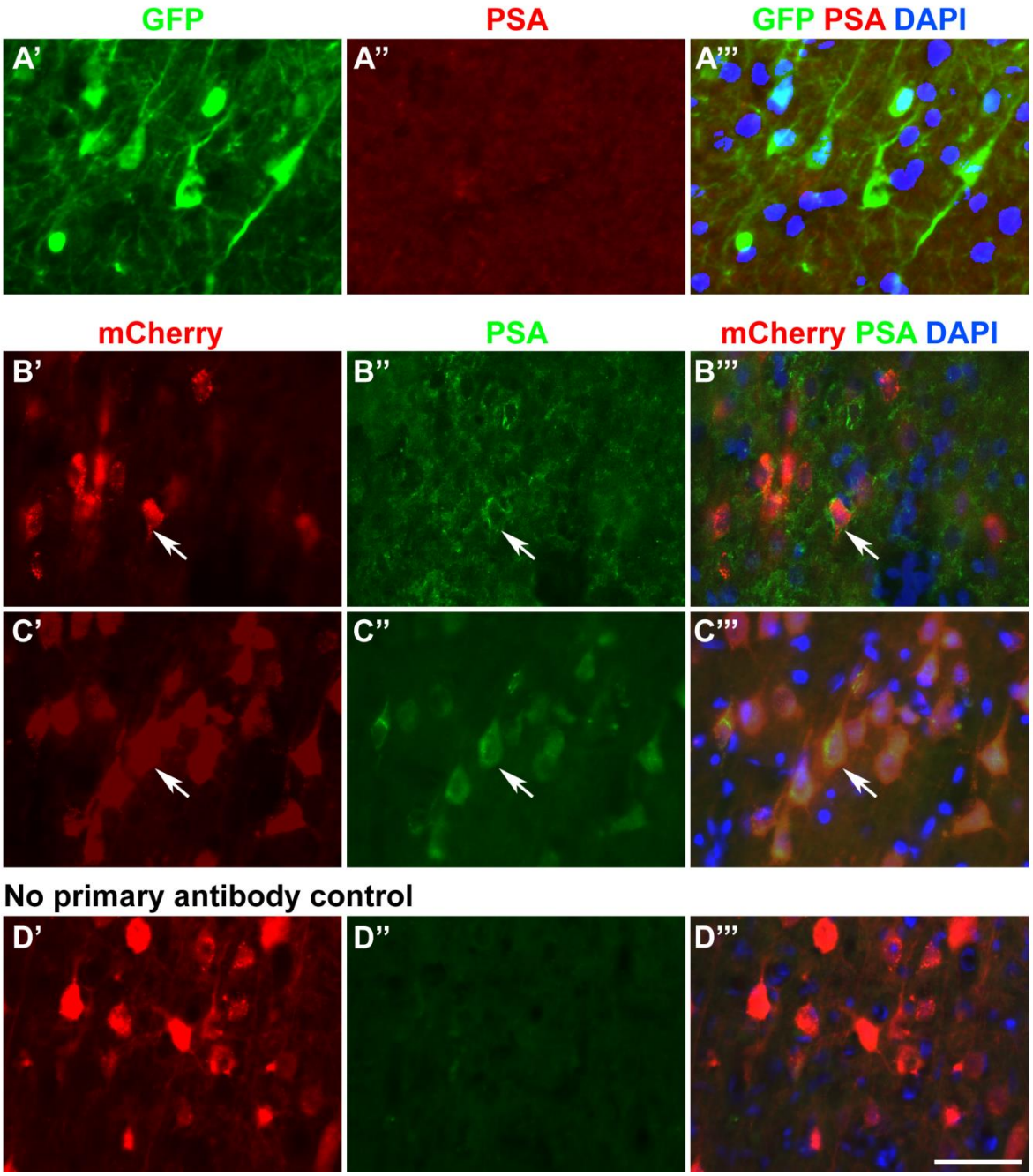

Figure 5.8. LV/Synapsin I-PST induced PSA expression in neurons.
(A'-A''') No PSA immunolabelling was observed surrounding neurons transduced by LV/Synapsin I-GFP following delivery to the cortex. **(B'-B''')** Some neurons transduced by LV/Synapsin I-PST expressed a ring-like PSA immunostaining that surrounded the neuronal cell body (arrows). **(C'-C''')** A separate population of transduced neurons had intracellular PSA immunolabelling (arrows). **(D'-D''')** GFP expression mediated by LV/Synapsin I-PST was not detected when the PSA primary antibody was excluded from the immunostaining. Scale bar = 50 μm.

5.2.5.2 Injured spinal cord

In the uninjured adult rat spinal cord, PSA expression in grey matter is generally confined to the superficial dorsal horns and surrounding the central canal (lamina X) (Bonfanti et al., 1992). In this study, PSA immunolabelling was absent around neurons when transduced by LV/Synapsin I-GFP (control, Figure 5.9A'-A'''). Conversely, PSA immunolabelling was abundant surrounding neurons when transduced by LV/Synapsin I-PST (Figure 5.9B'-B''').

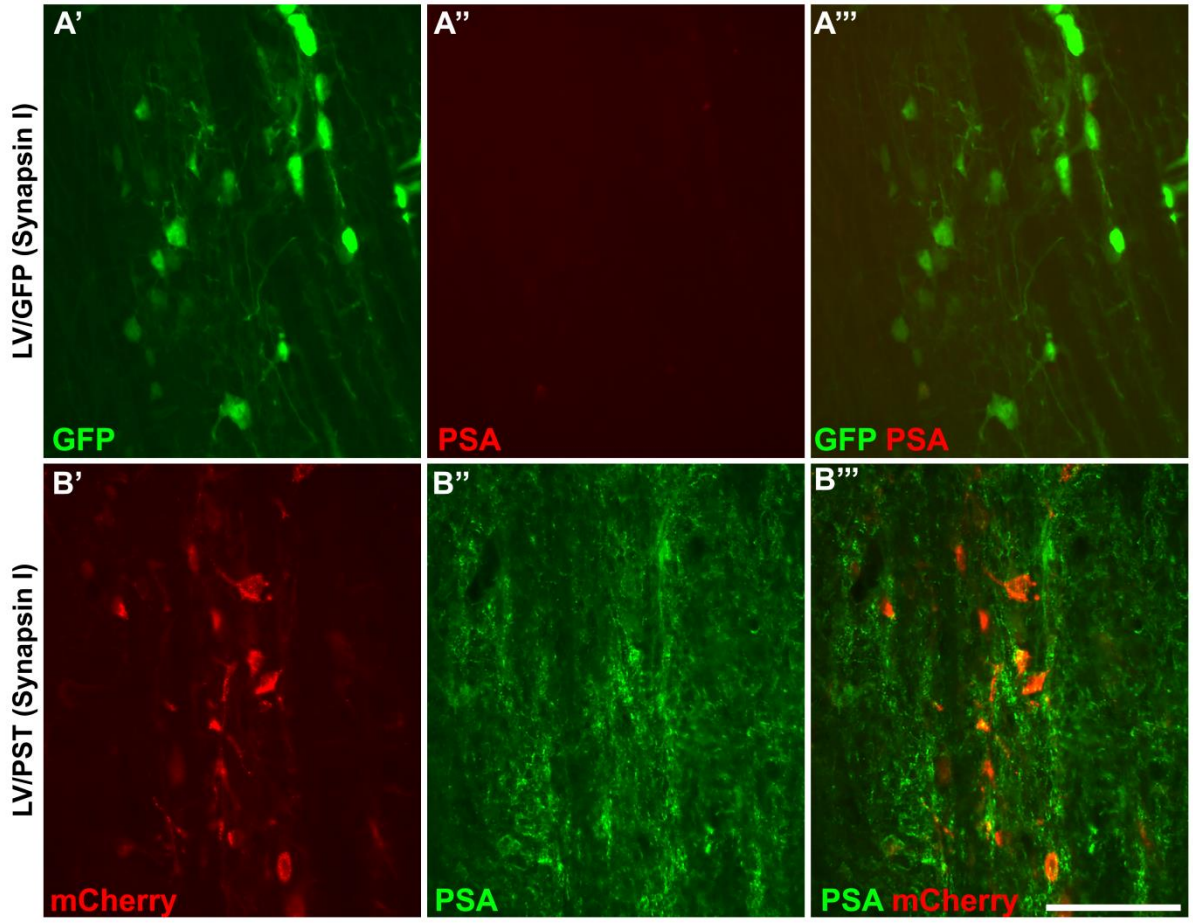

Figure 5.9. LV/Synapsin I-PST induced PSA expression in neurons of the injured spinal cord (A'-A''') PSA labelling was absent around neurons transduced by LV/Synapsin I-GFP at 2 weeks post-delivery to the injured cervical spinal cord. **(B'-B''')** Conversely, strong PSA labelling was found surrounding mCherry-positive neurons in the grey matter at 2 weeks post-delivery of LV/Synapsin I-PST. Scale bar = 100 μm.

5.2.6 Perineuronal net intensity following injection of lentiviral vectors into the sensorimotor cortex

Preliminary data from our laboratory suggested that re-expressing PSA in the spinal cord could reduce WFA labelling in PNNs (unpublished observation). To assess whether

overexpressing PSA in the adult sensorimotor cortex could reduce WFA binding to the PNN, adult rats received bilateral injections of LV vectors into the sensorimotor cortex; one cerebral hemisphere was injected with LV/Synapsin I-GFP, the other hemisphere was injected with LV/Synapsin I-PST. Brains were collected at 4 and 6 weeks post-injection and coronal sections containing the bilateral injection sites were labelled with WFA, which was visualised with streptavidin-conjugated Alexa Fluor 647.

At 4 weeks post-injection, transduction of neurons by LV/Synapsin I-GFP (control) or LV/Synapsin I-PST was strong (Figure 5.10). A fraction of neurons transduced by LV/Synapsin I-GFP were surrounded by WFA-labelled PNNs, suggesting that LV/Synapsin I-GFP can transduce PNN-expressing neurons *in vivo* (Figure 5.10A'-A'', arrows). Production of mCherry by LV/Synapsin I-PST was strongly observed using the red channel (excitation wavelength 543 nm) which also bled-through to the far red (excitation wavelength 647 nm) channel on an epifluorescence microscope (Figure 5.10B'-B'') and confocal microscope (Figure 5.10C'-C''). Several attempts were made to carry out WFA labelling using streptavidin-conjugated AMCA (using another excitation wavelength of 350 nm), but were all unsuccessful. Consequently, neither the number of transduced neurons with a PNN, or the density of individual PNNs were quantified. In summary, the issue of whether induced PSA expression could reduce WFA labelling remained undetermined.

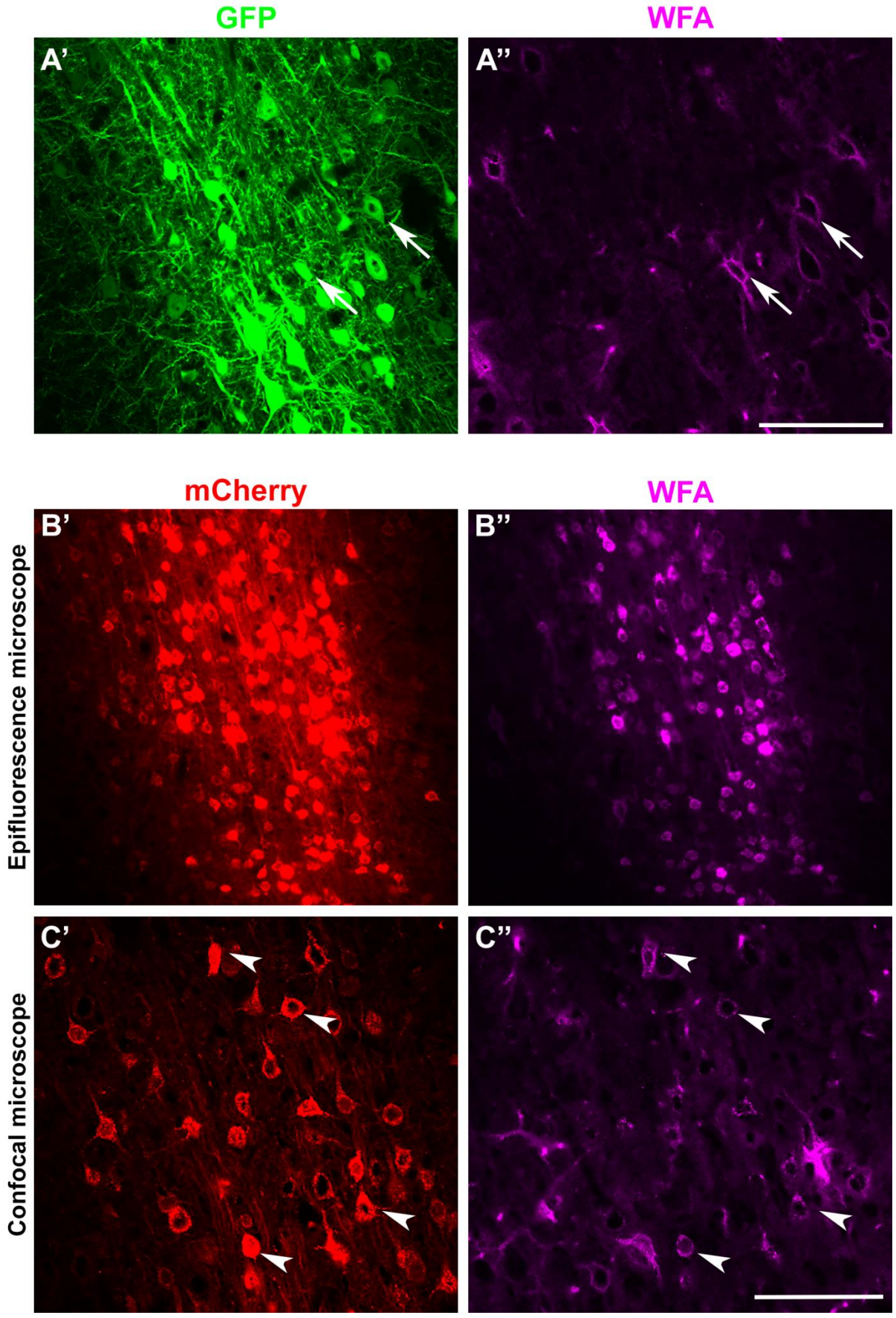
GFP
WFA
A'
A''
mCherry
WFA
B'
B''
Epifluorescence microscope
C'
C''
Confocal microscope

➤ **Figure 5.10. The relationship between induced PSA expression and the PNN was investigated *in vivo.***
(A'-A'') A large area of GFP-positive neurons was observed following LV/Synapsin I-GFP (control) delivery into the cortex. GFP-positive neurons were surrounded by WFA-labelled PNNs (arrows). **(B-C)** A large region of mCherry-positive neurons was observed following LV/Synapsin I-PST delivery into the cortex. mCherry fluorescence bled through to the far red channel on both an epifluorescence and confocal microscope (arrowheads), thus the effect of PSA expression on the PNN could not be investigated. Scale bar = 100 μm

5.3 Discussion

5.3.1 Generation of lentiviral vectors and delivery into the CNS

The use of LV vectors to drive gene expression in the CNS is becoming increasingly common, and vectors have been engineered to express enzymes, growth factors, receptors and siRNAs (reviewed by (Parr-Brownlie et al., 2015)). An increasing number of studies are using cell-type specific promoters to drive expression of transgenes in required cell types. The primary aim of this study was to generate two high-titre LV vectors, one to overexpress the polysialyltransferase (PST) gene, and a control vector to express the GFP only. A number of properties were required for these vectors for use in future studies, including the ability to (i) transduce specific neuronal cells in the CNS, (ii) transduce high numbers of neurons, (iii) produce high expression of PSA *in vivo* when using the LV/Synapsin I-PST and, (iv) result in long-term transgene expression.

In this chapter, three LV vectors were generated, all of which produced robust transgene expression at 2 weeks following intraparenchymal delivery into the CNS. Two LV vectors were driven by the human synapsin I promoter; LV/Synapsin I-GFP (control) and LV/Synapsin I-PST, the other one was driven by a CMV promoter (LV/CMV-GFP). Following delivery of viral vectors to the sensorimotor cortex, using a steel needle, there was visible needle tract damage as indicated by the presence of autofluorescent cells along the tract. However, this was not observed following LV delivery using a glass micropipette, thus this procedure was used for subsequent injections into both the sensorimotor cortex and the spinal cord. Using a glass micropipette to perform the injections allowed the precise delivery of viral vectors into the sensorimotor cortex, using stereotaxic coordinates, as previously described (Cetin et al., 2006).

There are many advantages that support the use of LV vectors in this study, compared to other types of viral vector. Firstly, previous studies from our laboratory, and others, have successfully used LV vectors carrying the PST gene to overexpress PSA in the injured nervous system, including rodent models of spinal cord injury (Zhang et al., 2007b; Zhang et al., 2007c). These studies showed the robust, long-term transgene expression following delivery of LV/PST into the injured spinal cord, and the resulting high-levels of PSA. Additionally, LV vectors are relatively easy to produce and purify in the laboratory, and it is simple to engineer the virus to transduce specific cell-types using specific promoter sequences. However, one downside to the use of LV vectors is that they are only able to transduce a relatively small area of the CNS. This is believed to be due (at least in part), to the relatively large size of the virion, compared to the size of the extracellular space of the rodent CNS (Cetin et al., 2006). This was also observed in this study, as transduced cells were often only found within a small region and in close vicinity to the injection site. Thus, it was necessary that multiple injections be used in future studies (at least 2 injections per site), to allow viral transduction of a wider area of the CNS. However, while delivering vectors using a glass micropipette causes considerably less tissue damage, compared to delivery using a steel needle, there will still be some minor damage to the CNS following injections using glass micropipettes. With multiple injections of LV vectors necessary to transduce a wide area of the CNS, this may cause some small, local areas of tissue damage that may affect the outcomes of any future experiments.

5.3.2 Cell types transduced by lentiviral vectors with a CMV promoter

As previously discussed, one of the LV produced in this study contained a CMV promoter, to non-specifically drive transgene expression in a number of CNS cell-types. Following direct microinjection into the sensorimotor cortex, transduction of neurons by LV/CMV-GFP was weak. Interestingly, however, transgene overexpression was robust in astrocytes, but absent in microglia. While it is well documented that CMV promoter sequences are able to transduce a wide range of cell types found in the CNS, the extent of neuronal transduction is disputed. In a similar study, Yaguchi *et al.,* noted strong transduction of cortical neurons by VSV-G pseudotyped LV with GFP under the control of a CMV promoter. Approximately 85% of transduced cells were reported to be immunolabelled with the neuronal marker NeuN,

and the remaining 10% of cells were astrocytes (Yaguchi et al., 2013). However, conflicting data was obtained from another study, by Hioki *et al.,* which noted approximately half of all transduced cells were neurons (Hioki et al., 2007). The disparity between our results compared to those obtained by other groups, may be explained by differences in viral titres, since some data suggests that the cellular tropism of LV vectors may change as a function of the titre of the viral vector (Yaguchi et al., 2013). Moreover, studies have noted that the pH of the medium used to harvest LV vectors can affect their tropism following delivery to the brain (Torashima et al., 2006).

Similarly, following LV/CMV-GFP injection into the cervical spinal cord, the transduction of neurons was poor, but transduction of astrocytes was high. This is consistent with other studies that have also noted strong transduction of spinal astrocytes (over 70% transduced cells) following delivery of a CMV promoter-driven LV into the rodent spinal cord (Hendriks et al., 2007; Peluffo et al., 2013) and weak or no transduction of microglia (Hendriks et al., 2007). A relatively low number of neurons were transduced by LV/CMV-GFP in the work presented in this study; a proportion of these were classified as motor neurons, based on their morphology and distribution. Similar findings have also been recently described by others (Peluffo et al., 2013).

Following completion of the GFAP labelling, it was found that the majority of GFP cells in both the cortex and the spinal cord were astrocytes, thereby it was decided to cease the further analysis of this tissue, and investigate LV vectors under the control of a neuronal-specific promoter.

5.3.3 Cell types transduced by synapsin I

In order to obtain selective neuronal cell transduction, LV with a synapsin I promoter was used in this study. Following microinjection into the cortex, both LV/Synapsin I-GFP (control) and LV/Synapsin I-PST selectively transduced cortical neurons at 2 weeks following injection. No transduction of either astrocytes or microglia was observed, but neuronal transduction was strong with either LV vector. These data are in agreement with a number of other published studies, that have noted almost exclusive transduction of neurons by synapsin I-driven LV following delivery into the CNS (Yaguchi et al., 2013). In the data

presented in this study, importantly, both LV/Synapsin I-GFP and LV/Synapsin I-PST could transduce PNN-expressing neurons following injection into the cortex. While no phenotypic analysis of the types of neurons transduced by LV/Synapsin I-GFP was carried out in this study, the presence of PNNs surrounding these neurons, suggests, at least in the cortex, these cells may be parvalbumin-positive inhibitory neurons, which have previously been documented to express high levels of WFA-labelled PNNs *in vivo* (Pizzorusso et al., 2002; Orlando and Raineteau, 2015). Additionally, based on the large size and ventral horn localisation of a population of transduced neurons in the spinal cord, it is clear that LV/Synapsin I-GFP can also transduce motor neurons, following intra-spinal delivery. While a strict analysis of the phenotypes of neurons transduced by LV vectors following delivery to the CNS was not performed here, this will be necessary in future studies if LV/Synapsin I-PST promotes functional recovery in a model of spinal cord injury. It will be important to investigate the neuronal circuitry responsible for this recovery of function.

5.3.4 PSA production by lentiviral vectors

Following injection of LV/Synapsin I-PST into the cortex or the cervical spinal cord, expression of PSA was widespread, and was found on the surface of transduced neurons in both regions of the CNS. Interestingly, in the cortex only, intracellular PSA immunostaining could also be observed. This may be due to the autopolysialylation of the PST enzyme, which has previously been shown to occur *in vivo* (Close and Colley, 1998). There was no PSA immunostaining present in the areas surrounding the control LV/Synapsin-GFP in either the cortex or the spinal cord, suggesting that the PSA produced in the CNS is due to expression of the PST enzyme. This data concurs with a number of other studies, that have noted selective PSA expression in the CNS following delivery of LV/Synapsin I-PST (Zhang et al., 2007b; Zhang et al., 2007c; Zhang et al., 2007a). Many of these studies have done so with the aim of assessing whether re-expressing PSA in the CNS can lead to enhanced regeneration of damaged axons in models of SCI, which is the focus of this thesis in Chapter 6.

One of the main aims of this chapter was to conduct a pilot study to investigate whether induced PSA expression in the cortex can lead to a reduction of WFA binding to its site within the PNN. As previously mentioned, there were some problems associated with this experiment, namely, the bleed-through of mCherry fluorescence (from LV/Synapsin I-PST)

onto other channels of both epifluorescence and confocal microscopes. This prevented the analysis of this tissue, due to the expression of GFP (as a consequence of LV/Synapsin I-GFP injection) in the other cerebral hemisphere rendering the use of FITC (or similar)-conjugated antibodies inadequate. Immunolabelling using AMCA-conjugated secondary antibody was attempted, however, staining was poor and was not strong enough for quantification. At this point, it was decided to replicate this study in the spinal cord, using separate animals for injection of LV/Synapsin I-GFP or LV/Synapsin I-PST, thus it was decided to discontinue this pilot study.

5.4 Conclusions

In this study, we have demonstrated successful generation of three high-titre LV vectors that can successfully transduce a high number of cells following stereotaxic injections into the cortex or cervical spinal cord. Two of these vectors (LV/Synapsin I-GFP and LV/Synapsin I-PST) that contain the neuron-specific promoter synapsin I, can result in selective transgene expression in neurons. Furthermore, LV/Synapsin I-PST, but not the control LV/Synapsin I-GFP can overexpress PSA in vivo. Therefore, these two vectors were used to assess the relationship between PSA and the PNN in the uninjured cervical spinal cord, in the following studies, and also to investigate whether PSA overexpression in a rodent model of SCI can promote neuroplasticity and behavioural improvement.

Chapter 6

Investigating whether induced PSA expression can promote locomotor recovery and neuroplasticity in a rodent model of spinal cord injury

Chapter 6: Investigating whether induced PSA expression can promote locomotor recovery and neuroplasticity in a rodent model of spinal cord injury

6.1 Introduction

In the previous chapter of this thesis, a lentiviral (LV) vector encoding the polysialyltransferase (PST) and mCherry genes under the control of two separate synapsin I promoters was generated (LV/PST). 2 weeks following delivery to either the naïve or injured cervical spinal cord, strong transduction of the grey matter was apparent, which was observed as numerous mCherry-positive neurons. Moreover, robust PSA expression was observed in the regions surrounding the mCherry-positive neurons. A control vector was also developed, which carried the gene for GFP only under the control of synapsin I promoter (LV/GFP). Following delivery to the naïve or injured spinal cord, strong neuronal transduction was observed. In contrast to LV/PST, PSA immunolabelling surrounding the injection sites was absent.

6.1.1 PSA-induced behavioural improvement in rodent models of SCI

As reviewed in chapter 1.4.4, a number of studies have investigated the effects of PSA in promoting functional improvements in models of SCI. For the most part, PSA expression has been achieved using a viral vector to induce expression of one of the polysialyltransferases that catalyses the formation of PSA *in vivo* (El Maarouf et al., 2006; Zhang et al., 2007b). A further set of studies have developed PSA mimetic peptides, that are delivered to the CNS via intrathecal catheters (Marino et al., 2009; Pan et al., 2014). All of these studies have utilised thoracic-level models of injury, and only a fraction of these have relied on behavioural testing to assess the extent of locomotor recovery. In the studies that used behavioural testing, a significant improvement in hindlimb locomotor function was observed in animals treated with PSA mimetic peptide, compared to controls. This recovery may have

been due to enhanced sprouting of serotonergic fibres caudal to the lesion site (Marino et al., 2009).

While the data obtained from the above studies is encouraging, there are questions that remain to be addressed, such as the efficacy of such treatments in a cervical-level model of SCI, and behavioural improvements associated with viral vector-mediated PSA expression. In our laboratory, we chose the use of viral vectors encoding the polysialyltransferase gene to induce PSA expression in the spinal cord, rather than the use of PSA mimetics. This allows us to direct PSA expression to specific cellular populations, and also, this allows long-term expression. The use of this viral vector in a mid-cervical model of SCI was investigated in more detail in this chapter.

6.1.2 Proposed relationship between PSA and the PNN *in vivo*

As described in chapter 1.5.4, preliminary observations from our laboratory suggest an inverse relationship between the expression of PSA and the formation of the PNN *in vivo*. This is based on results from a previous small histological study using sections of postnatal rat spinal cords, ranging from postnatal day 3 to day 21. This study noted the emergence of WFA-labelled PNNs following down-regulation of PSA expression in the spinal cord, and the lack of double-labelled neurons for both PSA and the PNN marker WFA (unpublished observation).

Thus far in this thesis, a cell culture model using primary neuronal cells was used to investigate whether removing PSA from the culture could exacerbate PNN formation, which would subsequently restrict synaptogenesis *in vitro.* Results from this study were negative, and no difference was observed in the proportion of PNNs or the density of synaptophysin-labelled terminals contacting cells with or without PSA (see Chapter 4). We hypothesised that the limitations of using a two-dimensional culture system may have affected the results obtained in this study. Additionally, in a pilot study, LV/PST and LV/GFP were injected into the adult rat sensorimotor cortex to investigate whether induced PSA expression could lead to a reduction in WFA labelling of PNNs *in vivo* (Chapter 5). Restrictions in immunostaining prevented further analysis of this tissue, therefore it was decided to re-examine this in the

cervical spinal cord, using the same viral vectors developed in Chapter 5, but only injecting one vector to the spinal cord of each animal.

6.1.3 Aims

Using the LV vectors described in chapter 5, the aims of this chapter were as follows. First, to evaluate whether induced PSA expression rostral and caudal to a cervical spinal cord lesion, could promote functional recovery by enhancing axonal sprouting and synaptogenesis. Second, to investigate whether PSA expression in the naïve cervical spinal cord can alter the binding of WFA lectin to its site within the PNN. Third, to see whether induced PSA expression in the naïve spinal cord can induce axonal sprouting and synaptogenesis.

6.2 Results

6.2.1 LV/PST induced functional recovery in rats with a cervical spinal cord injury

6.2.1.1 Open field locomotor assessment

To evaluate whether induced PSA expression via direct injection of LV/PST into the injured spinal cord can promote improvement in locomotor recovery, adult rats received unilateral injections of either LV/GFP or LV/PST, rostral and caudal to a lateral hemisection injury between the 5^{th} and 6^{th} cervical segments (henceforth known as Hx + LV/GFP and Hx + LV/PST, respectively). In the same study, additional groups of animals received injections of either LV/GFP or LV/PST only, in the absence of hemisection lesion, or sham surgery, which involved laminectomy only. Fore- and hindlimb function was assessed using a number of behavioural tests, starting 1 day following surgery and continued for the duration of the study.

The open field locomotor assessment can be used to score the forelimb and hindlimb locomotor function of rats, using the forelimb locomotor scale (FLS) and the Basso Beattie Bresnahan (BBB) scale, respectively. The FLS was developed as a tool to investigate acute recovery of forelimb function in the days following SCI. Baseline testing before surgery revealed normal forelimb function in all animals (FLS score 17 $\pm$ 0; consistent plantar stepping, parallel paw placement and consistent toe clearance, Figure 6.1A). 1 day post-surgery, all animals that received lateral hemisection injury had a drastic loss in forelimb function (FLS score 1 DPO; Hx + LV/GFP, 2.1 $\pm$ 1.0 and Hx + LV/PST, 0.8 $\pm$ 0.2, Figure 6.1A). Hx + LV/GFP animals showed a gradual improvement in forelimb function, which persisted until 16 days post-lesion (FLS score 16 DPO, 10.6 $\pm$ 1.4). There was little change beyond this time-point, and scores remained similar at the end of the study (FLS score 42 DPO, 11.3 $\pm$ 1.4, Figure 6.1A). Conversely, a gradual recovery of forelimb function was observed with Hx + LV/PST animals up to 8 days post-injury (FLS score 8 DPO, 9.7 $\pm$ 0.2, Figure 6.1A). Forelimb function remained consistent for approximately 2 weeks, then a moderate improvement was observed 26 days post-lesion (FLS score 26 DPO, 11.8 $\pm$ 1.7). A further improvement was observed 36 days post-injury (FLS score 36 DPO, 13.0 $\pm$ 1.8), then scores plateaued for

the remainder of the study. There was no difference in FLS scores in Hx + LV/PST versus Hx + LV/GFP animals at any examined time-point post-lesion (Figure 6.1A, $p > 0.05$, two-way ANOVA, Tukey's multiple comparisons test). Sham animals had a consistent FLS score of 17, indicating that the laminectomy procedure did not affect forelimb locomotor function (Figure 6.1A).

The BBB scale was designed to evaluate hindlimb function, ranging from complete hindlimb paralysis to normal movement (Basso et al., 1995). Pre-surgery, all animals in all treatment groups had BBB scores of 21, indicating normal hindlimb function (Figure 6.1B). This corresponds to consistent stepping, with paws placed in parallel to the animal's trunk, no toe dragging and consistent fore- and hindlimb coordination (see Figure 6.1). 1 day post-surgery, all animals that received the lateral hemisection lesion and either LV/GFP or LV/PST injections had a drastic loss in hindlimb motor function (BBB scores; LV/GFP, 5.6 ± 1.4 and LV/PST, 7.0 ± 1.8, respectively, Figure 6.1B). Up to 5 days post-lesion, injured animals showed a gradual improvement in hindlimb function but no difference was observed in the rate of recovery between treatment groups. By 7 days post-lesion, all Hx animals (in both treatment groups) had a BBB score of 11 (occasional stepping and fore- and hindlimb coordination). Hx + LV/GFP animals showed no further improvement in hindlimb function beyond the first week post-lesion. Conversely, hindlimb function of Hx + LV/PST animals continued to steadily improve beyond the first week post-injury and a significant improvement was observed 30 days post-lesion, compared to Hx + LV/GFP animals (BBB scores 30 DPO, 11.6 ± 0.3 vs. 13.8 ± 0.9, LV/GFP vs. LV/PST, p=0.009, two-way ANOVA, Tukey's multiple comparisons test, Figure 6.1B). This improvement in hindlimb function persisted for the remainder of the experiment. Sham animals had no difference in hindlimb function following surgery (BBB score 21 ± 0, Figure 6.1B).

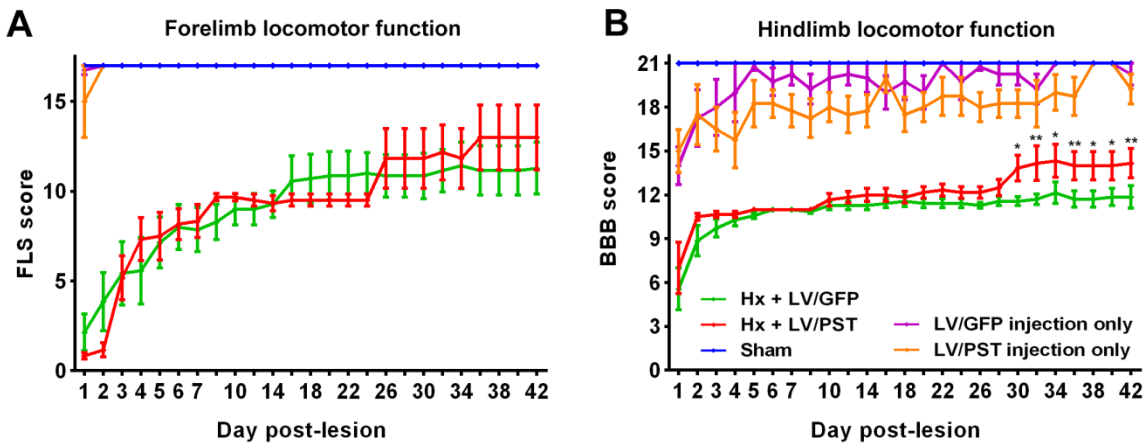

Figure 6.1. Intraspinal injection of LV/PST improved the hindlimb function of animals with mid-cervical SCI.
Open field locomotor testing was used to assess locomotor function of both the fore- and hindlimbs post-SCI. **(A)** The forelimb locomotor scale (FLS) was used to assess forelimb function in SCI-animals. 1 day post-lesion, both LV/PST and LV/GFP treated animals displayed a drastic loss in forelimb function. Animals in both treatment groups gradually regained forelimb function during the first 2 weeks, with no difference between groups (p>0.05). LV/GFP treated animals showed minimal improvement after 2 weeks, however, there was a minor improvement in function of LV/PST treated animals after 4 weeks. There was no difference between LV/PST and LV/GFP treated animals at any examined timepoint (p>0.05). Forelimb function in sham animals was unaffected. **(B)** The BBB scale was used to assess hindlimb function. One day post-lesion, both LV/PST and LV/GFP treated animals displayed a loss of hindlimb function. Some improvement was observed during the first week after surgery, however, in the LV/GFP group, no further improvement was observed after this timepoint. LV/PST treated animals showed a significant improvement in hindlimb function 30 days post-lesion, compared with LV/GFP treated rats (*p<0.05, **p<0.01). Hindlimb function in sham animals was unaffected by surgery. Sham, *n=3;* Hx + LV/PST*, n=6;* Hx + LV/GFP, *n*=6; LV/PST only, *n*=6 and; LV/GFP only, *n*=6.

6.2.1.2 Montoya staircase test

Modelling SCI at the cervical level allows assessment of tasks that require skilled movements, such as pellet retrieval, which cannot be assessed in models with injuries in the thoracic region. One of the most common behavioural tests for this purpose is the Montoya staircase test, a description of which can be found in chapter 2.4.2. This is a complex behavioural task, which requires at least two weeks of training. Two different outcomes can be measured from this behavioural test; first, gross locomotor function can be assessed by quantifying the number of food pellets displaced by each animal, and second, skilled

locomotor function can be assessed by quantifying the number of food pellets consumed per animal.

In this study, animals in all treatment groups were habituated to the Montoya staircase apparatus daily, for 2 weeks before surgery. Previous research has noted that rats may exhibit paw preference in behavioural tasks that involve retrieval of food pellets (Pençe, 2002). To ensure this was not the case with the animals used in this study, the number of food pellets displaced and consumed using the left (ipsilateral) and right (contralateral) paws was examined. Figure 6.2 shows the mean number of food pellets displaced or consumed during the training procedure, for all animals. There was no difference in the number of food pellets displaced by the left and right paws (p=0.96, two-way ANOVA) or any difference in the number of food pellets consumed (p=0.91, two-way ANOVA, Figure 6.2B) during training. Overall, there was an increase in the number of food pellets displaced or consumed during training. At the end of training, animals were randomly divided into treatment groups, thus in Figures 6.2C-F the same data is replotted according to their treatment groups.

On the first day of training, animals in all treatment groups could successfully displace one or multiple pellets from the staircase (Figure 6.2C). Generally, as training progressed, there was an increase in the average number of food pellets displaced by each group; one notable exception of this was the LV/PST injection only animals, which did not show much improvement with training (Figure 6.2C). There was no difference in the number of food pellets displaced by any treatment groups (p>0.05, two-way ANOVA). The number of food pellets consumed on the first day was low for all groups but increased as time progressed (Figure 6.2D). There was no difference in the number of food pellets consumed between treatment groups (p>0.05, two-way ANOVA). This data is replotted in Figures 6.2E and F. excluding the injection only groups for ease of viewing.

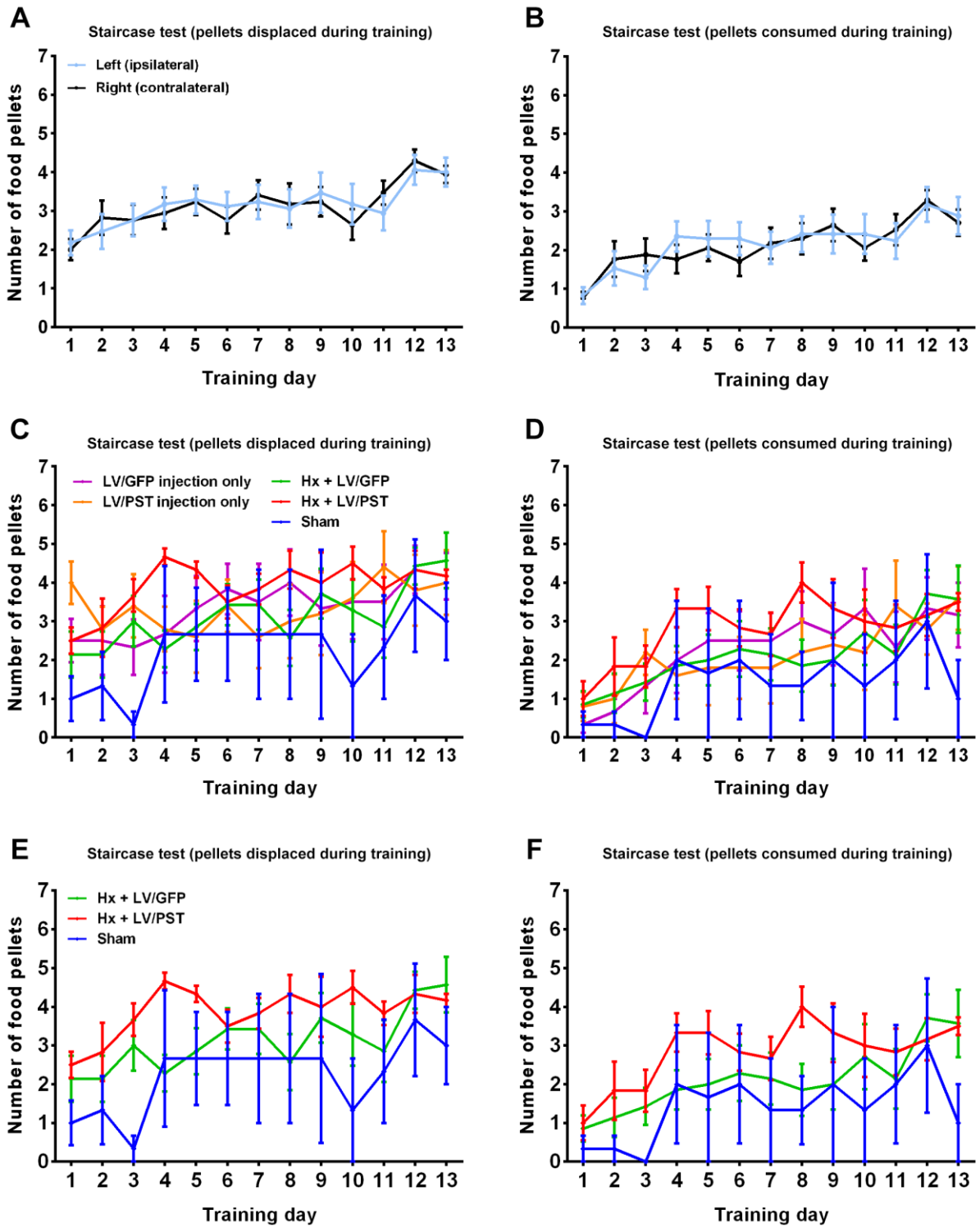

Figure 6.2. Animals were trained on the Montoya staircase test for 2 weeks prior to surgery.

The Montoya staircase test was used to assess skilled locomotor recovery following SCI. Animals were trained on this test daily for two weeks. **(A, B)** Mean (± SEM) number of food pellets displaced or consumed, respectively, by all animals during training. There was no difference in the number of pellets displaced or consumed by the left (ipsilateral) or right (contralateral) paws. **(C, D)** Mean number of food pellets displaced or consumed,

respectively, by each treatment group during training. There was no difference in either the mean number of food pellets displaced or consumed between treatment groups (p>0.05). **(E, F)** the data in figures **(C)** and **(D)** is presented again here, excluding LV/PST and LV/GFP injection only groups, to allow a direct comparison between Hx + LV/PST and Hx + LV/GFP animals more clearly. Sham, *n=3;* Hx + LV/PST*, n=6;* Hx + LV/GFP, *n*=6; LV/PST only, *n*=6 and; LV/GFP only, *n*=6.

The day before surgery, all animals were tested on the staircase test to obtain baseline values. No difference was observed between experimental groups in the number of food pellets displaced (LV/PST 3.6 $\pm$ 0.9, LV/GFP 3.3 $\pm$ 0.9, Hx + LV/GFP 3.7 $\pm$ 0.8, Hx + LV/PST 4.0 $\pm$ 0.5, Sham 2.5 $\pm$ 1.2, p>0.05, two-way ANOVA, Figure 6.3A). There was no difference in the number of pellets consumed between any experimental group, with one exception; Hx + LV/GFP animals consumed significantly more food pellets than sham animals (Hx + LV/GFP 3.1 $\pm$ 0.9, Sham 1.3 $\pm$ 0.6, p=0.02, two-way ANOVA, Figure 6.3B).

3 days post-surgery there was a minor reduction in the number of food pellets displaced by the LV/PST and LV/GFP injections only groups, compared to sham animals (LV/PST 2.0 $\pm$ 0.5, LV/GFP 2.2 $\pm$ 0.6, sham 4.3 $\pm$ 0.3). 10 days post-surgery, both groups had regained the ability to displace food pellets to the same level as baseline testing (Figure 6.3A). After this time point, the number of pellets displaced fluctuated depending on the testing day, however, there was a general trend towards an increase in the number of food pellets displaced (Figure 6.3A). There was no difference in the number of pellets displaced between the LV/GFP and LV/PST injection only groups throughout the duration of the study (p = 0.35*,* two-way ANOVA, Figure 6.3A). Moreover, there was no difference in the number of pellets displaced compared to sham animals (LV/PST, p = 0.62; LV/GFP, p = 0.99). Similarly, there was a minor reduction in the number of food pellets consumed by LV/PST and LV/GFP injection only animals, compared to sham, 3 days post-surgery (LV/PST 2.8 $\pm$ 1.0, LV/GFP 2.8 $\pm$ 0.9, sham 1.7 $\pm$ 0.7, Figure 6.3B). The number of pellets consumed had increased by 7 days, and further by 10 days post-surgery (Figure 6.3B). Following this there was a general trend towards an increase in the number of food pellets consumed over time, although there was some fluctuation on certain testing days (Figure 6.3B). There was no difference between the LV/PST and LV/GFP injection only groups in the number of pellets consumed following surgery (p= 0.06, Figure 6.3B). Furthermore, there was no difference in

the number of pellets consumed compared with sham animals (LV/PST, p = 0.42; LV/GFP, p = 0.97).

Compared with animals which received injection only or sham surgery, there was a drastic reduction in the number of pellets displaced by animals which had received lateral hemisection injuries. To visualise the results obtained from hemisection and sham animals more clearly, the data was re-plotted on a separate graph in figure 6.3A. There was a drastic reduction in the number of pellets displaced by both Hx + LV/PST and Hx + LV/GFP animals, compared to sham animals, 3 days post-lesion (Hx + LV/GFP 0 $\pm$ 0, Hx + LV/PST 0.5 $\pm$ 0.2, Sham 3.3 $\pm$ 1.1). 7 days post-lesion, some animals had regained the ability to displace food pellets, which was generally only 1 or 2 food pellets from the top position of the staircase. No difference was observed between treatment groups (Hx + LV/GFP 1.1 $\pm$ 0.6, Hx + LV/PST 2 $\pm$ 0.4, p=0.52, two-way ANOVA). By 14 days post-lesion, all animals in the Hx + LV/PST and Hx + LV/GFP groups could displace at least 1 food pellet. At most examined time points, the number of food pellets displaced by Hx + LV/PST was higher than the number of pellets displaced by Hx + LV/GFP animals. However, this did not reach statistical significance at any examined time (p>0.05, two-way ANOVA, Tukey's multiple comparisons test, Figure 6.3A). The number of food pellets displaced by hemisected animals was significantly lower than sham animals, for the duration of the study (Hx + LV/PST, p = 0.02; Hx + LV/GFP, p = 0.003, Figure 6.3A).

Similarly, the number of food pellets consumed by Hx + LV/PST, Hx + LV/GFP and sham animals was plotted on a separate graph in figure 6.3B. 3 days post-lesion, all Hx + LV/PST and Hx + LV/GFP animals lost the ability to retrieve food pellets from the staircase (Hx + LV/GFP 0 $\pm$ 0, Hx + LV/PST 0 $\pm$ 0, Sham 1.3 $\pm$ 0.6, Figure 6.3B). By 7 days post-surgery, 14% of Hx + LV/GFP and 50% of Hx + LV/PST animals could retrieve at least 1 food pellet (mean number food pellets consumed; Hx + LV/GFP 0.1 $\pm$ 0.1, Hx + LV/PST 0.7 $\pm$ 0.3). The number of food pellets consumed by all animals fluctuated throughout the duration of the study, and no difference was observed in the number of food pellets consumed at any time-point, between Hx + LV/PST and Hx + LV/GFP animals (p>0.05, two-way ANOVA, Figure 6.3B). 6 weeks post-lesion, there was, however, a higher percentage of Hx + LV/PST animals that could consume at least one food pellet from the staircase, compared to Hx + LV/GFP (83% vs 57%, respectively). The number of food pellets than consumed by hemisected animals was

significantly lower than sham animals throughout the study (LV/PST, p = 0.01; LV/GFP, p = 0.04, Figure 6.3B). This data is replotted in figures 6.3C and D, excluding the injection only groups for ease of viewing.

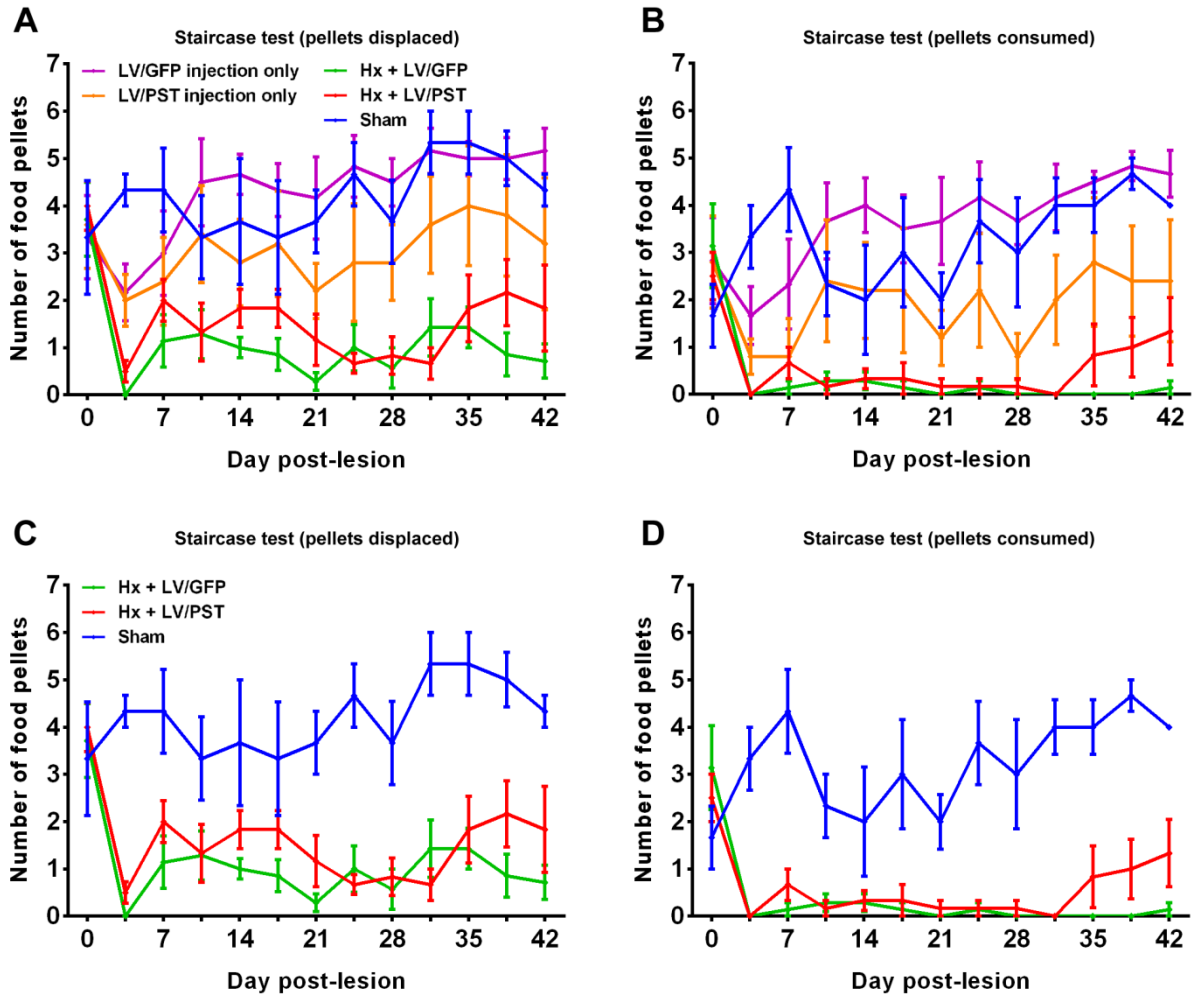

Figure 6.3. The intraspinal injection of LV/PST does not enhance performance on a skilled behavioural task, compared to LV/GFP injection.
The Montoya staircase test was used to assess the recovery of skilled forelimb locomotor function following surgery. **(A)** The number of food pellets displaced in the staircase can be used as a measure of gross forelimb locomotor function. 3 days post-surgery there was a reduction in the number of food pellets displaced by injection only and hemisection animals, irrespective of which treatment they received, compared to sham. One week post-surgery, animals had regained partial forelimb function. **(B)** Similarly, there was a reduction in the number of food pellets consumed by animals, 3 days post-surgery, in the injection only and hemisection groups, compared with sham animals. Some animals showed partial recovery 7 days post-surgery, which persisted for the duration of the study. **(C, D)** To visualise the results obtained from hemisection animals more clearly, the data presented in figures **(A)** and **(B)** was re-plotted to only include Hx + LV/PST, Hx + LV/GFP and sham animals. There

was no difference between Hx + LV/PST or Hx + LV/GFP animals in the number of food pellets displaced or consumed at any examined time-point (p>0.05, two-way ANOVA). Sham, *n=3;* Hx + LV/PST*, n=6;* Hx + LV/GFP, *n*=6; LV/PST only, *n*=6 and; LV/GFP only, *n*=6.

6.2.1.3 Grid exploratory test

To further evaluate the locomotor function of Hx + LV/PST animals, sensorimotor performance of the hindlimbs was assessed using the grid exploratory test. Animals were left to freely explore on a metal grid, and the number of incorrect steps (or missteps, when the animals' paw fell through the bottom of the grid) was quantified. Baseline testing revealed no difference in the number of missteps in any treatment group (Figure 6.4). As expected, one week after hemisection lesion, animals that received either LV/GFP (Hx + LV/GFP) or LV/PST (Hx + LV/PST) injections had an increased number of missteps, compared to sham and injection only groups. Interestingly, there was a difference in the number of missteps between Hx + LV/PST and Hx + LV/GFP animals one week post-lesion (11.3 $\pm$ 1.1 and 15.6 $\pm$ 0.8, respectively, p<0.05, two-way ANOVA, Figure 6.4). Over the timecourse of the study, both Hx + LV/GFP and Hx + LV/PST animals improved their performance at the grid exploratory test. Hx + LV/PST animals performed significantly better at this test between 4 and 6 weeks post-lesion, compared to Hx + GFP animals (p<0.05, two-way ANOVA, Figure 6.4). The number of missteps by animals that received sham surgery or injection of LV/PST or LV/GFP in the absence of hemisection injury was unaltered by surgery, and remained low for the duration of the study (Figure 6.4).

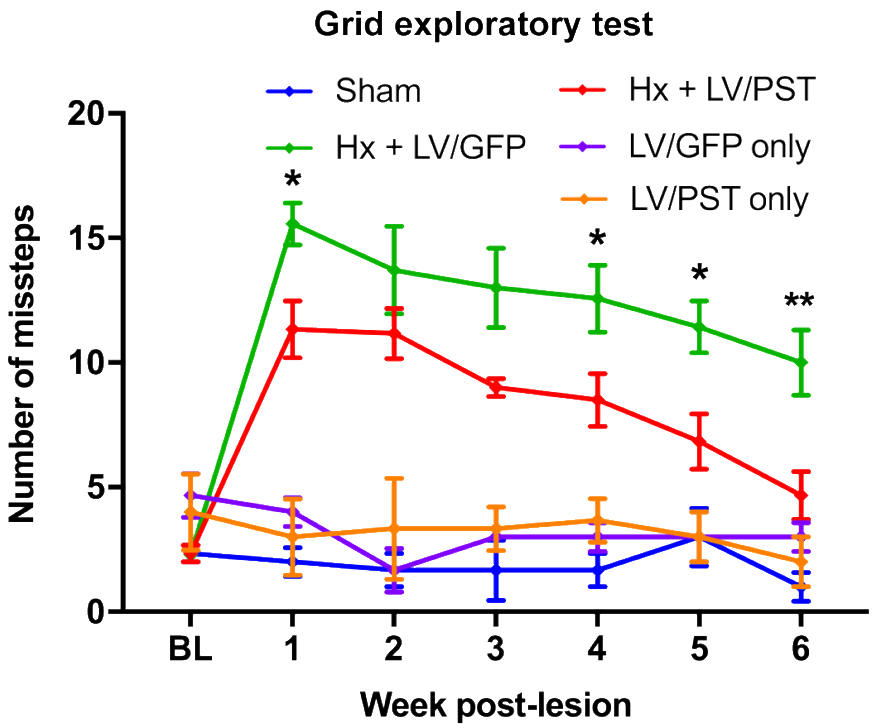

Figure 6.4. Intraspinal injection of LV/PST improved the hindlimb sensorimotor function of animals with mid-cervical SCI.
Animals' sensorimotor performance was assessed using the grid exploratory test. Prior to surgery, there was no difference observed in the number of missteps between treatment groups. One week post-surgery, however, animals that received lateral hemisection injury and injection of either LV/PST or LV/GFP had an increased number of missteps on the grid. Interestingly, Hx + LV/PST animals performed significantly better at the grid test one week post-lesion, and then between 4 and 6 weeks (*p<0.05, ** p<0.01, two-way ANOVA).

To summarise the behavioural data thus far, Hx + LV/PST animals showed a significant improvement in hindlimb locomotion, compared to Hx + LV/GFP animals, starting 4 weeks post-lesion and persisting for the duration of the study. There was no difference in forelimb function between Hx + LV/PST and Hx + LV/GFP animals, however there was a trend in both the open field locomotor assessment and the Montoya staircase test, which suggests a minor improvement in these animals. This improvement started 35 days post-lesion in the staircase test and 24 days post-lesion in the open field locomotor assessment. This data indicates there may be subtle improvements in forelimb locomotor, which cannot be detected by routine behavioural tests. To evaluate fine locomotor parameters, such as the forepaw print area, the automated gait analysis system Catwalk-XT was used.

6.2.1.4 Automated gait analysis

Animals were habituated to the Catwalk-XT system prior to surgery. Baseline values were obtained 2-3 days before surgery, then testing commenced when the majority of animals had regained frequent to consistent plantar stepping (3 weeks post-lesion). The Catwalk-XT system can be used to quantify both the intensity of the impact and the area occupied by individual paws, as they contact the glass walkway. Max contact max intensity is used to reveal the maximum intensity exerted by the paws, at the point at which they are in maximum contact with the glass walkway (Catwalk-XT User Manual). 3 weeks post-lesion, there was a reduction in the intensity of the ipsilateral forepaw placement in both Hx + LV/PST and Hx + LV/GFP animals, compared to sham animals, which persisted for the remainder of the study (Figure 6.5A). While no difference could be observed in the intensity of paw placement of Hx + LV/PST animals, when compared with Hx + LV/GFP, there was a marginal, non-significant improvement at all examined time points (p>0.05, two-way ANOVA, Figure 6.5A).

Following hemisection lesion, there was also a reduction in the print area of the ipsilateral forelimb, compared to sham animals. No difference was observed between the print area in Hx + LV/PST animals, compared to Hx + LV/GFP (Figure 6.5B), although the area was larger in Hx + LV/PST animals than in those that received Hx + LV/GFP injections, at all examined time points (Figure 6.5B).

Similarly, there was a reduction in the stride length of the ipsilateral forepaw in animals that received either Hx + LV/PST or Hx + LV/GFP animals, compared to sham animals. There was no difference between stride length in Hx + LV/PST and Hx + LV/GFP animals at any examined time point (Figure 6.5C)

While BBB scoring does take into account interlimb coordination, this is difficult to discern manually, and also relies on the animal completing three full step cycles in a row, without pause. While this is common in naïve animals, those with SCI do not move around the open field as frequently as naïve or sham animals, thus making it difficult to accurately gauge interlimb coordination. To assess coordination using the Catwalk-XT system, a parameter called ‘regularity index’ is used, which measures the number of normal stepping patterns taking place as an animal crosses the walkway, and represents this as a percentage of the

total number of stepping patterns. Baseline recordings for all animals showed a reliability index of close to 100%, suggesting constant interlimb coordination. Sham animals maintained this 100% reliability index, which indicates that the laminectomy procedure did not alter their ability to maintain consistent interlimb coordination. 3 weeks post-lesion, there was a decrease in the regularity index in both Hx + LV/PST and Hx + LV/GFP animals (Figure 6.5D); however, the values for Hx + LV/PST animals were closer to 100% than animals that received Hx + LV/GFP at all examined time points, suggesting a mild, non-significant improvement (Figure 6.5D)

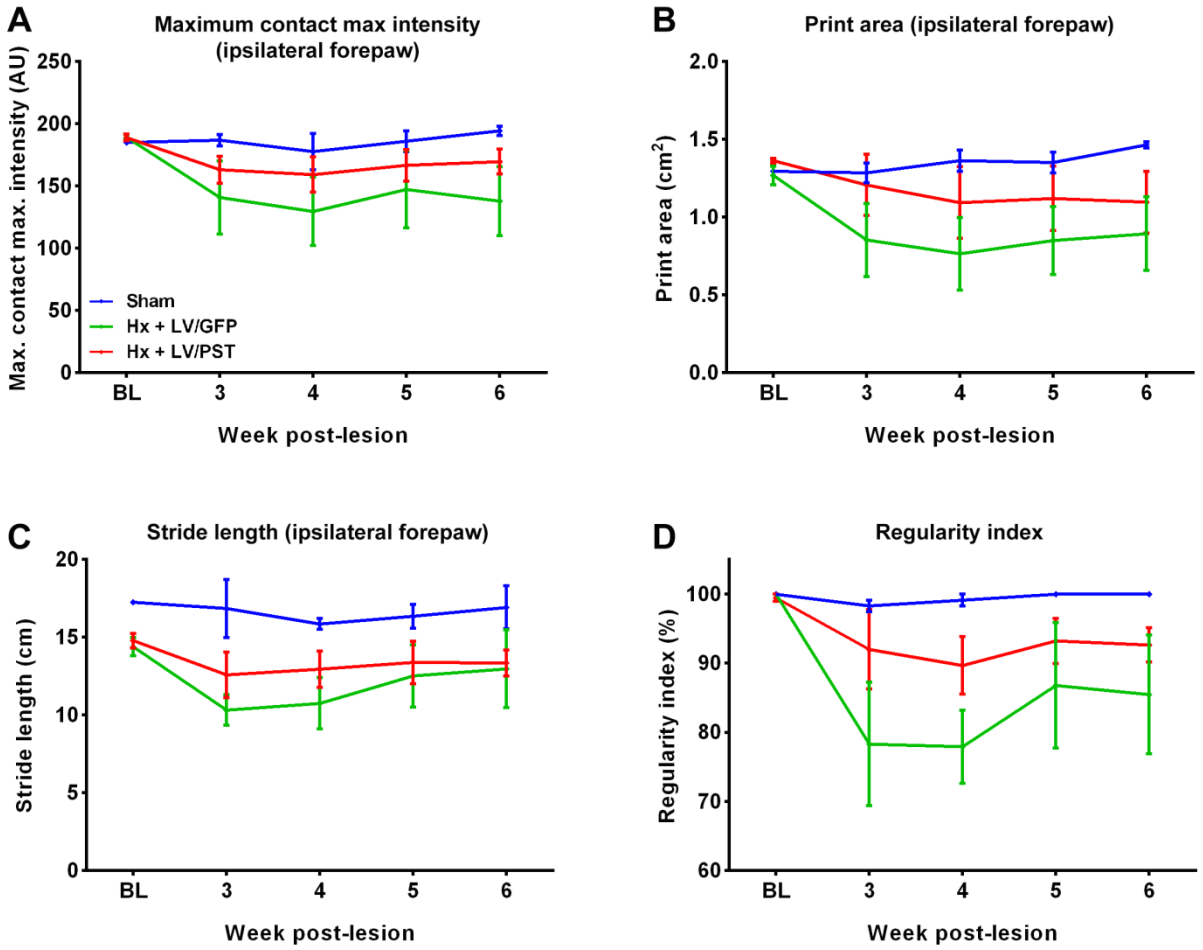

Figure 6.5. The LV/PST injections did not alter fine gait parameters, measured using the Catwalk-XT system.

Only animals that regained weight supported stepping were used for Catwalk-XT analysis. **(A)** The intensity of forepaw placement was unchanged between Hx + LV/PST and Hx + LV/GFP animals (p>0.05). **(B)** The print area of the ipsilateral forepaw was unchanged between Hx + LV/PST and Hx + LV/GFP animals (p>0.05). **(C)** Similarly, there was no difference in stride length between Hx + LV/PST and Hx + LV/GFP animals). **(D)** The

regularity index was close to 100% in all animals prior to surgery. After injury, there was a reduction in regularity index in both Hx + LV/GFP and Hx + LV/PST animals. There was no difference between Hx + LV/GFP and LV/PST at any examined time point. Sham, *n=3;* Hx + LV/PST*, n=6;* Hx + LV/GFP, *n*=6; LV/PST only, *n*=6 and; LV/GFP only, *n*=6.

6.2.2 LV/PST did not cause abnormal pain sensations

One of the possible adverse effects of inducing SCI in rodents is autotomy, which involves chewing of one or more of the digits of the animals' paws. In this study, no animals in the Hx + LV/GFP group developed autotomy at any time during the experiment. Conversely, 3 animals in the Hx + LV/PST group developed autotomy of the contralateral hindlimb and were culled according to Home Office instructions. The emergence of autotomy beyond the first couple of post-operative days suggested that Hx + LV/PST animals may be suffering from neuropathic pain. To investigate this further, animals were subjected to sensory testing to ensure that these animals did not have abnormal pain sensations. It should be noted that as animals with autotomy were immediately culled, sensory testing was performed on the remaining animals, which did not previously show signs of autotomy.

Responses to mechanical stimuli were assessed using Von Frey filaments. After 5 weeks post-lesion, there was no difference in the response to mechanical stimuli in Hx + LV/PST rats, compared to Hx + LV/GFP, in either the ipsilateral or contralateral hindpaws (Figure 6.6A, B, respectively). Similarly, there was no difference in the response to thermal stimuli observed 6 weeks post-lesion in either Hx + LV/PST or Hx + LV/GFP animals (Figure 6.6A, B). Responses to thermal stimuli were assessed using the plantar heat test (Hargreave's method). After 5 weeks post-lesion, there was no differences in the response to thermal stimuli in Hx + LV/PST animals, compared to those that received Hx + LV/GFP of either the ipsilateral or contralateral hindpaws (Figure 6.6C, D, respectively). Similarly, there was no difference in responses to thermal stimuli 6 weeks post-lesion in Hx + LV/PST or Hx + LV/GFP animals (Figure 6.6C,D).

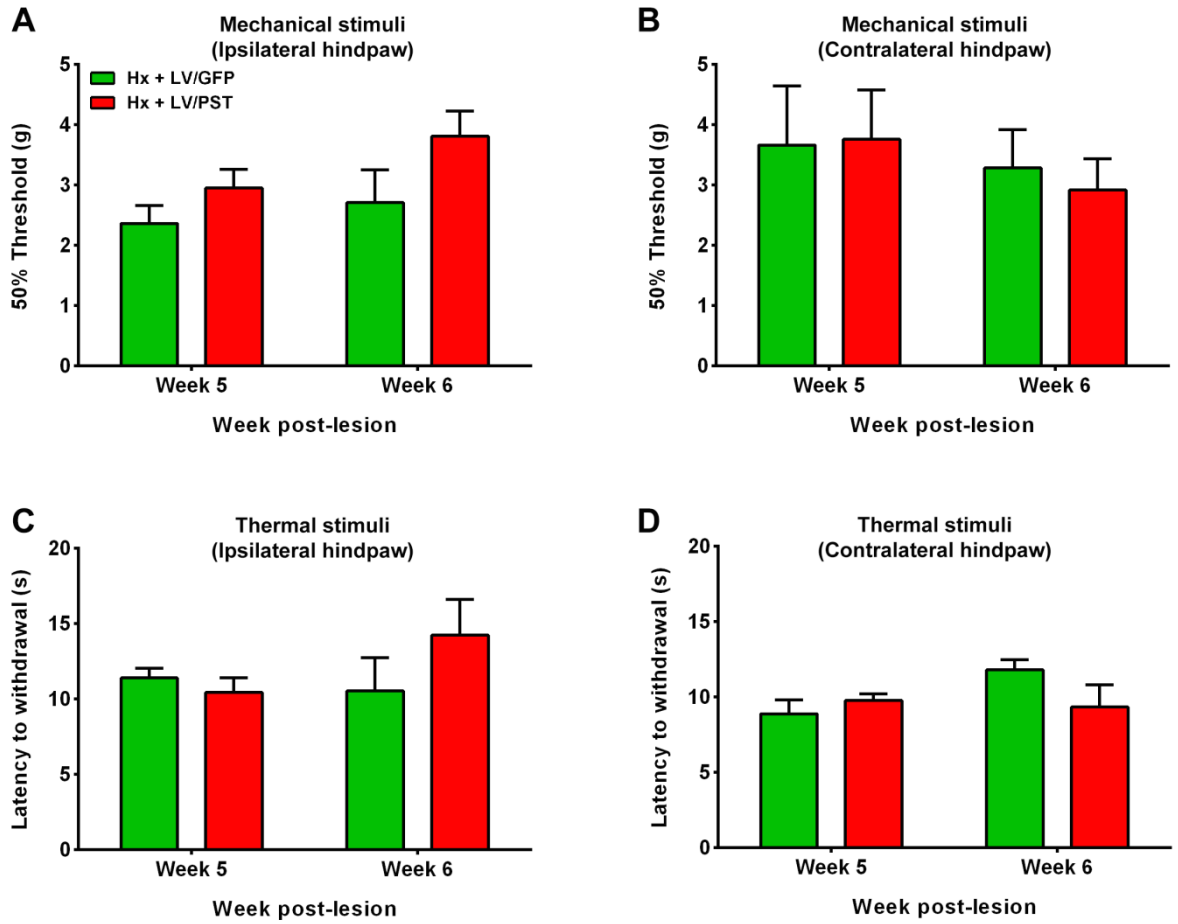

Figure 6.6. Testing of sensory function in animals that received lateral hemisection injury and viral vector treatment.
Following the development of autotomy in three animals that received Hx + LV/PST injections, sensory testing was performed to ensure that these animals were not suffering from neuropathic pain. **(A-B)** Responses to mechanical stimuli were assessed using Von Frey filaments. There was no difference in the response to stimulation with Von Frey filaments of either **(A)** ipsilateral or **(B)** contralateral hindpaws, in either Hx + LV/PST or Hx + LV/GFP animals. **(C-D)** Responses to thermal stimuli were assessed using the plantar heat test (Hargreave's method). There was no difference in the response to temperature of either the **(C)** ipsilateral or **(D)** contralateral hindpaws in either Hx + LV/PST or Hx + LV/GFP animals. Sham, *n=3;* Hx + LV/PST*, n=6;* Hx + LV/GFP, *n*=6; LV/PST only, *n*=6 and; LV/GFP only, *n*=6.

6.2.3 PSA expression was robust six weeks after LV/PST intraspinal injections

To verify PSA production following intraspinal injection of LV/PST viral vectors at the end of the experiment, horizontal sections of the cervical spinal cord containing the injury site (if present) and the injection sites, were immunolabelled using an antibody against PSA. Animals that received Hx + LV/PST injections had four regions of mCherry-positive cells in

the grey matter of the spinal cord, two rostral and two caudal to the hemisection lesion, representing the areas injected by the viral vector. Positive-cells were concentrated in the intermediate grey matter, some cells were also found in the dorsal and ventral horns. mCherry-positive cells were surrounded by strong PSA immunolabelling, suggesting strong expression of PSA by LV/PST, both rostral and caudal to the lesion site (Figure 6.7A, B). Conversely, no PSA immunolabelling was observed in animals that received Hx + LV/GFP injections. While large regions of GFP-expressing cells were observed in these animals (2 rostral and 2 caudal to the lesion site), no PSA labelling was found surrounding these cells (Figure 6.7C, D). Similarly to animals that received Hx + LV/PST injections, those that received injections alone had four regions of mCherry-positive cells, indicating the injection sites. Additionally, strong PSA labelling could be observed surrounding these mCherry-positive neurons (Figure 6.7E, F). Animals that received LV/GFP injections only showed a similar pattern to Hx + LV/GFP animals. Four regions of GFP-positive cells could be observed, and no PSA immunostaining was observed surrounding these cells (Figure 6.7G, H).

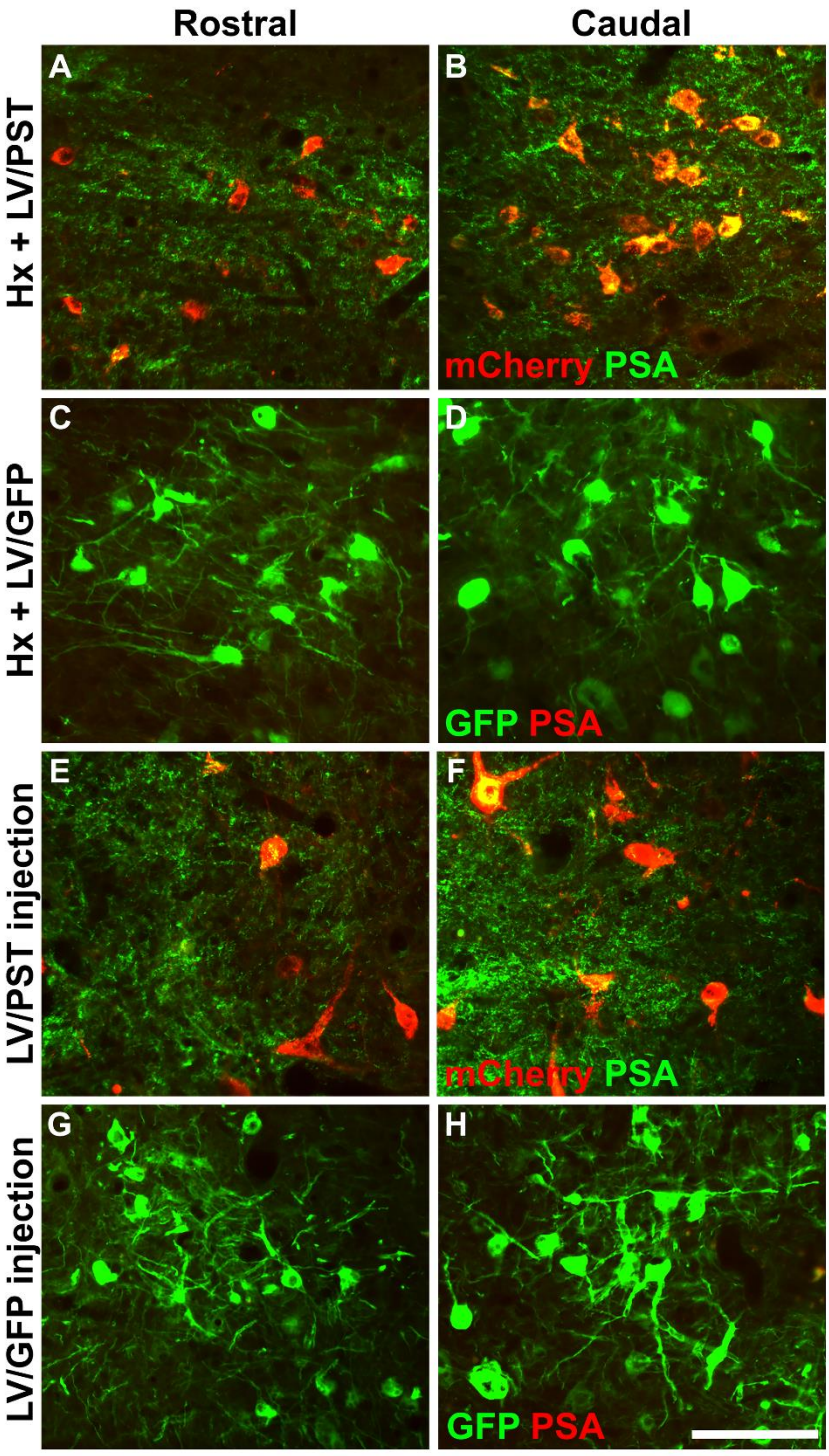

Figure 6.7. PSA labelling in the intermediate grey matter 6 weeks following injection of lentiviral vectors.

(A, B) Regions of mCherry-positive cells were observed in the cervical spinal cords of Hx + LV/PST animals, two rostral and two caudal to the lesion site. PSA labelling was strong surrounding mCherry-positive cells, suggesting PSA production by LV/PST. **(C, D)** Similarly, regions of GFP-positive cells were observed in the spinal cords of Hx + LV/GFP animals, 6 weeks post-injection. PSA immunolabelling was absent surrounding these cells. **(E, F)** LV/PST injection only, in the absence of hemisection injury resulted in mCherry-positive cells

in the spinal grey matter. These cells were surrounded by strong PSA immunolabelling. **(G, H)** GFP-positive cells were observed in the spinal cord of animals that received LV/GFP injection only. No PSA labelling was observed surrounding these cells. Scale bar = 100 μm.

To evaluate whether PSA expression was similar in Hx and injection only animals, the area occupied by PSA immunostaining was quantified 6 weeks following delivery to the spinal cord. As previously shown, there was no PSA expression in animals that received either Hx + LV/GFP injections or LV/GFP injections only, in the grey matter, in the areas surrounding the injection sites (Figure 6.8C, D and G, H). The area of PSA expression was high in both Hx + LV/PST and LV/PST injection only animals and was fairly variable between animals in the same treatment group. There was no difference between the PSA expression in animals that received Hx + LV/PST injection, compared to those that received LV/PST injection only (LV/PST 0.79 ± 0.21, Hx + LV/PST 0.46 ± 0.12, p>0.05, one-way ANOVA, Figure 6.8A). Moreover, there was no difference in PSA expression in the rostral or caudal injection sites in LV/PST injection only animals (Rostral 0.43 ± 0.16; Caudal 0.36 ± 0.1, p > 0.05, two-way ANOVA, Figure 6.8B), or rostral or caudal to the lesion in Hx + LV/PST animals (Rostral 0.22 ± 0.06; Caudal 0.24 ± 0.09, p > 0.05, Figure 6.8B)

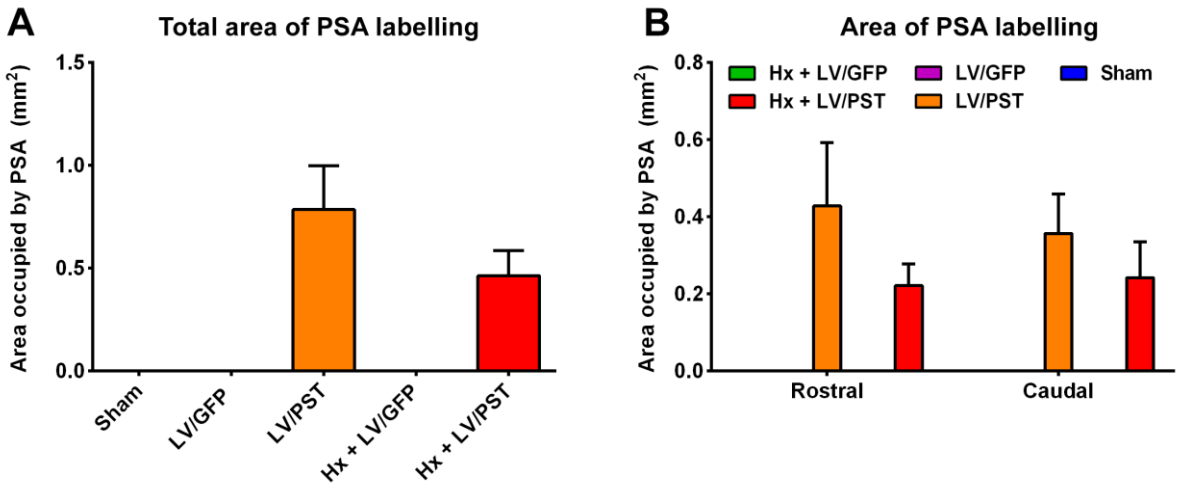

Figure 6.8. Quantification of PSA labelling following delivery of lentiviral vectors to the spinal cord.
The area occupied by PSA immunostaining was quantified 6 weeks following injection to the cervical spinal cord. **(A)** No PSA labelling was observed in sham animals, or those that received LV/GFP injections with or without hemisection injury. Conversely, strong PSA

labelling was observed in animals that received LV/PST injections. There was no difference observed between animals that received Hx + LV/PST or LV/PST injections only (p>0.05). **(B)** There was no difference between the area occupied by PSA labelling rostral and caudal to the injury site, in animals that received Hx + LV/PST. Moreover, there was no difference in the area occupied by PSA labelling in the rostral or caudal injections, in animals that received LV/PST injections only (p<0.05). Sham, *n=3;* Hx + LV/PST*, n=6;* Hx + LV/GFP, *n*=6; LV/PST only, *n*=6 and; LV/GFP only, *n*=6.

6.2.4 LV/PST-mediated PSA expression did not induce neuroplasticity six weeks after delivery to the cervical spinal cord

6.2.4.1 Serotonin immunolabelling

The delayed improvement in hindlimb motor function displayed by the LV/PST treated animals (starting 30 days post-lesion) may correspond to enhanced axonal sprouting and the formation of new spinal cord circuits. Serotonin is an important neuro-modulator, and sprouting of serotoninergic fibres has been demonstrated in a number of rodent models of SCI (Camand et al., 2004; Hawthorne et al., 2011). Moreover, a number of therapeutic agents have previously been shown to enhance sprouting of serotonergic fibres, including ChABC and PSA mimetic peptides (Barritt et al., 2006; Pan et al., 2014). To assess whether sprouting of serotonergic fibres was responsible for the improvement in motor function in LV/PST-treated animals, the spinal cords were immunolabelled using antibody raised against serotonin and the density of serotonergic inputs to individual mCherry or GFP-positive neurons in the intermediate grey matter-ventral horns was quantified.

The antibody used in this study strongly labelled serotonergic fibres, which were observed throughout the spinal cord, and with high density in the ventral horns. Serotonergic inputs to individual neurons could be clearly observed with a 40x objective on a standard epifluorescence microscope (Figure 6.9). In both Hx + LV/GFP and Hx + LV/PST animals, there appeared to be a lower density of serotonergic inputs to transduced neurons located caudal to the lesion site, compared to those in the rostral spinal cord (Figure 6.9A, D). This likely reflects the loss of descending serotonergic inputs to the caudal spinal cord, due to the hemisection lesion. There was no apparent difference in the density of serotonergic

inputs to mCherry-positive, compared to GFP-positive neurons, in animals that received intraspinal injections in the absence of hemisection injury (Figure 6.9E-H).

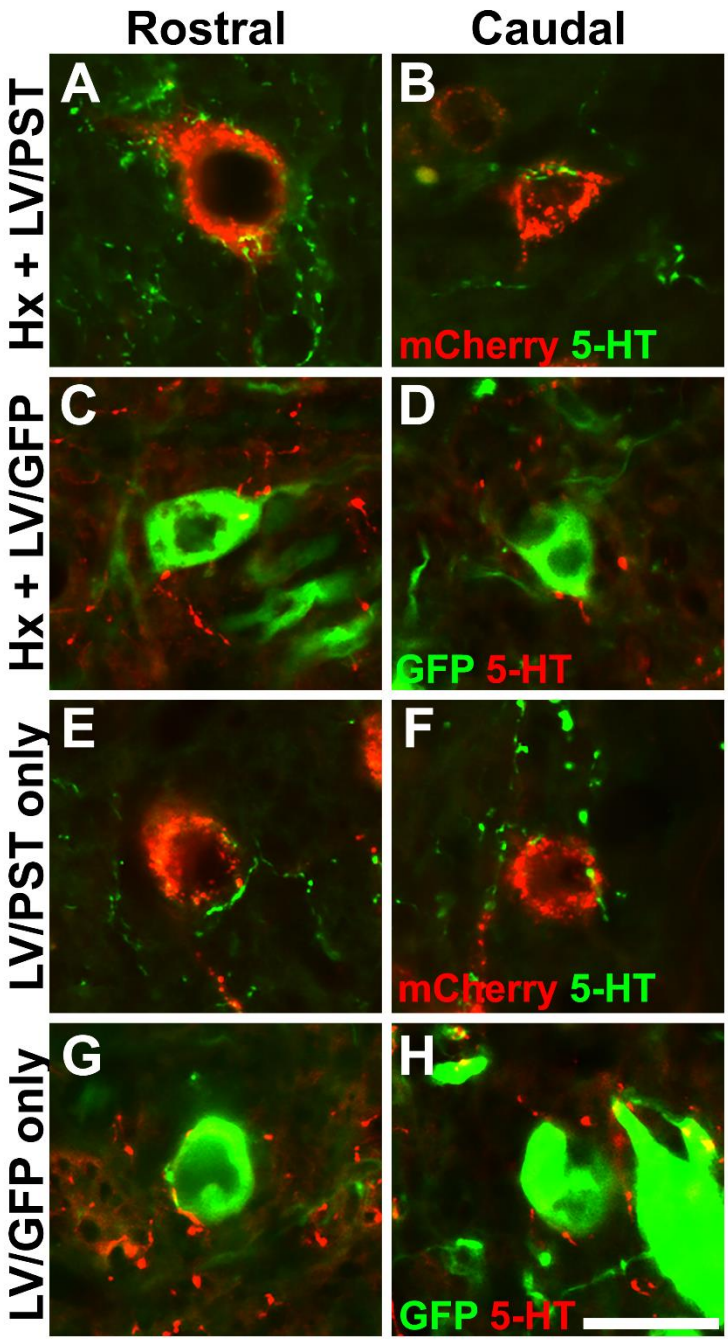

Figure 6.9. Representative photomicrographs showing serotonin labelling 6 weeks post-SCI and following delivery of viral vectors.
Immunolabelling was used to assess the density of serotonergic labelling onto GFP- or mCherry-positive neurons. **(A-B)** Strong serotonergic inputs were observed in animals that received Hx + LV/PST injections, rostral to SCI. Neurons located caudal to the injury appeared to receive lower levels of serotonergic inputs. **(C-D)** Similar results were observed in animals that received Hx + LV/GFP injections. **(E-H)** Similar levels of serotonergic inputs

were observed in animals that received LV/PST or LV/GFP injections only. Scale bar = 25 μm.

The quantification of the density of serotonergic labelling showed no difference in the density of inputs to either mCherry- or GFP-positive neurons in Hx + LV/PST or Hx + LV/GFP animals, respectively, rostral to the lesion (Hx + LV/PST 2.1 ± 0.5; Hx + LV/GFP 1.6 ± 0.4, $p > 0.05$, Figure 6.10). Similarly, there was no difference caudal to the lesion (Hx + LV/PST 1.6 ± 0.5; Hx + LV/GFP 1.0 ± 0.1, $p > 0.05$, Figure 6.10). There was also no difference in the density of serotonergic inputs to immunopositive neurons in animals that received injections of LV/PST alone, compared to LV/GFP, in the absence of hemisection injury (Rostral; LV/PST 2.2 ± 0.1; LV/GFP 2.7 ± 0.2, $p > 0.05$; Caudal; LV/PST 2.4 ± 0.4; LV/GFP 1.5 ± 0.2, $p > 0.05$, Figure 6.10).

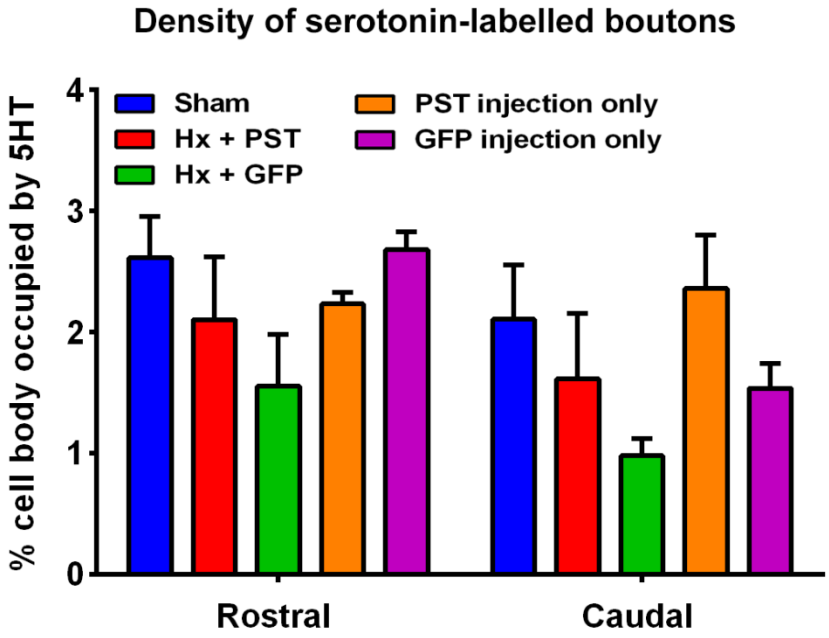

Figure 6.10. Quantification of the density of serotonin-labelled boutons contacting either mCherry- or GFP-positive neurons.
Six weeks following delivery of viral vectors to the cervical spinal cord, animals were culled and the spinal cords were assessed for serotonin labelling. There was no difference in the density of serotonergic inputs either rostral or caudal to the lesion site, in Hx + LV/PST and Hx + LV/GFP animals. Moreover, there was no difference between animals which received injections of either LV/PST or LV/GFP only and sham animals that received laminectomy ($p > 0.05$, two-way ANOVA). Sham, *n=3;* Hx + LV/PST, *n=6;* Hx + LV/GFP, *n*=6; LV/PST only, *n*=6; and LV/GFP only, *n*=6.

6.2.4.2 Synaptophysin immunolabelling

To assess whether induced PSA expression resulted in enhanced synaptic contacts to neurons with viral transgene expression, horizontal sections of spinal cord containing the intermediate grey matter were immunolabelled using antibody raised against synaptophysin and the density of synaptophysin-labelled boutons contacting individual mCherry or GFP-positive neurons was quantified. Strong synaptophysin labelling was observed throughout the spinal cord of animals in all experimental groups. There was no clear difference in the density of synaptophysin-labelled boutons contacting mCherry-positive, compared to GFP-positive neurons, in Hx + LV/PST and Hx + LV/GFP animals, respectively (Figure 6.11).

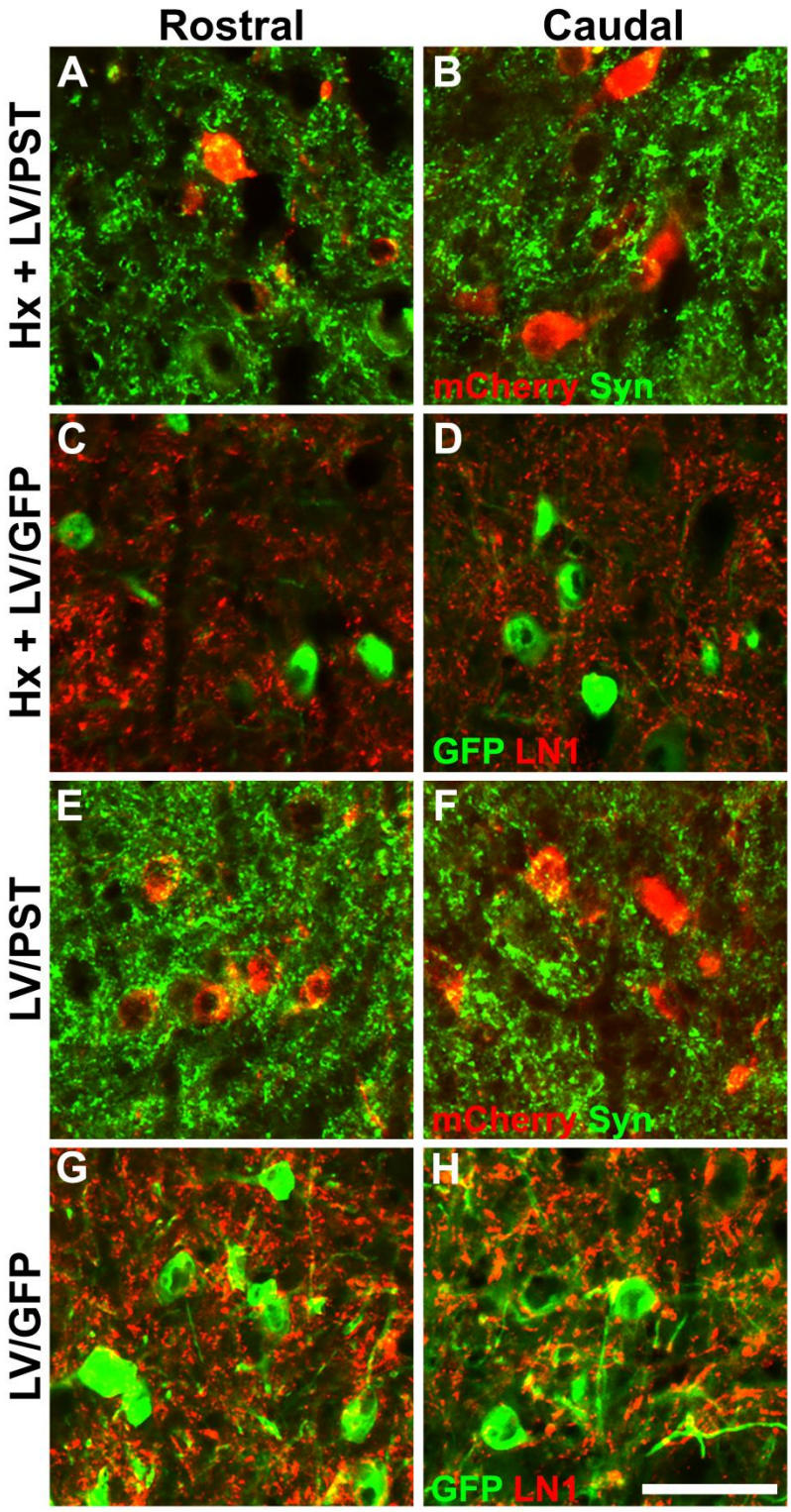

Figure 6.11. Representative photomicrographs showing synaptophysin immunolabelling following LV/PST or LV/GFP delivery to the spinal cord.

Immunolabelling was used to assess the density of synaptophysin-labelled boutons contacting GFP- or mCherry-positive neurons. **(A-D)** Examples of synaptophysin immunolabelling in animals which received Hx + LV/PST or LV/GFP injections. **(E-H)** Synaptophysin immunolabelling in animals which received injections of LV/PST or LV/GFP in the absence of hemisection injury. Scale bar = 50 μm.

The quantification of the density of synaptophysin immunolabelling showed no difference in the density of synaptic inputs to either mCherry-positive, or GFP-positive neurons in Hx + LV/PST or Hx + LV/GFP animals, respectively, rostral to the lesion site (16.1 ± 2.0, 13.4 ± 2.9, respectively, $p < 0.05$, Figure 6.12). Similarly, there was no difference caudal to the lesion (12.2 ± 1.8, 13.6 ± 2.9, respectively, $p < 0.05$, Figure 6.12). There was also no difference in the density of synaptophysin-labelled boutons to mCherry or GFP-positive neurons in animals that received injections of LV/PST alone, compared to LV/GFP, in the absence of hemisection injury (Rostral; 18.4 ± 2.5, 20.0 ± 3.2, respectively, Caudal; 17.0 ± 3.2, 16.3 ± 4.0, respectively, $p < 0.05$, Figure 6.12).

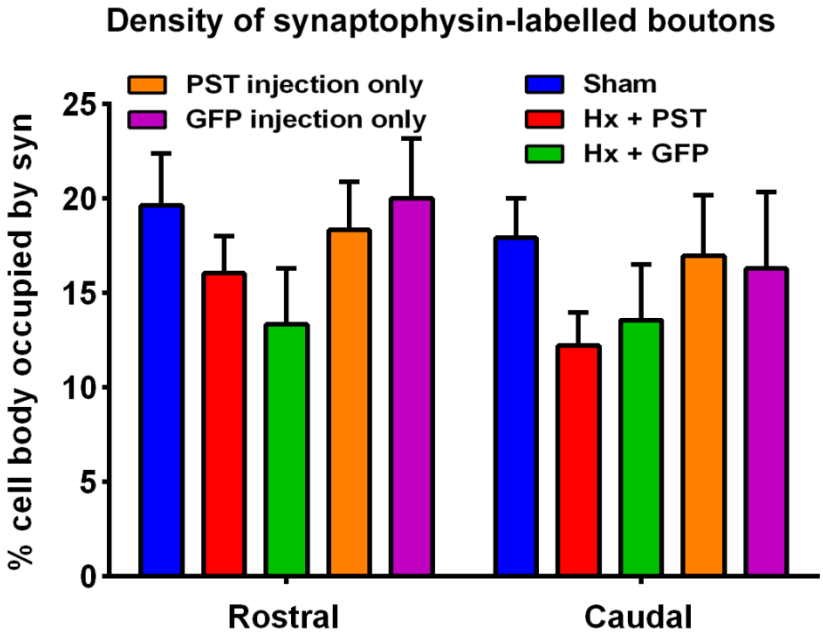

Figure 6.12. Quantification of the density of synaptophysin-labelled boutons contacting either mCherry- or GFP-positive neurons.
There was no difference in the density of synaptophysin-positive boutons either rostral or caudal to the lesion site in Hx + LV/PST and Hx + LV/GFP animals. Moreover, there was no difference between animals which received injections of either LV/PST or LV/GFP only and sham animals that received laminectomy ($p > 0.05$, two-way ANOVA). Sham, *n=3;* Hx + LV/PST*, n=6;* Hx + LV/GFP, *n*=6; LV/PST only, *n*=6 and; LV/GFP only, *n*=6.

6.2.5 LV/PST-mediated PSA expression did not alter the number of density of PNNs six weeks after delivery to the cervical spinal cord

6.2.5.1 WFA immunolabelling

To assess whether induced PSA expression in the spinal cord led to alterations in the PNN, sections were immunolabelled using WFA lectin, in addition to antibodies raised against LN1 and neurocan. Sham animals had PNNs distributed throughout the grey matter of the spinal cord, which were readily labelled by WFA lectin. Similarly, WFA-labelled PNNs were detected in animals in all the other experimental groups (Figure 6.13A). As previously described, Hx + LV/PST and Hx + LV/GFP injected animals had regions of mCherry-positive and GFP-positive neurons, respectively, in the intermediate grey matter-ventral horn. WFA-labelled PNNs were observed surrounding some mCherry/GFP-positive neurons in those animals (Figure 6.13A-D). Similarly, mCherry and GFP-positive neurons were observed in animals that received LV/PST and LV/GFP injections, respectively, in the absence of hemisection injury, and were surrounded by WFA-labelled PNNs (Figure 6.13E-H).

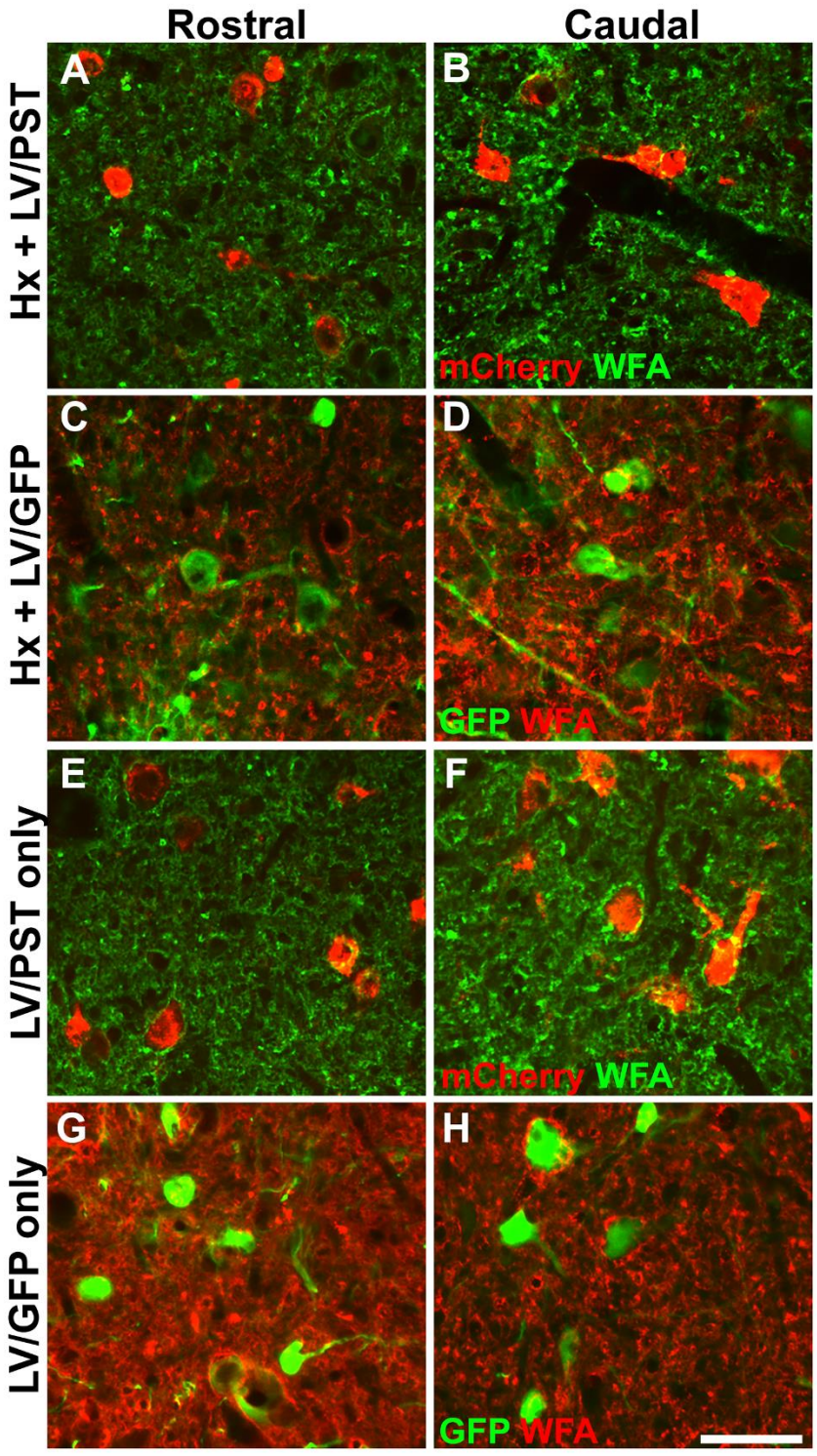

Figure 6.13. WFA labelled PNNs in animals injected with lentiviral vectors.
WFA-labelling was observed throughout the neuropil and condensed in PNNs in the spinal cords of animals in all treatment groups. **(A-B)** mCherry-positive neurons were surrounded by WFA-labelled PNNs rostral and caudal to the lesion in Hx + LV/PST animals. **(C-D)** Similarly, PNNs were observed surrounding GFP-positive neurons in Hx + LV/GFP animals. **(E-F)** WFA-labelled PNNs were found surrounding mCherry-positive neurons in animals that received LV/PST injections in the absence of hemisection injury. **(G-H)** GFP-positive neurons

were surrounded by WFA-labelled PNNs in LV/GFP injection only animals. Scale bar = 50 μm.

To evaluate whether there were any differences in WFA-labelled PNNs in animals that received LV/PST injections, compared to those that received LV/GFP injections, the proportion of transduced neurons with a WFA-labelled PNN, in addition to the density of WFA PNN labelling on individual neurons was quantified.

There was no difference in the proportion of mCherry or GFP-positive neurons with a WFA-labelled PNN in Hx + LV/PST and Hx + LV/GFP animals, respectively, rostral to the injury site (Hx + LV/PST 13.1 ± 3.2; Hx + LV/GFP 23.6 ± 7.0, $p > 0.05$, Figure 6.14A). Similarly, no difference was observed in animals that received injections of LV/PST or LV/GFP only, or sham (LV/PST 19.4 ± 2.4; LV/GFP 20.3 ± 3.1, $p > 0.05$, Figure 6.14A). Similar results were obtained caudal to the lesion site (Hx + LV/PST 18 ± 4.9; Hx + LV/GFP 16.2 ± 2.3; LV/PST 17.4 ± 4.5; LV/GFP 19.2 ± 6.3, $p > 0.05$, Figure 6.14A). To assess whether the induced PSA expression altered the density of PNN immunolabelling, the area occupied by PNN labelling on individual mCherry or GFP-positive neurons was quantified. There was no difference in the area occupied by WFA-PNN labelling in Hx + LV/PST or Hx + GFP animals, either rostral or caudal to the lesion site (Rostral; 28.6 ± 2.3 and 25.3 ± 6.7, respectively, $p > 0.05$; Caudal 30.2 ± 2.4 and 27 ± 3.8, respectively, $p > 0.05$, Figure 6.14B). There was also no difference in the density of WFA-PNN immunolabelling in LV/PST or LV/GFP injection only animals, rostral or caudal (Rostral; 26.8 ± 2.7 and 25.8 ±7.8, respectively, Caudal; 27.0 ± 5.3 and 28.9 ± 5.7 respectively, $p > 0.05$, Figure 6.14B).

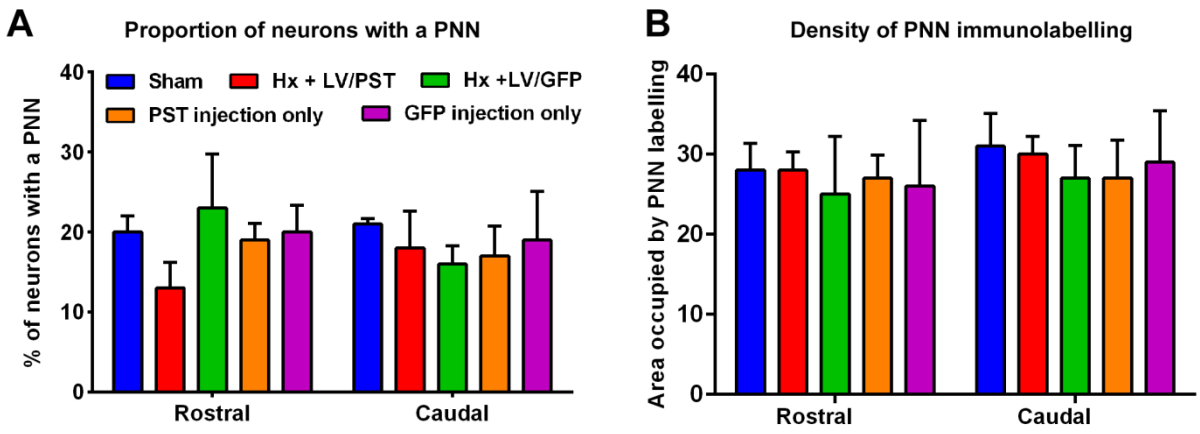

Figure 6.14. Quantification of WFA labelled PNNs following delivery of LV/PST and LV/GFP to the spinal cord.

(A) No difference was observed in the proportion of mCherry or GFP-positive neurons with a WFA-labelled PNN in Hx + LV/PST or Hx + LV/GFP animals, respectively. Moreover, there was no difference between animals that received injections of LV/PST or LV/GFP in the absence of injury, or sham animals. **(B)** There was no difference in the density of individual WFA-labelled PNNs in Hx + LV/PST or Hx + LV/GFP animals, rostral or caudal to the lesion site. Similarly, there was no difference in PNN density in LV/PST or LV/GFP injection only animals, or shams. Sham, *n=3;* Hx + LV/PST*, n=6;* Hx + LV/GFP, *n*=6; LV/PST only, *n*=6; and LV/GFP only, *n*=6.

6.2.5.2 LN1 immunolabelling

LN1-labelling was observed throughout the neuropil, and was concentrated in PNN structures in animals from all experimental groups (Figure 6.15). In all groups, a proportion of the mCherry or GFP-positive neurons were surrounded by LN1-labelled PNNs, which were found closely associated with the neuronal cell body. PNNs were also observed surrounding neurons devoid of mCherry or GFP labelling, but adjacent to those with expression of viral reporter genes (Figure 6.15).

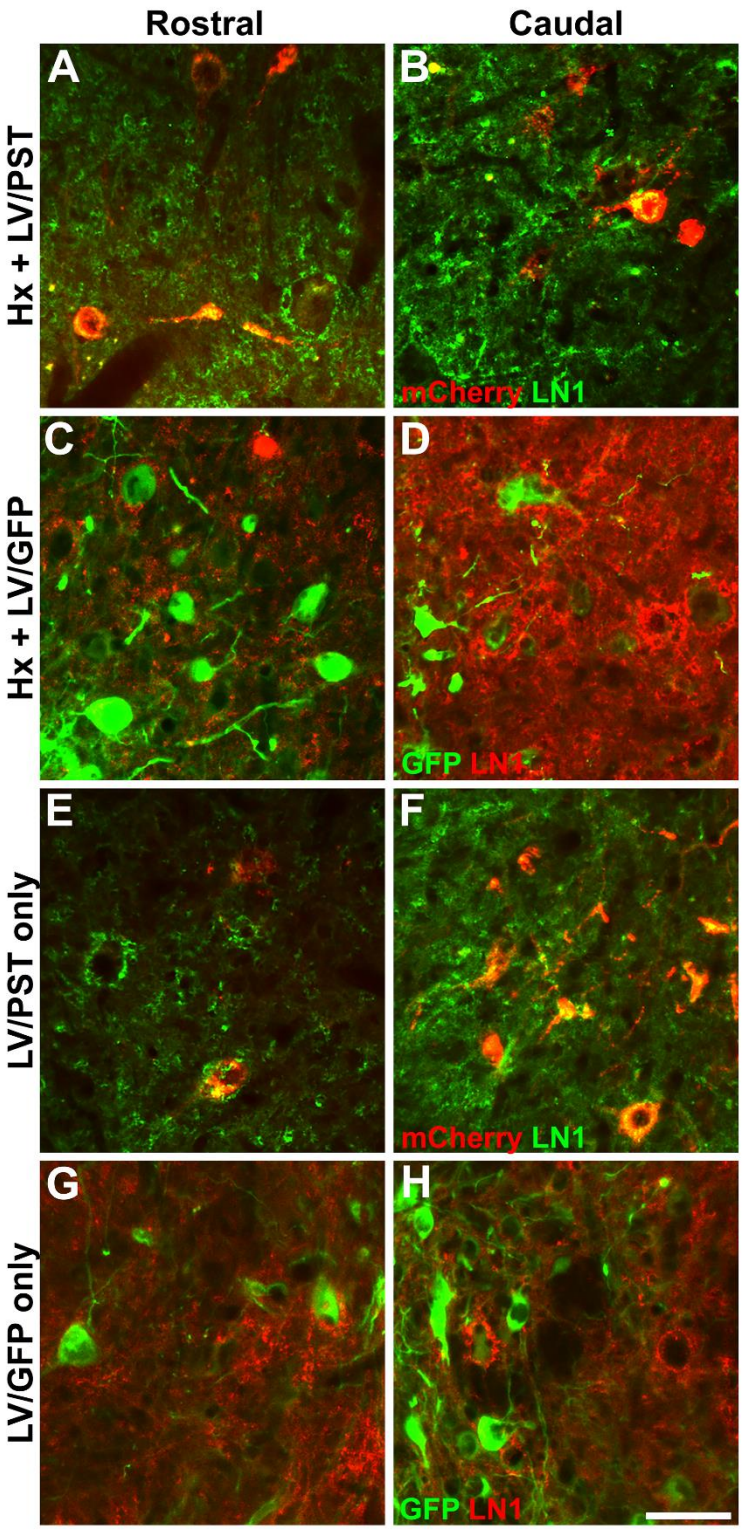

Figure 6.15. LN1-labelled PNNs were detected in the spinal cords of animals injected with viral vectors.

LN1 immunolabelling was observed throughout the cervical spinal cords of animals in all experimental groups, in both the neuropil and in PNNs. **(A-B)** PNNs were observed surrounding mCherry-positive neurons, and also neurons devoid of mCherry labelling, in animals that received Hx + LV/PST injections. **(C-D)** Similarly, LN1-labelled PNNs were found in GFP-positive, or negative, neurons in animals that received Hx + LV/GFP injections. **(E-H)**

PNN labelling was observed in animals that received injections of viral vectors only, in the absence of hemisection lesion. Scale bar = 50 μm.

To assess whether there was any difference in PNN immunolabelling in animals that received LV/PST injections, compared to those that received control viral vector (LV/GFP), the proportion of mCherry or GFP-positive neurons with a LN1-labelled PNN, in addition to the density of PNN immunolabelling was quantified.

There was no difference in the proportion of mCherry or GFP-positive neurons with a LN1-labelled PNN in Hx + LV/PST and Hx + LV/GFP animals, respectively, either rostral or caudal to the injury site (Rostral; Hx + LV/PST 14.3 ± 2.2 and Hx + LV/GFP 22.0 ± 2.3, Caudal; Hx + LV/PST 18.0 ± 2.3 and Hx + LV/GFP17.5 ± 2.9, $p > 0.05$, Figure 6.16A). Similarly, no difference was observed in animals that received injections of LV/PST or LV/GFP only, or sham animals (Rostral; LV/PST 20.0 ± 3.2 and LV/GFP 19.4 ± 3.2, Caudal; LV/PST 19.4 ± 3.2 and LV/GFP 17.5 ± 2.8, $p > 0.05$, Figure 6.16A). To assess whether the induced PSA expression altered the density of PNN immunolabelling, the area occupied by LN1-PNN labelling on individual mCherry-positive or GFP-positive neurons was quantified. There was no difference in the area occupied by LN1-PNN labelling in Hx + LV/PST or Hx + GFP animals, either rostral or caudal to the lesion site (Rostral; 20.0 ± 1.2 and 18.3 ± 3.1, respectively, $p > 0.05$; Caudal 22.5 ± 3.3 and 20.1 ± 1.4, respectively, $p > 0.05$, Figure 6.16B). There was also no difference in the density of LN1-PNN immunolabelling in LV/PST or LV/GFP animals, rostral or caudal (Rostral, 21.5 ± 6.2 and 22.4 ± 5.2, respectively; Caudal, 23.0 ± 7.3 and 20.8 ± 3.1, respectively, $p > 0.05$, Figure 6.16B).

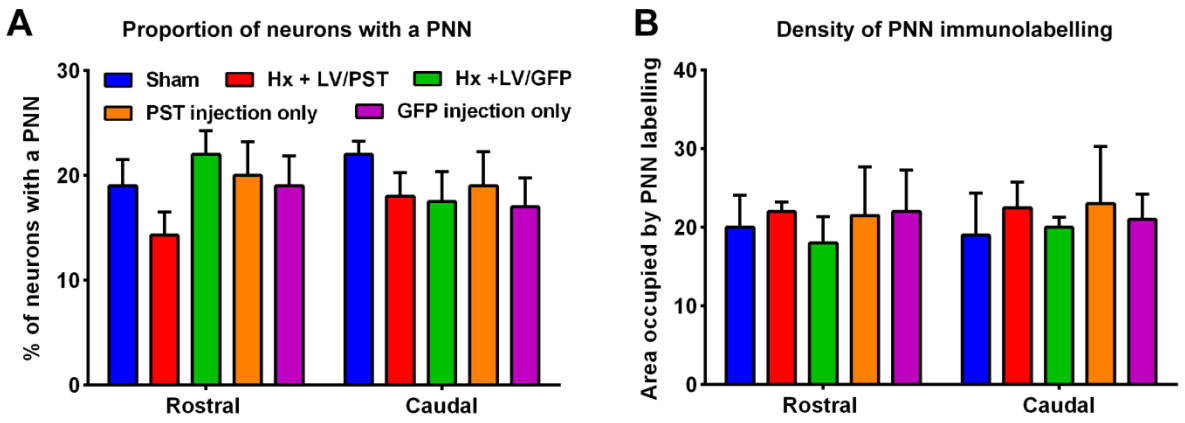

Figure 6.16. Quantification of LN1-labelled PNNs following delivery of LV/PST and LV/GFP to the spinal cord.
(A) No difference was observed in the proportion of mCherry or GFP-positive neurons with a WFA-labelled PNN in Hx + LV/PST or Hx + LV/GFP animals, respectively. Moreover, there was no difference between animals that received injections of LV/PST or LV/GFP in the absence of injury, or sham animals. **(B)** There was no difference in the density of individual WFA-labelled PNNs in Hx + LV/PST or Hx + LV/GFP animals, rostral or caudal to the lesion site. Similarly, there was no difference in PNN density in LV/PST or LV/GFP injection only animals, or shams. Sham, *n=3;* Hx + LV/PST*, n=6;* Hx + LV/GFP, *n*=6; LV/PST only, *n*=6 and; LV/GFP only, *n*=6.

6.3 Discussion

To summarise the data obtained in this chapter, first, a significant improvement in hindlimb locomotor function was observed following delivery of LV vector carrying the transgene for polysialyltransferase (LV/PST) rostral and caudal to a mid-cervical spinal cord lesion (Hx + LV/PST), compared to animals that received injections of control virus following injury (Hx + LV/GFP). This was not associated with an increase in the density of synaptophysin-positive boutons contacting neurons showing successful viral transgene expression, or an increase in the density of serotonergic inputs to these neurons. Moreover, no alterations were observed in either the proportion of neurons with a PNN, or the density of PNN immunolabelling on individual neurons. In a separate group of animals, injection of LV/PST in the absence of injury did not alter the proportion of neurons with a PNN, or the density of PNN immunolabelling. Furthermore, there was no increase in the density of synaptophysin-positive or serotonergic boutons contacting neurons showing viral transgene expression.

6.3.1 Locomotor function following delivery of lentiviral vectors

Targeted therapeutic interventions aiming to increase neuroplasticity in the injured spinal cord are increasing in popularity, due to the observation that the generation of novel spinal circuits may induce significant locomotor recovery, in the absence of long distance axonal regeneration (Bareyre et al., 2004). While regeneration of damaged axons across the glial scar may contribute to functional improvement in rodent models of SCI, in humans, the chances of this occurring are considerably lower due to the large distances (multiple centimetres) that regenerating axons must grow to cross the lesion site in order to reform functional connections.

In this study, hindlimb recovery was primarily assessed using the BBB scale, which is widely used in SCI research and has been used in a range of injury models including hemisection, contusion and compression lesions, in either cervical or thoracic spinal cord regions (Basso et al., 1995; García-Alías et al., 2011; Liu et al., 2015). One of the main benefits of this test is that it allows the investigation of a wide range of hindlimb movements, such as the individual movement of the ankle, knee and hip joints, interlimb coordination and the direction of paw placement (Basso et al., 1995). This allows monitoring of hindlimb locomotor function immediately following injury, which is generally not possible with other behavioural tests such as the grid exploratory test, or the automated gait analysis systems, as these tests typically require at least weight support or weight supporting stepping for accurate results.

Interestingly, hindlimb recovery following hemisection injury occurred at a similar rate in animals that received LV/PST or LV/GFP injections, for the first 4 weeks post-lesion. After this point, no further recovery was observed in Hx + LV/GFP animals. However, animals that received Hx + LV/PST injections continued to improve. A significant improvement in hindlimb function was observed starting 29 days post-lesion in Hx + LV/PST animals, compared to controls. This was due to an improvement in BBB scores from 11 to 14, which corresponds to an improvement in interlimb coordination. Additionally, there was a significant improvement observed in the hindlimb sensorimotor function of Hx + LV/PST animals, assessed using the grid exploratory test, compared to those that received Hx + LV/GFP. While the BBB scale is widely used in SCI research, there are a number of caveats with this test, one of which is the way in which interlimb coordination is assessed. To

examine this, an assessor must count the number of completed passes each animal undertakes (one completed pass equates to three complete step cycles), and observe whether fore and hindlimb placement occurs sequentially (Basso et al., 1995). This can be quite difficult to observe, especially as animals generally move around the open field apparatus at relatively fast speeds. Therefore, to obtain a quantified measure of interlimb coordination, in addition to other details regarding the animals locomotor performance, the automated gait analysis system Catwalk-XT was used.

Interestingly, there was no significant difference between the coordination (regularity index) of Hx + LV/GFP and Hx + LV/PST animals when assessed using the Catwalk-XT. There was, however, a trend to suggest a minor improvement in the regularity index. The differences observed in the BBB scores and Catwalk-XT regularity index values may have occurred for two reasons. First, as previously mentioned, the interlimb coordination measurement using the BBB scale may be inaccurately measured. Second, automated gait analysis systems, such as the Catwalk-XT, generally require a large number of animals for accurate results (Koopmans et al., 2007). Only 3-5 animals from each treatment group could perform weight-supported plantar placement of all four limbs, and thus it was only these animals that could be tested on the Catwalk. It is likely, therefore, that the Catwalk-XT study was underpowered, which may have affected the final results.

The FLS was developed as the forelimb counterpart to the BBB scale, and it measures similar parameters, such as paw placement, in addition to movement of the joints of the forearm (Cao et al., 2008). Interestingly, there was no improvement observed in forelimb locomotor function in Hx + LV/PST animals, compared to those that received LV/GFP injections. Similar to the BBB test, the FLS has a number of caveats, one of which is the broad criteria used to score the animals ((Cao et al., 2008) Supplementary Figure 2). Therefore, to complement the FLS, the forelimb locomotor function was also assessed using the Montoya staircase; however, no difference in locomotor function was observed between treatment groups. Moreover, forelimb function was examined using the Catwalk-XT system; however, no improvement was observed in any of the examined parameters.

While there was no drastic improvement observed in locomotor function following delivery of LV/PST after SCI, there was a trend to suggest a minor (non-significant) improvement in

all behavioural tests. This suggests that LV/PST delivery has caused a subtle improvement in locomotor function, but not such a large improvement as to reach statistical significance. Nonetheless, the behavioural data obtained in this study is still promising. Towards the end of this study (35 days post-lesion), Hx + LV/PST begin to show a slight improvement in the ability to retrieve food pellets in the Montoya staircase. It may be interesting to examine a longer timepoint, to see if the animals' performance on the staircase test continues to improve. Furthermore, mounting evidence suggests that rehabilitation used in combination with a targeted therapy can improve locomotor function beyond that observed with use of drug treatment alone ((Wang et al., 2011; Dietz and Fouad, 2014). There are a number of studies that have tried different paradigms of rehabilitation, including treadmill training, enriched cages, and task-specific rehabilitation, for example, pellet retrieval. Rehabilitation is also clinically relevant, as SCI patients are given a program of physiotherapy prior to their initial release from hospital after injury, and which they are encouraged to continue at home. Therefore, it would also be interesting to combine LV/PST injections with rehabilitation to see if this elicits a stronger behavioural improvement following SCI. In this case, it would be interesting to use a task-specific rehabilitation program, such as daily use of a pellet retrieval test (for example the Montoya staircase) to see if this leads to an improvement in forelimb locomotor function.

This study is the first to investigate the therapeutic benefit of PSA in the injured cervical spinal cord. Moreover, this is the first study to investigate the behavioural changes associated with LV/PST intraspinal injection in rats with SCI. To date there has been a number of studies investigating the therapeutic benefit of PSA expression in the injured thoracic spinal cord. Early research used a pseudotyped LV vector to engineer expression of polysialyltransferase in astrocytes in the injured spinal cord, which drives production of PSA (El Maarouf et al., 2006). Unfortunately, behavioural testing was not performed so comparisons between that study and ours cannot be performed. More recently, a couple of groups have developed PSA mimetic peptides, which can be continuously infused into the injured spinal cord using an osmotic minipump. So far, studies using these peptides have relied on contusion or corticospinal tract transection injuries in the thoracic spinal cord. The differences between the studies using the PSA mimetic and our study make direct comparisons difficult. Nonetheless, a significant recovery of motor function is observed in

our study with LV/PST treatment, and in studies using the PSA mimetic, compared to mice that received control peptide (Marino et al., 2009; Mehanna et al., 2010; Pan et al., 2014).

6.3.2 Autotomy in Hx + LV/PST animals

One of the possible adverse outcomes in experimental models of SCI is the emergence of autotomy, a behaviour during which the animal will consume part of its digits. Generally, two patterns of autotomy can be observed in rodent models of SCI (Hankenson, 2013). Firstly, autotomy can occur shortly after the initial injury (during the first few post-operative days), and is believed to be a direct consequence of the loss of sensation resulting from the damage to the spinal cord. Secondly, autotomy can also develop weeks after the injury, which is believed to be linked to the development of neuropathic pain. In this study three Hx + LV/PST animals developed autotomy of the digits of the contralateral hindlimb. This is in contrast to Hx + LV/GFP animals that did not exhibit any of this behaviour. The emergence of autotomy in Hx + LV/PST animals was observed between 2 and 3 weeks post-injury, which suggested that this might be caused by the development of neuropathic pain. Interestingly, however, responses to both thermal and mechanical stimuli were unaltered in Hx + LV/PST animals, compared to Hx + LV/GFP. Furthermore, animals that received Hx + LV/PST injections did not show any behavioural signs of pain (for example, unkept fur, weight loss), suggesting that these animals were not suffering from neuropathic pain. However, it should be noted that the animals that developed autotomy were not included in the sensory testing, as per Home Office requirements they were culled as soon as autotomy penetrated beyond the superficial skin of the digits. For this reason, it is likely that the data obtained from the sensory tests is not an accurate representation of all the animals in the Hx + LV/PST group.

The incidence of autotomy in other studies investigating PSA and SCI (using either viral vector-induced PSA expression, or PSA mimetic peptide) has not been reported, nor has any examination of sensory function. Previous data from our laboratory has, however, noted enhanced regeneration of sensory fibres following dorsal column lesion (Zhang et al., 2007b), so it could be speculated that in this study, enhanced regeneration/sprouting of sensory fibres in some Hx + LV/PST animals led to the development of neuropathic pain.

It is clear that this topic requires further research, as the emergence of neuropathic pain following therapeutic intervention to the spinal cord could be devastating and is an undesirable treatment outcome. If repeated, future studies should contain extensive sensory testing, including the plantar heat test (Hargreave's method) and the Von Frey test, and should include baseline testing and then regular testing following injury. Moreover, spinal cords from these animals could be immunolabelled to assess the sprouting of pain-related sensory axons. To investigate this at a cellular level, a relatively simple experiment could be to induce PSA expression in cultured dorsal root ganglion neurons, to examine (i) whether PSA induced significant neurite outgrowth (ie sprouting) of sensory neurons, and (ii) if so, which molecular factors may be responsible for this. Data from these studies would then provide robust evidence as to whether induced PSA expression in the injured spinal cord can result in the development of neuropathic pain.

6.2.3 LV/PST delivery resulted in strong PSA expression in the spinal cord

6 weeks following delivery of LV/PST to both the injured or uninjured spinal cord, multiple regions of mCherry-positive cells were observed, throughout most regions of the spinal cord, but concentrated in the intermediate grey matter. Following immunolabelling using an antibody against PSA, these cells were shown to be surrounded by strong PSA staining. This PSA labelling was not present in either injured or uninjured animals injected with LV/GFP. Previous studies using either viral vectors carrying the PST, or the STX transgene have also noted strong PSA labelling for up to six weeks (El Maarouf et al., 2006; Zhang et al., 2007b; Zhang et al., 2007c). It is likely that PSA expression will persist beyond six weeks, however, this has not yet been determined *in vivo.*

6.2.4 Induced PSA expression did not alter PNN structure or numbers

One of the primary aims of this thesis was to investigate the proposed relationship between PSA and the PNN in more detail. Thus far in this thesis, removing PSA from cultured hippocampal neurons during the first week *in vitro* did not affect the formation of PNNs. Moreover, a preliminary study using LV vectors to induce expression of PSA in the sensorimotor cortex was discontinued, due to the difficulty of analysing the tissue.

In the data described in this chapter, induced PSA expression using LV/PST in naïve rats, or animals that received lateral hemisection injury, did not affect either the number of neurons surrounded by either WFA or LN1-labelled PNNs, or the density of PNN immunostaining on individual neurons. The hypothesis that PSA expression may affect PNN development was based on preliminary data generated in the Bo laboratory, that noted (i) the down-regulation of PSA labelling prior to the formation of the PNN in the postnatal rat spinal cord and (ii) a reduction in WFA binding to its site within the PNN following induced PSA expression *in vivo.* Based on the evidence obtained in this study, it is unlikely that induced PSA expression can modulate the structure of the PNN *in vivo,* in either uninjured animals, or animals with a cervical level spinal cord injury.

6.2.5 Induced PSA expression does not enhance synaptogenesis *in vivo*

Six weeks following delivery of LV/PST to the injured spinal cord (Hx + LV/PST) there was no change in the density of synaptophysin- or serotonin-labelled boutons contacting neurons with viral transgene expression, compared to neurons in Hx + LV/GFP animals. Synaptophysin is a widely used marker of presynaptic terminals and a number of studies have shown an increase in the density of synaptophysin immunolabelling in the spinal cord to be associated with locomotor recovery following injury. Similarly, various studies are showing that enhanced sprouting of serotonergic neurons can also promote locomotor recovery from SCI (Barritt et al., 2006; Liu et al., 2015).

While there are no studies investigating sprouting of serotonergic fibres following LV-PST-mediated PSA expression after SCI, studies using PSA mimetic peptides have shown enhanced sprouting of serotonergic fibres following treatment with the mimetic, compared to control treatments (Marino et al., 2009; Pan et al., 2014). The study presented in this thesis did not assess the overall density of serotonergic fibres in the spinal cord, due to the limited area of induced PSA expression following delivery of LV/PST. Instead, the density of serotonin-labelled boutons contacting neurons with viral transgene expression was assessed. As previously mentioned in this thesis, there was no difference in the density of serotonergic boutons contacting neurons in Hx + LV/PST animals, compared to Hx + LV/GFP. While data from animals treated with PSA mimetic peptides suggests this treatment

enhances sprouting of serotonergic fibres, it may be possible that either (i) intraspinal delivery of LV/PST does not result in enhanced sprouting or increase synaptogenesis of serotonergic fibres *in vivo,* or (ii) LV/PST delivery may result in enhanced sprouting of serotonergic fibres, similar to treatment with PSA mimetic; however, these fibres do not form synaptic connections. Further work is required to assess this.

Currently, there is no other data available regarding synaptophysin immunolabelling following delivery of LV/PST to the injured spinal cord. Similarly, studies utilising PSA mimetic peptides have not investigated synaptophysin immunostaining. What is far more common, is the examination of specific types of synaptic markers, such as serotonin, VGLUT1 and ChAT (Mehanna et al., 2010). As previously mentioned, it has been reported that treatment with a PSA mimetic increases sprouting of serotonergic fibres following compression injury in mice. In a separate study, it was found that the density of both VGLUT1 and ChAT terminals were increased caudal to a thoracic-level injury in mice (Mehanna et al., 2010). It is likely that if synaptophysin immunolabelling were examined in these animals, the increase in the density of both VGLUT1 and ChAT-positive boutons would also be correlated with an increase in synaptophysin immunolabelling.

It is possible that the relatively limited expression of PSA following delivery of LV/PST to the spinal cord, in the data presented in this thesis, is responsible for both the lack of functional improvement and synaptogenesis in these animals. In other studies, the subdural administration of PSA mimetics allows the circulation of these peptides throughout the spinal cord (Marino et al., 2009; Mehanna et al., 2010; Pan et al., 2014), whereas the focal delivery method used in this study resulted in PSA expression in a relatively small area. It is likely that the number of injections of viral vector in this study was not sufficient to induce widespread PSA expression, which may explain both the limited behavioural recovery and limited synapse formation observed in Hx + LV/PST injected animals.

There was also no difference in the density of synaptophysin or serotonin-labelled boutons in animals injected with LV/PST only, in the absence of hemisection injury, compared to those injected with LV/GFP. This is not surprising, given that other studies investigating plasticity-promoting molecules, for example, ChABC, have not shown any alterations in plasticity or synaptogenesis in the absence of injury (Barritt et al., 2006).

6.3 Conclusions

In this study, we have demonstrated a mild improvement in locomotor function following LV vector-mediated PSA expression in a mid-cervical model of SCI. This slight improvement in locomotor function was not associated with an increase in the density of synaptophysin or serotonin-labelled boutons contacting neurons with transgene expression. Moreover, there was no difference in the number of PNNs or the density of PNN immunolabelling in animals treated with induced PSA expression. This study is the first to examine induced PSA expression mediated by LV vectors in a cervical-level model of SCI. Moreover, this is the first study to use behavioural testing to examine the efficacy of LV vector-mediated PSA expression in any model of SCI.

Chapter 7

General discussion and conclusions

Chapter 7: General discussion and conclusions

7.1 Conclusions

There are several conclusions that can be drawn from the data presented in this thesis.

Firstly, PNNs detected by WFA labelling, in addition to antibodies raised against molecules LN1 and neurocan, are ubiquitously distributed throughout the cervical spinal cord. Using double-immunofluorescent labelling it was found that WFA-labelled PNNs do not always contain LN1 or neurocan, and vice versa. Moreover, the proportion of neurons surrounded by PNNs is highly variable, depending on their location in the spinal cord. For example, the percentage of neurons with PNNs gradually increases as you move through the dorsal-ventral axis. It was also revealed that PNN-expressing neurons receive differing levels of serotonergic, cholinergic and inhibitory synaptic inputs.

Secondly, it was found that to allow high transgene expression in neurons in the cervical spinal cord and the sensorimotor cortex, lentiviral vectors should be driven by a synapsin I promoter, rather than a ubiquitous cell type promoter such as CMV. This results in strong transgene expression in neurons, but not astrocytes or microglial cells, 2 and 6 weeks following delivery to the CNS. Furthermore, using immunohistochemistry, it was shown that a lentiviral vector carrying the PST gene results in robust and long-term expression of PSA following delivery to the spinal cord and sensorimotor cortex.

Next, it was determined that while a decrease in PSA expression in cultures of embryonic hippocampal neurons corresponds to an increase in the proportion of cultured neurons with a PNN, enzymatic removal of PSA during the first week *in vitro* does not alter the development of PNNs. Moreover, removal of PSA does not affect the formation of synapses. Following on from this data, it was also shown that induced PSA in the adult spinal cord does not alter WFA binding to PNNs, or the detection of PNNs using LN1 antibody.

Finally, it was found that induced PSA expression above and below cervical SCI leads to a general improvement in hindlimb, but not forelimb locomotor function. No anatomical basis for this locomotor improvement could be determined in this thesis, as induced PSA

expression did not correspond to a reduction in the number of PNNs and did not alter the density of serotoninergic boutons contacting PSA-expressing neurons *in vivo.*

7.2 Discussion

Previous research has revealed the heterogeneous distribution and composition of PNNs in the spinal cord (Vitellaro-Zuccarello et al., 2007; Galtrey et al., 2008). In chapter 3 of this thesis, more neurons were surrounded by PNNs in the ventral regions of the spinal cord, compared to the dorsal horn, and dorsal regions of the intermediate grey matter. Some PNNs lacked labelling for the supporting molecule LN1, which is interesting considering that previous studies using LN1 knockout mice, in addition to *in vitro* studies, have suggested LN1 expression is critical for the production of condensed PNNs (Carulli et al., 2010; Kwok et al., 2010). Similarly, some PNNs also lacked labelling for the CSPG neurocan, which is unsurprising, given that other studies have noted relatively low expression of neurocan in the spinal cord compared to expression of other CSPGs (Galtrey et al., 2008). Thus, it is likely that the PNNs devoid of neurocan labelling contain other CSPGs, such as versican, aggrecan or phosphacan.

To date, there is relatively little available data regarding the phenotype and function of neurons located in lamina X of the spinal cord. In data presented in chapter 3 of this thesis, a population of neurons in lamina X were surrounded by dense, WFA-labelled PNNs, that showed little LN1 or neurocan labelling. Phenotypic analysis of these neurons suggested some were positive for the calcium-binding protein parvalbumin, but not for calbindin, or the cholinergic neuronal marker ChAT, and received low serotonergic and cholinergic inputs. Some studies have suggested that a population of lamina X neurons may be activated during stimulated locomotion, and others have suggested the presence of propriospinal neurons in lamina X (Dai et al., 2005; Siebert et al., 2010b). It would be interesting to further characterise these neurons, to try to elucidate their phenotype.

While previous studies have characterised the types of PNN-expressing neurons in the spinal cord, there is little available data regarding the types and relative amounts of synaptic inputs received by these cells. With mounting research suggesting that modulation of PNNs can promote neuroplasticity and locomotor recovery after SCI (Alilain et al., 2011; Dyck and

Karimi-Abdolrezaee, 2015), it is therefore vital to understand the circuitry of PNN-expressing neurons, to be able to accurately predict the consequences of manipulating inputs to these neurons after injury. This study revealed that PNN-expressing neurons receive varying levels of serotonergic, cholinergic and GABAergic inputs, depending on their location in the spinal cord. Moreover, there was no correlation observed between the density of specific types of synaptic inputs to PNN-expressing cells and the density of PNN immunolabelling. Although the development of PNNs coincides with the stabilisation of synapses *in vivo*, it may be that the amount of matrix deposited on the neuronal surface is not dependent on the density, or type of synaptic inputs to these neurons.

Currently, there is little data available regarding the molecular cues or interactions responsible for initiation of PNN formation *in vivo.* Based on preliminary data from our laboratory, we proposed that down-regulation of PSA may correspond to the time at which PNN formation is commenced in the spinal cord. This was addressed further in chapter 4, and to a lesser extent, chapters 5 and 6 of this thesis. In chapter 4, it was found that cultured hippocampal neurons expressed high levels of PSA during the first two weeks *in vitro,* following which levels declined. Conversely, few PNNs were found in culture until the second week *in vitro*, but they increased during the third week. While these observations are consistent with preliminary data obtained in this laboratory, attempts to validate a causal relationship between PSA down-regulation and PNN formation by enzymatically removing PSA from culture were unsuccessful. While two-dimensional cultures, like the system used in chapter 4 of this thesis, are commonly used in research, the cells share little similarity with those found *in vivo*. This is partly based on the complex, three-dimensional cytoarchitecture of the CNS, which consists of closely-associated neurons and glial cells, ensheathed by the interstitial extracellular matrix. Consequently, in chapters 5 and 6 of this thesis, the proposed relationship between PSA and PNNs was addressed *in vivo.*

Based on preliminary data, it was hypothesised that induced PSA expression *in vivo* can reduce WFA binding to its site within the PNN (unpublished observation, Dr Xuenong Bo and Dr Yi Zhang). The data presented in chapter 5 of this thesis showed strong PSA expression following delivery of a lentiviral vector carrying the PST transgene to the sensorimotor cortex. Due to problems with the immunolabelling of this tissue, the number and density of PNNs in the area of induced PSA expression could not be reliably analysed, thus this study

was discontinued and was repeated in the cervical spinal cord. In chapter 6, it was found that induced PSA expression in the spinal cord did not affect either the proportion of neurons with a PNN, or the density of PNN labelling on individual neurons. This, coupled with the data presented in chapter 4, suggests that PSA is unable to affect the development, or the maintenance, of PNN expression either *in vitro* or *in vivo.* This is interesting, considering the preliminary data obtained from this laboratory suggesting an inverse relationship between PSA expression and PNN formation *in vivo,* in addition to published studies from other laboratories suggesting contrasting functions of PSA and PNNs in the regulation of neuroplasticity in the visual cortex (Pizzorusso et al., 2002; Di Cristo et al., 2007a).

While the data presented in this thesis did not support a direct relationship between PSA and the PNN, at least in the adult CNS, chapter 6 of this thesis aimed to address whether induced expression of PSA using LV/PST could still promote neuroplasticity and locomotor recovery following cervical-level SCI. While there was no improvement in forelimb locomotor function in animals with LV/PST, there was a minor improvement in hindlimb function, observed from four weeks following injury. It was also found that enhanced synaptogenesis, and specifically, involving serotonergic neurons, was not responsible for this functional improvement. While no other studies have investigated serotonergic sprouting following LV/PST delivery to the injured spinal cord, enhanced sprouting has been observed following delivery of PSA mimetic peptide (Pan et al., 2014). What has been observed, however, is enhanced sprouting of corticospinal neurons (El Maarouf et al., 2006). In the study presented in this thesis, BDA was injected into the contralateral sensorimotor cortex, to assess the sprouting of corticospinal fibres post-injury. Unfortunately, however, BDA labelling was very poor and was difficult to observe in the grey matter of both Hx + LV/GFP and Hx + LV/PST animals (Supplementary Figure 4), but could be seen in the dorsal columns (Supplementary Figure 5). For this reason, corticospinal axons could not be quantified here, however, it could be proposed that enhanced axonal sprouting of corticospinal neurons, and the formation of new spinal circuits could be responsible for the recovery of function observed in this study.

Enhanced regeneration of sensory neurons in a dorsal column transection lesion, following delivery of LV/PST has previously been observed by the Bo laboratory (Zhang et al., 2007b).

In the final results chapter, it was found that hemisected animals with LV/PST delivery had a higher incidence of autotomy, compared to those injected with control viral vector. Some studies indicate that autotomy in experimental models of SCI may be due to the development of neuropathic pain, a common adverse effect of SCI in rodents and humans alike (Zhang et al., 2005; Wang et al., 2016). While no signs of neuropathic pain were observed in animals treated with LV/PST in this study, the animals with severe autotomy were not included in this behavioural testing, thus the data is not an accurate representation of all LV/PST treated animals and is likely skewed. As LV/PST delivery has been shown to enhance regeneration of sensory neurons following SCI (Zhang et al., 2007b), one hypothesis that could be drawn from this data is that LV/PST delivery has resulted in the enhanced sprouting of sensory neurons, which has led to the development of neuropathic pain.

7.3 Future work

While the data presented in chapter 3 of this thesis has provided a detailed characterisation of LN1 and neurocan labelled PNNs in the cervical spinal cord, what is lacking from this study is information regarding other components of the PNN, such as additional members of the CSPG family (aggrecan, versican and phosphacan), in addition to other supporting molecules such as hyaluronan and tenascin-R. Recent work has identified the chemorepulsive protein semaphorin 3A as a component of PNNs in the rodent brain. It would be interesting to include semaphorin 3A in future studies, as little information is currently available regarding this molecule and PNNs in the spinal cord. The reasons LN1 and neurocan were selected for analysis in this thesis were, firstly, previous research has shown LN1 expression to be vital for the development of PNNs both *in vivo* and *in vitro* (Carulli et al., 2010; Kwok et al., 2010). Secondly, both LN1 and neurocan expression has been shown in PNNs in the spinal cord, in addition to in cultures of embryonic neurons (Miyata et al., 2005; Galtrey et al., 2008). Future work, building on the data presented in this thesis, should therefore, examine other components of PNNs, and could also examine the distribution of PNNs in the thoracic and lumbosacral spinal cord, to examine whether there are differences in PNNs along the rostrocaudal axis of the spinal cord.

Chapter 3 also showed the heterogeneous distribution of PNNs throughout the dorsoventral axis of the spinal cord. One region of particular interest in this study was lamina X, where a population of neurons expressing dense, WFA-labelled PNNs, were located. While the data presented here showed that a proportion of these neurons are positive for the calcium-binding protein parvalbumin, the phenotype of other lamina X PNN-expressing neurons is still unknown. It would be interesting to investigate these neurons in more detail, to elucidate the phenotype of the parvalbumin-negative, PNN-expressing neurons in lamina X.

The *in vitro* experiments performed in chapter 4 provided no evidence to suggest a causal relationship between PSA down-regulation and the formation of PNNs. However, as previously mentioned, two-dimensional cultures do not accurately represent the environment *in vivo,* therefore may not have been the optimal cellular model. For example, in the data presented in this thesis, removal of PSA from cultured neurons did not alter the formation of synapses to PNN-expressing neurons or affect the global density of synaptophysin labelling. Interestingly, however, removing PSA from the cortex in organotypic slice cultures has been shown to promote early maturation of inhibitory synapses, and was consistent with additional data obtained *in vivo* (Di Cristo et al., 2007a). For this reason, it would be interesting to repeat the experiments performed in chapter 4, using organotypic cultures, which more accurately represent the tissue environment *in vivo.* Moreover, the quantification method used to assess synaptophysin-labelled boutons in contact with PNN-expressing neurons in these cultures did not permit the evaluation of inputs to dendrites; only boutons in contact with the neuronal cell body could be assessed. As previous research has shown endo-N-mediated PSA removal from cultured hippocampal neurons resulted in a reduction in the density of synaptic inputs to dendrites, it may be that the quantification method used in this thesis was not sufficient.

Building on this, it would also be interesting to examine the effect of PSA removal *in vivo* on the formation and structure of PNNs. There are two ways in which this could be performed. Firstly, intraventricular or intracortical delivery of endo-N to postnatal animals, to selectively cleave PSA from the surface of cells *in vivo.* This technique has been performed in a number of studies, and results in widespread loss of PSA throughout the brain (Daston et al., 1996; Di Cristo et al., 2007a; Battista and Rutishauser, 2010). Secondly, using knockout mice devoid of one or both of the polysialyltransferase enzymes (Eckhardt et al., 2000; Oltmann-

Norden et al., 2008; Röckle and Hildebrandt, 2016). Subsequent histological analysis could then be performed at different time points to assess whether PSA removal had any effect on the development of the PNN. Performing these experiments would provide additional information regarding the proposed relationship between PSA and the PNN *in vivo.*

The final results chapter in this thesis showed an improvement in hindlimb locomotor recovery in hemisected rats following intraspinal delivery of LV/PST, compared to those that received injections of control virus. While no improvement in the density of synaptophysin or serotonergic-labelled boutons was observed contacting neurons which displayed expression of viral transgenes, it would be interesting to evaluate other types of synaptic markers, including those that have previously been shown to be altered in other studies investigating LV/PST delivery to the injured spinal cord, or those using PSA mimetic peptide. Examples of these include cholinergic and corticospinal synapses (El Maarouf et al., 2006; Mehanna et al., 2010; Pan et al., 2014).

While no improvement in forelimb function was observed in animals treated with LV/PST, there was a general trend towards improvement in all behavioural tests. This suggests that induced PSA expression has a minor effect in spinal cord injured animals, but not enough to elicit functional improvement. Although four intraspinal injections were used in the study presented in chapter 6 of this thesis, and PSA expression encompassed a fairly large region of the spinal cord, other studies revealing functional improvement have relied on the use of PSA mimetic peptide, delivered intrathecally (Mehanna et al., 2010; Pan et al., 2014). Thus, it would be interesting to deliver LV/PST using more injections, to try to cover a wider region of the spinal cord, or using a different type of viral vector, such as adeno-associated vectors, that are able to transduce a relatively large area of the CNS following direct delivery (McCown, 2011). Moreover, in this study, LV/PST was only delivered to the ipsilateral side of the spinal cord. It is now well-regarded that spontaneous axonal sprouting occurs after injury, and axons have been shown to cross across the spinal cord midline, from the contralateral to the ipsilateral side of the spinal cord. Thus, it would be interesting to also inject LV/PST into the contralateral side of the spinal cord, as well as rostral and caudal to the lesion site, to try encourage the sprouting of axons across the midline.

With a strong trend towards locomotor recovery observed in the Montoya staircase test, a measure of skilled locomotor function, in animals injected with LV/PST, it could be speculated that combining LV/PST administration with daily neurorehabilitation would result in more significant improvement in forelimb locomotor function. Mounting evidence is showing the beneficial role of rehabilitation in improving locomotor recovery from SCI, particularly when used in combination with targeted therapeutics (García-Alías et al., 2009; Wang et al., 2011).

Although considered a good model for the evaluation of neuroplasticity and axonal regeneration in rodents, stab lesions, such as the hemisection model that was used in this study are rarely observed in clinical SCI (SpinalResearch, 2016). Commonly, lesions to the spinal cord are a result of compression or contusion injury, resulting from dislodgement of one of more of the vertebrae (SpinalResearch, 2016). Therefore, it would also be interesting to evaluate intraspinal delivery of LV/PST following either contusion or compression injury in rodents. A reliable, hemi-contusion model of SCI has been developed for the mid-cervical spinal cord, which would allow the evaluation of both fore and hindlimb locomotor function following delivery of LV/PST (Dunham et al., 2010; Mondello et al., 2015).

7.4 Concluding remarks

One of the main aims of this thesis was to evaluate the proposed relationship between expression of PSA and the development of PNNs in more detail. While the data presented here does not suggest a link between the two, there are subsequent experiments that could be performed to evaluate this in more detail. This thesis also evaluated the detailed distribution of WFA, LN1 or neurocan-labelled PNNs in the cervical spinal cord and the relationship between the density of PNN and synaptic immunolabelling. Finally, induced PSA expression using a lentiviral vector was shown to improve locomotor recovery following SCI. However, the cause of this functional improvement has not yet been determined. This study was the first to evaluate any PSA-based therapy in a cervical-level injury, and also the first to investigate the behavioural improvements associated with viral vector-mediated induced PSA expression.

Appendices

Supplementary Figure 1. Average size of PNN-expressing neurons in the cervical spinal cord

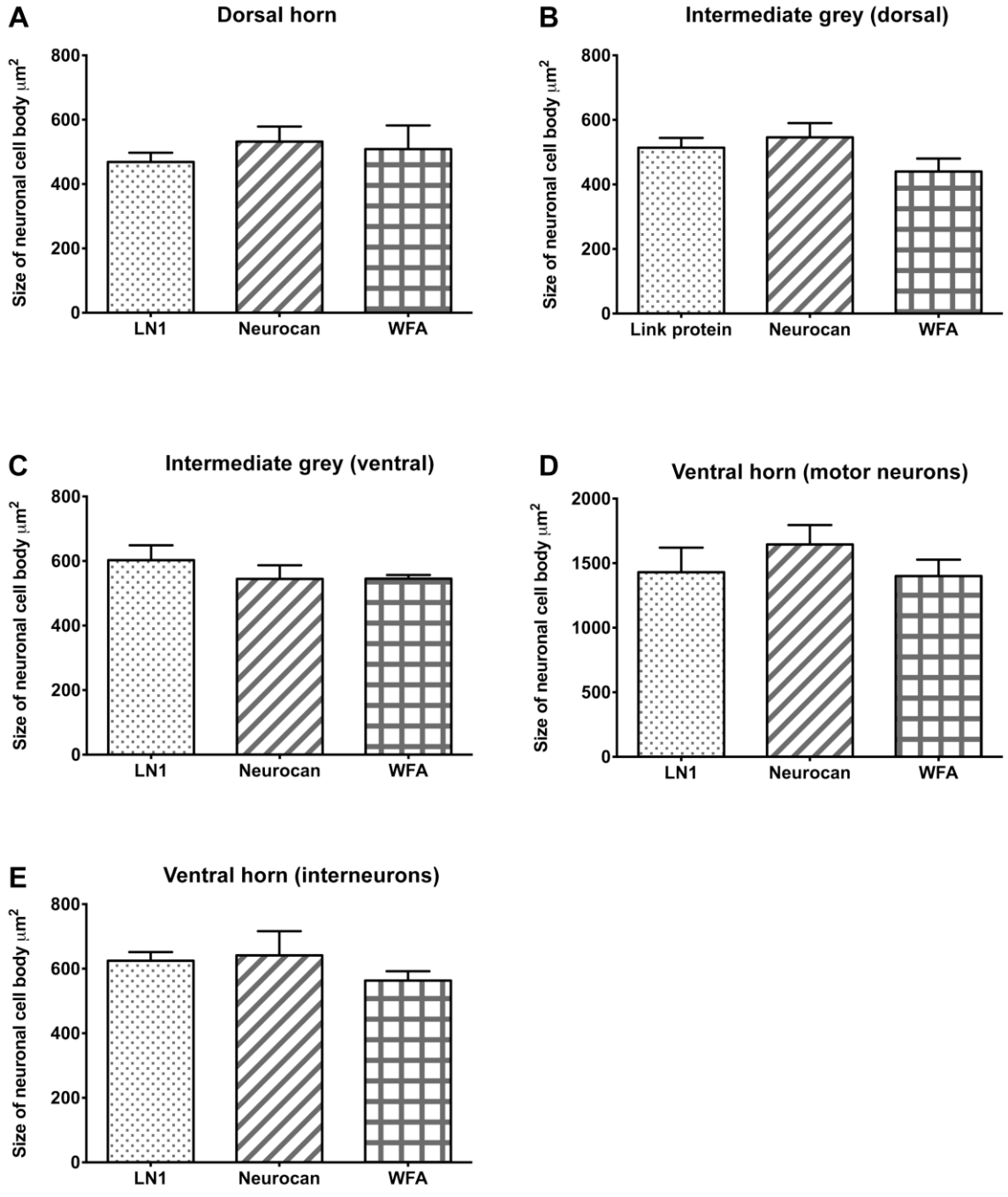

Supplementary Figure 1. Average size of PNN-expressing neurons in the cervical spinal cord.

Quantification of the mean size of the cell bodies of neurons expressing LN1, neurocan or WFA-labelled PNNs in the **(A)** dorsal horn, **(B)** dorsal intermediate grey matter, **(C)** ventral intermediate grey matter, **(D)** ventral horn (motor neurons) and **(E)** ventral horn (interneurons). No difference was observed in the mean size of neurons in any region of the spinal cord ($p>0.05$, one-way ANOVA, *n=3)*

Supplementary Figure 2. BBB scoring system.

0	No observable hind limb (HL) movement.
1	Slight movement of one or two joints, usually the hip and/or knee.
2	Extensive movement of one joint or extensive movement of one joint and slight movement of one other joint.
3	Extensive movement of two joints.
4	Slight movement of all three joints of the HL.
5	Slight movement of two joints and extensive movement of the third.
6	Extensive movement of two joints and slight movement of the third.
7	Extensive movement of all three joints of the HL.
8	Sweeping with no weight support or plantar placement of the paw with no weight support.
9	Plantar placement of the paw with weight support in stance only (i.e., when stationary) or occasional, frequent, or consistent weight supported dorsal stepping and no plantar stepping.
10	Occasional weight supported plantar steps, no forelimb (FL)-HL coordination.
11	Frequent to consistent weight supported plantar steps and no FL-HL coordination.
12	Frequent to consistent weight supported plantar steps and occasional FL-HL coordination.
13	Frequent to consistent weight supported plantar steps and frequent FL-HL coordination.
14	Consistent weight supported plantar steps, consistent FL-HL coordination; and predominant paw position during locomotion is rotated (internally or externally) when it makes initial contact with the surface as well as just before it is lifted off at the end of stance or frequent plantar stepping, consistent FL-HL coordination, and occasional dorsal stepping.
15	Consistent plantar stepping and consistent FL-HL coordination; and no toe clearance or occasional toe clearance during forward limb advancement; predominant paw position is parallel to the body at initial contact.
16	Consistent plantar stepping and consistent FL-HL coordination during gait; and toe clearance occurs frequently during forward limb advancement; predominant paw position is parallel at initial contact and rotated at lift off.
17	Consistent plantar stepping and consistent FL-HL coordination during gait; and toe clearance occurs frequently during forward limb advancement; predominant paw position is parallel at initial contact and lift off.
18	Consistent plantar stepping and consistent FL-HL coordination during gait; and toe clearance occurs consistently during forward limb advancement; predominant paw position is parallel at initial contact and rotated at lift off.
19	Consistent plantar stepping and consistent FL-HL coordination during gait; and toe clearance occurs consistently during forward limb advancement; predominant paw position is parallel at initial contact and lift off; and tail is down part or all of the time.
20	Consistent plantar stepping and consistent coordinated gait; consistent toe clearance; predominant paw position is parallel at initial contact and lift off; tail consistently up; and trunk instability.
21	Consistent plantar stepping and coordinated gait, consistent toe clearance, predominant paw position is parallel throughout stance, consistent trunk stability, tail consistently up.

Originally published in Journal of Neurotrauma, Volume 12, Number 1, 1995.

Supplementary Figure 3. FLS scoring system.

Forelimb Locomotor Scale (FLS)

0. No movements of the forelimb (shoulder, elbow or wrist joints)
1. Slight movements of one or two joints of the forelimb
2. Extensive movement of one joint and slight movement of another joint of the forelimb
3. Slight movement of all three joints of the forelimb
4. Extensive movement of one joint and slight movement of two joints of the forelimb
5. Extensive movement of two joints and slight movement of one joint of the forelimb
6. Extensive movement of all three joints of the forelimb
7. Plantar placement of the forelimb with no weight support
8. Dorsal stepping only
9. Dorsal stepping and/or occasional plantar stepping
10. Frequent plantar stepping
11. Continuous plantar stepping
12. Continuous plantar stepping with paw position rotated (either at initial contact, lift off or both)
13. Continuous plantar stepping with paw position parallel (either at initial contact, lift off or both)
14. Continuous plantar stepping with paw position rotated (either at initial contact, lift off or both) and occasional toe clearance
15. Continuous plantar stepping with paw position parallel (either at initial contact, lift off or both) and occasional toe clearance
16. Continuous plantar stepping with paw position parallel (either at initial contact, lift off or both) and frequent toe clearance
17. Continuous plantar stepping with paw position parallel (either at initial contact, lift off or both) and continuous toe clearance

Supplementary Figure 4. BDA labelling in SCI animals

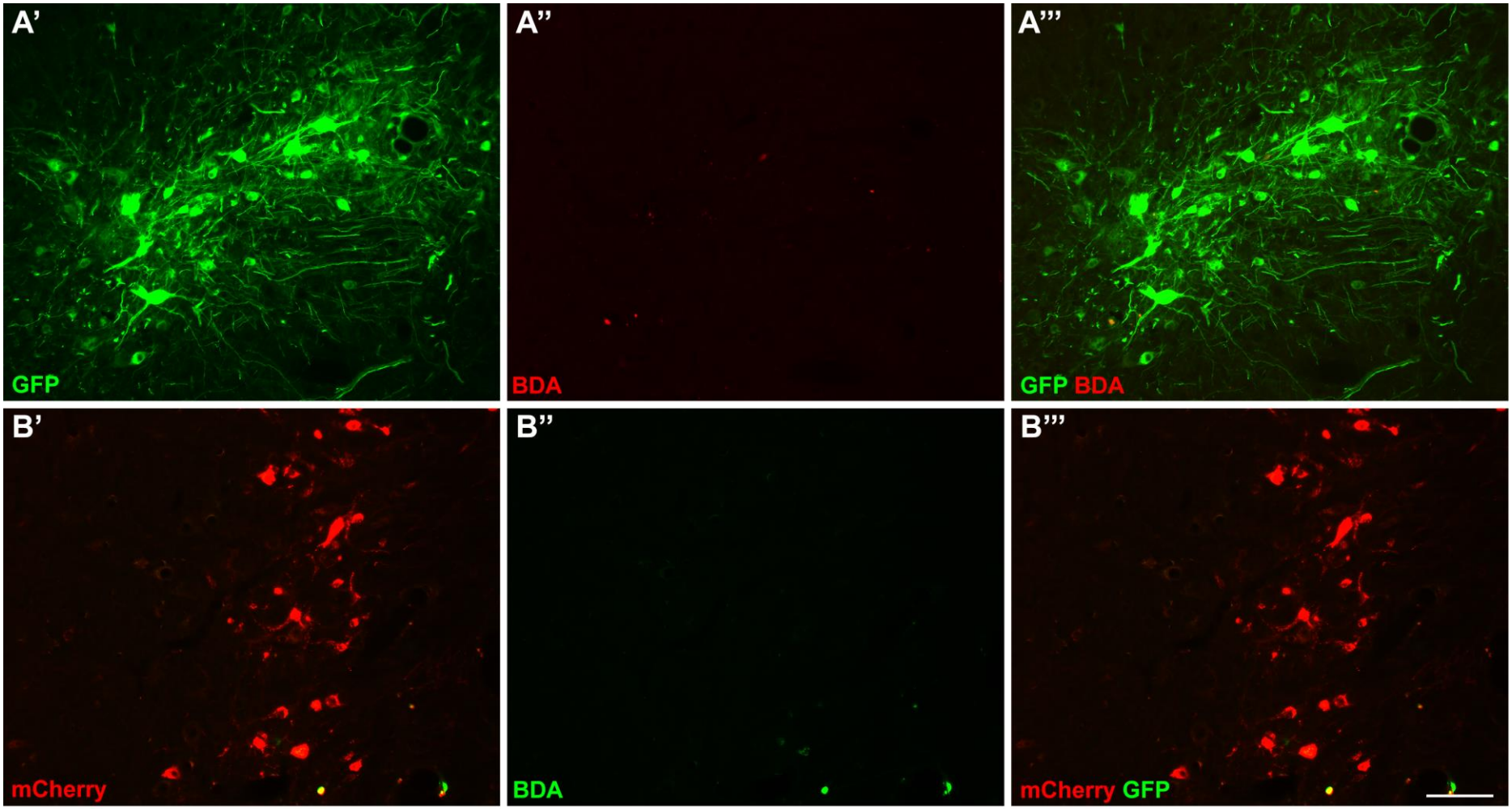

Supplementary Figure 4. BDA labelling in injured animals.

Quantification of BDA was not possible due to the poor labelling observed in the hemisected spinal cord, 6 weeks post-lesion. (A) BDA labelling was weak in the ipsilateral spinal cord of animals in the Hx + LV/GFP treatment group. (B) Similarly, BDA labelling was weak in the ipsilateral spinal cord of animals in the Hx + LV/PST group. Scale bar = 100 μm.

Supplementary Figure 5. BDA labelling in the dorsal columns of SCI animals.

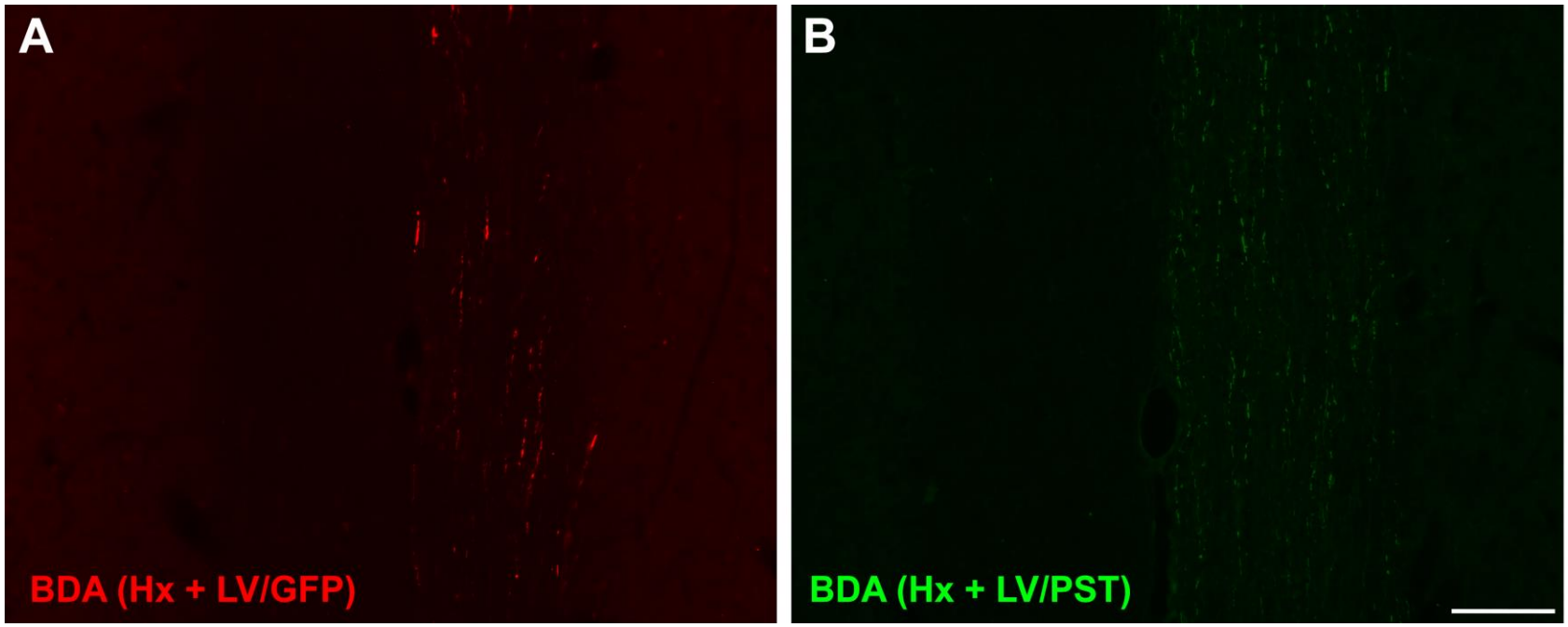

Supplementary Figure 5. BDA labelling in the dorsal columns of injured animals.
As previously shown, BDA labelling was poor in the ipsilateral grey matter and could not be used for quantification. However, BDA labelling was observed in the dorsal columns of both (A) Hx + LV/GFP and (B) Hx + LV/PST treated animals. Scale bar = 100 μm.

Bibliography

Aaron LI, Chesselet MF (1989) Heterogeneous distribution of polysialylated neuronal-cell adhesion molecule during post-natal development and in the adult: an immunohistochemical study in the rat brain. Neuroscience 28:701-710.

Akbik F, Cafferty WB, Strittmatter SM (2012) Myelin associated inhibitors: a link between injury-induced and experience-dependent plasticity. Exp Neurol 235:43-52.

Alilain WJ, Horn KP, Hu H, Dick TE, Silver J (2011) Functional regeneration of respiratory pathways after spinal cord injury. Nature 475:196-200.

Alluin O, Delivet-Mongrain H, Gauthier MK, Fehlings MG, Rossignol S, Karimi-Abdolrezaee S (2014) Examination of the combined effects of chondroitinase ABC, growth factors and locomotor training following compressive spinal cord injury on neuroanatomical plasticity and kinematics. PLoS One 9:e111072.

Almad A, Sahinkaya FR, McTigue DM (2011) Oligodendrocyte fate after spinal cord injury. Neurotherapeutics 8:262-273.

Andrews MR, Czvitkovich S, Dassie E, Vogelaar CF, Faissner A, Blits B, Gage FH, ffrench-Constant C, Fawcett JW (2009) Alpha9 integrin promotes neurite outgrowth on tenascin-C and enhances sensory axon regeneration. J Neurosci 29:5546-5557.

Ankeny DP, Lucin KM, Sanders VM, McGaughy VM, Popovich PG (2006) Spinal cord injury triggers systemic autoimmunity: evidence for chronic B lymphocyte activation and lupus-like autoantibody synthesis. J Neurochem 99:1073-1087.

Arranz AM, Perkins KL, Irie F, Lewis DP, Hrabe J, Xiao F, Itano N, Kimata K, Hrabetova S, Yamaguchi Y (2014) Hyaluronan deficiency due to Has3 knock-out causes altered neuronal activity and seizures via reduction in brain extracellular space. J Neurosci 34:6164-6176.

Aspberg A, Miura R, Bourdoulous S, Shimonaka M, Heinegârd D, Schachner M, Ruoslahti E, Yamaguchi Y (1997) The C-type lectin domains of lecticans, a family of aggregating chondroitin sulfate proteoglycans, bind tenascin-R by protein-protein interactions independent of carbohydrate moiety. Proc Natl Acad Sci U S A 94:10116-10121.

Azzouz M, Kingsman SM, Mazarakis ND (2004) Lentiviral vectors for treating and modeling human CNS disorders. The journal of gene medicine 6:951-962.

BackUp (2016) About spinal cord injury. In.

Bao F, Brown A, Dekaban GA, Omana V, Weaver LC (2011) CD11d integrin blockade reduces the systemic inflammatory response syndrome after spinal cord injury. Exp Neurol 231:272-283.

Barber RP, Phelps PE, Houser CR, Crawford GD, Salvaterra PM, Vaughn JE (1984) The morphology and distribution of neurons containing choline acetyltransferase in the adult rat spinal cord: an immunocytochemical study. J Comp Neurol 229:329-346.

Bareyre FM, Kerschensteiner M, Raineteau O, Mettenleiter TC, Weinmann O, Schwab ME (2004) The injured spinal cord spontaneously forms a new intraspinal circuit in adult rats. Nat Neurosci 7:269-277.

Baron EJ (1996) In: Medical Microbiology, 4th Edition (Baron S, ed). Galveston (TX).

Barritt AW, Davies M, Marchand F, Hartley R, Grist J, Yip P, McMahon SB, Bradbury EJ (2006) Chondroitinase ABC promotes sprouting of intact and injured spinal systems after spinal cord injury. J Neurosci 26:10856-10867.

Barros CS, Franco SJ, Müller U (2011) Extracellular matrix: functions in the nervous system. Cold Spring Harb Perspect Biol 3:a005108.

Bartanusz V, Jezova D, Alajajian B, Digicaylioglu M (2011) The blood-spinal cord barrier: morphology and clinical implications. Ann Neurol 70:194-206.

Bartus K, James ND, Bosch KD, Bradbury EJ (2012) Chondroitin sulphate proteoglycans: key modulators of spinal cord and brain plasticity. Exp Neurol 235:5-17.

Bartus K, James ND, Didangelos A, Bosch KD, Verhaagen J, Yáñez-Muñoz RJ, Rogers JH, Schneider BL, Muir EM, Bradbury EJ (2014) Large-scale chondroitin sulfate proteoglycan digestion with

chondroitinase gene therapy leads to reduced pathology and modulates macrophage phenotype following spinal cord contusion injury. J Neurosci 34:4822-4836.
Basso DM, Beattie MS, Bresnahan JC (1995) A sensitive and reliable locomotor rating scale for open field testing in rats. J Neurotrauma 12:1-21.
Battista D, Rutishauser U (2010) Removal of polysialic acid triggers dispersion of subventricularly derived neuroblasts into surrounding CNS tissues. J Neurosci 30:3995-4003.
Beck KD, Nguyen HX, Galvan MD, Salazar DL, Woodruff TM, Anderson AJ (2010) Quantitative analysis of cellular inflammation after traumatic spinal cord injury: evidence for a multiphasic inflammatory response in the acute to chronic environment. Brain : a journal of neurology 133:433-447.
Beier KT, Saunders A, Oldenburg IA, Miyamichi K, Akhtar N, Luo L, Whelan SP, Sabatini B, Cepko CL (2011) Anterograde or retrograde transsynaptic labeling of CNS neurons with vesicular stomatitis virus vectors. Proceedings of the National Academy of Sciences of the United States of America 108:15414-15419.
Bekku Y, Saito M, Moser M, Fuchigami M, Maehara A, Nakayama M, Kusachi S, Ninomiya Y, Oohashi T (2012) Bral2 is indispensable for the proper localization of brevican and the structural integrity of the perineuronal net in the brainstem and cerebellum. J Comp Neurol 520:1721-1736.
Benson MD, Romero MI, Lush ME, Lu QR, Henkemeyer M, Parada LF (2005) Ephrin-B3 is a myelin-based inhibitor of neurite outgrowth. Proc Natl Acad Sci U S A 102:10694-10699.
Boato F, Hendrix S, Huelsenbeck SC, Hofmann F, Grosse G, Djalali S, Klimaschewski L, Auer M, Just I, Ahnert-Hilger G, Höltje M (2010) C3 peptide enhances recovery from spinal cord injury by improved regenerative growth of descending fiber tracts. J Cell Sci 123:1652-1662.
Bonfanti L (2006) PSA-NCAM in mammalian structural plasticity and neurogenesis. Prog Neurobiol 80:129-164.
Bonfanti L, Merighi A, Theodosis DT (1996) Dorsal rhizotomy induces transient expression of the highly sialylated isoform of the neural cell adhesion molecule in neurons and astrocytes of the adult rat spinal cord. Neuroscience 74:619-623.
Bonfanti L, Olive S, Poulain DA, Theodosis DT (1992) Mapping of the distribution of polysialylated neural cell adhesion molecule throughout the central nervous system of the adult rat: an immunohistochemical study. Neuroscience 49:419-436.
Bonfanti L, Peretto P, Merighi A, Fasolo A (1997) Newly-generated cells from the rostral migratory stream in the accessory olfactory bulb of the adult rat. Neuroscience 81:489-502.
Bonin RP, Bories C, De Koninck Y (2014) A simplified up-down method (SUDO) for measuring mechanical nociception in rodents using von Frey filaments. Molecular pain 10:26.
Bowes AL, Yip PK (2014) Modulating inflammatory cell responses to spinal cord injury: all in good time. J Neurotrauma 31:1753-1766.
Bradbury EJ, Moon LD, Popat RJ, King VR, Bennett GS, Patel PN, Fawcett JW, McMahon SB (2002) Chondroitinase ABC promotes functional recovery after spinal cord injury. Nature 416:636-640.
Bretzner F, Plemel JR, Liu J, Richter M, Roskams AJ, Tetzlaff W (2010) Combination of olfactory ensheathing cells with local versus systemic cAMP treatment after a cervical rubrospinal tract injury. J Neurosci Res 88:2833-2846.
Bruckner G, Kacza J, Grosche J (2004) Perineuronal nets characterized by vital labelling, confocal and electron microscopy in organotypic slice cultures of rat parietal cortex and hippocampus. Journal of molecular histology 35:115-122.
Bruckner G, Szeoke S, Pavlica S, Grosche J, Kacza J (2006) Axon initial segment ensheathed by extracellular matrix in perineuronal nets. Neuroscience 138:365-375.
Bruckner G, Grosche J, Schmidt S, Hartig W, Margolis RU, Delpech B, Seidenbecher CI, Czaniera R, Schachner M (2000) Postnatal development of perineuronal nets in wild-type mice and in a mutant deficient in tenascin-R. The Journal of comparative neurology 428:616-629.

Brückner G, Grosche J (2001) Perineuronal nets show intrinsic patterns of extracellular matrix differentiation in organotypic slice cultures. Exp Brain Res 137:83-93.

Budinich CS, Chen H, Lowe D, Rosenberger JG, Bernstock JD, McCabe JT (2012) Mouse brain PSA-NCAM levels are altered by graded-controlled cortical impact injury. Neural Plast 2012:378307.

Bukalo O, Schachner M, Dityatev A (2001) Modification of extracellular matrix by enzymatic removal of chondroitin sulfate and by lack of tenascin-R differentially affects several forms of synaptic plasticity in the hippocampus. Neuroscience 104:359-369.

Burgess A, Wainwright SR, Shihabuddin LS, Rutishauser U, Seki T, Aubert I (2008) Polysialic acid regulates the clustering, migration, and neuronal differentiation of progenitor cells in the adult hippocampus. Developmental neurobiology 68:1580-1590.

Cabungcal JH, Steullet P, Morishita H, Kraftsik R, Cuenod M, Hensch TK, Do KQ (2013) Perineuronal nets protect fast-spiking interneurons against oxidative stress. Proc Natl Acad Sci U S A 110:9130-9135.

Caggiano AO, Zimber MP, Ganguly A, Blight AR, Gruskin EA (2005) Chondroitinase ABCI improves locomotion and bladder function following contusion injury of the rat spinal cord. Journal of neurotrauma 22:226-239.

Cai D, Qiu J, Cao Z, McAtee M, Bregman BS, Filbin MT (2001) Neuronal cyclic AMP controls the developmental loss in ability of axons to regenerate. J Neurosci 21:4731-4739.

Camand E, Morel MP, Faissner A, Sotelo C, Dusart I (2004) Long-term changes in the molecular composition of the glial scar and progressive increase of serotoninergic fibre sprouting after hemisection of the mouse spinal cord. Eur J Neurosci 20:1161-1176.

Cao Y, Shumsky JS, Sabol MA, Kushner RA, Strittmatter S, Hamers FP, Lee DH, Rabacchi SA, Murray M (2008) Nogo-66 receptor antagonist peptide (NEP1-40) administration promotes functional recovery and axonal growth after lateral funiculus injury in the adult rat. Neurorehabil Neural Repair 22:262-278.

Carulli D, Rhodes KE, Fawcett JW (2007) Upregulation of aggrecan, link protein 1, and hyaluronan synthases during formation of perineuronal nets in the rat cerebellum. The Journal of comparative neurology 501:83-94.

Carulli D, Foscarin S, Faralli A, Pajaj E, Rossi F (2013) Modulation of semaphorin3A in perineuronal nets during structural plasticity in the adult cerebellum. Mol Cell Neurosci 57:10-22.:10.1016/j.mcn.2013.1008.1003. Epub 2013 Aug 1030.

Carulli D, Pizzorusso T, Kwok JC, Putignano E, Poli A, Forostyak S, Andrews MR, Deepa SS, Glant TT, Fawcett JW (2010) Animals lacking link protein have attenuated perineuronal nets and persistent plasticity. Brain : a journal of neurology 133:2331-2347.

Cetin A, Komai S, Eliava M, Seeburg PH, Osten P (2006) Stereotaxic gene delivery in the rodent brain. Nature protocols 1:3166-3173.

Charles P, Reynolds R, Seilhean D, Rougon G, Aigrot MS, Niezgoda A, Zalc B, Lubetzki C (2002) Re-expression of PSA-NCAM by demyelinated axons: an inhibitor of remyelination in multiple sclerosis? Brain : a journal of neurology 125:1972-1979.

Cheah M, Andrews MR, Chew DJ, Moloney EB, Verhaagen J, Fassler R, Fawcett JW (2016) Expression of an Activated Integrin Promotes Long-Distance Sensory Axon Regeneration in the Spinal Cord. J Neurosci 36:7283-7297. doi: 7210.1523/JNEUROSCI.0901-7216.2016.

Chen J, Wu J, Apostolova I, Skup M, Irintchev A, Kügler S, Schachner M (2007) Adeno-associated virus-mediated L1 expression promotes functional recovery after spinal cord injury. Brain 130:954-969.

Chen YJ, Zhu H, Zhang N, Shen L, Wang R, Zhou JS, Hu JG, Lü HZ (2015) Temporal kinetics of macrophage polarization in the injured rat spinal cord. J Neurosci Res 93:1526-1533.

Chuong CM, Edelman GM (1984) Alterations in neural cell adhesion molecules during development of different regions of the nervous system. J Neurosci 4:2354-2368.

Close BE, Colley KJ (1998) In vivo autopolysialylation and localization of the polysialyltransferases PST and STX. J Biol Chem 273:34586-34593.

Close BE, Tao K, Colley KJ (2000) Polysialyltransferase-1 autopolysialylation is not requisite for polysialylation of neural cell adhesion molecule. The Journal of biological chemistry 275:4484-4491.

Costa LM, Pereira JE, Filipe VM, Magalhães LG, Couto PA, Gonzalo-Orden JM, Raimondo S, Geuna S, Maurício AC, Nikulina E, Filbin MT, Varejão AS (2013) Rolipram promotes functional recovery after contusive thoracic spinal cord injury in rats. Behav Brain Res 243:66-73.

Cregg JM, DePaul MA, Filous AR, Lang BT, Tran A, Silver J (2014) Functional regeneration beyond the glial scar. Exp Neurol 253:197-207.

Cremer H, Lange R, Christoph A, Plomann M, Vopper G, Roes J, Brown R, Baldwin S, Kraemer P, Scheff S (1994a) Inactivation of the N-CAM gene in mice results in size reduction of the olfactory bulb and deficits in spatial learning. Nature 367:455-459.

Cremer H, Lange R, Christoph A, Plomann M, Vopper G, Roes J, Brown R, Baldwin S, Kraemer P, Scheff S, et al. (1994b) Inactivation of the N-CAM gene in mice results in size reduction of the olfactory bulb and deficits in spatial learning. Nature 367:455-459.

Crowe MJ, Bresnahan JC, Shuman SL, Masters JN, Beattie MS (1997) Apoptosis and delayed degeneration after spinal cord injury in rats and monkeys. Nat Med 3:73-76.

Curreli S, Arany Z, Gerardy-Schahn R, Mann D, Stamatos NM (2007) Polysialylated neuropilin-2 is expressed on the surface of human dendritic cells and modulates dendritic cell-T lymphocyte interactions. J Biol Chem 282:30346-30356.

Dai H, MacArthur L, McAtee M, Hockenbury N, Tidwell JL, McHugh B, Mansfield K, Finn T, Hamers FP, Bregman BS (2009) Activity-based therapies to promote forelimb use after a cervical spinal cord injury. J Neurotrauma 26:1719-1732.

Dai X, Noga BR, Douglas JR, Jordan LM (2005) Localization of spinal neurons activated during locomotion using the c-fos immunohistochemical method. J Neurophysiol 93:3442-3452.

Danilov CA, Steward O (2015) Conditional genetic deletion of PTEN after a spinal cord injury enhances regenerative growth of CST axons and motor function recovery in mice. Exp Neurol 266:147-160.

Daston MM, Bastmeyer M, Rutishauser U, O'Leary DD (1996) Spatially restricted increase in polysialic acid enhances corticospinal axon branching related to target recognition and innervation. The Journal of neuroscience : the official journal of the Society for Neuroscience 16:5488-5497.

Davalos D, Grutzendler J, Yang G, Kim JV, Zuo Y, Jung S, Littman DR, Dustin ML, Gan WB (2005) ATP mediates rapid microglial response to local brain injury in vivo. Nat Neurosci 8:752-758.

David S, Kroner A (2011) Repertoire of microglial and macrophage responses after spinal cord injury. Nat Rev Neurosci 12:388-399.

de Castro R, Jr., Hughes MG, Xu GY, Clifton C, Calingasan NY, Gelman BB, McAdoo DJ (2004) Evidence that infiltrating neutrophils do not release reactive oxygen species in the site of spinal cord injury. Experimental neurology 190:414-424.

Deboy CA, Xin J, Byram SC, Serpe CJ, Sanders VM, Jones KJ (2006) Immune-mediated neuroprotection of axotomized mouse facial motoneurons is dependent on the IL-4/STAT6 signaling pathway in CD4(+) T cells. Exp Neurol 201:212-224. Epub 2006 Jun 2027.

Deepa SS, Carulli D, Galtrey C, Rhodes K, Fukuda J, Mikami T, Sugahara K, Fawcett JW (2006) Composition of perineuronal net extracellular matrix in rat brain: a different disaccharide composition for the net-associated proteoglycans. J Biol Chem 281:17789-17800.

Demircan K, Yonezawa T, Takigawa T, Topcu V, Erdogan S, Ucar F, Armutcu F, Yigitoglu MR, Ninomiya Y, Hirohata S (2013) ADAMTS1, ADAMTS5, ADAMTS9 and aggrecanase-generated proteoglycan fragments are induced following spinal cord injury in mouse. Neurosci Lett 544:25-30.

Deng LX, Deng P, Ruan Y, Xu ZC, Liu NK, Wen X, Smith GM, Xu XM (2013) A novel growth-promoting pathway formed by GDNF-overexpressing Schwann cells promotes propriospinal axonal regeneration, synapse formation, and partial recovery of function after spinal cord injury. J Neurosci 33:5655-5667.

Dergham P, Ellezam B, Essagian C, Avedissian H, Lubell WD, McKerracher L (2002) Rho signaling pathway targeted to promote spinal cord repair. J Neurosci 22:6570-6577.

Di Cristo G, Chattopadhyaya B, Kuhlman SJ, Fu Y, Bélanger MC, Wu CZ, Rutishauser U, Maffei L, Huang ZJ (2007a) Activity-dependent PSA expression regulates inhibitory maturation and onset of critical period plasticity. Nat Neurosci 10:1569-1577.

Di Cristo G, Chattopadhyaya B, Kuhlman SJ, Fu Y, Belanger MC, Wu CZ, Rutishauser U, Maffei L, Huang ZJ (2007b) Activity-dependent PSA expression regulates inhibitory maturation and onset of critical period plasticity. Nature neuroscience 10:1569-1577.

Dickendesher TL, Baldwin KT, Mironova YA, Koriyama Y, Raiker SJ, Askew KL, Wood A, Geoffroy CG, Zheng B, Liepmann CD, Katagiri Y, Benowitz LI, Geller HM, Giger RJ (2012) NgR1 and NgR3 are receptors for chondroitin sulfate proteoglycans. Nat Neurosci 15:703-712.

Didangelos A, Iberl M, Vinsland E, Bartus K, Bradbury EJ (2014) Regulation of IL-10 by chondroitinase ABC promotes a distinct immune response following spinal cord injury. J Neurosci 34:16424-16432.

Dietz V, Fouad K (2014) Restoration of sensorimotor functions after spinal cord injury. Brain 137:654-667.

Dimou L, Schnell L, Montani L, Duncan C, Simonen M, Schneider R, Liebscher T, Gullo M, Schwab ME (2006) Nogo-A-deficient mice reveal strain-dependent differences in axonal regeneration. J Neurosci 26:5591-5603.

Dityatev A, Dityateva G, Sytnyk V, Delling M, Toni N, Nikonenko I, Muller D, Schachner M (2004) Polysialylated neural cell adhesion molecule promotes remodeling and formation of hippocampal synapses. The Journal of neuroscience : the official journal of the Society for Neuroscience 24:9372-9382.

Dromard C et al. (2008) Adult human spinal cord harbors neural precursor cells that generate neurons and glial cells in vitro. J Neurosci Res 86:1916-1926.

Du K, Zheng S, Zhang Q, Li S, Gao X, Wang J, Jiang L, Liu K (2015) Pten Deletion Promotes Regrowth of Corticospinal Tract Axons 1 Year after Spinal Cord Injury. J Neurosci 35:9754-9763.

Dunham KA, Siriphorn A, Chompoopong S, Floyd CL (2010) Characterization of a graded cervical hemicontusion spinal cord injury model in adult male rats. J Neurotrauma 27:2091-2106.

Dyck SM, Karimi-Abdolrezaee S (2015) Chondroitin sulfate proteoglycans: Key modulators in the developing and pathologic central nervous system. Exp Neurol 269:169-187.

Echeverry S, Shi XQ, Rivest S, Zhang J (2011) Peripheral nerve injury alters blood-spinal cord barrier functional and molecular integrity through a selective inflammatory pathway. J Neurosci 31:10819-10828.

Eckhardt M, Mühlenhoff M, Bethe A, Koopman J, Frosch M, Gerardy-Schahn R (1995) Molecular characterization of eukaryotic polysialyltransferase-1. Nature 373:715-718.

Eckhardt M, Bukalo O, Chazal G, Wang L, Goridis C, Schachner M, Gerardy-Schahn R, Cremer H, Dityatev A (2000) Mice deficient in the polysialyltransferase ST8SiaIV/PST-1 allow discrimination of the roles of neural cell adhesion molecule protein and polysialic acid in neural development and synaptic plasticity. J Neurosci 20:5234-5244.

El Maarouf A, Petridis AK, Rutishauser U (2006) Use of polysialic acid in repair of the central nervous system. Proc Natl Acad Sci U S A 103:16989-16994.

Eva R, Fawcett J (2014) Integrin signalling and traffic during axon growth and regeneration. Curr Opin Neurobiol 27:179-185.

Faulkner JR, Herrmann JE, Woo MJ, Tansey KE, Doan NB, Sofroniew MV (2004) Reactive astrocytes protect tissue and preserve function after spinal cord injury. J Neurosci 24:2143-2155.

Fawcett JW, Asher RA (1999) The glial scar and central nervous system repair. Brain Res Bull 49:377-391.

Fawcett JW et al. (2007) Guidelines for the conduct of clinical trials for spinal cord injury as developed by the ICCP panel: spontaneous recovery after spinal cord injury and statistical power needed for therapeutic clinical trials. Spinal Cord 45:190-205.

Fiore R, Püschel AW (2003) The function of semaphorins during nervous system development. Front Biosci 8:s484-499.

Fisher D, Xing B, Dill J, Li H, Hoang HH, Zhao Z, Yang XL, Bachoo R, Cannon S, Longo FM, Sheng M, Silver J, Li S (2011) Leukocyte common antigen-related phosphatase is a functional receptor for chondroitin sulfate proteoglycan axon growth inhibitors. J Neurosci 31:14051-14066.

Fletcher TL, Cameron P, De Camilli P, Banker G (1991) The distribution of synapsin I and synaptophysin in hippocampal neurons developing in culture. The Journal of neuroscience : the official journal of the Society for Neuroscience 11:1617-1626.

Foscarin S, Ponchione D, Pajaj E, Leto K, Gawlak M, Wilczynski GM, Rossi F, Carulli D (2011) Experience-dependent plasticity and modulation of growth regulatory molecules at central synapses. PLoS One 6:e16666. doi: 16610.11371/journal.pone.0016666.

Fournier AE, GrandPre T, Strittmatter SM (2001) Identification of a receptor mediating Nogo-66 inhibition of axonal regeneration. Nature 409:341-346.

Freund P, Schmidlin E, Wannier T, Bloch J, Mir A, Schwab ME, Rouiller EM (2006) Nogo-A-specific antibody treatment enhances sprouting and functional recovery after cervical lesion in adult primates. Nat Med 12:790-792.

Freund P, Schmidlin E, Wannier T, Bloch J, Mir A, Schwab ME, Rouiller EM (2009) Anti-Nogo-A antibody treatment promotes recovery of manual dexterity after unilateral cervical lesion in adult primates--re-examination and extension of behavioral data. Eur J Neurosci 29:983-996.

Friedlander DR, Milev P, Karthikeyan L, Margolis RK, Margolis RU, Grumet M (1994) The neuronal chondroitin sulfate proteoglycan neurocan binds to the neural cell adhesion molecules Ng-CAM/L1/NILE and N-CAM, and inhibits neuronal adhesion and neurite outgrowth. The Journal of cell biology 125:669-680.

Frischknecht R, Heine M, Perrais D, Seidenbecher CI, Choquet D, Gundelfinger ED (2009) Brain extracellular matrix affects AMPA receptor lateral mobility and short-term synaptic plasticity. Nat Neurosci 12:897-904.

Fry EJ, Chagnon MJ, López-Vales R, Tremblay ML, David S (2010) Corticospinal tract regeneration after spinal cord injury in receptor protein tyrosine phosphatase sigma deficient mice. Glia 58:423-433.

Galtrey CM, Kwok JC, Carulli D, Rhodes KE, Fawcett JW (2008) Distribution and synthesis of extracellular matrix proteoglycans, hyaluronan, link proteins and tenascin-R in the rat spinal cord. Eur J Neurosci 27:1373-1390.

Galuska SP, Rollenhagen M, Kaup M, Eggers K, Oltmann-Norden I, Schiff M, Hartmann M, Weinhold B, Hildebrandt H, Geyer R, Mühlenhoff M, Geyer H (2010) Synaptic cell adhesion molecule SynCAM 1 is a target for polysialylation in postnatal mouse brain. Proc Natl Acad Sci U S A 107:10250-10255.

Garcia-Alias G, Truong K, Shah PK, Roy RR, Edgerton VR (2015) Plasticity of subcortical pathways promote recovery of skilled hand function in rats after corticospinal and rubrospinal tract injuries. Experimental neurology 266:112-119.

García-Alías G, Barkhuysen S, Buckle M, Fawcett JW (2009) Chondroitinase ABC treatment opens a window of opportunity for task-specific rehabilitation. Nat Neurosci 12:1145-1151.

García-Alías G, Petrosyan HA, Schnell L, Horner PJ, Bowers WJ, Mendell LM, Fawcett JW, Arvanian VL (2011) Chondroitinase ABC combined with neurotrophin NT-3 secretion and NR2D expression promotes axonal plasticity and functional recovery in rats with lateral hemisection of the spinal cord. J Neurosci 31:17788-17799.

Geissler M, Gottschling C, Aguado A, Rauch U, Wetzel CH, Hatt H, Faissner A (2013) Primary hippocampal neurons, which lack four crucial extracellular matrix molecules, display abnormalities of synaptic structure and function and severe deficits in perineuronal net formation. The Journal of neuroscience : the official journal of the Society for Neuroscience 33:7742-7755.

Gensel JC, Zhang B (2015) Macrophage activation and its role in repair and pathology after spinal cord injury. Brain Res 1619:1-11.

Geoffroy CG, Lorenzana AO, Kwan JP, Lin K, Ghassemi O, Ma A, Xu N, Creger D, Liu K, He Z, Zheng B (2015) Effects of PTEN and Nogo Codeletion on Corticospinal Axon Sprouting and Regeneration in Mice. J Neurosci 35:6413-6428.

Ghosh M, Tuesta LM, Puentes R, Patel S, Melendez K, El Maarouf A, Rutishauser U, Pearse DD (2012) Extensive cell migration, axon regeneration, and improved function with polysialic acid-modified Schwann cells after spinal cord injury. Glia 60:979-992.

Giamanco KA, Matthews RT (2012) Deconstructing the perineuronal net: cellular contributions and molecular composition of the neuronal extracellular matrix. Neuroscience 218:367-384.

Giamanco KA, Morawski M, Matthews RT (2010) Perineuronal net formation and structure in aggrecan knockout mice. Neuroscience 170:1314-1327.

Giza J, Biederer T (2010) Polysialic acid: a veteran sugar with a new site of action in the brain. Proc Natl Acad Sci U S A 107:10335-10336.

Glass JD, Lee W, Shen H, Watanabe M (1994) Expression of immunoreactive polysialylated neural cell adhesion molecule in the suprachiasmatic nucleus. Neuroendocrinology 60:87-95.

Glomsda BA, Blaheta RA, Hailer NP (2003) Inhibition of monocyte/endothelial cell interactions and monocyte adhesion molecule expression by the immunosuppressant mycophenolate mofetil. Spinal Cord 41:610-619.

Gogolla N, Caroni P, Lüthi A, Herry C (2009) Perineuronal nets protect fear memories from erasure. Science 325:1258-1261.

Goh EL, Young JK, Kuwako K, Tessier-Lavigne M, He Z, Griffin JW, Ming GL (2008) beta1-integrin mediates myelin-associated glycoprotein signaling in neuronal growth cones. Mol Brain 1:10.

Gonzenbach RR, Gasser P, Zörner B, Hochreutener E, Dietz V, Schwab ME (2010) Nogo-A antibodies and training reduce muscle spasms in spinal cord-injured rats. Ann Neurol 68:48-57.

Gonzenbach RR, Zoerner B, Schnell L, Weinmann O, Mir AK, Schwab ME (2012) Delayed anti-nogo-a antibody application after spinal cord injury shows progressive loss of responsiveness. J Neurotrauma 29:567-578.

GrandPré T, Li S, Strittmatter SM (2002) Nogo-66 receptor antagonist peptide promotes axonal regeneration. Nature 417:547-551.

GrandPré T, Nakamura F, Vartanian T, Strittmatter SM (2000) Identification of the Nogo inhibitor of axon regeneration as a Reticulon protein. Nature 403:439-444.

Granger N, Blamires H, Franklin RJ, Jeffery ND (2012) Autologous olfactory mucosal cell transplants in clinical spinal cord injury: a randomized double-blinded trial in a canine translational model. Brain 135:3227-3237.

Greenhalgh AD, David S (2014) Differences in the phagocytic response of microglia and peripheral macrophages after spinal cord injury and its effects on cell death. J Neurosci 34:6316-6322.

Gris D, Marsh DR, Oatway MA, Chen Y, Hamilton EF, Dekaban GA, Weaver LC (2004) Transient blockade of the CD11d/CD18 integrin reduces secondary damage after spinal cord injury, improving sensory, autonomic, and motor function. J Neurosci 24:4043-4051.

Grumet M, Flaccus A, Margolis RU (1993) Functional characterization of chondroitin sulfate proteoglycans of brain: interactions with neurons and neural cell adhesion molecules. The Journal of cell biology 120:815-824.

Hall ED, Braughler JM (1986) Role of lipid peroxidation in post-traumatic spinal cord degeneration: a review. Cent Nerv Syst Trauma 3:281-294.

Hamilton LK, Truong MK, Bednarczyk MR, Aumont A, Fernandes KJ (2009) Cellular organization of the central canal ependymal zone, a niche of latent neural stem cells in the adult mammalian spinal cord. Neuroscience 164:1044-1056.

Han S, Arnold SA, Sithu SD, Mahoney ET, Geralds JT, Tran P, Benton RL, Maddie MA, D'Souza SE, Whittemore SR, Hagg T (2010) Rescuing vasculature with intravenous angiopoietin-1 and alpha v beta 3 integrin peptide is protective after spinal cord injury. Brain 133:1026-1042.

Hane M, Matsuoka S, Ono S, Miyata S, Kitajima K, Sato C (2015) Protective effects of polysialic acid on proteolytic cleavage of FGF2 and proBDNF/BDNF. Glycobiology 25:1112-1124.

Hankenson FC (2013) Critical Care Management for Laboratory Mice and Rats. In.

Harrill JA, Chen H, Streifel KM, Yang D, Mundy WR, Lein PJ (2015) Ontogeny of biochemical, morphological and functional parameters of synaptogenesis in primary cultures of rat hippocampal and cortical neurons. Molecular brain 8:10.

Harris NG, Mironova YA, Hovda DA, Sutton RL (2010) Pericontusion axon sprouting is spatially and temporally consistent with a growth-permissive environment after traumatic brain injury. J Neuropathol Exp Neurol 69:139-154.

Hata K, Fujitani M, Yasuda Y, Doya H, Saito T, Yamagishi S, Mueller BK, Yamashita T (2006) RGMa inhibition promotes axonal growth and recovery after spinal cord injury. J Cell Biol 173:47-58. Epub 2006 Apr 2003.

Hausmann ON (2003) Post-traumatic inflammation following spinal cord injury. Spinal Cord 41:369-378.

Hawthorne AL, Hu H, Kundu B, Steinmetz MP, Wylie CJ, Deneris ES, Silver J (2011) The unusual response of serotonergic neurons after CNS Injury: lack of axonal dieback and enhanced sprouting within the inhibitory environment of the glial scar. J Neurosci 31:5605-5616.

Hellal F, Hurtado A, Ruschel J, Flynn KC, Laskowski CJ, Umlauf M, Kapitein LC, Strikis D, Lemmon V, Bixby J, Hoogenraad CC, Bradke F (2011) Microtubule stabilization reduces scarring and causes axon regeneration after spinal cord injury. Science 331:928-931.

Hendriks WT, Eggers R, Verhaagen J, Boer GJ (2007) Gene transfer to the spinal cord neural scar with lentiviral vectors: predominant transgene expression in astrocytes but not in meningeal cells. J Neurosci Res 85:3041-3052.

Hesp ZC, Goldstein EZ, Goldstein EA, Miranda CJ, Kaspar BK, McTigue DM (2015) Chronic oligodendrogenesis and remyelination after spinal cord injury in mice and rats. J Neurosci 35:1274-1290.

Hildebrandt H, Becker C, Mürau M, Gerardy-Schahn R, Rahmann H (1998) Heterogeneous expression of the polysialyltransferases ST8Sia II and ST8Sia IV during postnatal rat brain development. J Neurochem 71:2339-2348.

Hines DJ, Hines RM, Mulligan SJ, Macvicar BA (2009) Microglia processes block the spread of damage in the brain and require functional chloride channels. Glia 57:1610-1618.

Hioki H, Kameda H, Nakamura H, Okunomiya T, Ohira K, Nakamura K, Kuroda M, Furuta T, Kaneko T (2007) Efficient gene transduction of neurons by lentivirus with enhanced neuron-specific promoters. Gene therapy 14:872-882.

Horn KP, Busch SA, Hawthorne AL, van Rooijen N, Silver J (2008) Another barrier to regeneration in the CNS: activated macrophages induce extensive retraction of dystrophic axons through direct physical interactions. J Neurosci 28:9330-9341.

Houle JD, Côté MP (2013) Axon regeneration and exercise-dependent plasticity after spinal cord injury. Ann N Y Acad Sci 1279:154-163.

Howell MD, Gottschall PE (2012) Lectican proteoglycans, their cleaving metalloproteinases, and plasticity in the central nervous system extracellular microenvironment. Neuroscience 217:6-18.

Hu F, Strittmatter SM (2008) The N-terminal domain of Nogo-A inhibits cell adhesion and axonal outgrowth by an integrin-specific mechanism. J Neurosci 28:1262-1269.

Hu H, Tomasiewicz H, Magnuson T, Rutishauser U (1996) The role of polysialic acid in migration of olfactory bulb interneuron precursors in the subventricular zone. Neuron 16:735-743.

Huang WL, George KJ, Ibba V, Liu MC, Averill S, Quartu M, Hamlyn PJ, Priestley JV (2007) The characteristics of neuronal injury in a static compression model of spinal cord injury in adult rats. Eur J Neurosci 25:362-372.

Huebner EA, Strittmatter SM (2009) Axon regeneration in the peripheral and central nervous systems. Results Probl Cell Differ 48:339-351.

Humpel C (2015) Organotypic brain slice cultures: A review. Neuroscience 305:86-98.

Hunanyan AS, Petrosyan HA, Alessi V, Arvanian VL (2013) Combination of chondroitinase ABC and AAV-NT3 promotes neural plasticity at descending spinal pathways after thoracic contusion in rats. J Neurophysiol 110:1782-1792.

Hunt D, Coffin RS, Anderson PN (2002) The Nogo receptor, its ligands and axonal regeneration in the spinal cord; a review. J Neurocytol 31:93-120.

Hutchinson KJ, Gómez-Pinilla F, Crowe MJ, Ying Z, Basso DM (2004) Three exercise paradigms differentially improve sensory recovery after spinal cord contusion in rats. Brain 127:1403-1414.

Hutson TH, Verhaagen J, Yanez-Munoz RJ, Moon LD (2012) Corticospinal tract transduction: a comparison of seven adeno-associated viral vector serotypes and a non-integrating lentiviral vector. Gene therapy 19:49-60.

Jager C, Lendvai D, Seeger G, Bruckner G, Matthews RT, Arendt T, Alpar A, Morawski M (2013) Perineuronal and perisynaptic extracellular matrix in the human spinal cord. Neuroscience 238:168-184.

Jakovcevski I, Wu J, Karl N, Leshchyns'ka I, Sytnyk V, Chen J, Irintchev A, Schachner M (2007) Glial scar expression of CHL1, the close homolog of the adhesion molecule L1, limits recovery after spinal cord injury. J Neurosci 27:7222-7233.

James ND, Shea J, Muir EM, Verhaagen J, Schneider BL, Bradbury EJ (2015) Chondroitinase gene therapy improves upper limb function following cervical contusion injury. Exp Neurol 271:131-135.

Ji B, Li M, Wu WT, Yick LW, Lee X, Shao Z, Wang J, So KF, McCoy JM, Pepinsky RB, Mi S, Relton JK (2006) LINGO-1 antagonist promotes functional recovery and axonal sprouting after spinal cord injury. Mol Cell Neurosci 33:311-320.

Jin D, Liu Y, Sun F, Wang X, Liu X, He Z (2015) Restoration of skilled locomotion by sprouting corticospinal axons induced by co-deletion of PTEN and SOCS3. Nat Commun 6:8074.

John N, Krugel H, Frischknecht R, Smalla KH, Schultz C, Kreutz MR, Gundelfinger ED, Seidenbecher CI (2006) Brevican-containing perineuronal nets of extracellular matrix in dissociated hippocampal primary cultures. Molecular and cellular neurosciences 31:774-784.

Johnson CP, Fujimoto I, Rutishauser U, Leckband DE (2005) Direct evidence that neural cell adhesion molecule (NCAM) polysialylation increases intermembrane repulsion and abrogates adhesion. J Biol Chem 280:137-145.

Jones TB, Hart RP, Popovich PG (2005) Molecular control of physiological and pathological T-cell recruitment after mouse spinal cord injury. J Neurosci 25:6576-6583.

Kajana S, Goshgarian HG (2009) Systemic administration of rolipram increases medullary and spinal cAMP and activates a latent respiratory motor pathway after high cervical spinal cord injury. J Spinal Cord Med 32:175-182.

Kallapur SG, Akeson RA (1992) The neural cell adhesion molecule (NCAM) heparin binding domain binds to cell surface heparan sulfate proteoglycans. J Neurosci Res 33:538-548.

Kanno H, Pressman Y, Moody A, Berg R, Muir EM, Rogers JH, Ozawa H, Itoi E, Pearse DD, Bunge MB (2014) Combination of engineered Schwann cell grafts to secrete neurotrophin and chondroitinase promotes axonal regeneration and locomotion after spinal cord injury. J Neurosci 34:1838-1855.

Keyvan-Fouladi N, Raisman G, Li Y (2003) Functional repair of the corticospinal tract by delayed transplantation of olfactory ensheathing cells in adult rats. J Neurosci 23:9428-9434.
Kigerl KA, Gensel JC, Ankeny DP, Alexander JK, Donnelly DJ, Popovich PG (2009) Identification of two distinct macrophage subsets with divergent effects causing either neurotoxicity or regeneration in the injured mouse spinal cord. J Neurosci 29:13435-13444.
Kim JE, Li S, GrandPré T, Qiu D, Strittmatter SM (2003) Axon regeneration in young adult mice lacking Nogo-A/B. Neuron 38:187-199.
Kiselyov VV, Skladchikova G, Hinsby AM, Jensen PH, Kulahin N, Soroka V, Pedersen N, Tsetlin V, Poulsen FM, Berezin V, Bock E (2003) Structural basis for a direct interaction between FGFR1 and NCAM and evidence for a regulatory role of ATP. Structure 11:691-701.
Kjellen L, Lindahl U (1991) Proteoglycans: structures and interactions. Annual review of biochemistry 60:443-475.
Koopmans GC, Deumens R, Brook G, Gerver J, Honig WM, Hamers FP, Joosten EA (2007) Strain and locomotor speed affect over-ground locomotion in intact rats. Physiol Behav 92:993-1001.
Koppe G, Bruckner G, Brauer K, Hartig W, Bigl V (1997) Developmental patterns of proteoglycan-containing extracellular matrix in perineuronal nets and neuropil of the postnatal rat brain. Cell and tissue research 288:33-41.
Kwok JC, Carulli D, Fawcett JW (2010) In vitro modeling of perineuronal nets: hyaluronan synthase and link protein are necessary for their formation and integrity. Journal of neurochemistry 114:1447-1459.
Lang BT, Cregg JM, DePaul MA, Tran AP, Xu K, Dyck SM, Madalena KM, Brown BP, Weng YL, Li S, Karimi-Abdolrezaee S, Busch SA, Shen Y, Silver J (2015) Modulation of the proteoglycan receptor PTPσ promotes recovery after spinal cord injury. Nature 518:404-408.
Lasiene J, Shupe L, Perlmutter S, Horner P (2008) No evidence for chronic demyelination in spared axons after spinal cord injury in a mouse. J Neurosci 28:3887-3896.
Lau LW, Cua R, Keough MB, Haylock-Jacobs S, Yong VW (2013) Pathophysiology of the brain extracellular matrix: a new target for remyelination. Nat Rev Neurosci 14:722-729.
Lavdas AA, Franceschini I, Dubois-Dalcq M, Matsas R (2006) Schwann cells genetically engineered to express PSA show enhanced migratory potential without impairment of their myelinating ability in vitro. Glia 53:868-878.
Lee HJ, Bian S, Jakovcevski I, Wu B, Irintchev A, Schachner M (2012) Delayed applications of L1 and chondroitinase ABC promote recovery after spinal cord injury. J Neurotrauma 29:1850-1863.
Lee JK, Chan AF, Luu SM, Zhu Y, Ho C, Tessier-Lavigne M, Zheng B (2009) Reassessment of corticospinal tract regeneration in Nogo-deficient mice. J Neurosci 29:8649-8654.
Lee JY, Choi HY, Ahn HJ, Ju BG, Yune TY (2014) Matrix metalloproteinase-3 promotes early blood-spinal cord barrier disruption and hemorrhage and impairs long-term neurological recovery after spinal cord injury. The American journal of pathology 184:2985-3000.
Lein PJ, Barnhart CD, Pessah IN (2011) Acute hippocampal slice preparation and hippocampal slice cultures. Methods Mol Biol 758:115-134.
Lemarchant S, Pruvost M, Hébert M, Gauberti M, Hommet Y, Briens A, Maubert E, Gueye Y, Féron F, Petite D, Mersel M, do Rego JC, Vaudry H, Koistinaho J, Ali C, Agin V, Emery E, Vivien D (2014) tPA promotes ADAMTS-4-induced CSPG degradation, thereby enhancing neuroplasticity following spinal cord injury. Neurobiol Dis 66:28-42.
Lemons ML, Condic ML (2008) Integrin signaling is integral to regeneration. Exp Neurol 209:343-352.
Li M, Husic N, Lin Y, Christensen H, Malik I, McIver S, LaPash Daniels CM, Harris DA, Kotzbauer PT, Goldberg MP, Snider BJ (2010) Optimal promoter usage for lentiviral vector-mediated transduction of cultured central nervous system cells. Journal of neuroscience methods 189:56-64.
Li S, Strittmatter SM (2003) Delayed systemic Nogo-66 receptor antagonist promotes recovery from spinal cord injury. J Neurosci 23:4219-4227.

Li Y, Raisman G (1995) Sprouts from cut corticospinal axons persist in the presence of astrocytic scarring in long-term lesions of the adult rat spinal cord. Exp Neurol 134:102-111.
Li Y, Decherchi P, Raisman G (2003) Transplantation of olfactory ensheathing cells into spinal cord lesions restores breathing and climbing. J Neurosci 23:727-731.
Liebscher T, Schnell L, Schnell D, Scholl J, Schneider R, Gullo M, Fouad K, Mir A, Rausch M, Kindler D, Hamers FP, Schwab ME (2005) Nogo-A antibody improves regeneration and locomotion of spinal cord-injured rats. Ann Neurol 58:706-719.
Liehl B, Hlavaty J, Moldzio R, Tonar Z, Unger H, Salmons B, Gunzburg WH, Renner M (2007) Simian immunodeficiency virus vector pseudotypes differ in transduction efficiency and target cell specificity in brain. Gene therapy 14:1330-1343.
Lin R, Kwok JC, Crespo D, Fawcett JW (2008) Chondroitinase ABC has a long-lasting effect on chondroitin sulphate glycosaminoglycan content in the injured rat brain. J Neurochem 104:400-408.
Liu BP, Fournier A, GrandPré T, Strittmatter SM (2002) Myelin-associated glycoprotein as a functional ligand for the Nogo-66 receptor. Science 297:1190-1193.
Liu G, Detloff MR, Miller KN, Santi L, Houlé JD (2012) Exercise modulates microRNAs that affect the PTEN/mTOR pathway in rats after spinal cord injury. Exp Neurol 233:447-456.
Liu K, Lu Y, Lee JK, Samara R, Willenberg R, Sears-Kraxberger I, Tedeschi A, Park KK, Jin D, Cai B, Xu B, Connolly L, Steward O, Zheng B, He Z (2010) PTEN deletion enhances the regenerative ability of adult corticospinal neurons. Nat Neurosci 13:1075-1081.
Liu XZ, Xu XM, Hu R, Du C, Zhang SX, McDonald JW, Dong HX, Wu YJ, Fan GS, Jacquin MF, Hsu CY, Choi DW (1997) Neuronal and glial apoptosis after traumatic spinal cord injury. J Neurosci 17:5395-5406.
Liu ZH, Yip PK, Adams L, Davies M, Lee JW, Michael GJ, Priestley JV, Michael-Titus AT (2015) A Single Bolus of Docosahexaenoic Acid Promotes Neuroplastic Changes in the Innervation of Spinal Cord Interneurons and Motor Neurons and Improves Functional Recovery after Spinal Cord Injury. J Neurosci 35:12733-12752.
Loers G, Cui YF, Neumaier I, Schachner M, Skerra A (2014) A Fab fragment directed against the neural cell adhesion molecule L1 enhances functional recovery after injury of the adult mouse spinal cord. Biochem J 460:437-446.
Loers G, Saini V, Mishra B, Gul S, Chaudhury S, Wallqvist A, Kaur G, Schachner M (2016) Vinorelbine and epirubicin share common features with polysialic acid and modulate neuronal and glial functions. J Neurochem 136:48-62.
Lu J, Féron F, Mackay-Sim A, Waite PM (2002) Olfactory ensheathing cells promote locomotor recovery after delayed transplantation into transected spinal cord. Brain 125:14-21.
Lu P, Yang H, Jones LL, Filbin MT, Tuszynski MH (2004) Combinatorial therapy with neurotrophins and cAMP promotes axonal regeneration beyond sites of spinal cord injury. J Neurosci 24:6402-6409.
Luo J, Bo X, Wu D, Yeh J, Richardson PM, Zhang Y (2010) Promoting survival, migration, and integration of transplanted Schwann cells by over-expressing polysialic acid. Glia.
Maier IC, Ichiyama RM, Courtine G, Schnell L, Lavrov I, Edgerton VR, Schwab ME (2009) Differential effects of anti-Nogo-A antibody treatment and treadmill training in rats with incomplete spinal cord injury. Brain 132:1426-1440.
Maness PF, Schachner M (2007) Neural recognition molecules of the immunoglobulin superfamily: signaling transducers of axon guidance and neuronal migration. Nat Neurosci 10:19-26.
Marino P, Norreel JC, Schachner M, Rougon G, Amoureux MC (2009) A polysialic acid mimetic peptide promotes functional recovery in a mouse model of spinal cord injury. Experimental neurology 219:163-174.
Masson RL, Sparkes ML, Ritz LA (1991) Descending projections to the rat sacrocaudal spinal cord. J Comp Neurol 307:120-130.

McAdoo DJ, Xu GY, Robak G, Hughes MG (1999) Changes in amino acid concentrations over time and space around an impact injury and their diffusion through the rat spinal cord. Exp Neurol 159:538-544.

McCown TJ (2011) Adeno-Associated Virus (AAV) Vectors in the CNS. Curr Gene Ther 11:181-188.

McRae PA, Porter BE (2012) The perineuronal net component of the extracellular matrix in plasticity and epilepsy. Neurochem Int 61:963-972.

McRae PA, Rocco MM, Kelly G, Brumberg JC, Matthews RT (2007) Sensory deprivation alters aggrecan and perineuronal net expression in the mouse barrel cortex. The Journal of neuroscience : the official journal of the Society for Neuroscience 27:5405-5413.

Mehanna A, Jakovcevski I, Acar A, Xiao M, Loers G, Rougon G, Irintchev A, Schachner M (2010) Polysialic acid glycomimetic promotes functional recovery and plasticity after spinal cord injury in mice. Mol Ther 18:34-43.

Mendiratta SS, Sekulic N, Lavie A, Colley KJ (2005) Specific amino acids in the first fibronectin type III repeat of the neural cell adhesion molecule play a role in its recognition and polysialylation by the polysialyltransferase ST8Sia IV/PST. J Biol Chem 280:32340-32348.

Mi S, Lee X, Shao Z, Thill G, Ji B, Relton J, Levesque M, Allaire N, Perrin S, Sands B, Crowell T, Cate RL, McCoy JM, Pepinsky RB (2004) LINGO-1 is a component of the Nogo-66 receptor/p75 signaling complex. Nat Neurosci 7:221-228.

Miles GB, Hartley R, Todd AJ, Brownstone RM (2007) Spinal cholinergic interneurons regulate the excitability of motoneurons during locomotion. Proc Natl Acad Sci U S A 104:2448-2453.

Miller PD, Styren SD, Lagenaur CF, DeKosky ST (1994) Embryonic neural cell adhesion molecule (N-CAM) is elevated in the denervated rat dentate gyrus. The Journal of neuroscience : the official journal of the Society for Neuroscience 14:4217-4225.

Mills CD, Hains BC, Johnson KM, Hulsebosch CE (2001) Strain and model differences in behavioral outcomes after spinal cord injury in rat. J Neurotrauma 18:743-756.

Miyata S, Nishimura Y, Hayashi N, Oohira A (2005) Construction of perineuronal net-like structure by cortical neurons in culture. Neuroscience 136:95-104.

Miyata S, Komatsu Y, Yoshimura Y, Taya C, Kitagawa H (2012) Persistent cortical plasticity by upregulation of chondroitin 6-sulfation. Nature neuroscience 15:414-422, S411-412.

Mondello SE, Sunshine MD, Fischedick AE, Moritz CT, Horner PJ (2015) A Cervical Hemi-Contusion Spinal Cord Injury Model for the Investigation of Novel Therapeutics Targeting Proximal and Distal Forelimb Functional Recovery. J Neurotrauma 32:1994-2007.

Monnier PP, Sierra A, Schwab JM, Henke-Fahle S, Mueller BK (2003) The Rho/ROCK pathway mediates neurite growth-inhibitory activity associated with the chondroitin sulfate proteoglycans of the CNS glial scar. Mol Cell Neurosci 22:319-330.

Morris AW, Carare RO, Schreiber S, Hawkes CA (2014) The Cerebrovascular Basement Membrane: Role in the Clearance of beta-amyloid and Cerebral Amyloid Angiopathy. Frontiers in aging neuroscience 6:251.

Mörgelin M, Heinegård D, Engel J, Paulsson M (1994) The cartilage proteoglycan aggregate: assembly through combined protein-carbohydrate and protein-protein interactions. Biophys Chem 50:113-128.

Mühlenhoff M, Eckhardt M, Bethe A, Frosch M, Gerardy-Schahn R (1996) Autocatalytic polysialylation of polysialyltransferase-1. EMBO J 15:6943-6950.

Nacher J, Blasco-Ibanez JM, McEwen BS (2002) Non-granule PSA-NCAM immunoreactive neurons in the rat hippocampus. Brain research 930:1-11.

Nait Oumesmar B, Vignais L, Duhamel-Clerin E, Avellana-Adalid V, Rougon G, Baron-Van Evercooren A (1995a) Expression of the highly polysialylated neural cell adhesion molecule during postnatal myelination and following chemically induced demyelination of the adult mouse spinal cord. The European journal of neuroscience 7:480-491.

Nait Oumesmar B, Vignais L, Duhamel-Clérin E, Avellana-Adalid V, Rougon G, Baron-Van Evercooren A (1995b) Expression of the highly polysialylated neural cell adhesion molecule during

postnatal myelination and following chemically induced demyelination of the adult mouse spinal cord. Eur J Neurosci 7:480-491.
Nakayama J, Fukuda M (1996) A human polysialyltransferase directs in vitro synthesis of polysialic acid. J Biol Chem 271:1829-1832.
Nandini CD, Sugahara K (2006) Role of the sulfation pattern of chondroitin sulfate in its biological activities and in the binding of growth factors. Adv Pharmacol 53:253-279.
Neirinckx V, Coste C, Franzen R, Gothot A, Rogister B, Wislet S (2014) Neutrophil contribution to spinal cord injury and repair. J Neuroinflammation 11:150.
Neumann S, Bradke F, Tessier-Lavigne M, Basbaum AI (2002) Regeneration of sensory axons within the injured spinal cord induced by intraganglionic cAMP elevation. Neuron 34:885-893.
Nikulina E, Tidwell JL, Dai HN, Bregman BS, Filbin MT (2004) The phosphodiesterase inhibitor rolipram delivered after a spinal cord lesion promotes axonal regeneration and functional recovery. Proc Natl Acad Sci U S A 101:8786-8790.
Noble LJ, Donovan F, Igarashi T, Goussev S, Werb Z (2002) Matrix metalloproteinases limit functional recovery after spinal cord injury by modulation of early vascular events. The Journal of neuroscience : the official journal of the Society for Neuroscience 22:7526-7535.
Oka S, Bruses JL, Nelson RW, Rutishauser U (1995) Properties and developmental regulation of polysialyltransferase activity in the chicken embryo brain. The Journal of biological chemistry 270:19357-19363.
Oltmann-Norden I, Galuska SP, Hildebrandt H, Geyer R, Gerardy-Schahn R, Geyer H, Mühlenhoff M (2008) Impact of the polysialyltransferases ST8SiaII and ST8SiaIV on polysialic acid synthesis during postnatal mouse brain development. J Biol Chem 283:1463-1471.
Ong E, Nakayama J, Angata K, Reyes L, Katsuyama T, Arai Y, Fukuda M (1998) Developmental regulation of polysialic acid synthesis in mouse directed by two polysialyltransferases, PST and STX. Glycobiology 8:415-424.
Oohashi T, Edamatsu M, Bekku Y, Carulli D (2015) The hyaluronan and proteoglycan link proteins: Organizers of the brain extracellular matrix and key molecules for neuronal function and plasticity. Exp Neurol 274:134-144.
Orlando C, Raineteau O (2015) Integrity of cortical perineuronal nets influences corticospinal tract plasticity after spinal cord injury. Brain structure & function 220:1077-1091.
Pan HC, Shen YQ, Loers G, Jakovcevski I, Schachner M (2014) Tegaserod, a small compound mimetic of polysialic acid, promotes functional recovery after spinal cord injury in mice. Neuroscience 277:356-366.
Papastefanaki F, Chen J, Lavdas AA, Thomaidou D, Schachner M, Matsas R (2007) Grafts of Schwann cells engineered to express PSA-NCAM promote functional recovery after spinal cord injury. Brain : a journal of neurology 130:2159-2174.
Parr-Brownlie LC, Bosch-Bouju C, Schoderboeck L, Sizemore RJ, Abraham WC, Hughes SM (2015) Lentiviral vectors as tools to understand central nervous system biology in mammalian model organisms. Frontiers in molecular neuroscience 8:14.
Pearse DD, Sanchez AR, Pereira FC, Andrade CM, Puzis R, Pressman Y, Golden K, Kitay BM, Blits B, Wood PM, Bunge MB (2007) Transplantation of Schwann cells and/or olfactory ensheathing glia into the contused spinal cord: Survival, migration, axon association, and functional recovery. Glia 55:976-1000.
Peluffo H, Foster E, Ahmed SG, Lago N, Hutson TH, Moon L, Yip P, Wanisch K, Caraballo-Miralles V, Olmos G, Llado J, McMahon SB, Yanez-Munoz RJ (2013) Efficient gene expression from integration-deficient lentiviral vectors in the spinal cord. Gene therapy 20:645-657.
Pençe S (2002) Paw preference in rats. J Basic Clin Physiol Pharmacol 13:41-49.
Pizzorusso T, Medini P, Berardi N, Chierzi S, Fawcett JW, Maffei L (2002) Reactivation of ocular dominance plasticity in the adult visual cortex. Science 298:1248-1251.

Popovich PG, Stokes BT, Whitacre CC (1996) Concept of autoimmunity following spinal cord injury: possible roles for T lymphocytes in the traumatized central nervous system. J Neurosci Res 45:349-363.

Pyka M, Wetzel C, Aguado A, Geissler M, Hatt H, Faissner A (2011) Chondroitin sulfate proteoglycans regulate astrocyte-dependent synaptogenesis and modulate synaptic activity in primary embryonic hippocampal neurons. The European journal of neuroscience 33:2187-2202.

Qiu J, Cai D, Dai H, McAtee M, Hoffman PN, Bregman BS, Filbin MT (2002) Spinal axon regeneration induced by elevation of cyclic AMP. Neuron 34:895-903.

Rahim AA, Wong AM, Howe SJ, Buckley SM, Acosta-Saltos AD, Elston KE, Ward NJ, Philpott NJ, Cooper JD, Anderson PN, Waddington SN, Thrasher AJ, Raivich G (2009) Efficient gene delivery to the adult and fetal CNS using pseudotyped non-integrating lentiviral vectors. Gene therapy 16:509-520.

Raisman G, Li Y (2007) Repair of neural pathways by olfactory ensheathing cells. Nat Rev Neurosci 8:312-319.

Rhodes KE, Fawcett JW (2004) Chondroitin sulphate proteoglycans: preventing plasticity or protecting the CNS? Journal of anatomy 204:33-48.

Rockle I, Seidenfaden R, Weinhold B, Muhlenhoff M, Gerardy-Schahn R, Hildebrandt H (2008) Polysialic acid controls NCAM-induced differentiation of neuronal precursors into calretinin-positive olfactory bulb interneurons. Developmental neurobiology 68:1170-1184.

Rolls A, Shechter R, Schwartz M (2009) The bright side of the glial scar in CNS repair. Nat Rev Neurosci 10:235-241.

Romberg C, Yang S, Melani R, Andrews MR, Horner AE, Spillantini MG, Bussey TJ, Fawcett JW, Pizzorusso T, Saksida LM (2013) Depletion of perineuronal nets enhances recognition memory and long-term depression in the perirhinal cortex. J Neurosci 33:7057-7065.

Roonprapunt C, Huang W, Grill R, Friedlander D, Grumet M, Chen S, Schachner M, Young W (2003) Soluble cell adhesion molecule L1-Fc promotes locomotor recovery in rats after spinal cord injury. J Neurotrauma 20:871-882.

Rutishauser U (1998) Polysialic acid at the cell surface: biophysics in service of cell interactions and tissue plasticity. J Cell Biochem 70:304-312.

Röckle I, Hildebrandt H (2016) Deficits of olfactory interneurons in polysialyltransferase- and NCAM-deficient mice. Dev Neurobiol 76:421-433.

Sandrow-Feinberg HR, Houlé JD (2015) Exercise after spinal cord injury as an agent for neuroprotection, regeneration and rehabilitation. Brain Res 1619:12-21.

Schwab JM, Conrad S, Monnier PP, Julien S, Mueller BK, Schluesener HJ (2005) Spinal cord injury-induced lesional expression of the repulsive guidance molecule (RGM). Eur J Neurosci 21:1569-1576.

Schwab ME, Caroni P (2008) Antibody against myelin-associated inhibitor of neurite growth neutralizes nonpermissive substrate properties of CNS white matter. Neuron 60:404-405.

Seki T, Arai Y (1991) The persistent expression of a highly polysialylated NCAM in the dentate gyrus of the adult rat. Neuroscience research 12:503-513.

Seki T, Arai Y (1993) Highly polysialylated neural cell adhesion molecule (NCAM-H) is expressed by newly generated granule cells in the dentate gyrus of the adult rat. The Journal of neuroscience : the official journal of the Society for Neuroscience 13:2351-2358.

Serpe CJ, Coers S, Sanders VM, Jones KJ (2003) CD4+ T, but not CD8+ or B, lymphocytes mediate facial motoneuron survival after facial nerve transection. Brain Behav Immun 17:393-402.

Shen F, Kuo R, Milon-Camus M, Han Z, Jiang L, Young WL, Su H (2013) Intravenous delivery of adeno-associated viral vector serotype 9 mediates effective gene expression in ischemic stroke lesion and brain angiogenic foci. Stroke; a journal of cerebral circulation 44:252-254.

Shen Y, Tenney AP, Busch SA, Horn KP, Cuascut FX, Liu K, He Z, Silver J, Flanagan JG (2009) PTPsigma is a receptor for chondroitin sulfate proteoglycan, an inhibitor of neural regeneration. Science 326:592-596.

Siebert JR, Middelton FA, Stelzner DJ (2010a) Intrinsic response of thoracic propriospinal neurons to axotomy. BMC Neurosci 11:69.
Siebert JR, Middleton FA, Stelzner DJ (2010b) Long descending cervical propriospinal neurons differ from thoracic propriospinal neurons in response to low thoracic spinal injury. BMC Neurosci 11:148.
Siebert JR, Conta Steencken A, Osterhout DJ (2014) Chondroitin sulfate proteoglycans in the nervous system: inhibitors to repair. Biomed Res Int 2014:845323.
Silver J, Miller JH (2004) Regeneration beyond the glial scar. Nat Rev Neurosci 5:146-156.
Smith CC, Mauricio R, Nobre L, Marsh B, Wüst RC, Rossiter HB, Ichiyama RM (2015) Differential regulation of perineuronal nets in the brain and spinal cord with exercise training. Brain Res Bull 111:20-26.
Snow DM, Lemmon V, Carrino DA, Caplan AI, Silver J (1990) Sulfated proteoglycans in astroglial barriers inhibit neurite outgrowth in vitro. Experimental neurology 109:111-130.
Sofroniew MV, Vinters HV (2010) Astrocytes: biology and pathology. Acta Neuropathol 119:7-35.
Soleman S, Yip PK, Duricki DA, Moon LD (2012) Delayed treatment with chondroitinase ABC promotes sensorimotor recovery and plasticity after stroke in aged rats. Brain 135:1210-1223.
SpinalResearch (2016) Facts and figures. In.
Stamegna JC, Felix MS, Roux-Peyronnet J, Rossi V, Féron F, Gauthier P, Matarazzo V (2011) Nasal OEC transplantation promotes respiratory recovery in a subchronic rat model of cervical spinal cord contusion. Exp Neurol 229:120-131.
Starkey ML, Bartus K, Barritt AW, Bradbury EJ (2012) Chondroitinase ABC promotes compensatory sprouting of the intact corticospinal tract and recovery of forelimb function following unilateral pyramidotomy in adult mice. The European journal of neuroscience 36:3665-3678.
Steward O, Sharp K, Yee KM, Hofstadter M (2008) A re-assessment of the effects of a Nogo-66 receptor antagonist on regenerative growth of axons and locomotor recovery after spinal cord injury in mice. Exp Neurol 209:446-468.
Steward O, Sharp K, Selvan G, Hadden A, Hofstadter M, Au E, Roskams J (2006) A re-assessment of the consequences of delayed transplantation of olfactory lamina propria following complete spinal cord transection in rats. Exp Neurol 198:483-499.
Stirling DP, Liu S, Kubes P, Yong VW (2009) Depletion of Ly6G/Gr-1 leukocytes after spinal cord injury in mice alters wound healing and worsens neurological outcome. The Journal of neuroscience : the official journal of the Society for Neuroscience 29:753-764.
Stirling DP, Cummins K, Mishra M, Teo W, Yong VW, Stys P (2014) Toll-like receptor 2-mediated alternative activation of microglia is protective after spinal cord injury. Brain 137:707-723.
Stone D, Liu Y, Li ZY, Strauss R, Finn EE, Allen JM, Chamberlain JS, Lieber A (2008) Biodistribution and safety profile of recombinant adeno-associated virus serotype 6 vectors following intravenous delivery. Journal of virology 82:7711-7715.
Storms SD, Rutishauser U (1998) A role for polysialic acid in neural cell adhesion molecule heterophilic binding to proteoglycans. J Biol Chem 273:27124-27129.
Suttkus A, Rohn S, Weigel S, Glockner P, Arendt T, Morawski M (2014) Aggrecan, link protein and tenascin-R are essential components of the perineuronal net to protect neurons against iron-induced oxidative stress. Cell death & disease 5:e1119.
Tabakow P, Raisman G, Fortuna W, Czyz M, Huber J, Li D, Szewczyk P, Okurowski S, Miedzybrodzki R, Czapiga B, Salomon B, Halon A, Li Y, Lipiec J, Kulczyk A, Jarmundowicz W (2014) Functional regeneration of supraspinal connections in a patient with transected spinal cord following transplantation of bulbar olfactory ensheathing cells with peripheral nerve bridging. Cell Transplant 23:1631-1655.
Takami T, Oudega M, Bates ML, Wood PM, Kleitman N, Bunge MB (2002) Schwann cell but not olfactory ensheathing glia transplants improve hindlimb locomotor performance in the moderately contused adult rat thoracic spinal cord. J Neurosci 22:6670-6681.

Tan CL, Kwok JC, Patani R, Ffrench-Constant C, Chandran S, Fawcett JW (2011) Integrin activation promotes axon growth on inhibitory chondroitin sulfate proteoglycans by enhancing integrin signaling. J Neurosci 31:6289-6295.

Tassew NG, Mothe AJ, Shabanzadeh AP, Banerjee P, Koeberle PD, Bremner R, Tator CH, Monnier PP (2014) Modifying lipid rafts promotes regeneration and functional recovery. Cell Rep 8:1146-1159. doi: 1110.1016/j.celrep.2014.1106.1014. Epub 2014 Aug 1147.

Tauchi R, Imagama S, Ohgomori T, Natori T, Shinjo R, Ishiguro N, Kadomatsu K (2012a) ADAMTS-13 is produced by glial cells and upregulated after spinal cord injury. Neurosci Lett 517:1-6.

Tauchi R, Imagama S, Natori T, Ohgomori T, Muramoto A, Shinjo R, Matsuyama Y, Ishiguro N, Kadomatsu K (2012b) The endogenous proteoglycan-degrading enzyme ADAMTS-4 promotes functional recovery after spinal cord injury. J Neuroinflammation 9:53.

Theodosis DT, Bonfanti L, Olive S, Rougon G, Poulain DA (1994) Adhesion molecules and structural plasticity of the adult hypothalamo-neurohypophysial system. Psychoneuroendocrinology 19:455-462.

Tom VJ, Steinmetz MP, Miller JH, Doller CM, Silver J (2004) Studies on the development and behavior of the dystrophic growth cone, the hallmark of regeneration failure, in an in vitro model of the glial scar and after spinal cord injury. J Neurosci 24:6531-6539.

Tom VJ, Sandrow-Feinberg HR, Miller K, Domitrovich C, Bouyer J, Zhukareva V, Klaw MC, Lemay MA, Houlé JD (2013) Exogenous BDNF enhances the integration of chronically injured axons that regenerate through a peripheral nerve grafted into a chondroitinase-treated spinal cord injury site. Exp Neurol 239:91-100.

Tomasiewicz H, Ono K, Yee D, Thompson C, Goridis C, Rutishauser U, Magnuson T (1993) Genetic deletion of a neural cell adhesion molecule variant (N-CAM-180) produces distinct defects in the central nervous system. Neuron 11:1163-1174.

Torashima T, Yamada N, Itoh M, Yamamoto A, Hirai H (2006) Exposure of lentiviral vectors to subneutral pH shifts the tropism from Purkinje cell to Bergmann glia. Eur J Neurosci 24:371-380.

Totoiu MO, Keirstead HS (2005) Spinal cord injury is accompanied by chronic progressive demyelination. J Comp Neurol 486:373-383.

Trivedi A, Olivas AD, Noble-Haeusslein LJ (2006) Inflammation and Spinal Cord Injury: Infiltrating Leukocytes as Determinants of Injury and Repair Processes. Clin Neurosci Res 6:283-292.

Tsien RY (2013) Very long-term memories may be stored in the pattern of holes in the perineuronal net. Proceedings of the National Academy of Sciences of the United States of America 110:12456-12461.

Vitellaro-Zuccarello L, Bosisio P, Mazzetti S, Monti C, De Biasi S (2007) Differential expression of several molecules of the extracellular matrix in functionally and developmentally distinct regions of rat spinal cord. Cell Tissue Res 327:433-447.

Vo T, Carulli D, Ehlert EM, Kwok JC, Dick G, Mecollari V, Moloney EB, Neufeld G, de Winter F, Fawcett JW, Verhaagen J (2013) The chemorepulsive axon guidance protein semaphorin3A is a constituent of perineuronal nets in the adult rodent brain. Mol Cell Neurosci 56:186-200.

Vutskits L, Djebbara-Hannas Z, Zhang H, Paccaud JP, Durbec P, Rougon G, Muller D, Kiss JZ (2001) PSA-NCAM modulates BDNF-dependent survival and differentiation of cortical neurons. The European journal of neuroscience 13:1391-1402.

Walberer M, Stolz E, Müller C, Friedrich C, Rottger C, Blaes F, Kaps M, Fisher M, Bachmann G, Gerriets T (2006) Experimental stroke: ischaemic lesion volume and oedema formation differ among rat strains (a comparison between Wistar and Sprague-Dawley rats using MRI). Lab Anim 40:1-8.

Wang D, Fawcett J (2012) The perineuronal net and the control of CNS plasticity. Cell and tissue research 349:147-160.

Wang D, Ichiyama RM, Zhao R, Andrews MR, Fawcett JW (2011) Chondroitinase combined with rehabilitation promotes recovery of forelimb function in rats with chronic spinal cord injury. J Neurosci 31:9332-9344.

Wang H, Katagiri Y, McCann TE, Unsworth E, Goldsmith P, Yu ZX, Tan F, Santiago L, Mills EM, Wang Y, Symes AJ, Geller HM (2008) Chondroitin-4-sulfation negatively regulates axonal guidance and growth. J Cell Sci 121:3083-3091.

Wang KC, Kim JA, Sivasankaran R, Segal R, He Z (2002) P75 interacts with the Nogo receptor as a co-receptor for Nogo, MAG and OMgp. Nature 420:74-78.

Wang RR, Lou GD, Yu J, Hu TT, Hou WW, Chen Z, Zhang SH, Seltzer Z (2016) Oral Administration of Pregabalin in Rats before or after Nerve Injury Partially Prevents Spontaneous Neuropathic Pain and Long Outlasts the Treatment Period. Pharmacology 97:251-258.

Warden P, Bamber NI, Li H, Esposito A, Ahmad KA, Hsu CY, Xu XM (2001) Delayed glial cell death following wallerian degeneration in white matter tracts after spinal cord dorsal column cordotomy in adult rats. Exp Neurol 168:213-224.

Watson C, Paxinos G, Kayalioglu G, Heise C (2008) The Spinal Cord.

Weber P, Bartsch U, Rasband MN, Czaniera R, Lang Y, Bluethmann H, Margolis RU, Levinson SR, Shrager P, Montag D, Schachner M (1999) Mice deficient for tenascin-R display alterations of the extracellular matrix and decreased axonal conduction velocities in the CNS. J Neurosci 19:4245-4262.

Weinhold B, Seidenfaden R, Rockle I, Muhlenhoff M, Schertzinger F, Conzelmann S, Marth JD, Gerardy-Schahn R, Hildebrandt H (2005) Genetic ablation of polysialic acid causes severe neurodevelopmental defects rescued by deletion of the neural cell adhesion molecule. The Journal of biological chemistry 280:42971-42977.

Weishaupt N, Mason AL, Hurd C, May Z, Zmyslowski DC, Galleguillos D, Sipione S, Fouad K (2014) Vector-induced NT-3 expression in rats promotes collateral growth of injured corticospinal tract axons far rostral to a spinal cord injury. Neuroscience 272:65-75.

Wells JE, Rice TK, Nuttall RK, Edwards DR, Zekki H, Rivest S, Yong VW (2003) An adverse role for matrix metalloproteinase 12 after spinal cord injury in mice. The Journal of neuroscience : the official journal of the Society for Neuroscience 23:10107-10115.

Wu B, Matic D, Djogo N, Szpotowicz E, Schachner M, Jakovcevski I (2012) Improved regeneration after spinal cord injury in mice lacking functional T- and B-lymphocytes. Exp Neurol 237:274-285.

Wu J, Leung PY, Sharp A, Lee HJ, Wrathall JR (2011) Increased expression of the close homolog of the adhesion molecule L1 in different cell types over time after rat spinal cord contusion. J Neurosci Res 89:628-638.

Xu B, Park D, Ohtake Y, Li H, Hayat U, Liu J, Selzer ME, Longo FM, Li S (2015) Role of CSPG receptor LAR phosphatase in restricting axon regeneration after CNS injury. Neurobiol Dis 73:36-48.

Xu W, Chi L, Xu R, Ke Y, Luo C, Cai J, Qiu M, Gozal D, Liu R (2005) Increased production of reactive oxygen species contributes to motor neuron death in a compression mouse model of spinal cord injury. Spinal Cord 43:204-213.

Yaguchi M, Ohashi Y, Tsubota T, Sato A, Koyano KW, Wang N, Miyashita Y (2013) Characterization of the properties of seven promoters in the motor cortex of rats and monkeys after lentiviral vector-mediated gene transfer. Human gene therapy methods 24:333-344.

Yang L, Ge Y, Tang J, Yuan J, Ge D, Chen H, Zhang H, Cao X (2015a) Schwann Cells Transplantation Improves Locomotor Recovery in Rat Models with Spinal Cord Injury: a Systematic Review and Meta-Analysis. Cell Physiol Biochem 37:2171-2182.

Yang P, Yin X, Rutishauser U (1992) Intercellular space is affected by the polysialic acid content of NCAM. J Cell Biol 116:1487-1496.

Yang S, Cacquevel M, Saksida LM, Bussey TJ, Schneider BL, Aebischer P, Melani R, Pizzorusso T, Fawcett JW, Spillantini MG (2015b) Perineuronal net digestion with chondroitinase restores memory in mice with tau pathology. Exp Neurol 265:48-58.

Ying Z, Roy RR, Edgerton VR, Gómez-Pinilla F (2005) Exercise restores levels of neurotrophins and synaptic plasticity following spinal cord injury. Exp Neurol 193:411-419.

Yip PK, Wong LF, Sears TA, Yáñez-Muñoz RJ, McMahon SB (2010) Cortical overexpression of neuronal calcium sensor-1 induces functional plasticity in spinal cord following unilateral pyramidal tract injury in rat. PLoS Biol 8:e1000399.

Yip PK, Wong LF, Pattinson D, Battaglia A, Grist J, Bradbury EJ, Maden M, McMahon SB, Mazarakis ND (2006) Lentiviral vector expressing retinoic acid receptor beta2 promotes recovery of function after corticospinal tract injury in the adult rat spinal cord. Human molecular genetics 15:3107-3118.

Yiu G, He Z (2006) Glial inhibition of CNS axon regeneration. Nat Rev Neurosci 7:617-627.

Yuan YM, He C (2013) The glial scar in spinal cord injury and repair. Neurosci Bull 29:421-435.

Zhang B, Bailey WM, Kopper TJ, Orr MB, Feola DJ, Gensel JC (2015) Azithromycin drives alternative macrophage activation and improves recovery and tissue sparing in contusion spinal cord injury. J Neuroinflammation 12:218.

Zhang H, Xie W, Xie Y (2005) Spinal cord injury triggers sensitization of wide dynamic range dorsal horn neurons in segments rostral to the injury. Brain Res 1055:103-110.

Zhang H, Chang M, Hansen CN, Basso DM, Noble-Haeusslein LJ (2011) Role of matrix metalloproteinases and therapeutic benefits of their inhibition in spinal cord injury. Neurotherapeutics : the journal of the American Society for Experimental NeuroTherapeutics 8:206-220.

Zhang SX, Huang F, Gates M, Holmberg EG (2013) Role of endogenous Schwann cells in tissue repair after spinal cord injury. Neural Regen Res 8:177-185.

Zhang Y, Zhang X, Yeh J, Richardson P, Bo X (2007a) Engineered expression of polysialic acid enhances Purkinje cell axonal regeneration in L1/GAP-43 double transgenic mice. The European journal of neuroscience 25:351-361.

Zhang Y, Ghadiri-Sani M, Zhang X, Richardson PM, Yeh J, Bo X (2007b) Induced expression of polysialic acid in the spinal cord promotes regeneration of sensory axons. Mol Cell Neurosci 35:109-119.

Zhang Y, Zhang X, Wu D, Verhaagen J, Richardson PM, Yeh J, Bo X (2007c) Lentiviral-mediated expression of polysialic acid in spinal cord and conditioning lesion promote regeneration of sensory axons into spinal cord. Molecular therapy : the journal of the American Society of Gene Therapy 15:1796-1804.

Zhao RR, Andrews MR, Wang D, Warren P, Gullo M, Schnell L, Schwab ME, Fawcett JW (2013) Combination treatment with anti-Nogo-A and chondroitinase ABC is more effective than single treatments at enhancing functional recovery after spinal cord injury. Eur J Neurosci 38:2946-2961.

Zhao RR, Muir EM, Alves JN, Rickman H, Allan AY, Kwok JC, Roet KC, Verhaagen J, Schneider BL, Bensadoun JC, Ahmed SG, Yáñez-Muñoz RJ, Keynes RJ, Fawcett JW, Rogers JH (2011) Lentiviral vectors express chondroitinase ABC in cortical projections and promote sprouting of injured corticospinal axons. J Neurosci Methods 201:228-238.

Zheng B, Ho C, Li S, Keirstead H, Steward O, Tessier-Lavigne M (2003) Lack of enhanced spinal regeneration in Nogo-deficient mice. Neuron 38:213-224.

Zhou HX, Li XY, Li FY, Liu C, Liang ZP, Liu S, Zhang B, Wang TY, Chu TC, Lu L, Ning GZ, Kong XH, Feng SQ (2014a) Targeting RPTPσ with lentiviral shRNA promotes neurites outgrowth of cortical neurons and improves functional recovery in a rat spinal cord contusion model. Brain Res 1586:46-63.

Zhou X, He X, Ren Y (2014b) Function of microglia and macrophages in secondary damage after spinal cord injury. Neural Regen Res 9:1787-1795.

Zuber C, Lackie PM, Catterall WA, Roth J (1992) Polysialic acid is associated with sodium channels and the neural cell adhesion molecule N-CAM in adult rat brain. J Biol Chem 267:9965-9971.

Zukor K, Belin S, Wang C, Keelan N, Wang X, He Z (2013) Short hairpin RNA against PTEN enhances regenerative growth of corticospinal tract axons after spinal cord injury. J Neurosci 33:15350-15361.